EXPERIMENTAL INVESTIGATION OF NARROW GAP IMPROVED ELECTROSLAG WELDING FOR HPS 70W HIGH-PERFORMANCE STEEL

by

Andrei Denes
A Thesis
Submitted to the
Graduate Faculty
of
George Mason University
in Partial Fulfillment of
The Requirements for the Degree
of
Master of Science
Civil and Infrastructure Engineering

Committee:

___________________________	Dr. Girum Urgessa, Thesis Director
___________________________	Dr. David Lattanzi, Committee Member
___________________________	Dr. Anthony Battistini, Committee Member
___________________________	Dr. Liza Durant, Department Chair
___________________________	Dr. Kenneth S. Ball, Dean, Volgenau School of Engineering
Date: ______________________	Spring Semester 2017 George Mason University Fairfax, VA

Experimental Investigation of Narrow Gap Improved Electroslag Welding for HPS 70W High-Performance Steel

A Thesis submitted in partial fulfillment of the requirements for the degree of Master of Science at George Mason University

by

Andrei Denes
Bachelor of Science
Technical University of Cluj-Napoca, 2005

Director: Girum Urgessa, Associate Professor
Sid and Reva Dewberry Department of Civil, Environmental, and Infrastructure Engineering

Spring Semester 2017
George Mason University
Fairfax, VA

ACKNOWLEDGEMENTS

I would like to thank the staff at Turner Fairbanks Highway Research Center for allowing me to perform the work described in this research thesis. I especially would like to thank Dr. Justin Ocel for allowing this study to happen as well as for his guidance, mentoring and support along the way. The same amount of gratitude goes to my thesis advisor Dr. Girum Urgessa as his advice and guidance were invaluable to the completion of this thesis. I am extremely grateful for having him as my advisor for his knowledge, comments and suggestions. I would like to thank my committee members, Dr. David Lattanzi and Dr. Anthony Battistini for their warm support. I would also like to thank my coworkers Michael Gawron, Kevin Deasy, William K. Lee and Timothy Tuggle who helped me perform the tests, and Thomas Parker who machined all the testing specimens. And lastly, but most importantly, I would like to thank my beautiful wife, Alina Horvath, for all the patience, support and inspiration she provided me.

TABLE OF CONTENTS

LIST OF TABLES

LIST OF FIGURES

LIST OF EQUATIONS

LIST OF ABBREVIATIONS AND SYMBOLS

Accelerated Bridge Construction	ABC
American Association of State Highway and Transportation Officials	AASHTO
American Society of Testing and Material	ASTM
American Welding Society	AWS
Area	A
Base Metal Tension Specimen	B
Base Metal Test Plate	BMP
Bend Specimen	BD
Center Line	CL
Charpy V-notch	CVN
Charpy V-Notch Absorbed Energy Regressed Transition Curve	Y, gc_i
Charpy V-Notch API model parameters	A, B, C, D
Charpy V-Notch MPM model parameters	a_1, a_2, a_3, a_4
Charpy V-Notch MPM model squared residual	r_i^2
Charpy V-Notch Number of Tested Specimens	n
Charpy V-Notch Test Absorbed Energy	Y_i, v_i
Charpy V-Notch Test Testing Temperature	T_i
Crosshead Speed for Tension Testing	CS
CVN Lateral Expansion Measurements	L_{ex}
CVN Lateral Expansion Measurement parameters	A1, A2, A3, A4
CVN Specimen Orientation with Notch Aligned to DOR	TL
CVN Specimen Orientation with Notch Transverse to DOR	LT
Data Acquisition System	DAQ
Direction of Roll	DOR
Electroslag Welding	ESW
Federal Highway Administration	FHWA
Flux-cored Arc Welding	FCAW
Fusion Line	FL
Gas Metal Arc Welding	GMAW
Guided Bent Test Jig	BTJ
Heat Affected Zone	HAZ

High Performance Steel …………………………………………………………….HPS
Macroetch Specimen ………………………………………………………………… M
Narrow Gap Improved Electroslag Welding …………………………………… ESW-NG
Not Applicable ……………………………………………………………………….. N/A
Orientation of Specimen Aligned with DOR …………………………………………… L
Orientation of Specimen Transverse to DOR ...………………………………………… T
Reduced Round Tension Specimen …………………………………………………… RR
Reduced Section Tension Specimen ……………………………………………………. S
Round Tension Specimen ……………………………………………………………… R
Shielded Metal Arc Welding …………………………………………………... SMAW
Specimen Diameter for Tension Testing …………………………….…...... D_1, D_2, d1, d2
Specimen Width for Tension Testing ………………………………………………….. W
Static Yield Stress ……………………………………………………………………. SYS
Structural Stability Research Council ……………………………………………… SSRC
Submerged Arc Welding ……………………………………………………………. SAW
Test Plate A ……………………………………………………………………………. PA
Test Plate B ……………………………………………………………………………. PB
Thickness for Tension Testing ……….……………………………………………. T, t_1, t_2, t_3
Vickers Hardness Diagonal Measurement …………………………………………. d1, d2
Vickers Hardness Force ………………………………………………………………… P
Vickers Hardness Value …………………………………………………………….…… HV
Welding Procedure Specifications ………………………………………………….. WPS
Weld Tension Specimen ……………………………………………………………….. W

ABSTRACT

EXPERIMENTAL INVESTIGATION OF NARROW GAP IMPROVED ELECTROSLAG WELDING FOR HPS 70W HIGH-PERFORMANCE STEEL

Andrei Denes, M.S.

George Mason University, 2017

Thesis Director: Dr. Girum Urgessa

This thesis presents an experimental investigation of the Narrow Gap Improved Electroslag (ESW-NG) welding method when applied on HPS 70W high-performance steel and the associated tests required for qualification of the welding method under the American Welding Society D1.5:2010 (AWS) bridge welding code. The welding process is studied in detail through testing of two weld qualification plates and the base metal. Tension testing, toughness testing and hardness testing of specimens with various geometries and orientations within the two plates and the base metal were performed, in addition to the tests required for weld qualification. The testing methods and specimens used are thoroughly described and their significance is explained. The experimental results achieved the objective of determining and characterizing the mechanical properties of HPS 70W high-performance steel when welded with ESW-NG. However, the research revealed that ESW-NG cannot be pre-qualified for HPS 70W per the AWS code at this time due to the failure of the all-weld tension specimens.

CHAPTER 1: INTRODUCTION

1.1. Motivation

Over the years, the size and complexity of infrastructure systems have steadily increased due to the increase in global population. Therefore, it is fitting that the components of our infrastructure systems evolve and adapt to better suit this increase in global demand for communication, energy or transportation. While the construction industry still relies on many proven, conventional means of delivery of services and products, progress and innovation are welcomed and they are useful means of enhancing the final product.

In the bridge construction industry specifically, a new philosophy to build and rehabilitate bridges has been conceived and pioneered by The Federal Highway Administration (FHWA), in order to reduce the time required for construction or repair of bridges. This method is known as Accelerated Bridge Construction (ABC) and it involves the use of "innovative planning, design, materials, and construction methods" in order to reduce the construction time required to construct new or replace existing bridge structures while keeping the project safe and cost-effective (Culmo, 2011).

Steel bridges are preferred in ABC because structural members can potentially leave fabrication shops and can be installed on the same day. This is in contrast to concrete structural members that must be joined via cast in place grout or concrete joint systems that require extended curing time, prolonging the impact of construction on traffic systems.

Steel structural members are typically formed from molten steel, which is cast into the near-net shape of the final cross section and then hot-rolled in the steel mill to the required geometry. These standard shapes are commonly used in building and bridge construction; however, due to the heavy loading supported by bridges, standard structural members are not adequate. For that reason, custom shapes built up from steel plates, which are designed to provide more strength, need to be used. In these instances, the plates have to be joined to create a homogenous structural member. Typically, this is achieved through welding of the plates. Currently the favored method of joining steel plates for bridges is Submerged Arc Welding (SAW), which is a time-consuming process. Descriptions of this welding process and other commonly used welding methods for structural steel are provided in the literature review.

The alternative to SAW and other commonly used arc welding processes is the Electroslag Welding (ESW) welding process. ESW is a single pass high deposition weld well suited for joining thicker materials. The method was widely used in the 1950’s and 1960’s. However, the original ESW method used at that time proved to be prone to defects and the weld metal experienced low toughness properties. FHWA improved the original ESW method and was able to mitigate the initial problems observed. The improved ESW method is referred to as Narrow Gap Improved Electroslag Welding (ESW-NG). A detailed description of the process, its history and applications are presented in the literature review.

As of today, the ESW-NG method is not pre-qualified by the American Welding Society (AWS) and the American Association of State Highway and Transportation Officials (AASHTO) for use on high-performance steel above yield strength of 50 ksi. The use of high-performance steel is significantly increasing in the bridge construction industry. However, there is sparse research available on the use of ESW-NG on high-performance steel. For this reason, the weld has a low adoption rate in the industry. Adopting ESW-NG as a viable joining method for thick steel plates in design guidelines is expected to improve productivity, reduce costs and dramatically reduce the time required to produce, connect and even repair large steel members.

This thesis presents experimental investigations on the efficacy of using ESW-NG for joining HPS 70W high-performance steel structural members. Results from this thesis are expected to be invaluable in informing relevant code writing committees in AWS and AASHTO when provisions to pre-qualify the ESW-NG process are contemplated.

1.2. Objective and Scope of the Experimental Investigation

The experimental investigation set out to find the material properties of the ESW-NG weld when performed on high-performance steel and prequalify the weld for use under AWS. To accomplish these objectives, a series of tests were performed using AWS qualification requirements as a guide.

The tests were performed following standardized methods which insure repeatability. The results were thoroughly catalogued and analyzed in order to provide meaningful information on strength, toughness and hardness performance of ESW-NG on HPS 70W high-performance steel. This data can further establish the possibility of using

ESW-NG on fracture critical members and can determine the temperature zones listed in AASHTO in which it may be used. Prequalification under AWS would ensure a higher rate of adoption of the welding process in the construction industry. Implementation of ESW-NG over submerged arc welding as a leading welding method would reduce costs and increase productivity.

In order to achieve the stated objectives, two welded plates were commissioned and 442 individual specimens, including spares, were manufactured by the Federal Highway Administration. The specimens were tested at the Turner Fairbanks Research Center in Mclean, VA using both destructive and non-destructive testing methods. A statistically meaningful number of specimens were tested for most of the testing methods. Where this was not achieved, specimens were tested to lay the foundation for future investigations.

1.3. Thesis Organization

The thesis is organized in five chapters and an appendix. Chapter 1 presents a short introduction and motivation of the research problem, and the scope and desired objectives of the investigation.

Chapter 2 presents a literature review of commonly available bridge welding methods, a detailed description of the ESW-NG method, historical research efforts surrounding the use of ESW-NG in steel members, and basic summary of interpreting experimental results used to determine toughness of specimens.

Chapter 3 presents the experimental testing program. Welding Procedure Specifications (WPS), a detailed description of two welded plates used in this research, and the associated testing methods are included. The testing methods include macroetch, side and face-bend testing, tension testing (both reduced and standard sections), toughness testing, and hardness testing on the base metal and welded plates.

The results from the experimental testing are presented in Chapter 4. Observations, trends, and discussions are provided for results obtained from each testing method.

Chapter 5 presents conclusions, limitations of the research and recommendations for future work.

The Appendix presents the data that was not reported in Chapters 3 and 4 from the tension testing, toughness testing and hardness. The data is organized in tables based on the specific test type and method.

CHAPTER 2: LITERATURE REVIEW

2.1. Bridge Construction Welding Methods

There are many types of welding procedures in use today, but not all of them are suitable for safely joining structural steel members. Commonly used welding methods and brief descriptions of each welding procedure are presented below. These procedures are: Shielded Metal Arc Welding (SMAW), Flux-cored Arc Welding (FCAW), Gas Metal Arc Welding (GMAW), Submerged Arc Welding (SAW), and Electroslag Welding (ESW).

The most well-known welding method is SMAW, commonly referred to as stick welding or manual welding. As shown in Figure 2.1, this welding process involves the use of electrodes covered in flux that strike an arc with the metal creating a puddle of molten filler material. The flux covers the weld and protects it from contamination and oxidation while the core of the electrodes is the filler material. This process is very versatile and widely used, but it has limitations. It is relatively costly and depends heavily on operator skills (Blodgett, Funderburk, Miller, & Quintana, 1999).In addition, because there is only so much material that can be filled at once, there is a need for multiple passes over one area to complete the weld. This proves to be time consuming and dramatically increases the likelihood of forming defects.

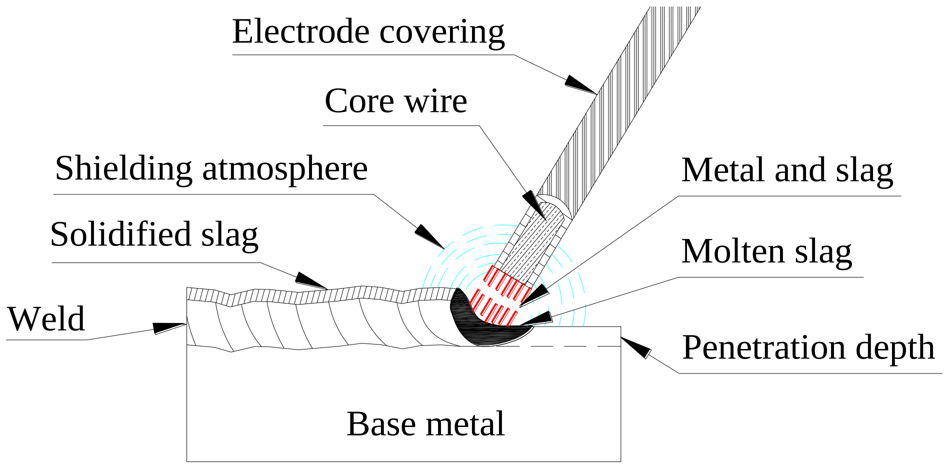

Figure 2.1. Shielded Metal Arc Welding

FCAW is another popular welding process for steel fabrication. As shown in Figure 2.2, FCAW is an automatic or semi-automatic process that uses an arc between a continuous filler metal electrode and the molten metal pool. The electrode for this type of welding is always tubular and contains a mixture of metallic powder and flux. This welding type has two major advantages over SMAW. The main advantage is that since the electrode is continuous, lengthy welds can be achieved without the need to stop and restart the welding process. Start and stops not only reduce productivity but also introduce potential discontinuities and defects in the weld. A second advantage of this welding process is that increased amperage can be used for increasing welding speed (Blodgett, Funderburk, Miller, & Quintana, 1999).

GMAW, also known as "MIG welding," is very similar to FCAW and while it is more popular than FCAW, it is rarely used in structural steel fabrication or erection because of its sensitivity to mill scale, rust and shielding loss. GMAW, as the name entails, uses gas to protect the weld from contamination. The main difference between FCAW and GMAW is that the latter leaves almost no slag and uses a solid (metal) cored electrode.

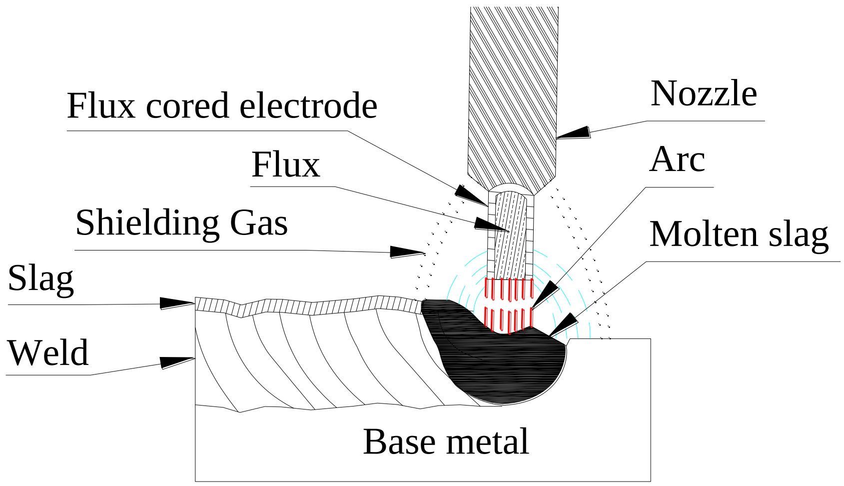

Figure 2.2. Flux Cored Arc Welding

As shown in Figure 2.3, SAW differs from the other arc welding processes because the arc stays submerged under a layer of flux that protects the weld from contaminations and provides optimal conditions for the weld. Due to the placement of the flux, the actual welding process cannot be observed, requiring the use of automated processes to achieve high quality welds. This welding procedure is used extensively in the industry due its high deposition rates. Another disadvantage, in contrast to the welding procedures presented before, is that the weld can only be performed horizontally due to the granular nature of the flux (Blodgett, Funderburk, Miller, & Quintana, 1999).

However, SAW is still widely used in fabricating structural steel plates and shapes regardless of its aforementioned disadvantages.

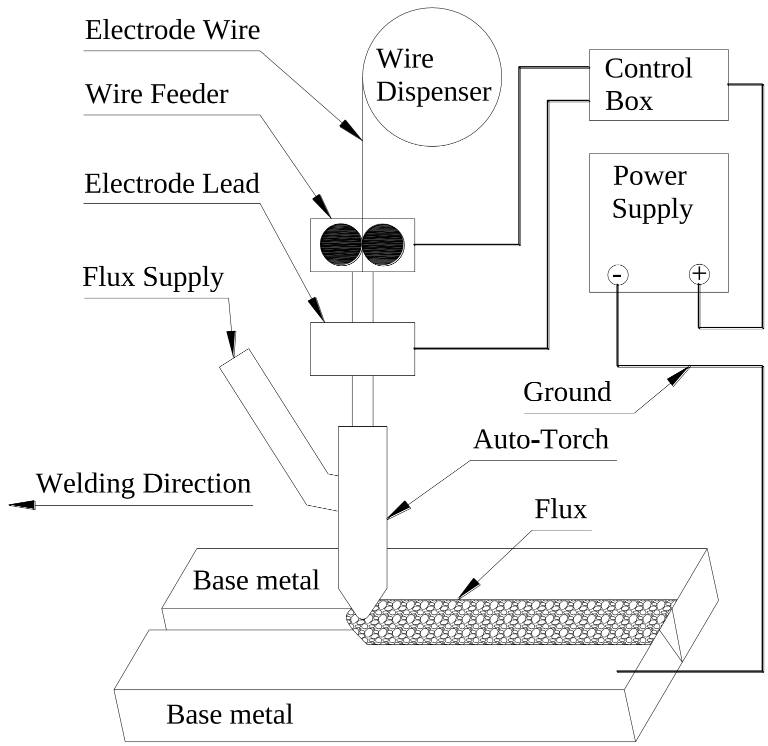

Figure 2.3. Submerged Arc Welding

ESW is a single pass vertical up high deposition weld that is well suited for joining thicker materials. Narrow Gap Improved - Electroslag Weld (ESW-NG) is an improved method of generating ESW welds. An in-depth description of the process, its history and applications are presented in section 2.2 due to the focus of this thesis on the efficacy of ESW-NG for high-performance steel applications.

It is very important to note that the welding methods widely used for joining structural steel involve arc welding and they require special preparation of the base metal at the joint before welding. In general, for a successful weld the joint requires a certain geometry and pre-heating before creating the weld. The use of ESW-NG is advantageous because it does not require any pre-heating and the geometry at union is straight.

2.2. Summary of Electroslag Welding – Narrow Gap (ESW-NG)

ESW is considered to be the most productive method of welding thick parts. While all the other methods presented before have limitations to the depth and deposition rate they can achieve in a single pass, ESW can successfully weld, in theory, any thickness of material over ¾ inches in a single pass. The process was developed at the Paton Institute of Electric Welding in Kiev in the early 1950s. In 1959, the first ESW unit was introduced in the United States (American Welding Society, 2009). After the process was introduced in the US, it was widely used on bridges during the 1960s and 1970s mainly due to its high productivity (Federal Highway Administration, 1996). However, certain welding problems began to surface in the 1970s. ESW welds at that time consistently resulted in welds with defects and diminished toughness properties (Bennett, Swanson, & Linzell, 2009). These issues culminated with the discovery of a 10 foot long crack on the Neville Island Bridge on I-79 in western Pennsylvania in the winter of 1977. This prompted FHWA to prohibit the use of ESW on tension members, effectively eliminating the use of ESW on bridge construction (Verma, 2001). In the 1980s extensive research was done to improve ESW through the efforts of FHWA. The method was improved by reducing the gap between the components being joined and adjusting other welding parameters, such as the electrode size and material and current input, resulting in the Narrow Gap Improved Electroslag Welding (ESW-NG) welding process. AWS/AASHTO D1.5:2010 both refer to the Narrow Gap Improved method as ESW-NG. ESW-NG has comparable mechanical properties to arc welding methods while eliminating the possibility for weld cracking (Chambers, Electroslag Welding Facts for Structural Engineers, 2015).

An ESW weld, as opposed to the other welding procedures presented in section 2.1, is done in the vertical position. This presents a unique set of challenges to the weld execution. In order to be able to perform the weld, the two metal plates to be joined are positioned in a vertical position with at least ¾ inch of spacing in between the root opening. Figure 2.4 presents a typical set-up of parts required to produce an ESW-NG weld.

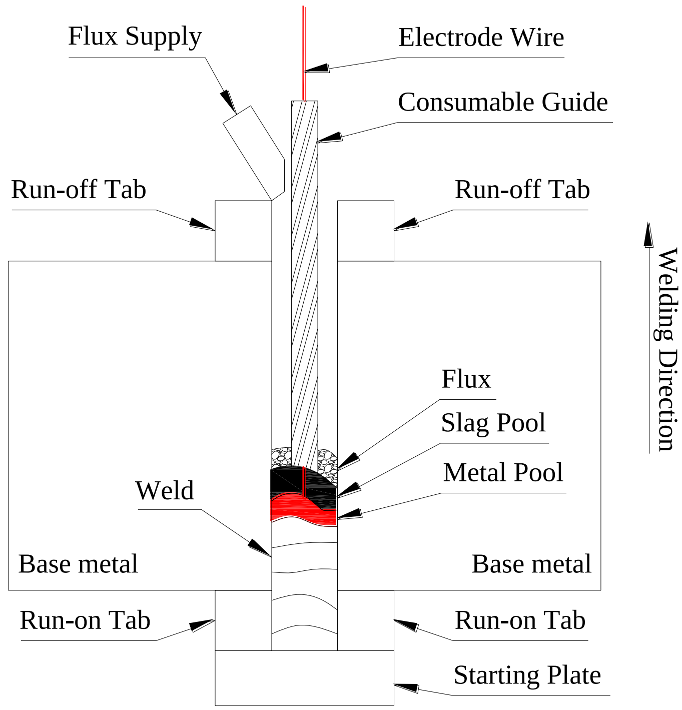

Figure 2.4. ESW-NG Weld Set-up

A receptacle, called sump, for the molten slag and metal pool is welded to the bottom of the plates to be joined. The sump consists of a starting plate, the base of the receptacle, and two more plates, known as run-on tabs to serve as sides to the sump. In order to terminate the weld beyond the joined parts, two more plates are added at the top, known as run-off tabs. Electrode wires encased in a consumable guide are positioned inside the root opening. Retaining shoes are placed on the exposed sides of the root opening, along the face of the plates to be joined, to enclose the weld area. In order to initiate the process, an arc is produced between the electrode and the sump. At the same time flux is introduced through a metered flux feeder. Although the original reaction is similar to that of submerged arc welding, as the flux and consumable guides melt the reaction changes making this a non-arc welding procedure. The flux creates a molten slag pool and the electrode wire or wires create a molten weld pool. The consumable guide also adds metal to the molten weld pool. Following the initial arc required to start the weld, the slag conducts the current from the electrode to the steel plates. The molten weld pool is comprised of added metal and around fifty percent molten base metal. To prevent short-circuiting between the consumable guide and the plates, insulators are used. As the insulators melt, they also add to the molten slag pool that covers and protects the weld. The electrode wires are designed to meet the weld metal composition and properties in order to reduce sensitivity to hot cracking and increase productivity. The shape of the guide is designed to distribute heat more evenly and reduce the possibility of incomplete fusion. After weld completion the retaining shoes, the sump and the run-off tabs are removed and the weld is ground flush with the steel (Verma, 2001).

Figure 2.5 presents the typical machinery and tools set-up required to produce an ESW-NG weld. A disadvantage of early ESW welds was that the process was controlled through human interaction, which resulted in inconsistencies within the weld. During the early ESW welding process the correct ratio of wire, flux and electric current could not be achieved due to the lack of automated control. This was rectified in ESW-NG by using a control box as shown in Figure 2.5 that controls the whole welding process. The weld, after the initial set-up of the plates, is performed by applying current to the electrode wire from a controllable power source. Ground wires are connected to the plates allowing for the current flows from the power supply to the electrodes passing through the plates. The electrode wire is incased into the consumable guide, which is held in place by a guide holder. A wire feeder equipped with a wire meter is placed above the guide holder. The wire feeder receives material from a wire dispenser. At the same time, flux is fed to the weld via the flux feeder. The control box receives data from the power source, wire feeder and flux feeder adjusting continuously for an optimal relationship between them. It has been found that constant potential power supplies with variable balance through AC power on a square wave are the ideal means of performing NGI-ESW welds (Chambers & Medlock, 2015). Water cooled retaining shoes encase the outside of the weld and a data acquisition (DAQ) system is used to record the parameters of the weld.

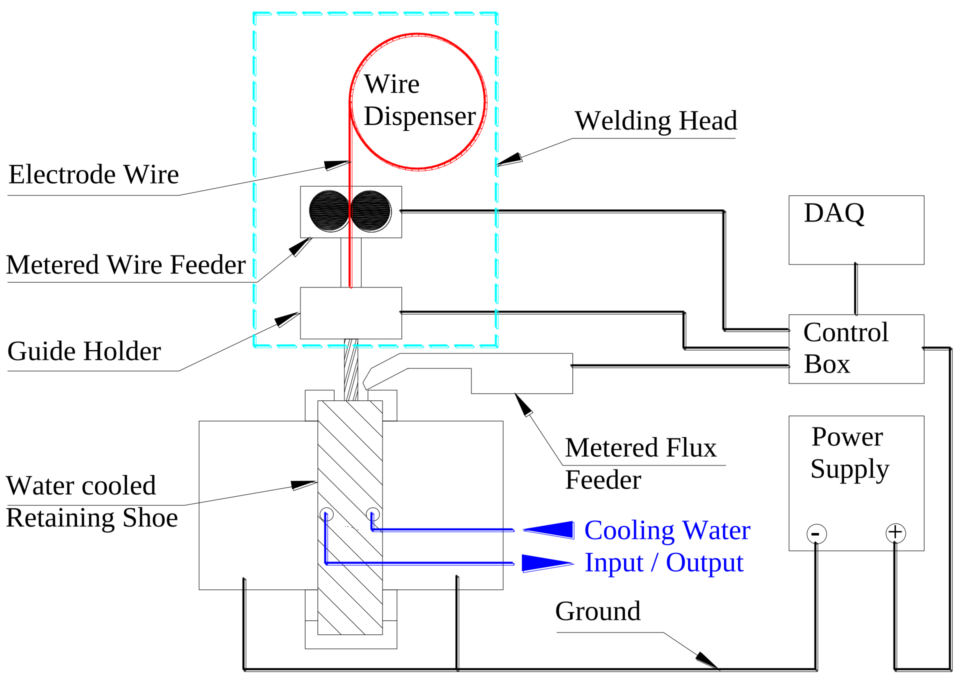

Figure 2.5. ESW-NG Weld Equipment

As mentioned before, one of the main differences between ESW and ESW-NG is the size of the root opening. A two-inch plate would typically have a 1¼-inch groove opening (root opening) for the ESW welding process but only a ¾-inch root opening for the ESW-NG process (Chambers & Medlock, Electroslag Welding Facts for Structural Engineers , 2015). A minimum of ¾-inch gap is needed for sufficient slag bath size, good slag circulation and clearance for the consumable guide. A root opening that is too large, besides causing economical issues from the wasted filler material, can also cause a reduction in the form factor and prevent good fusion (American Welding Society, 2009). The reduced size of the root opening in ESW-NG forced a redesign of the consumable guide making it winged, whereas in ESW the consumable guide was round. The round consumable guide consistently resulted in welds with incomplete fusion at the edges. A winged consumable guide spreads much more evenly with the generated heat eliminating the problem. Figure 2.6 presents a schematic of the two consumable guides.

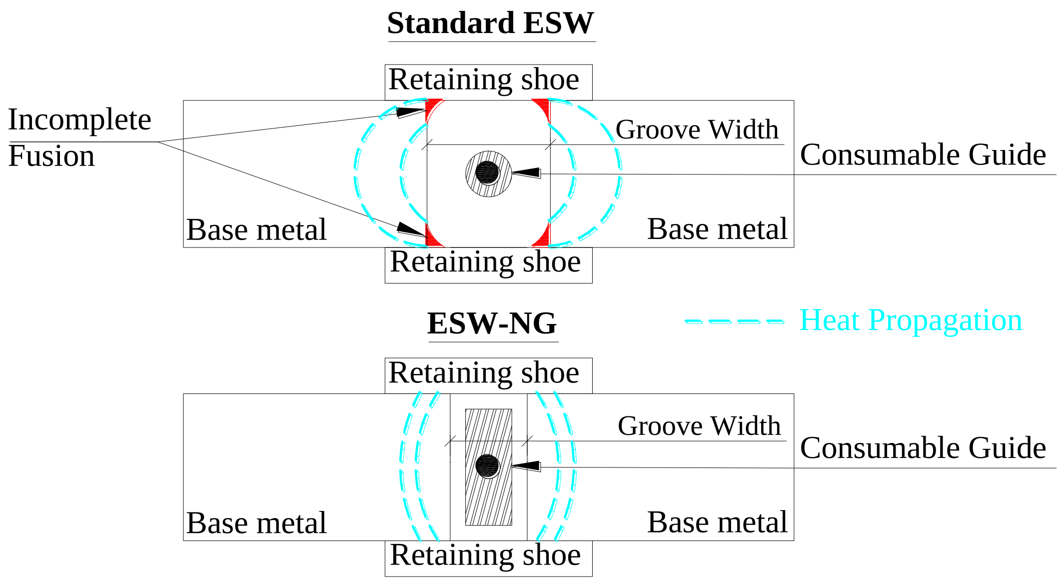

Figure 2.6. NGI-ESW vs ESW consumable tube section

In summary, the main advantages of ESW-NG include a very high deposition rate, an ability to weld very thick materials (up to 36-inch welds have been reported), not requiring preheating of surfaces, high quality weld deposit, minimum preparation of joining parts, automated process, low flux consumption, and minimum welding time (American Welding Society, 2009).

The ESW-NG process has its own limitations. Currently, it is only usable on carbon and low alloy steels and some stainless steels. In addition, vertical positioning of the weld is required. Once welding has started, it must be carried out to completion; otherwise defects will form. The welding method cannot be used on materials thinner than ¾ inches and it is very difficult to weld complex material shapes such as “I” shapes (American Welding Society, 2009).

2.3. Previous Research Efforts on the Use of ESW and ESW-NG

Since the bridge failures due to ESW in the late 1970s, it has been known that the toughness capacity of traditional ESW welds is unacceptable for bridge design using AASHTO and AWS codes. While AASHTO requires a minimum Charpy V-notch (CVN) toughness of 20 J (15 ft-lbs) on non-fracture critical members, ESW welds consistently received values of 3–4 J (2.2-3 ft-lbs) on tests, which is well below the minimum requirements. Starting in the 1980s, FHWA recognizing the advantages of ESW, commissioned new research to improve the process so that it could be once again used on bridge members. The result of this research was the ESW-NG weld. The main improvement from a structural viewpoint was the increased CVN toughness of the welded joints, as well as the increased welding speed (Federal Highway Administration, 1996). In 1996, FHWA conducted tests meant to qualify and promote the use of ESW-NG on joining A36 and A588 steels.

A major focus of FHWA's effort was to improve CVN toughness because the parameter correlates directly with the weld structure and quality. The agency was able to achieve its goals by optimizing the welding procedure and defining relationships between the welding process and the microstructure of the weld. Five-hundred CVN specimens in over 200 experimental conditions were tested in order to determine the optimum process parameters (Federal Highway Administration, 1996).

The strength of a weld, if done by the proper design codes, is greater than the joined material. This is why usually the weakest part of a joining process will generally be found either at the fusion line (FL) or in the heat affected zone (HAZ). Although quantification of HAZ toughness was not the principal objective of the FHWA study, tests were conducted on a number of CVN specimens with the notch at designated distances from the FL within the HAZ. AWS does not require testing within the HAZ, neither does it provide limits for toughness, except with-in the weld metal. As a result, toughness was compared to the toughness of the base metal because the HAZ is outside of the weld nugget, effectively a part of the base metal. Specimens were tested at 1-mm (0.04 in) increments starting at the FL. It was observed that using ESW-NG, even with the reduced CVN toughness in the HAZ, resulted in values that were far above the values obtained in toughness tests done previously on the core material of traditional ESW welds.

Through its research, FHWA also managed to increase the speed of the ESW process. This was achieved by increasing the welding current, decreasing the root opening, using tubular powder-cored wire and using a new, special consumable guide (Federal Highway Administration, 1996). For ESW-NG, the current was effectively doubled from 550–600 A to 1000–1350 A. It was observed that the relationship between the current and heat input is non-linear and after a maximum value is attained, the heat input decreases. Heat input is an important variable of the weld as it controls the size of the HAZ; the lower the heat input, the smaller the HAZ. At the same time, a higher current increases the welding speed. (Federal Highway Administration, 1996).

Reducing the size of the root opening increases the welding speed and reduces the heat input as well. Root opening and heat input in this case are linearly related which means that reducing the gap actually reduces the heat input. Since a smaller root opening requires less material to fill, the speed of the weld also increases (Federal Highway Administration, 1996).

The use of a tubular wire and a special winged consumable guide allows for a more even distribution of the heat and a higher current to pass through. Two types of consumable guides were designed in order to accommodate different thickness of plates, these consumables represent the standard for ESW-NG today. Figure 2.7 presents the consumable guides developed by FHWA compared to the standard ESW consumable guides (Federal Highway Administration, 1996).

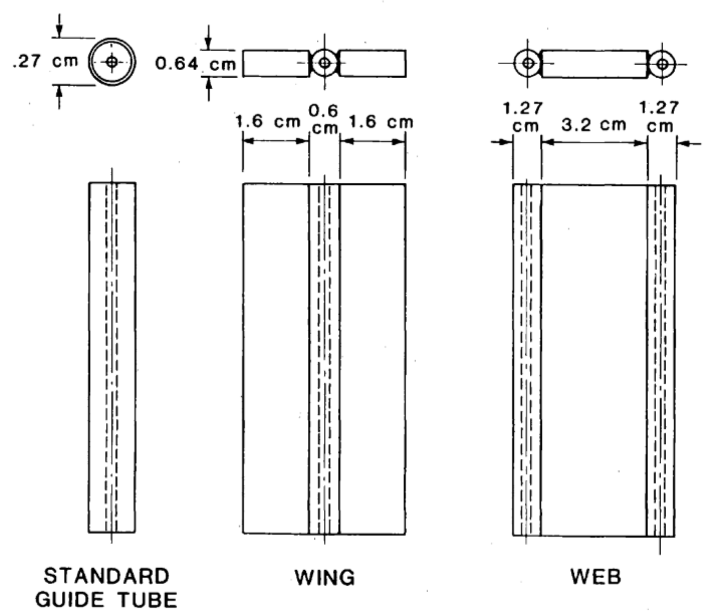

Figure 2.7. Consumable guides: Wing and Web design for NGI-ESW vs standard ESW (Federal Highway Administration, 1996)

The 1996 FHWA study concluded that ESW-NG is able to produce consistent and reliable welds with insignificant imperfections. ESW-NG welds were identified as a prime candidate for joining A36 and A588 steels for up to 3 in in thickness due to the high productivity and above toughness requirements set forth by AASHTO and AWS. Also, defects such as hot cracking which led to the I-79 bridge defect can be reliably detected using non-destructive methods, or simply be prevented by applying the weld properly.

Since 1996, structural steel members have evolved, making the conclusions of the prior FHWA study limited. This is due to the fact that the steels used in the prior FHWA study (A36 and A588) have been and are being replaced for bridge construction by lighter, stronger and more weldable high performance steel's such as HPS 70W. In 2005, under the sponsorship of the Ohio DOT and FHWA, a field and lab study was conducted to find the performance of HPS-485W, known today as HPS 70W, steels for bridge construction. Various connection types were also evaluated and a comparison of SAW versus ESW-NG fatigue performance was conducted (Swanson, Linzell, & Bennett, 2006).

HPS 70W steel is a weathering steel that satisfies AASHTO Zone 3 toughness requirements and has improved weldability. HPS 70W is produced by quenching and tempering (Q&T) or Thermal-Mechanical Controlled Processing (TMCP). The main difference between HPS 70W steel and previous grade 70 steels is in its chemical composition which allows for vastly improved fatigue and fracture characteristics and enhanced welding properties due to the reduced carbon content. This makes the steel less susceptible to hydrogen cracking and HAZ hardening (Federal Highway Administration, 2002).

In order to investigate the behavior of HPS-70W butt-welded joints under fatigue loading, Swanson et al. (2006) constructed ten specimens out of a welded plate. Five specimens were SAW welds and five were ESW-NG welds. Each specimen was subjected to fatigue loading consistent with the AASHTO fatigue life equation. All specimens reached a preset infinite fatigue lifecycle of 2.3 million cycles. Some of the specimens, two from each weld, were additionally tested for up to a cumulative of 5 million cycles. All specimens reached and surpassed their expected performance (Swanson, Linzell, & Bennett, 2006).

The above study concluded that HPS-70W welded butt-splices performed at least as good as similar connections created using SAW. Both types of weld showed performance far above the predicted fatigue life calculated from the AASHTO life equation. Based on these findings, the authors concluded that ESW-NG is an appropriate method for joining HPS-70W and should be included in the AWS D1.5 weld standard.

The study performed by FHWA on toughness properties of ESW-NG and the study conducted by Verma (2000) resulted in the rescinding of the 1977 moratorium banning ESW welds for bridge construction, provided that the improved ESW-NG method is used.

2.4. Curve Fitting for Charpy V-Notch Toughness Data

The theory behind standard testing methods, such as tension testing, is widely published and not repeated in this literature review. However, a description of curve fitting approaches for analyzing data obtained from the toughness testing was deemed important to be included here, as material toughness was one of the original issues with ESW and is required for AWS qualification.

Toughness properties of a material can be examined through multiple methods. A cost effective method of testing toughness for metallic materials is the Charpy V-Notch test (CVN). Test results from CVN testing are very important to structural engineers as they provide an accurate representation of a steel's brittle or ductile behavior at different temperatures. Steel is brittle at low temperatures and ductile at high temperature. Therefore, it is very important to recognize exactly where steel starts to exhibit ductile or brittle behavior, when the change from brittle to ductile behavior happens, and how quickly this change occurs. The temperature range where the transition occurs can be determined through regression. This change determines if the material is suited for the region where the design will be implemented. For an inherently brittle steel, application in a cold environment is prohibited by AASHTO. The relationship between temperature and absorbed energy can be accurately modeled graphically through a transition curve graph.

Due to the known properties of steel, it is expected that a transition curve will have a lower and upper shelf where the steel behaves brittle or ductile, respectively, and a "S" shaped portion in-between where the transition occurs. While there are many functions that can model a combination of rectilinear and curved behavior, a hyperbolic tangent function has been found to be the most suited for modeling toughness. Two models have emerged as useful means to establish the transition curve: The API and MPM model.

The API model is shown in Equation 2.1. The graphical interpretation of the equation is presented in Figure 2.8. The transition curve is modeled based on four parameters A, B, C and D. Each parameter is defined in the equations from Equation 2.2 to Equation 2.5. All parameters are only related to the absorbed energy Y_i and test temperature T_i. "Y" represents the curve and "n" represents the total number of tests (Yeager). This model does not use optimization and it creates a mirrored curve based on the median of the tested temperatures, inflection point D.

$$Y = A + B \tanh\left(\frac{T-D}{C}\right) \qquad \text{Equation (2-1)}$$

$$A = \frac{\Sigma_i Y_i}{n} \qquad \text{Equation (2-2)}$$

$$B = \frac{\max(Y_i) - \min(Y_i)}{2} \qquad \text{Equation (2-3)}$$

$$C = \frac{\max(T_i) - \min(T_i)}{2} \qquad \text{Equation (2-4)}$$

$$D = median(T_i) \qquad \text{Equation (2-5)}$$

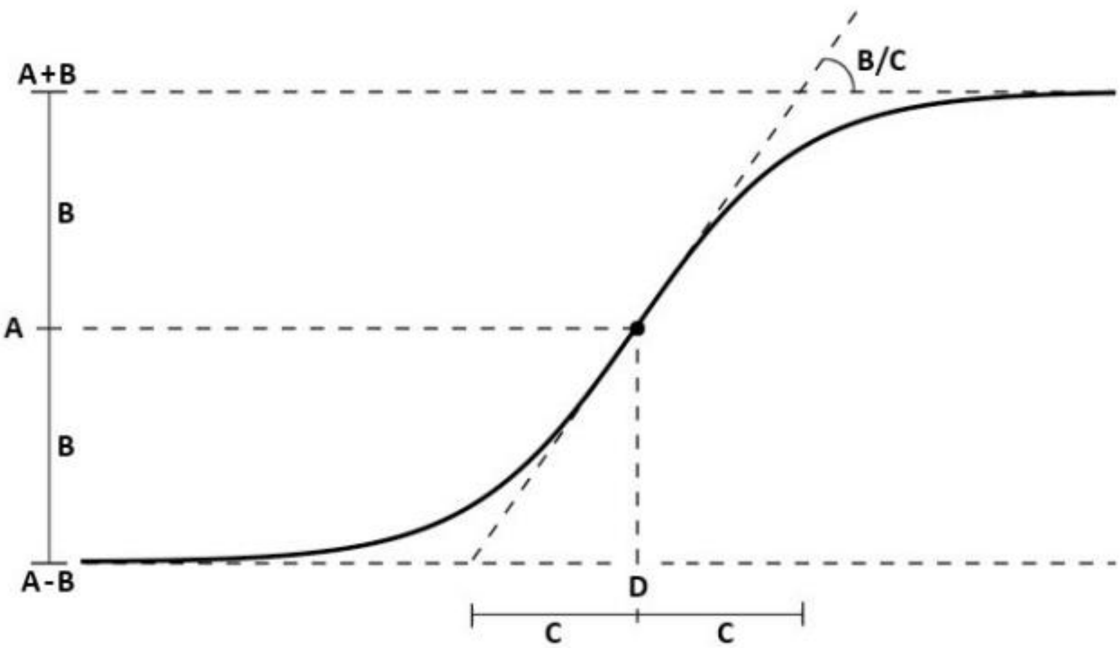

Figure 2.8. Graphical representation of the API function (Yeager)

The MPM model, used by MPM Technologies in their CharpyFit™ software is a model based on optimization. An optimization software is required for application of this method. For the purposes of this experimental research Solver for Excel was used. In Figure 2.9, a typical snapshot of the excel window is shown. The formula used for this model is presented in Equation 2.6. In this equation T_i is the tested temperature, Y is the function, and the other variables are explained in the following paragraphs. The objective of the optimization is to reach the lowest possible squared residual, r_i^2, as shown in Equation 2.7. This is achieved by manipulating variables a1 through a4. It can be observed that in Equation 2.7, a1 must be positive as it represents the lower shelf value of the energy and energy cannot be negative. The variable a2 is the upper shelf energy, a3 is the point of inflection and a4 is the temperature range of transition. Equation 2.8 shows how r_i^2 is calculated. Here gc_i is the guessed curve, the result, and v_i is the actual recorded result of the CVN test. The graphical representation of the function and its parameters is presented in Figure 2.10.

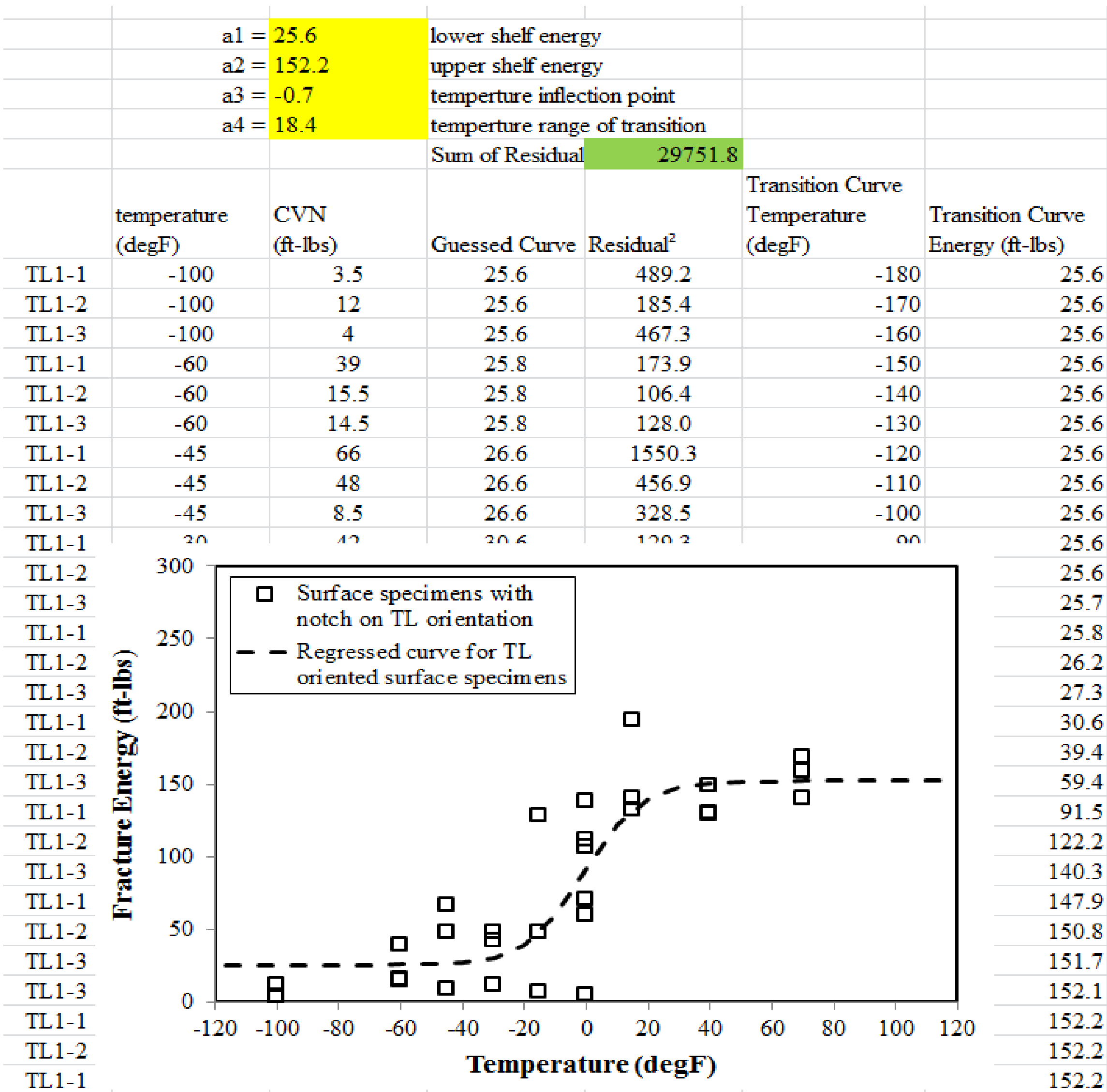

	a1 =	25.6	lower shelf energy			
	a2 =	152.2	upper shelf energy			
	a3 =	-0.7	temperture inflection point			
	a4 =	18.4	temperture range of transition			
			Sum of Residual	29751.8		
	temperature (degF)	CVN (ft-lbs)	Guessed Curve	Residual^2	Transition Curve Temperature (degF)	Transition Curve Energy (ft-lbs)
TL1-1	-100	3.5	25.6	489.2	-180	25.6
TL1-2	-100	12	25.6	185.4	-170	25.6
TL1-3	-100	4	25.6	467.3	-160	25.6
TL1-1	-60	39	25.8	173.9	-150	25.6
TL1-2	-60	15.5	25.8	106.4	-140	25.6
TL1-3	-60	14.5	25.8	128.0	-130	25.6
TL1-1	-45	66	26.6	1550.3	-120	25.6
TL1-2	-45	48	26.6	456.9	-110	25.6
TL1-3	-45	8.5	26.6	328.5	-100	25.6
TL1-1						25.6
TL1-2						25.6
TL1-3						25.7
TL1-1						25.8
TL1-2						26.2
TL1-3						27.3
TL1-1						30.6
TL1-2						39.4
TL1-3						59.4
TL1-1						91.5
TL1-2						122.2
TL1-3						140.3
TL1-1						147.9
TL1-2						150.8
TL1-3						151.7
TL1-3						152.1
TL1-1						152.2
TL1-2						152.2
TL1-1						152.2

Figure 2.9. Optimization method snapshot.

$$Y = \frac{a_1}{2}\left[1 - \tanh\left(\frac{T_i - a_3}{a_4}\right)\right] + \frac{a_2}{2}\left[1 + \tanh\left(\frac{T_i - a_3}{a_4}\right)\right]$$

Equation (2-6)

$$objective = \min_{a_1 \geq 0} \sum_{i=1}^{n} r_i^2$$ ` Equation (2-7)

$$r_i^2 = (gc_i - v_i)^2$$ Equation (2-8)

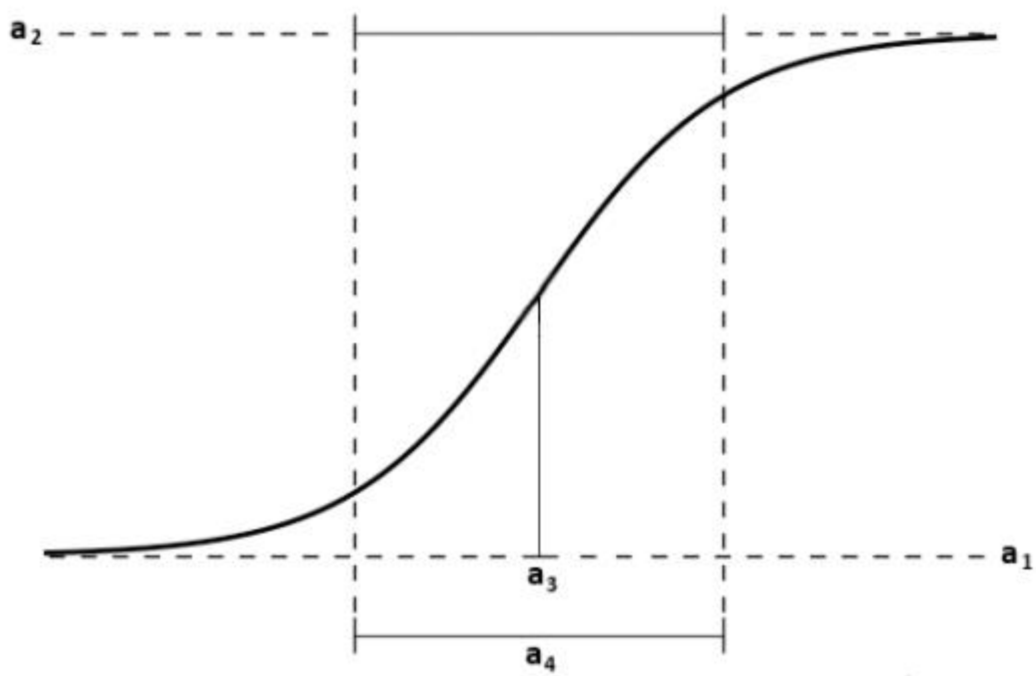

Figure 2.10. Graphical representation of the MPM model (Yeager)

A comparison between MPM and API was performed on the base metal plate (BMP) toughness testing results. The two methods were used to represent the data collected from each of the four types of specimens tested on BMP. The results are presented in Figure 2.11 through Figure 2.14.

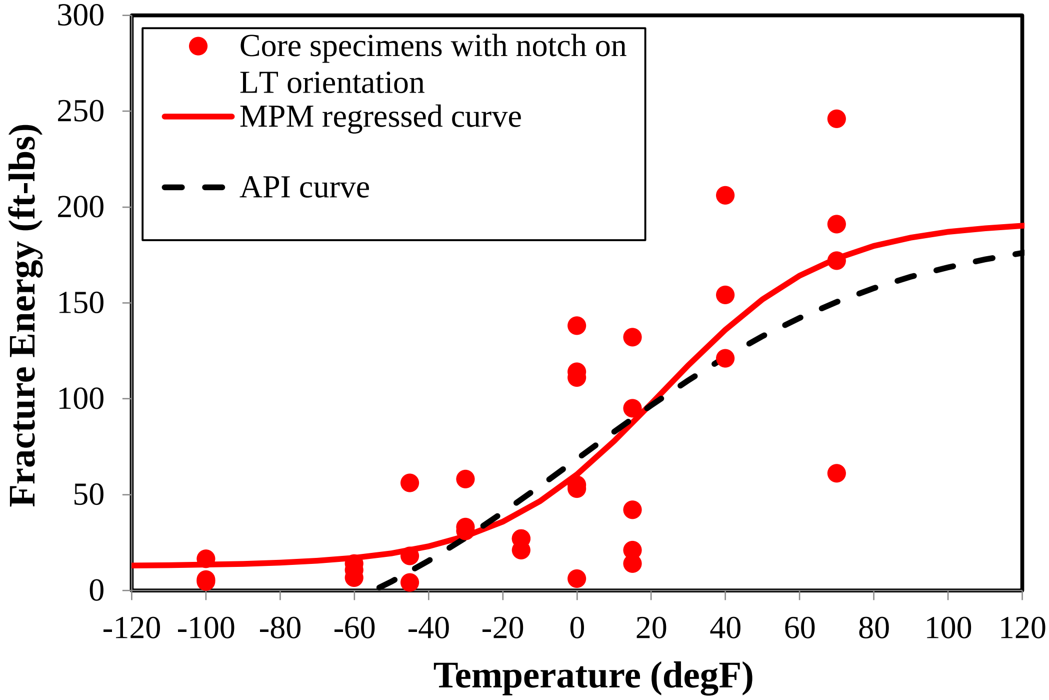

Figure 2.11. Best fit curves from LT Core data

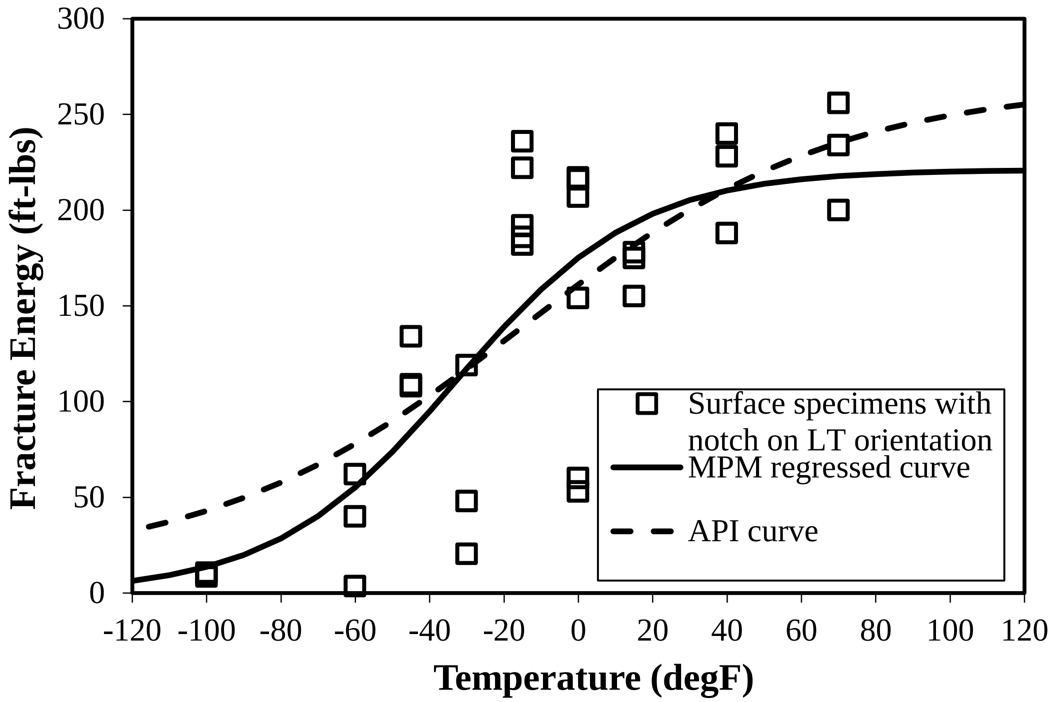

Figure 2.12. Best fit curves from LT Surface data

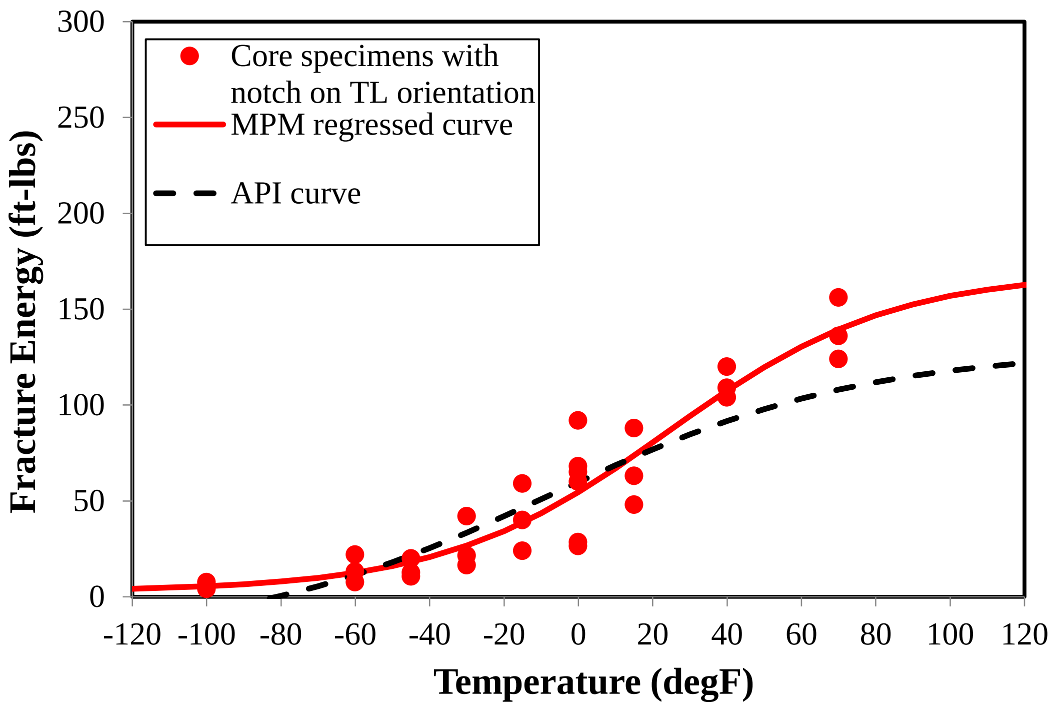

Figure 2.13. Best fit curves from TL Core data

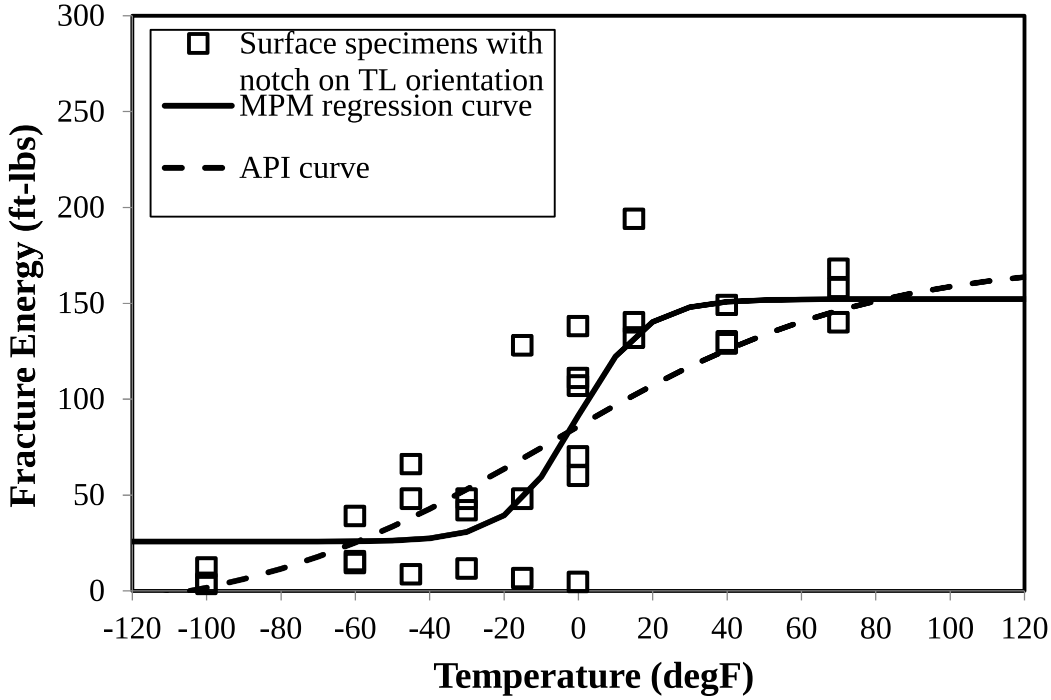

Figure 2.14. Best fit curves from TL Surface data

The comparison yielded that MPM is more accurate in portraying the transition curve for BMP. Due to the nature of API, the inflection point (A,D) from Figure 2.8 will always be at the median of the temperature and the average of the toughness values. As such, for the model to work it is imperative to collect the same number of specimens at every temperature and test over a temperature gradient symmetrical to D. The data collected from BMP did not follow these restrictions, but rather followed one of the requirements set by this experimental program which is to identify behavior at lower temperatures. In the case of the data collected from BMP, the API model shows negative energy for the lower shelf on all the specimen types due to the higher number specimens tested at lower temperatures so it does not portray an accurate transition curve. Since MPM uses optimization by minimizing the error between the guessed curve and the actual data, it can accurately identify or extrapolate the transition curve parameters with less samples and no symmetry requirements. For these reasons, the decision made in thesis is to use the MPM method for predicting all transition curves of the CVN results.

2.5. Summary of Literature Review

In the literature review, a brief description of commonly used welding methods was presented, followed by a detailed description of the ESW welding method. ESW is a highly productive welding method which is susceptible to toughness issues. Previous research sponsored by FHWA analyzed the problems in depth and provided an improved welding method, ESW-NG. However, the previous FHWA research was focused on the steel in use at that time (Grade 50 or lower) and as such only those types of steels are pre-qualified for ESW-NG welding in AWS.

In order to quantify the toughness properties of ESW-NG when performed on HPS 70W steel, two modeling methods were discussed. These modeling methods transform the data obtained from CVN testing into transition curves displaying the lower and upper shelf energies, and the transition region. The literature review substantiated the rationale for choosing the MPM method. This resulted in a lesser number of CVN specimens required in the testing program described in chapter 3.

ESW-NG requires a reduced quantity of consumables, virtually no surface preparation and can produce a weld in one pass.

Hence, adoption of ESW-NG over SAW as the leading method for welding thick steel parts would result in a significant increase in productivity and great cost savings.

CHAPTER 3: EXPERIMENTAL PROGRAM

A series of tests was performed in order to determine mechanical and material properties of the ESW-NG weld and HPS 70W base metal. For these tests, the provisions of AWS D1.5 were used as a guideline. These provisions must be followed to qualify a welding procedure for use in bridge construction. Chapter 5 Part A of AWS details the requirements for qualification of the Welding Procedure Specifications (WPS), while Part B presents the requirements for qualification of welding personnel. The requirements for welding personnel are not covered under the scope of this thesis. Therefore, Part B is not investigated. While the majority of the tests performed in support of this thesis are based on Part A of the AWS requirements, the testing program has been expanded beyond the scope of the AWS prequalification in order to build on FHWA's past research on ESW-NG. This chapter presents the standard testing methods used for weld qualification as stipulated in the AWS code and the additional tests conducted by the research program supporting this thesis.

3.1. Experimental Program Overview

A wide array of tests was performed under this experimental program. The testing was performed on two HPS 70W plates joined with the ESW-NG welding method and one HPS 70W virgin base metal plate from the same run of the mill. A detailed description of the tested plates, their properties and the tests performed is presented in the following subchapters.

The test specimens were sampled to maximize their number and gather the largest possible amount of data. Where possible, spare and extra specimens were manufactured. 1 shows the number of specimens manufactured versus the number of specimens tested by type. A detailed description of the type of specimen, its significance and testing method is provided further in this chapter.

Table 3.1. Total specimen count by type.

Test Type	Manufactured	Tested
Macroetch	7	7
Hardness	7	7
Sidebend	6	6
Facebend	4	4
Tension	70	40
Toughness	348	325
TOTAL	**442**	**389**

3.2. AWS Welding Procedure Specifications for Qualification Testing

For weld qualification, an array of tests must be performed on a qualification welded plate. The code requires non-destructive tests, mechanical tests and etching of test welds to be performed on the joined plate and base metal. The focus of this research is to determine mechanical and material properties of the weld and base metal. As such the mechanical and etching test’s will be detailed in the following paragraphs. The required tests by the AWS code are presented in Table 3.2. The orientation of each specimen is presented with respect to the direction of roll (DOR) of the base metal. All specimens aligned to DOR were transverse to the weld and were designated by the orientation “L”. The transverse to DOR specimens that were aligned with the weld were designated “T”. Figure 3.1 presents the orientation layout with respect to a typical WPS plate.

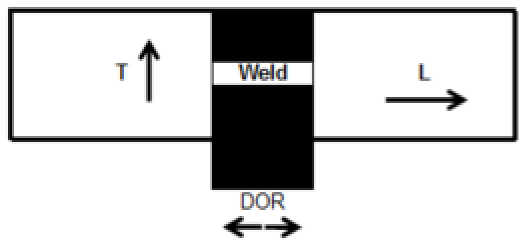

Figure 3.1. Schematic of the specimen orientation designations.

Table 3.2. Code required specimens for qualification.

Type	Count	Depth	Orientation
Macroetch	3	-	T
Sidebend	4	-	T
Reduced Section Tension	2	-	T
CVN at center of weld	8	Core	T
Round Tension, all weld	1	Core	L

The location of each test specimen must follow the guidelines laid out in Figure 3.2. This figure presents a minimum length of the standard test plate as well as the specimen location on the plate per AWS for qualification purposes. In order to mitigate start-stop issues, a portion of the test plate on both the bottom and top is discarded and not used as test specimen. Required macroetch, sidebend and reduced section tension are positioned transverse to the weld in a symmetrical setup with respect to the vertical center of the plate. The Round Tension all weld metal and the Charpy V-Notch (CVN) test specimens are placed close to the vertical center, where the weld is most consistent.

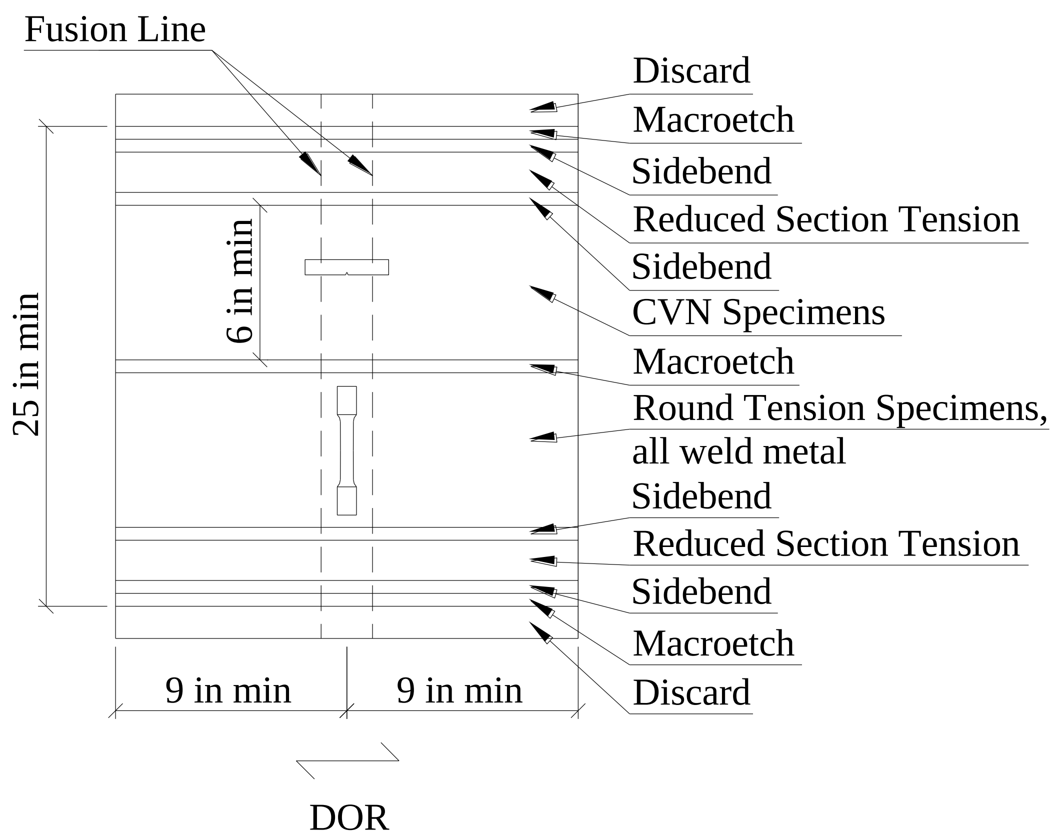

Figure 3.2. Location of required test samples per AWS D1.5 2010

3.3. Supplemental Testing for Mechanical Properties Assessment

In addition to the required testing to qualify the WPS, several auxiliary tests were performed as part of this research. The impetus is to provide an extensive assessment of the properties of the weld and the heat-affected zone (HAZ). The location of the supplemental test specimens was chosen so that there will be a minimal impact on the overall shape of the WPS test plate and the location of the required tests for qualification.

The auxiliary tests performed on the WPS testing plates are longitudinal macroetch, hardness, face-bend, CVN and tension tests. On the base metal, similar hardness and tension tests were performed.

3.4. Welded Testing Plates

In order to investigate the properties of the ESW-NG weld on HPS 70W (HPS 485W) steel, a 72 in long WPS plate was proposed. The WPS plate was commissioned from a contractor, which manufactured it at its own shop. During welding of the steel, the wire feeder jammed approximately 18 in into the process, effectively stopping the welding process at around 23 in from the sump. An additional issue was also noticed during the welding process. The electrical ground was only in contact with one of the plates resulting in a much higher heat input on that side of the weld. To mitigate these issues, a “start/stop” was installed at this point and the welding was restarted. This was deemed acceptable because it was not a production weld and the start/stop area could just be cut off and discarded at specimen slicing. Since this was done late in the day, the manufacturer decided to restart the process the following day. Overnight due to the weld contracting, the run-off tab cracked and dislocated from its position, jamming the consumable guide completely. The viable solution at this point was to split the plate into two separate plates resulting in two different WPS plates for testing.

At the completion of the welding process, NDT tests were performed by the manufacturer on both plates and the ESW-NG welds were deemed sound and free of defects. The first plate in this research was designated as Plate A (PA), while the second plate was designated as Plate B (PB).

3.4.1. Plate A

Figure 3.3 shows the first plate, PA. In order to keep track of the potential ground issue, each side of PA was assigned a distinctive alphanumeric designation. The side where the ground was originally placed was designated as 1, while the side with the faulty ground was designates as 2. PA was 23 in long and 40 in wide.

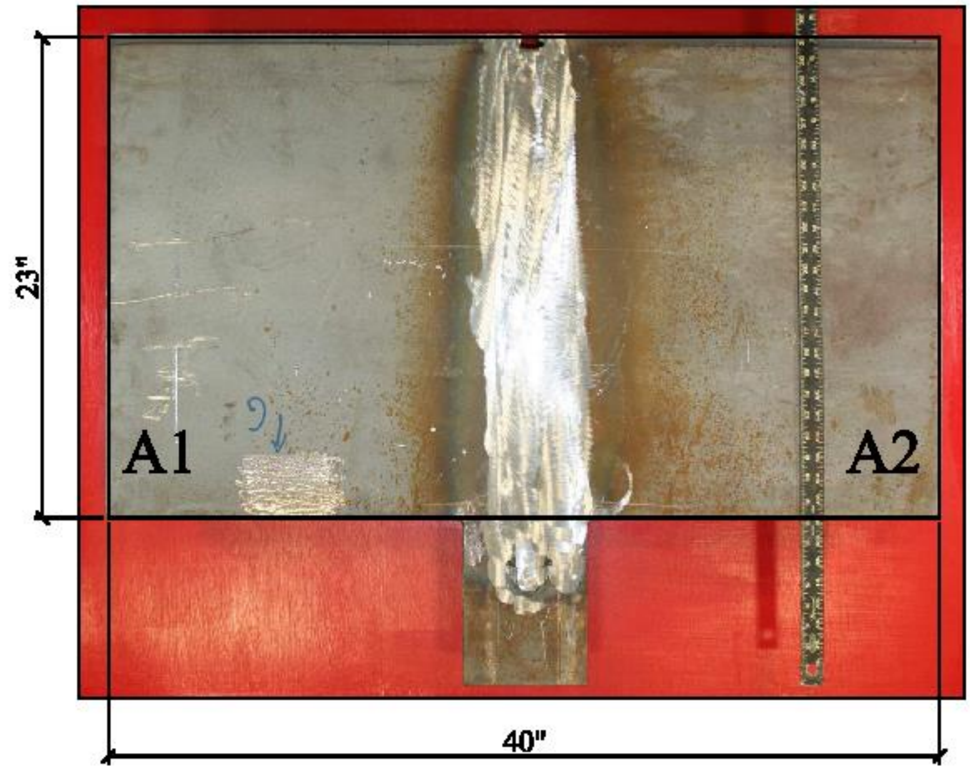

Figure 3.3. Testing Plate A

0 presents the type and number of each specimen manufactured from this plate at Turner Fairbanks Highway Research Center (TFHRC). All specimens aligned to DOR are transverse to the weld and designated by L, while all specimens transverse to DOR are aligned to the weld and designated by T as presented in Figure 3.1. There were 79 specimens overall manufactured from PA.

Table 3.3. Specimen count for Plate A

Type	Number of Specimens Manufactured	Number of Specimens Tested	Depth	Orientation
Macroetch	2	2	-	L
Hardness	2	2	-	L
Reduced Section Tension	2	2	-	L
Sidebend	2	2	-	L
CVN at center of weld	8	7	Core	L
CVN at center of weld	8	7	Surface	L
CVN at Fusion Line	12	12	Core	L
CVN at Fusion Line	12	12	Surface	L
CVN at 0.04 in within HAZ	12	12	Core	L
CVN at 0.04 in within HAZ	12	12	Surface	L
Round Tension, all weld	3	3	Core	T
Reduced Round Tension, all weld	3	3	Core	T
Round Tension	1	1	Core	L
TOTAL	**79**	**77**	-	-

Figure 3.4 shows the location of each specimen along the plate. A 1 ¼ in slice from the bottom of the plate and a 1 ¾ in section from the top were discarded to ensure that no areas with potential start/stop issues will be tested. At both ends of the remaining plate two macroetch and hardness testing specimens were located. Hardness was performed on the macroetch specimens after re-polishing as detailed in section 3.10. Next to the macroetch/hardness specimens, the Reduced Section Tension specimens were cut, followed by the sidebend specimens.

On the lower end of the plate, above the lower sidebend specimen, two tension specimens crossing the weld were sampled in the L orientation. A round tension specimen and a reduced round tension specimen were taken within the thickness of the plate as detailed in the tension testing in section 3.8.

The experimental program has an emphasis on toughness properties. As such, PA had two sizeable areas dedicated to CVN specimens as shown in Figure 3.4. Each area contained the same number of toughness specimens. The size, location, and preparation method of the specimens are presented in the toughness testing section 3.9.

At the midway point between the top and bottom of the plate, the all weld tension tests were sampled. For PA, three round tension and three reduced round tension specimens were manufactured. The size, location and preparation method of the specimens are presented in the tension testing section in 3.8.

The base metal test plate was also cut out from the A1 side of PA. A detailed account of the specimens manufactured, location and type are presented in the base metal section in 3.5.

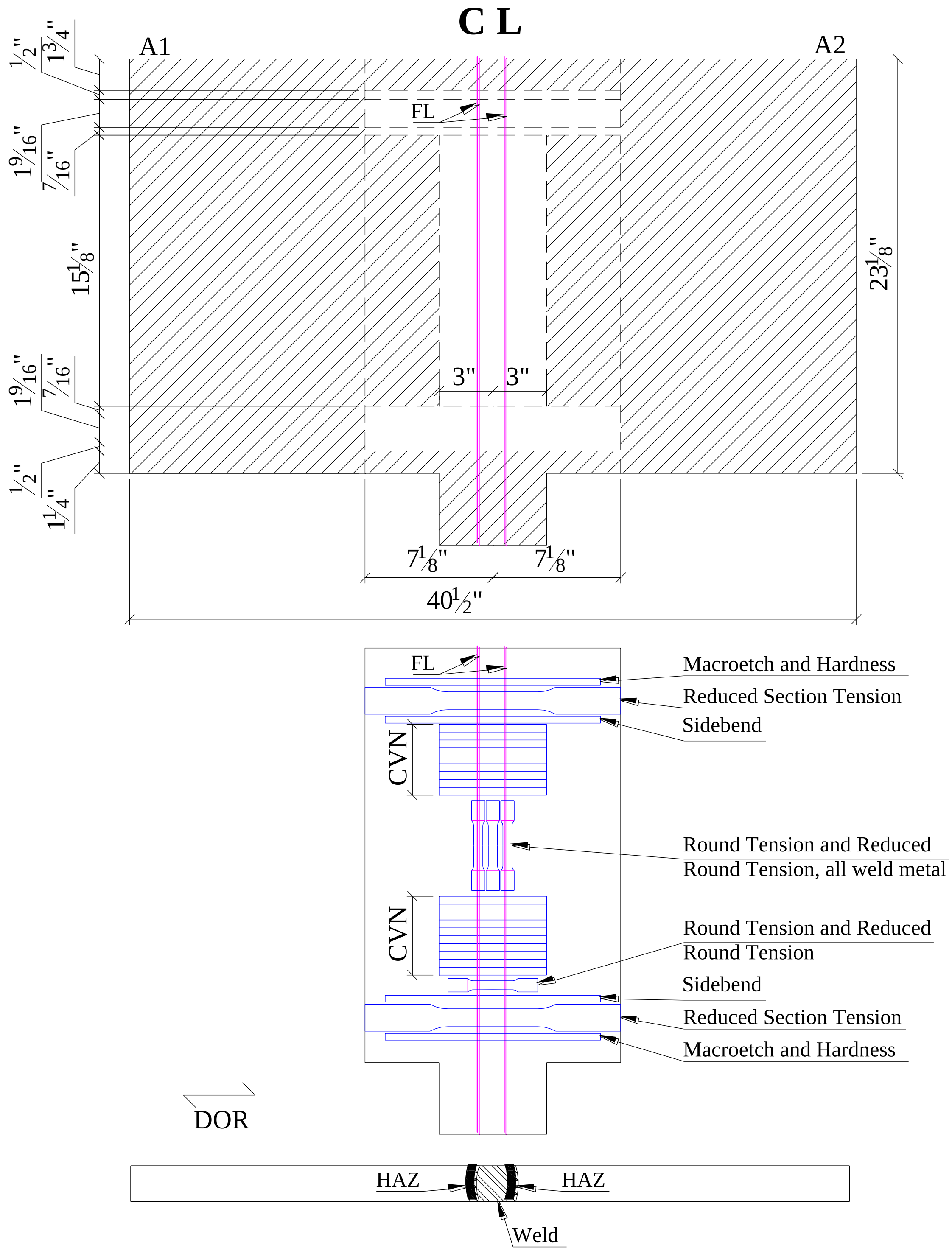

Figure 3.4. Plate A sectioning plan and specimen lay-out

3.4.2. Plate B

Figure 3.5 shows the second plate, PB. This plate had a good ground connected to each base metal plate before welding. PB was 48 in long and 40 in wide. No apparent issues were observed during welding. PB was sectioned per the dimensions shown in Figure 3.6. Each specimen was subsequently manufactured to the specifications required for testing.

Figure 3.5. Testing Plate B

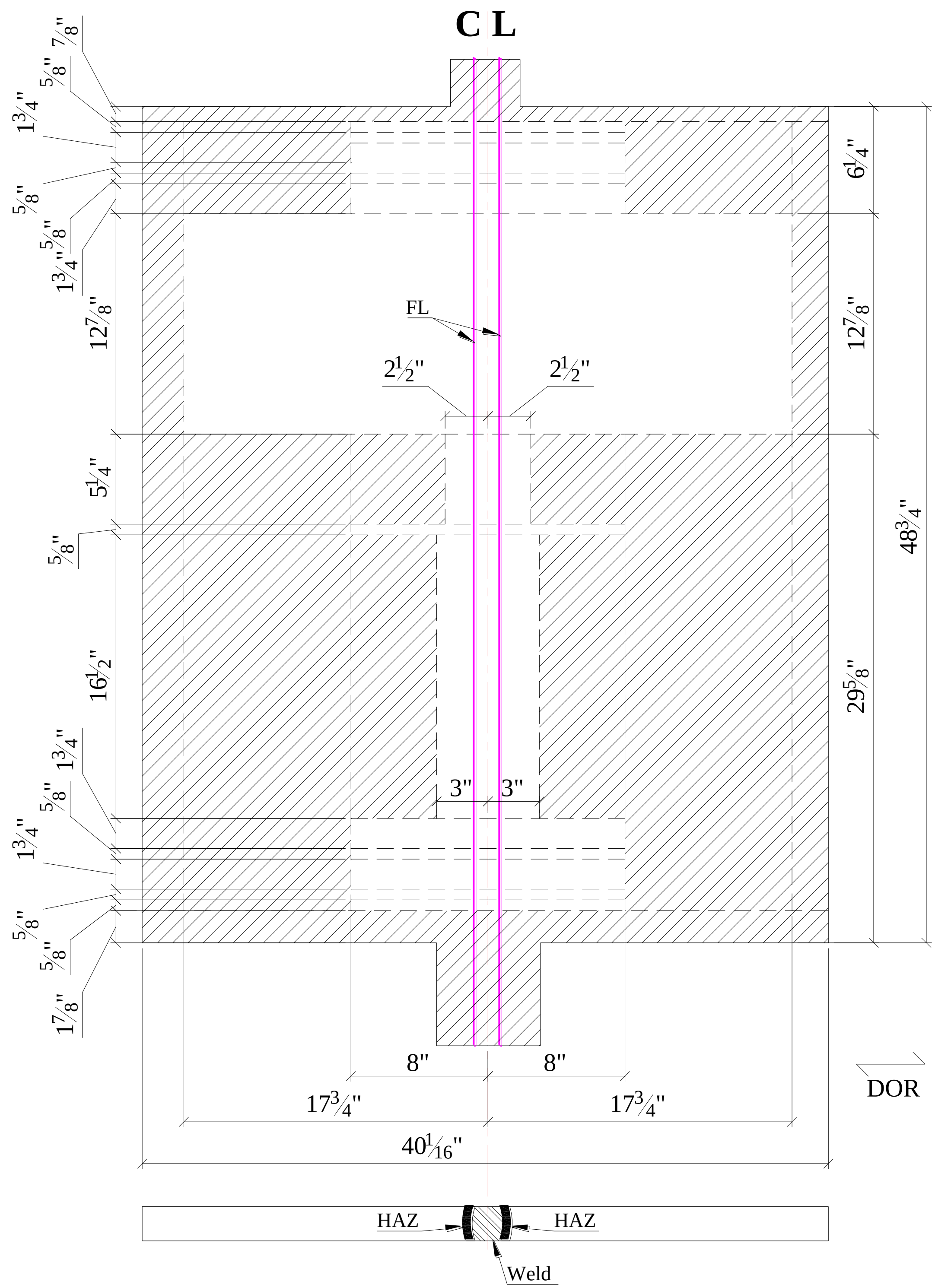

Figure 3.6. Plate B sectioning plan

Table 3.4 presents the specimen type and total number of each specimen manufactured from PB. The designations of the specimen orientations are similar to Figure 3.1. A total of 180 specimens were manufactured from Plate B (PB).

Table 3.4. Specimen count for Plate B

Type	Number of Specimens Manufactured	Number of Specimens Tested	Depth	Orientation
Macroetch	3	3	-	L
Hardness	3	3	-	L
Sidebend	4	4	-	L
Reduced Section Tension	2	2	-	L
Facebend	4	4	Surface	L
Macroetch[a]	2	2	Core	L
Hardness[a]	2	2	Core	L
Large Tension	3	0	-	L
Round Tension, all weld	5	5	-	T
CVN at center of weld	10	16[b]	Core	L
CVN at center of weld	10	14[b]	Surface	L
CVN at Fusion Line	22	18	Core	L
CVN at Fusion Line	22	18	Surface	L
CVN at 0.04 in within HAZ	22	18	Core	L
CVN at 0.04 in within HAZ	22	18	Surface	L
CVN at 0.2 in within HAZ	22	18	Core	L
CVN at 0.2 in within HAZ	22	18	Surface	L
TOTAL	**180**	**163**	-	-

[a] Longitudinal specimens
[b] Extra specimens were manufactured from one of the large tension specimens

Figure 3.7 shows the location of each specimen manufactured from PB. As shown in Figure 3.6, a 1 7/8 in slice from the bottom of the plate and a 7/8 in section from the top were discarded to ensure that no areas with potential start/stop issues will be tested. At both ends of the remaining plate two full depth macroetch and hardness testing specimens aligned with DOR were placed.

The third full depth macroetch and hardness specimen was placed approximately midway along the plate. Additionally, two more longitudinal macroetch, facebend and hardness specimens were prepared. These specimens are meant to illustrate the structure, toughness and hardness properties of the weld as it progressed upwards. Similar to PA, hardness was performed on all macroetch specimens of PB after re-polishing. The size, location and preparation method of the specimens are presented in the hardness testing section in 0. The full-width large tension specimens shown in Figure 3.7 are prepared for future testing and they are not included in the scope of this research.

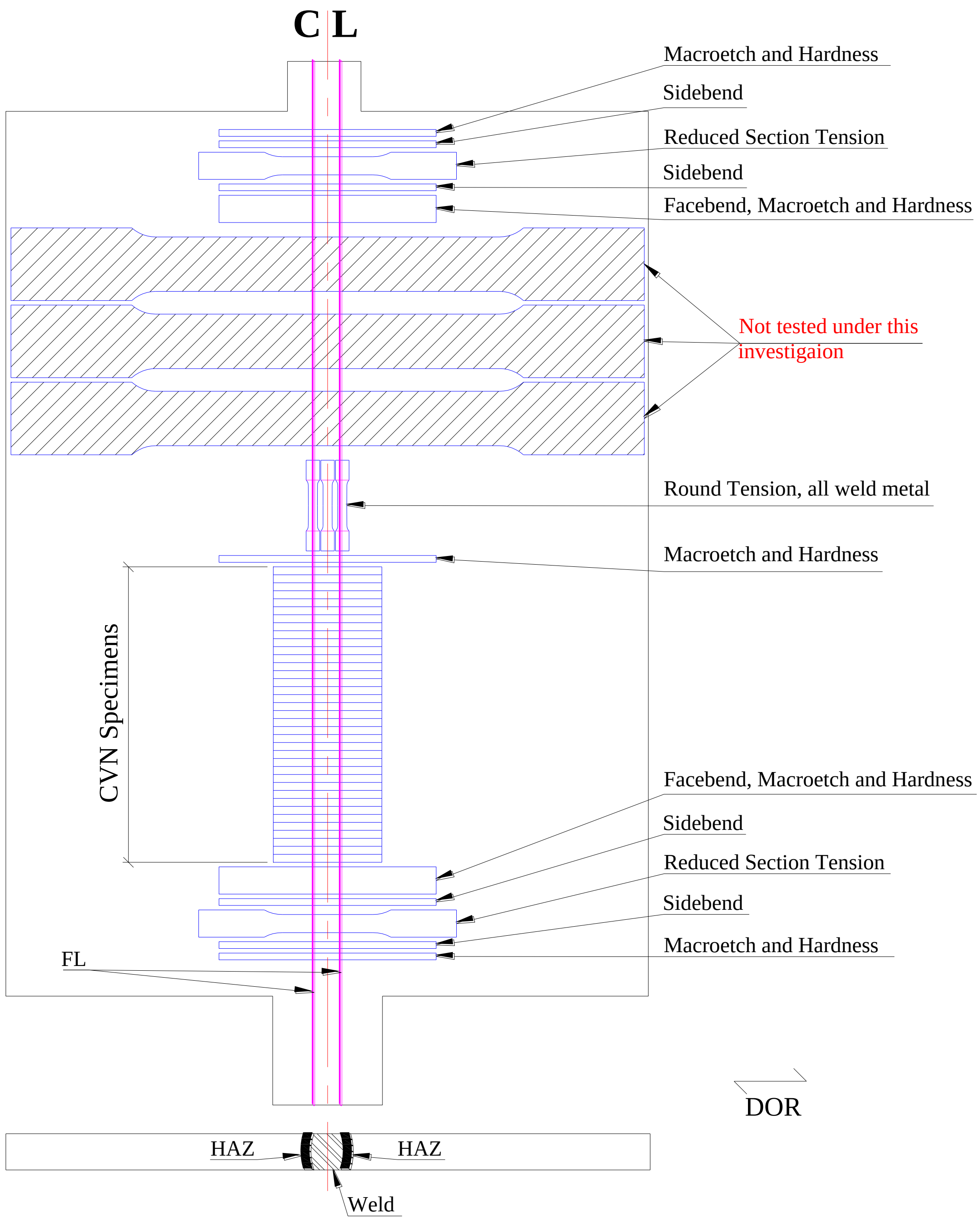

Figure 3.7. Plate B specimen lay-out

3.5. Base Metal Testing Plate

HPS 70W is an unlisted base metal in AWS. As such, for WPS qualification it must follow the requirements set-out in the code for unlisted steels with $F_y \geq 70$ ksi. To be accepted as a base metal the steel must have a minimum of five-year history of successful use as a base metal, acceptance by other national codes and records of past welding verifying adequate resistance to cracking. HPS 70W successfully satisfies these conditions. AWS does also require additional CVN tests within the HAZ for ESW welds when using an unlisted steel such as HPS 70W.

Table 3.5 presents the tensile and toughness properties of the HPS 70W plate that was used for this experimental program as received from the mill. The chemical composition of the plate is presented in Table 3.6. This data was extracted from the mill test certificate provided by the manufacturer.

Table 3.5. HPS 70W base metal plate strength properties from manufacturer

Yield Strength (ksi)	Ultimate Tensile Strength (ksi)	Elongation with 2in gage (%)	Absorbed Energy at -10 ºF (ft-lbs)
77.6	90.6	26	135.5

Table 3.6. HPS 70W base metal plate chemical composition

C	M	P	S	CU	SI	NI	CR	MO	V	AL	CB	N
0.11	1.18	0.008	0.002	0.31	0.38	0.32	0.57	0.06	0.0.49	0.027	0.001	0.008

The base metal testing plate (BMP) was cut out of PA. In order to provide a thorough analysis of the properties of the tested base metal, an array of mechanical tests was performed on BMP. For the sake of comparison to the ESW qualification plates, all mechanical tests done on PA and PB were also matched with similar tests on BMP, even if not required for mechanical properties characterization.

Multiple tension and toughness specimens were cut from the BMP. Table 3.7 presents the specimen type and total number of each specimen manufactured from BMP, as well as the orientation with respect to DOR and approximate location within depth.

Table 3.7. Specimen Count for Base Metal Testing Plate

Type	Number of Specimens Manufactured	Number of Specimens Tested	Depth	Orientation
Reduced Section Tension	3	3	-	L
Reduced Round Tension	6	3	Core	L
Reduced Round Tension	6	3	Surface	L
Reduced Round Tension	6	3	Core	T
Reduced Round Tension	6	3	Surface	T
Round Tension	12	6	-	L
Round Tension	12	3	-	T
CVN LT orientation	33	33	Core	L
CVN LT orientation	33	32	Surface	L
CVN TL orientation	33	30	Core	T
CVN TL orientation	33	30	Surface	T
Total:	**183**	**149**	-	-

Figure 3.8 presents a schematic of the BMP in which the location and orientation of each specimen is shown. All specimens were placed at least 1 1/2 in from the edges of the plate in order to mitigate thermal effects that might have appeared from the cutting of the plate. CVN and tension specimens were prepared both aligned with DOR and

transverse to DOR. The specimens were oriented in this manner to showcase the mechanical properties of the material in both directions. A detailed account of the specimen geometry and location is provided in the respective testing method description.

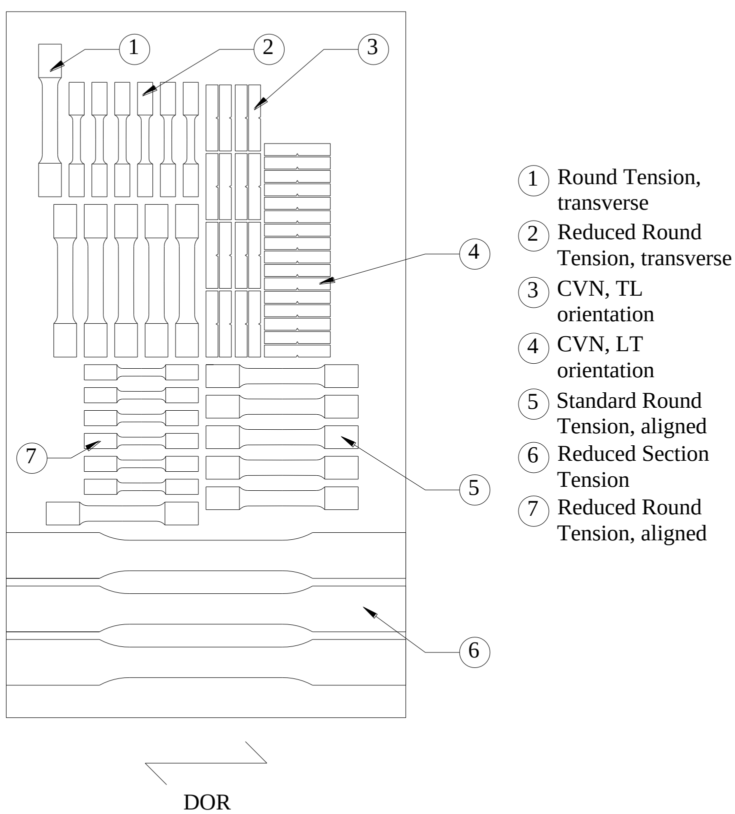

Figure 3.8. Base metal testing plate lay-out

3.6. Macroetch Testing

Macroetch is a non-destructive testing method involving the use of an acid based substance which highlights the macrostructure of a metal. The test involves minimal resources, but provides a clear picture of the macrostructure of the weld and HAZ.

The first step in performing the test is cutting the sample from the WPS plate. The specimen is then polished using progressively finer abrasives until an almost “mirror” like finish is obtained. A solution containing 10% Nitric Acid and 90% water is then applied to the sample. The solution highlights the grain structure of the weld and base metal. The specimens are then washed and dried. After completion of the preparation process the sample clearly shows the weld, fusion line and HAZ.

For qualification, all samples must be inspected visually and be free of defects. The sample must not present any cracks and have a thorough fusion between weld metal and base metal with no discontinuities exceeding 1/32 in.

Table 3.8 presents the designation, type and plate of origin of the tested specimens.

Table 3.8. Macroetch (M) specimens and characteristics

Designation[1]	Plate of origin	Type
M1	PA	Transverse
M2	PA	Transverse
M3	PB	Transverse
M4	PB	Longitudinal
M5	PB	Transverse
M6	PB	Longitudinal
M7	PB	Transverse

[1]designation is incremental with respect to the upward progression of the weld and plate assignment

A typical transverse specimen is presented in Figure 3.9. To aid in the polishing process all specimens were machine finished. The sample was cut to approximately 6in wide and centered on the weld. The width of the sample ensures the weld, HAZ and base material is treated prior to the assessment.

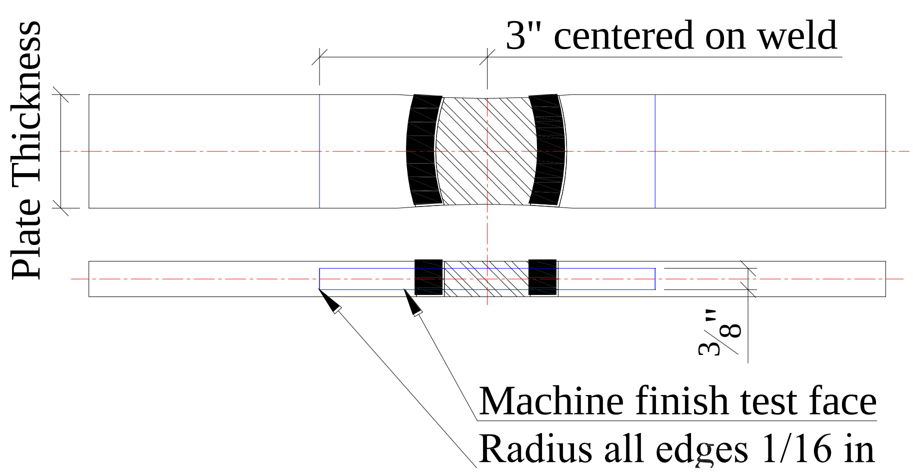

Figure 3.9. Typical transverse macroetch specimen.

Figure 3.10 shows a typical longitudinal macroetch specimen. These specimens were only manufactured for PB, and they were 1 ½ in wide and 3/8 in thick. The specimens were sampled from the core of the weld.

After sample preparation, all macroetch specimens were visually inspected and high resolution photos were taken of each specimen. A typical photo of a transverse specimen produced for macroetch evaluation is shown in Figure 3.11, while Figure 3.12 shows a typical longitudinal macroetch sample.

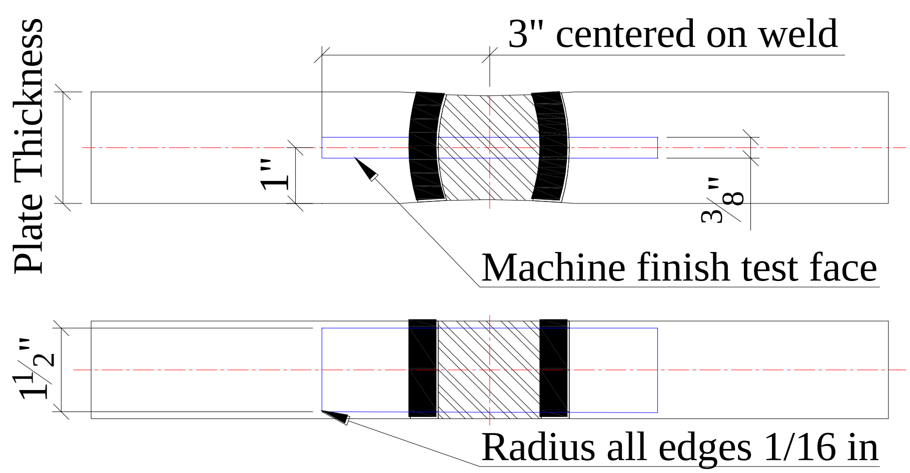

Figure 3.10. PB Longitudinal macroetch specimen

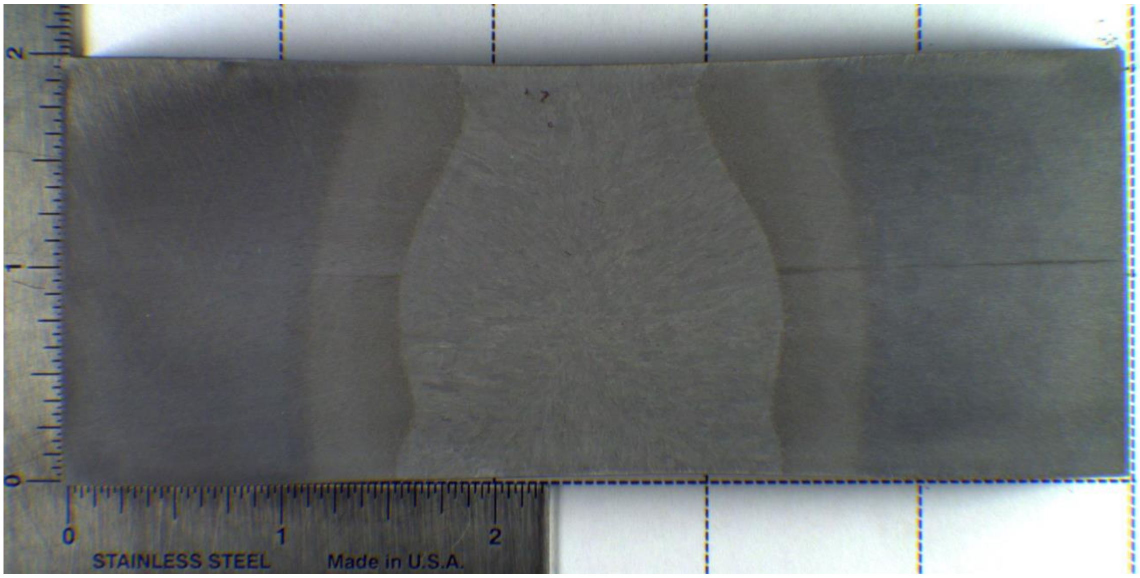

Figure 3.11. Typical transverse macroetch specimen after preparation

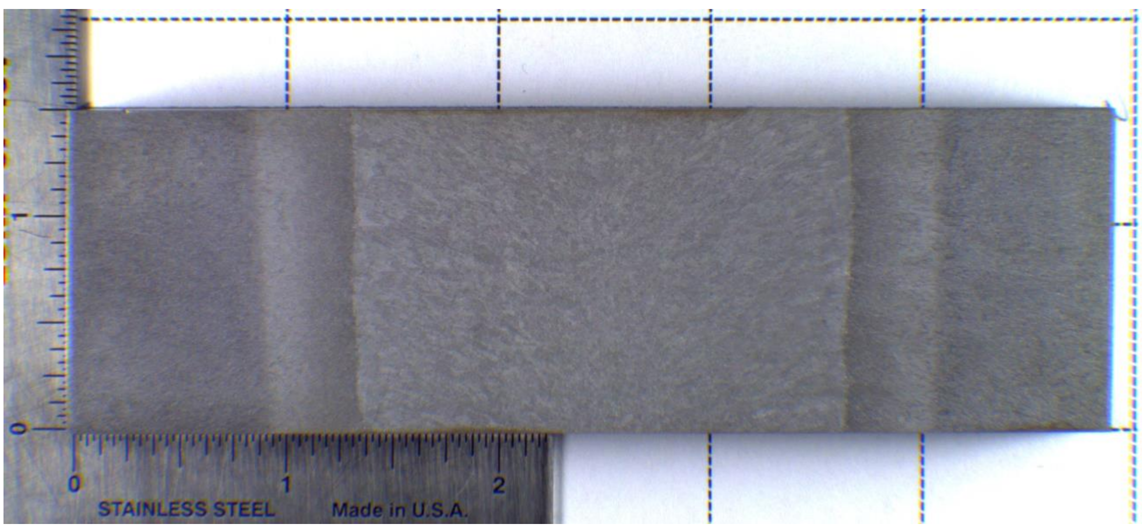

Figure 3.12. Typical longitudinal macroetch specimen after preparation

3.7. Side-bend and Face-bend Testing

The side-bend and face-bend tests are meant as a quick evaluation of the weld quality. They require minimum machinery and set-up to perform. The side-bend specimens represent a transverse section through the weld, while the face-bend specimens represent a longitudinal cut of the weld. The length of the samples must be at minimum 10 in while insuring that the weld, HAZ and sufficient base metal are encompassed within the surface of the specimen. The specimens, both side-bend and face-bend, are centered on the weld. Specimens for both tests are required to be 3/8 in thick and must have the edge machined with a radius of up to 1/8 in for preventing concentration of stresses. The width of the side-bend specimen depends on the thickness of the material. For PA, full thickness specimens were tested. On PB, the specimen width was reduced to 1 ½ in for comparison with the face-bend samples. The AWS code allows for a reduction of the width of the specimen as long as the specimen is still centered on the weld. Figure 3.13 presents a typical side-bend specimen from PA, while Figure 3.14 illustrates a typical specimen for PB.

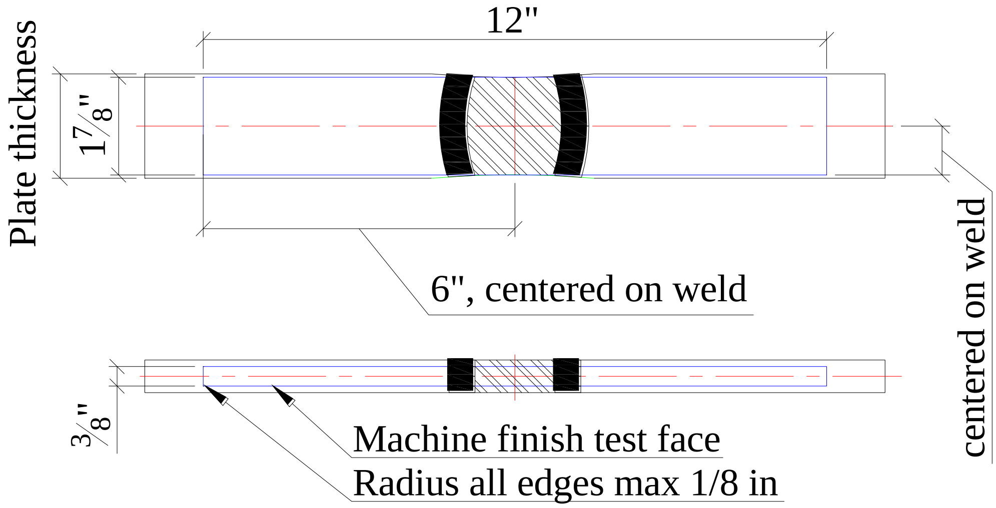

Figure 3.13. Typical PA side-bend specimen geometry

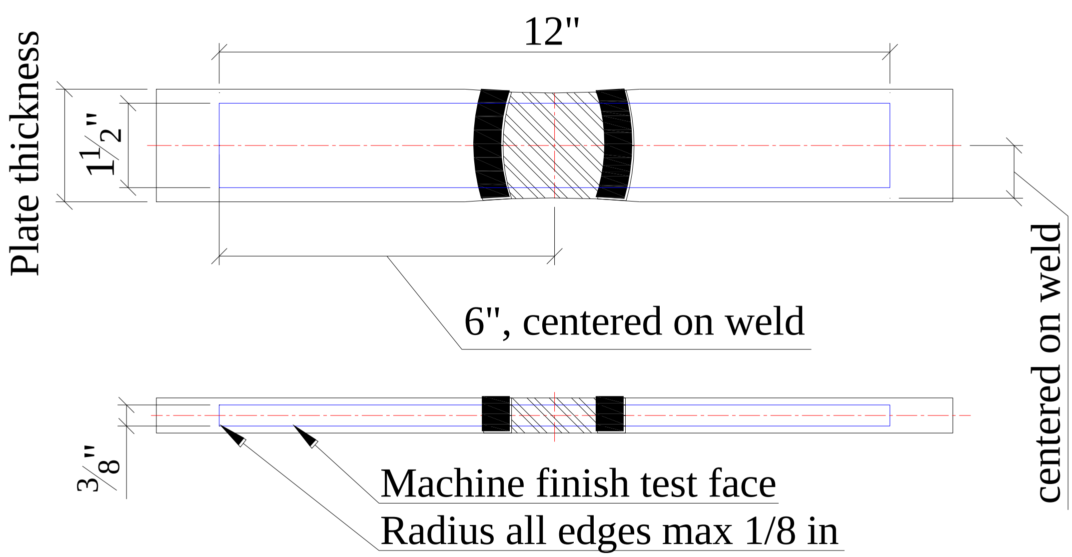

Figure 3.14. Typical PB side-bend specimen geometry

The face-bend specimens must be 1 1/2 in per AWS. They were sampled from the same cut as the longitudinal macroetch at 11/16 in from the center of the plate. The geometry and the location of the specimens is presented in Figure 3.15.

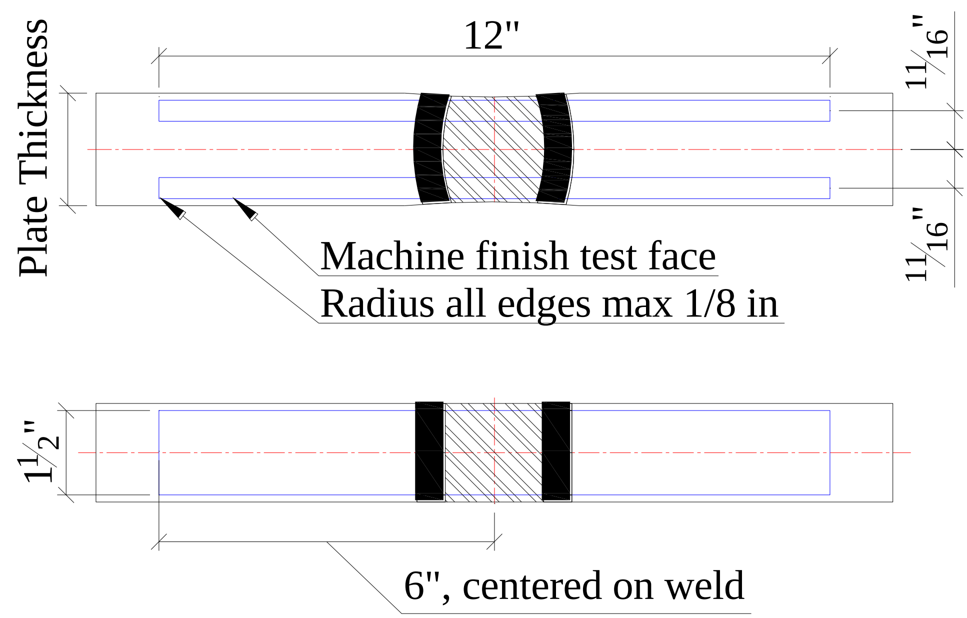

Figure 3.15. Typical PB face-bend specimen geometry and location

Figure 3.16 shows a typical side-bend and face-bend specimen after preparation for testing. The specimen designation, type and plate of origin is presented in Table 3.9.

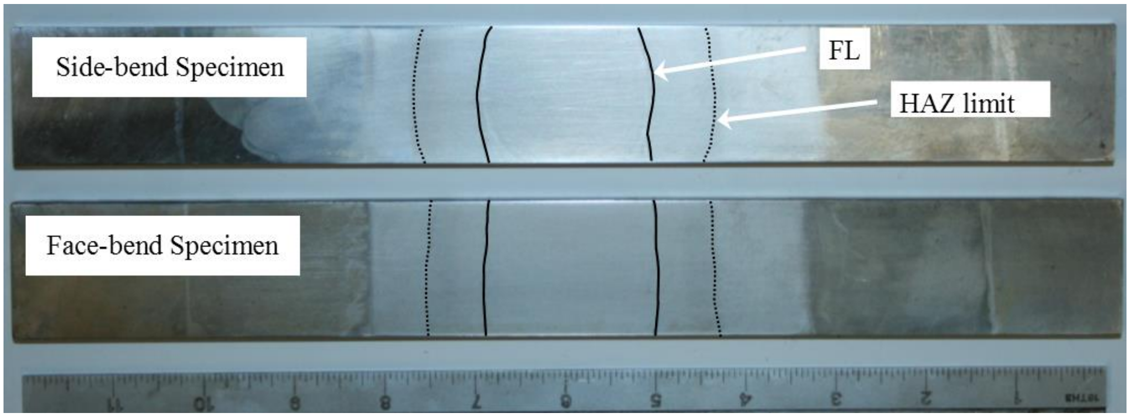

Figure 3.16. Side-bend and face-bend specimens

Table 3.9. Bend (BD) specimens and characteristics

Designation[1]	Plate of origin	Type
BD1	PA	Side-bend
BD2	PA	Side-bend
BD3	PB	Side-bend
BD4	PB	Side-bend
BD5	PB	Face-bend
BD6	PB	Face-bend
BD7	PB	Face-bend
BD8	PB	Face-bend
BD9	PB	Side-bend
BD10	PB	Side-bend

[1]designation is incremental with respect to the upward progression of the weld and plate assignment

The specimens were tested in a Guided Bent Test Jig (BTJ). The jig is comprised of two main parts. A stationary die on which the specimen is placed and a mobile plunger which pushes the sample through the die. The specimen is placed on the die centered on the weld with the help of alignment bolts. The face of the weld is placed downward towards the gap. The plunger pushes the specimen through the die and ejects it through the ejection hole. Any convenient means of moving the plunger is allowed per AWS, as such a hydraulic jack was used to perform testing. A successfully tested specimen will have a "U" shape and the weld, including HAZ, must be completely within the bent portion of the sample. Figure 3.17 illustrates the BTJ used for testing.

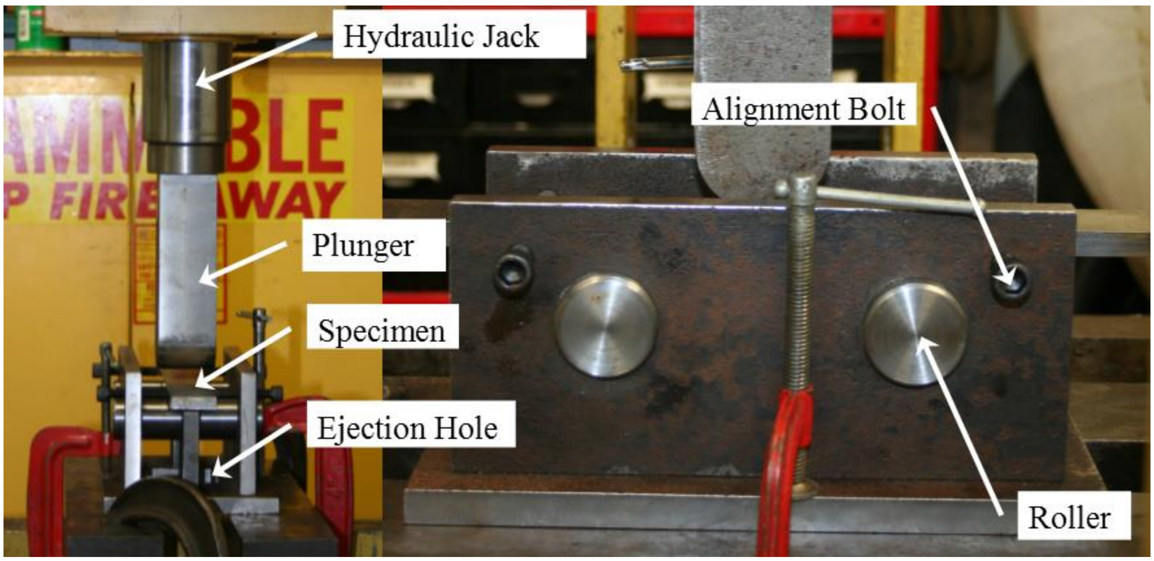

Figure 3.17. Guided Bend Test Jig (BTJ)

The dimensions of the BTJ are governed by the type of base metal used. For Grade 70 steel the dimensions are presented in Table 3.10. All the required dimensions conform to (AWS B4.0:2007). The plunger is machined finished and the rollers hardened.

Table 3.10. Die and plunger dimensions for the BTJ

Base Metal Yield Strength	Plunger Diameter	Plunger Radius	Face to Face distance between rollers	Roller Radius
Over 50 ksi to 90 ksi	2 in	1 in	2-7/8 in	3/4 in

The test results required for this procedure involve a visual examination of the specimen for defects. The tested specimen shall not have any discontinuities more than 1/8 in and the sum of all discontinuities larger than 1/32 in shall not be greater than 3/8 in on the surface. Any specimens with corner cracks larger than ¼ in are also considered failed except if that crack is from a slag inclusion. In the latter case the 1/8 in limit from the surface condition still applies. If one of the specimens fails, two re-tests from the same WPS plate must be performed and both tests must pass the requirements.

3.8. Tension Testing

Tension testing performed under uniaxial loading provides information on the strength and ductility of the material. This is useful information for comparing materials, quality control and alloy development (ASTM International, 2013). As such, tension tests are very useful in assessing the strength of a weld versus that of the base metal. For a fair comparison, the test specimens are of a standard, repeatable geometry and the method is also standardized. A detailed description of both method and sample geometries is presented in the following paragraphs.

For WPS qualification, two reduced section tension specimens and one all weld metal round specimen must be successfully tested. AWS requires that the specimens be tested per (ASTM A370 - 12a) and be prepared per (AWS B4.0:2007). ASTM A 370 is a broader standard covering all mechanical test methods pertaining to steel. ASTM A370 uses a less detailed, production oriented, version of ASTM E8/E8M for tension testing of metallic materials. Due to this reason and from the desire to test further variations of sample geometry, covered under ASTM E8/E8M, the later standard was used for testing the tension coupons. The specimen geometry and test method was duplicated between weld test plate and base metal. In the following sections, the method used for testing is presented in detail.

If the testing method is applied correctly, it will provide elongation, area reduction, yield and tensile strength information on the tested steel.

3.8.1. General Specimen Considerations

The specimen size for tension testing can be full size or machined down if permitted by the product specification. In order to maximize accuracy and prevent inadequate results particular care must be given to machining the specimens. The surface of the reduced section of the specimen needs to be free of notches, chatter marks, cold work, gouges, burrs, rough surfaces or sharp edges (ASTM E8/E8M - 13a, 2013). Finishing of the edges on the reduced section of rectangular specimens should not result in a significant change in the cross-sectional calculated area. Fillet radii are to be implemented at the transition from reduced section to gripping section. The smallest cross-sectional area of the specimen has to be at the center. A small taper is permitted by ASTM E8 as detailed in the specimen descriptions presented in the following sections. The specimen geometry has to be machined within specified tolerances.

The tension specimens originated from PA and PB were assigned the designation "W" followed by an alphanumerical character. All BMP tension specimens were assigned the designation "B" followed by an alphanumerical character. The specimen designation, plate of origin and reduced area geometry is presented in Table 3.11.

Table 3.11. Tension specimens pre-test measurements

ID	Plate of origin	Type[2]	Orient-ation[3]	Thickness / Diameter 1 (in)	Width / Diameter 2 (in)	Area (in^2)
W1[1]	PA	S	L	1.8137	0.9982	1.8104
W2[1]	PA	S	L	1.8328	0.9993	1.8315
W3[1]	PA	R	L	0.4990	0.4980	0.1952
W4[1]	PA	R	T	0.4990	0.4990	0.1956
W5[1]	PA	R	T	0.4970	0.4980	0.1944
W6[1]	PA	R	T	0.5010	0.5010	0.1971
W7[1]	PA	RR	T	0.2520	0.2520	0.0499
W8[1]	PA	RR	T	0.2490	0.2500	0.0489
W9[1]	PA	RR	T	0.2520	0.2520	0.0499
W10[1]	PB	S	L	1.4960	0.9965	1.4908
W11[1]	PB	S	L	1.4975	0.9979	1.4944
W12[1]	PB	R	T	0.4990	0.5000	0.1960
W13[1]	PB	R	T	0.4980	0.4980	0.1948
W14[1]	PB	R	T	0.4990	0.4980	0.1952
W15[1]	PB	R	T	0.4990	0.4990	0.1956
W16[1]	PB	R	T	0.5000	0.4990	0.1960
B1	BMP	S	L	1.8728	1.0032	1.8788
B2	BMP	S	L	1.8737	1.0017	1.8769
B3	BMP	S	L	1.8733	1.0028	1.8785
B4	BMP	R	L	0.49700	0.4980	0.1944
B5	BMP	R	L	0.49800	0.4960	0.1940
B6	BMP	R	L	0.50000	0.4980	0.1956
B7	BMP	R	L	0.49800	0.4980	0.1948
B8	BMP	R	L	0.49800	0.4980	0.1948
B9	BMP	R	L	0.49700	0.4960	0.1936
B10	BMP	R	T	0.49700	0.4960	0.1936
B11	BMP	R	T	0.49500	0.4960	0.1928

B12	BMP	R	T	0.49600	0.4950	0.1928
B13	BMP	RR	T	0.25000	0.2520	0.0495
B14	BMP	RR	T	0.25200	0.2520	0.0499
B15	BMP	RR	T	0.24900	0.2490	0.0487
B16	BMP	RR	L	0.24500	0.2470	0.0475
B17	BMP	RR	L	0.24800	0.2470	0.0481
B18	BMP	RR	L	0.24800	0.2480	0.0483
B19	BMP	RR	L	0.24700	0.2500	0.0485
B20	BMP	RR	L	0.24900	0.2490	0.0487
B21	BMP	RR	L	0.25000	0.2500	0.0491
B22	BMP	RR	T	0.25000	0.2490	0.0489
B23	BMP	RR	T	0.24900	0.2490	0.0487
B24	BMP	RR	T	0.25000	0.2510	0.0493

[1]Designation is incremental with respect to the upward progression of the weld, type of coupon and plate assignment
[2]Types are as follows: S – reduced section; R – round; RR – reduced round
[3]Orientation with respect to DOR: L – aligned to DOR; T – transverse to DOR

3.8.2. Reduced Section Tension Specimens

The reduced section tension specimens are transverse samples that encompass the weld, HAZ and base metal. The coupon must be centered on the weld and the reduced section at the center must be long enough to include the weld, HAZ and a minimum of 1/4 in on each side. The thickness of the specimen depends on the thickness test plate (T). In the case that T is thicker than 1 in, T can be divided into multiple strips of equal thickness. However, for ESW AWS presents a special provision requiring that the minimum thickness of the coupon shall not be less than 0.5 T. If the tested specimen has a thickness between 0.5 and T, the weld may be qualified for T. This effectively limits the number of specimens to one per slice. The width of the reduced section is set to 1 in. The fillet radius between the reduced section and the grip section is limited to a minimum of 2 in. The grip section length has to be a minimum of 2/3 of the grip on the testing apparatus, while its width will be 1-1/2 in (American Welding Society, 2010). The reduced section is centered on the grip section of the specimen. A 4 in gage is also marked on the specimens reduced section as required by ASTM E8/E8M-13a. Figure 3.18 presents the reduced section tension specimen and its geometry for PA and base metal specimens. Figure 3.19 shows the geometry of the coupons for PB.

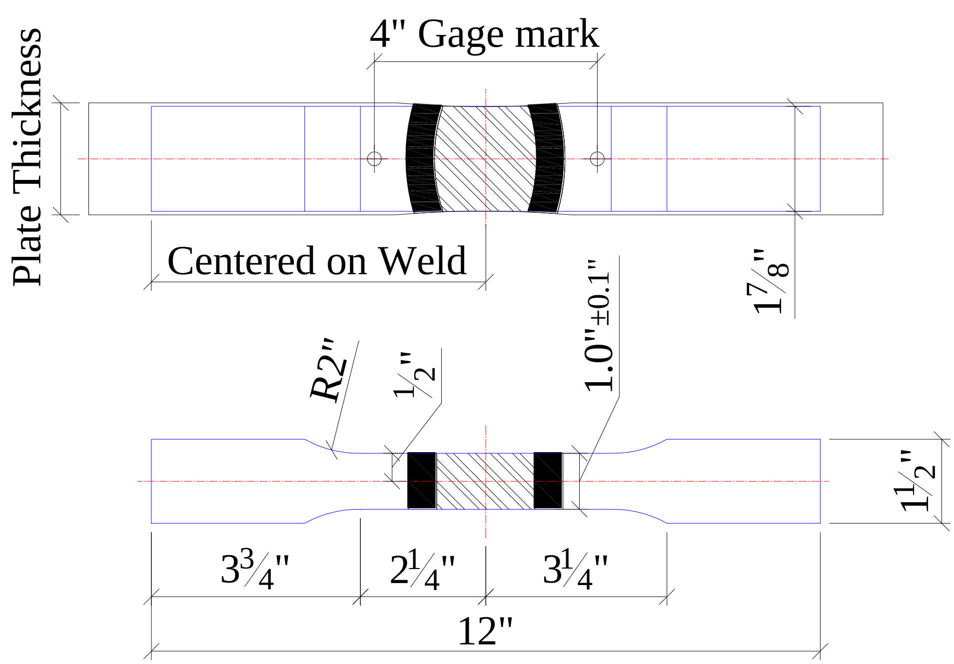

Figure 3.18. Plate A (PA) Standard Reduced Section Tension Specimen (S)

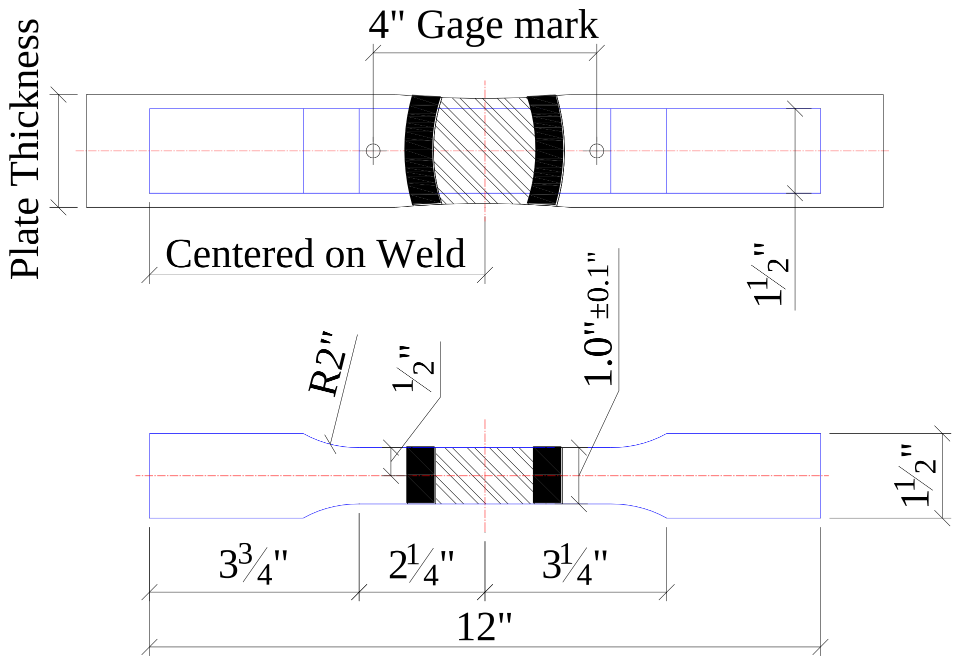

Figure 3.19. Plate B (PB) Standard Reduced Section Tension Specimen (S)

The cross-sectional geometric properties of the reduced section stay the same from fillet to fillet on the welded specimens as per AWS D1.5M/D1.5:2010. For the BMP coupons on the other hand a slight area reduction can be applied from the middle of the specimen to the fillet side of the specimen. This reduction in area results from the slight reduction of the width of the specimen which creates a controlling section. ASTM E8/E8M-13a allows for this slight taper along the length of the specimen. As the applied load on the specimen is uniaxial tension, a reduction in either strength or area would induce a probable point of failure, rupture, along the reduced section of the specimen. Since the standard requires that failure occurs close to the center of the specimens, a controlling section is desired to ensure failure within the specification. Reducing the area, but keeping the same load on the specimen creates a concentration of stresses at the lesser area inducing failure at the controlling section. The width at the ends of the reduced section, beginning of fillet, must not be more that 101% than the width at the center of the coupon. In Figure 3.20 the typical BMP reduced section tension specimen is presented.

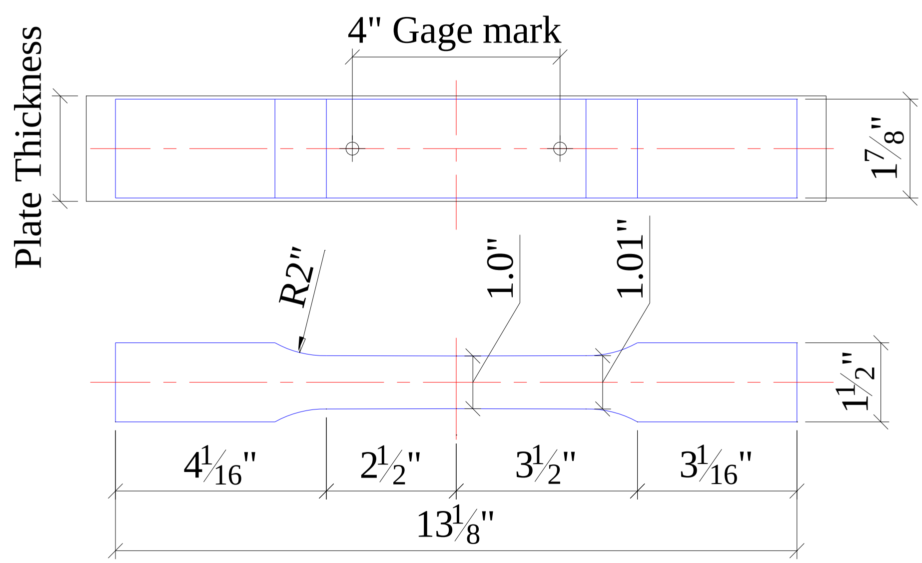

Figure 3.20. Base Metal Plate (BMP) Reduced Section Tension Specimen (S)

3.8.3. Standard Round Tension Specimens

AWS requires testing one all weld metal tension specimen. The specimen is a standard round specimen and will be aligned with the weld, transverse to DOR. Also, additionally, standard round weld tension specimens of the same geometry aligned with

DOR, transverse to the weld, are tested in this investigation. For comparison purposes coupons from the base metal aligned and transverse to DOR are also tested.

The standard round specimen has a diameter of 0.5 in of the reduced section and minimum total length of 5 in. The reduced section from fillet to fillet must be at least 2-1/4 in. A 2 in gage length is marked on the reduced section centered on the middle of the specimen. The tolerance for the gage mark is ± 0.005 in. The fillet has a radius of 3/8 in and the length of the non-reduced section has to be sufficient for proper griping (ASTM International, 2013). AWS presents a treaded gripping section, but ASTM E8 allows for use of other finishes for the gripping section. This is due to the nature of modern testing frames which are able to grip much better than previous models and do not require a treaded end. For the purposes of this investigation, non-treaded specimens were used. Figure 3.21 presents the standard round specimen.

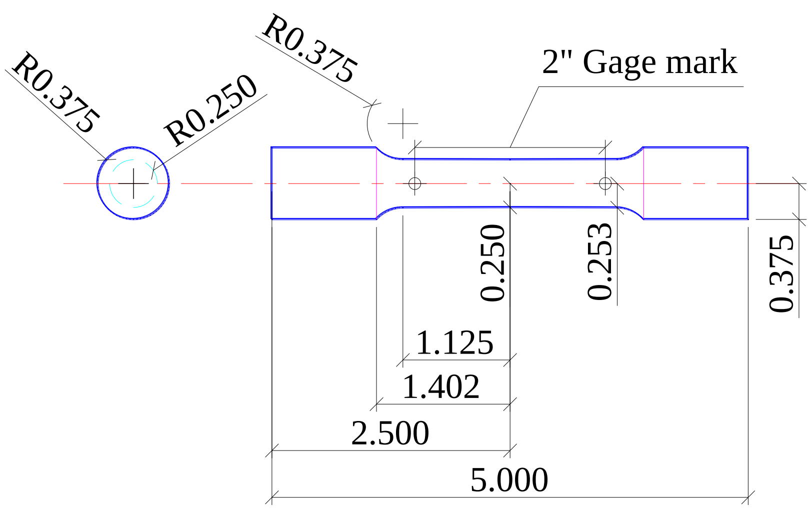

Figure 3.21. Standard Round Specimen (R), all units in inches

All specimens are tapered from center toward the fillet in order to increase the diameter to 101% of center diameter and create a controlling section as allowed per ASTM E8-13a. This procedure was described in detail in the previous section 0.

On both PA and PB the location within depth of the round tension specimens was determined by the desire to produce as many coupons as possible. For PA the three round all weld tension specimens, W4, W5 and W6, were placed per Figure 3.22. Specimen W6 is the center specimen as required by AWS. The location of W3 is illustrated in Figure 3.23. Figure 3.24 presents the position of the five all weld round tension specimens from PB. The location of the coupons extracted from BMP is presented in Figure 3.25 and is independent on the orientation of the specimen.

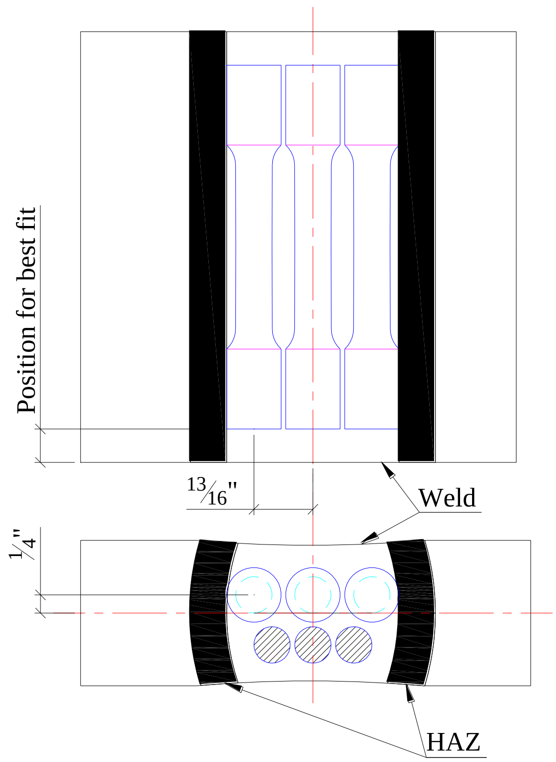

Figure 3.22. PA, R type specimens sampling plan.

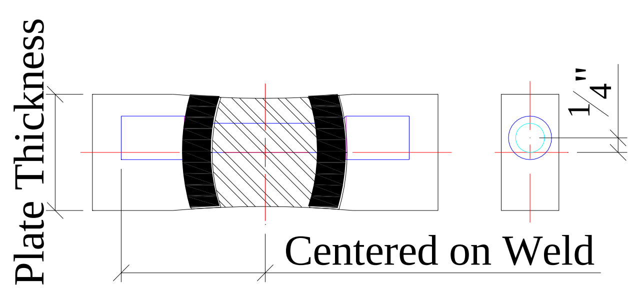

Figure 3.23. PA, location of round specimen W3

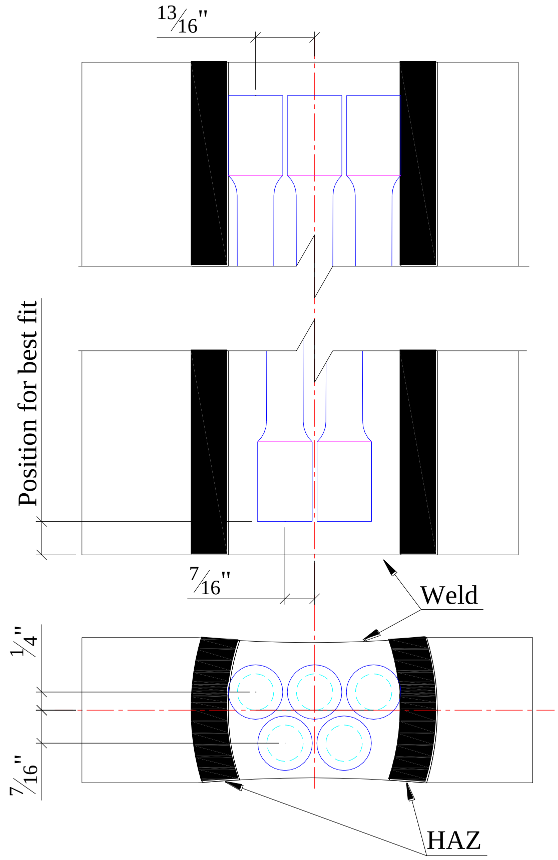

Figure 3.24. PB R type specimens sampling plan.

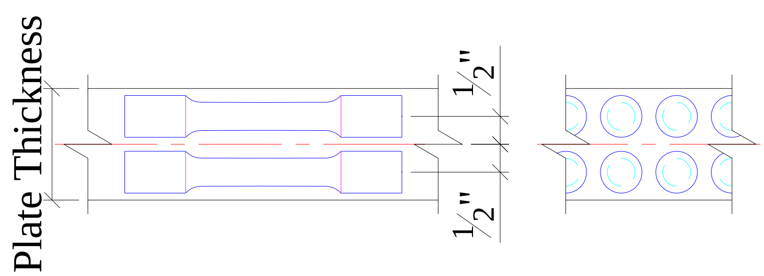

Figure 3.25. BMP round tension specimen’s location within depth.

3.8.4. Reduced Round Tension Specimens

The area of a test specimen is in direct correlation with the capacity of the testing frame required to perform the test. As such, ASTM E8-13a allows testing of smaller size specimens, proportional to the standard specimens. This allows laboratories with smaller capacity load frames to still compare results with better equipped testing facilities. In the desire to explore the possibility of using reduced section specimens to characterize the weld, smaller size round specimen are also tested under this testing program. These specimens are outside of the scope of AWS, but are covered under ASTM E8-13a.

Smaller specimen sizes allow testing at different depths of the plate. This allows investigation of the tension properties of the material at core and at surface.

The test specimens used here have a similar geometry to the standard round specimen, but all the dimensions are reduced by a factor of 2. The diameter of the reduced section at the center is 0.25 in, the gage length is 1 in, and the distance from fillet to fillet is a minimum of 1-1/4 in. As for the standard round sections, the gripping portion has to be sufficient for proper gripping. The diameter at the fillet is 101% the diameter at center. Figure 3.26 presents the typical sampled specimen.

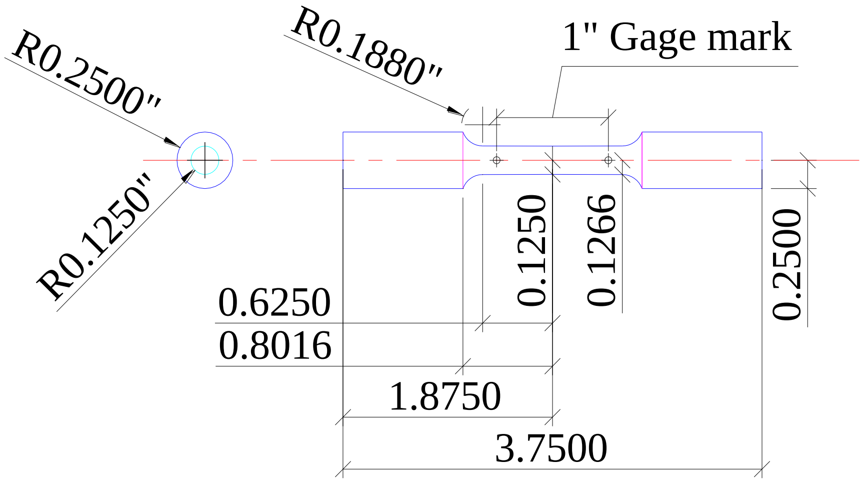

Figure 3.26. Standard RR-type Tension Specimen, all units in inches

PA provided specimens transverse to DOR as presented in Figure 3.27, while aligned and transverse specimens were extracted from BMP. Specimen W8 is the coupon located at the center in Figure 3.27, and it represents a scaled down equivalent of the AWS required tension testing specimen. On BMP, the reduced round tension specimens were sampled as shown in Figure 3.28.

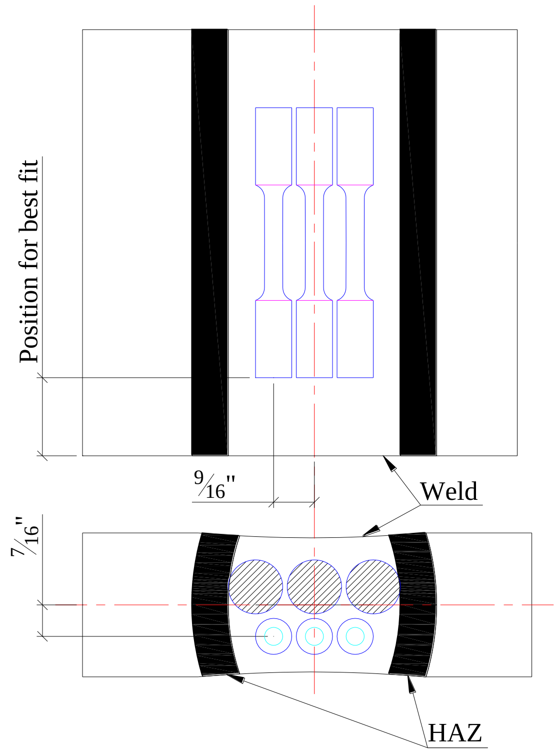

Figure 3.27. PA RR type specimens location.

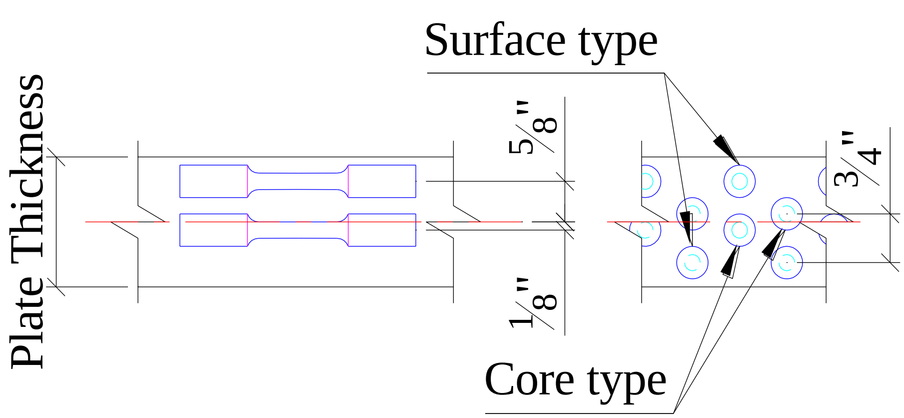

Figure 3.28. BMP RR type specimens location.

3.8.5. Apparatus

In order to perform a tension test, a hydraulic frame equipped with a force transducer and a displacement measuring device has to be used. The force transducer has to be verified, properly calibrated and have a measuring range wide enough to cover yield and tensile strength measurements. Typically, specimens are attached to the frame using wedge grips. For best results, wedge grips should be supported over their entire lengths by the head of the testing machine. Figure 3.29 presents a typical tension-testing frame. The hydraulic actuator must be warmed up to normal operating temperatures in order to minimize errors resulting from transient conditions (ASTM E8/E8M - 13a, 2013). The frame presented in Figure 3.29 employs a highly accurate loop command and control system allowing for very precise control of the testing conditions, well beyond those required by the ASTM.

Dimension measuring devices used to measure specimen geometry need to be accurate and precise to at least half the smallest unit of the individual dimension required to be measured. The apparatus most commonly used to measure precise dimensions is the micrometer. A typical micrometer is presented in Figure 3.30.

Figure 3.29. Typical tension testing frame

Figure 3.30. Typical micrometer

For elongation measurement during testing extensometers are required for accuracy. ASTM E8 requires specific gage lengths over which elongation is to be measured for repeatability. The extensometers shall be verified to include the strains corresponding to the yield strength and elongation. The gage lengths for determining yield strength shall not exceed 80% of the distance between grips (ASTM International, 2013). Figure 3.31 presents a typical extensometer. This type of extensometer was used for testing all round and reduced round specimens.

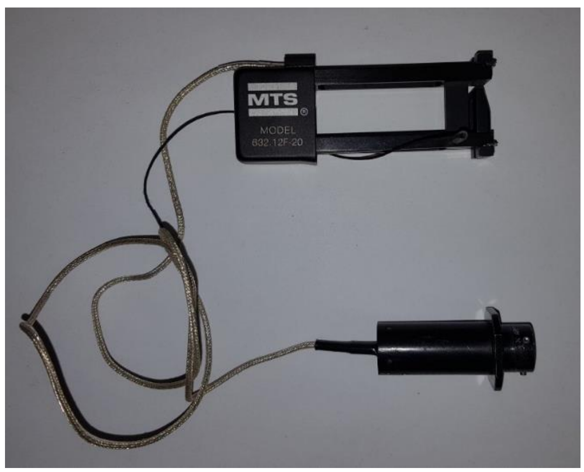

Figure 3.31. Typical extensometer

For all reduced section tension coupons, a more advanced video extensometer was used. This type of extensometer is presented in Figure 3.32. The video extensometer permits measurement of an infinite number of extensometers at the same time, allowing for strain measurements in multiple locations at once. Also, the test is recorded and a rerun of the test with different extensometers and gage lengths is also possible.

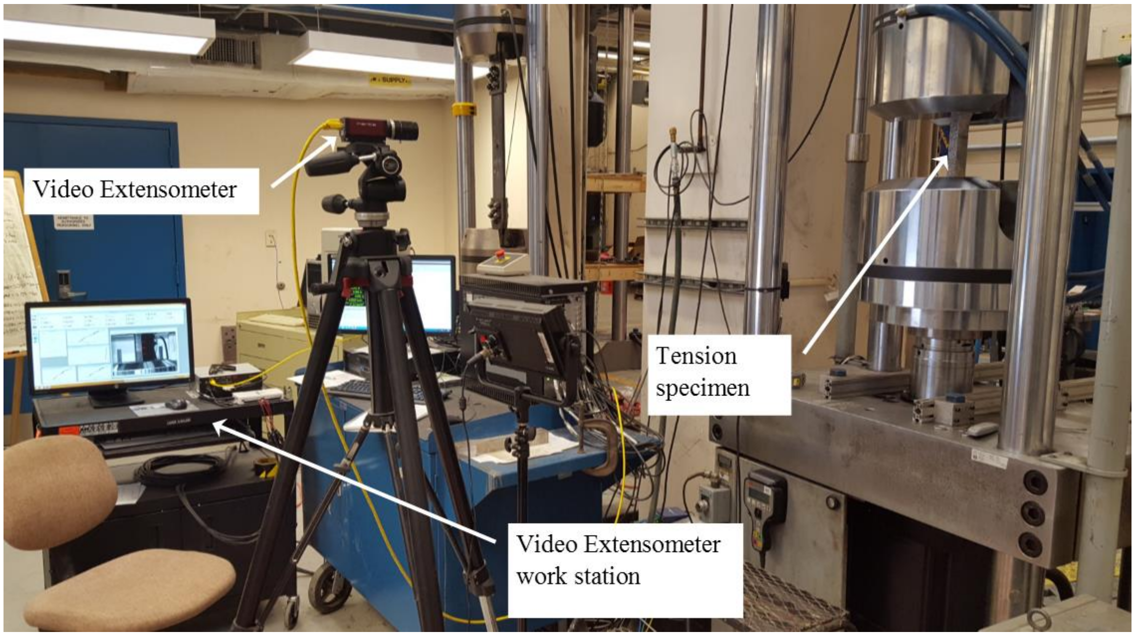

Figure 3.32. Video Extensometer set-up.

3.8.6. Method

To establish the tensile properties of the test coupons detailed measurements of their geometry must be taken first. For specimens with the smallest dimension greater than 0.2 in the measurements have to be accurate to the nearest 0.001 in. This includes all tension coupons tested under this investigation. Typical measurements for an accurate description of the specimen are gage length and cross-sectional measurements at center and gage marks. Using these measurements, the least cross-sectional area within the reduced section is determined. This least area, if taper is applied, will be at the center of the reduced section. The area for rectangular specimens is calculated using Equation 3.1, where W is the width of the specimen and T is the thickness. The area for round specimens is calculated using Equation 3.2 where D_1 is the first diameter measured at center and D_2 is the second distinct measurement normal to the first diameter measurement (ASTM E8/E8M - 13a, 2013).

$$A = W \times T \qquad \text{Equation (3-1)}$$

$$A = \frac{\pi \times (\frac{D_1 + D_2}{2})^2}{4} \qquad \text{Equation (3-2)}$$

The gage length used to determine specimen elongation may be marked by stamping lightly the specimen with a punch, scribing it or making with ink. To determine elongation less than 3%, the original elongation needs to be measured to the nearest 0.002 in prior to testing.

The testing machine needs to be set-up in such a way that a zero force indication signifies zero applied axial tension on the specimen. Any axial tension force introduced to the specimen from gripping must be either recorded and kept throughout testing or removed through movement of the actuator. If there is any load present after gripping zeroing the force transducer is prohibited as it would affect the results.

The speed of testing is very important as a higher speed of testing results in higher strength results from the material due to dynamic effects. For this reason, ASTM E8 presents five suitable methods of control for the testing speed. Each method has its advantages and disadvantages., but in general they are designed in such a way that they cover the multitude of testing machines available to testing labs. For this investigation, the method of "crosshead speed" (CS) control was chosen because it is very suitable for use with advanced loop control systems. For this method, in order to determine yield properties, the CS needs to be set between 0.012 and 0.018 in/in/min elongation with respect to the original reduced section. In determining tensile strength, after determining yield properties, CS can be set to any speed between 0.05 and 0.5 in/in/min of the length of the reduced section.

For the speed rate control methods, ASTM E8 provides multiple methods for determining yield strength. The most commonly used, as well as the method used for this research, is the offset method. For yield strength determinations by the offset method, a stress-strain curve is to be obtained and a parallel of the first portion of the curve, the linear portion, is to be drawn at 0.2% strain. At the intersection between the parallel line and the stress-strain curve, the yield value is recorded. When reporting yield strength using this method the offset value needs to be provided in parenthesis next to the yield strength. If the straight portion of the graph does not originate at the origin of the axes, the offset must be applied starting where the straight line drawn by the slope intersects the strain axis.

The Modulus of Elasticity (E) is calculated as the slope of the initial straight portion of the stress-strain curve. To insure that only the straight portion of the curve is considered, the slope is calculated at the stress value equivalent to 75 % of the yield stress.

Tensile strength, or ultimate strength, is the maximum force carried by the specimen divided by the original cross-sectional area of the specimen. During testing, the maximum load is easily recorded by modern testing equipment.

For elongation, the original gauge length must be known. Using an extensometer, the incremental values are recorded. Elongation is reported as percentage increase from the original gage length. If possible it is recommended that the extensometer be kept in touch with the specimen throughout the test as to record the elongation at rupture. If the extensometer is to be removed, the two separated pieces are to be fitted together and the distance between gauge marks measured. This can only be performed if elongation is 3% or more than 0.5% of the extensometer scale. Elongation needs to be recorded to the nearest 0.2% or 0.002 in (ASTM E8/E8M - 13a, 2013).

Reduction of area is calculated at the minimum cross-section at the location of fracture. The reduction of area is expressed as a percentage of the original area of the cross-section. The reduction of area is to be expressed to the nearest 0.5% if the reduction is between 0 and 10% and 1% if the reduction is greater than 10%. The area of the reduced section for rectangular specimens is assumed to be parabolic. Therefore, Equation 3.3 is used for calculation. In Equation 3.3, W is the measured width after testing, t_1 and t_3 are the thicknesses at the corners and t_2 is the thickness at center. For round specimens, the area will be geometrically represented by an ellipse. This results in the calculation of the area conforming to Equation 3.4 where d1 is the least diameter and d2 is the greater diameter.

$$A = \frac{(t_1 + 4 \times t_2 + t_3)}{6} \times W \qquad \text{Equation (3-3)}$$

$$A = \frac{\pi \times d1 \times d2}{2} \qquad \text{Equation (3-4)}$$

Retests are allowed under the following circumstances:

- Poorly machined surfaces;
- Original specimen had wrong dimensions;
- Specimen properties have been changed by wrong machining practices;
- Incorrect test procedures;
- Fracture was outside of middle half of gauge length;
- Malfunctioning testing equipment.

At the end of the testing process the following data must be reported per ASTM E8/E8M-13a:

- Reference to the standard used;
- Material and sample identification;
- Specimen type;

- Yield strength and method used to determine it;
- Yield point elongation;
- Tensile strength;
- Elongation, including original gauge length and method used to determine elongation;
- Reduction of area;
- Specimen section dimensions before and after testing including equations used to calculate cross-sectional areas;
- Speed and method used to determine testing speed;
- Method used for rounding test results;
- Reason for replacing specimens.

3.9. Toughness Testing

Toughness can be accurately evaluated by using the Notched Bar Impact Test, also known as the Charpy V-notch test or CVN. Impact testing on notched specimens is well proven to be in correlation with service experience. Impact testing correctly predicts brittle fractures and ductile behavior of steel products (ASTM E23-12c, 2012).

The most important characteristics of an impact test are a recognized, standardized, specimen, a set of anvils and specimen supports, a moving mass and an absorbed energy measuring apparatus. The sample is positioned on the anvil supports and receives blow from the standardized moving mass. The absorbed energy required to break the specimen is then measured.

Toughness evaluation of the weld and FL, is a requirement in AWS for ESW-NG qualification. AWS requires toughness testing to be done according to ASTM A370. ASTM A370 references for CVN toughness testing ASTM E23, as such the latter will be used for the purpose of gathering toughness information on the BMP and WPS. In addition to the mandatory specimens required for qualification, multiple specimens were tested on PA and PB at the FL and within HAZ. The purpose of these additional tests was to establish reliable transition curves as presented in section 2.4. For a thorough investigation of BMP's toughness properties two orientations of the specimens were investigated.

3.9.1. CVN Toughness Specimens

For the WPS to pass, eight specimens need to be tested at the core of plate and center of weld at set temperatures and they must meet or exceed minimum requirements specified in AWS.

The most common specimen geometry used for toughness testing is the Type A specimen, or simple beam Charpy specimen, as designated by (ASTM E23-12c) and is presented in Figure 3.33.

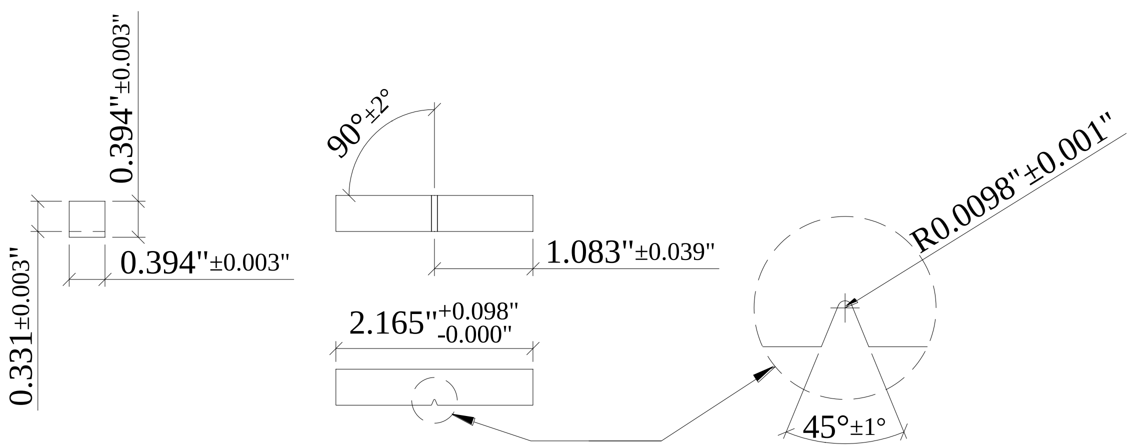

Figure 3.33. Standard Charpy V-Notch (CVN) specimen

The notch is machined smooth without polishing. Since the most variation in test results comes from defects in notch machining, it is of high importance to adhere to the listed tolerances. The finish requirement for the notched surface and the opposite side is $R_a \leq 2$ µm, while for the other sides it is $R_a \leq 4$ µm. The identification marks for the specimen must not be placed on the notched side. They can be placed either on the square ends of the specimen or any other side as long as no markings are closer than 0.394 in from the center of the notch. The marking method shall not involve excessive heat, which could damage the specimen.

The placement of the specimens within the depth of the plates was chosen to maximize the number of samples. In order to manufacture the specimens, the areas of the testing plates reserved for CVN testing were first cut to 7/16 in slices. Whit-in each slice 4 samples were prepared. All CVN core specimens were sampled at approximately 1/4 in from the core of each testing plate, while all surface specimens were sampled at approximately 11/16 in from the core of the plates. 0 and Table 3.4 present the number and types of specimens manufactured from PA and PB.

Figure 3.34 shows the typical lay-out for the CVN at the center of weld for PA and PB. The specimens were aligned with the center of the weld and the notch was positioned towards the sump of the weld as required by code (Bridge Welding Code AASHTO/AWS D1.5M/D1.5).

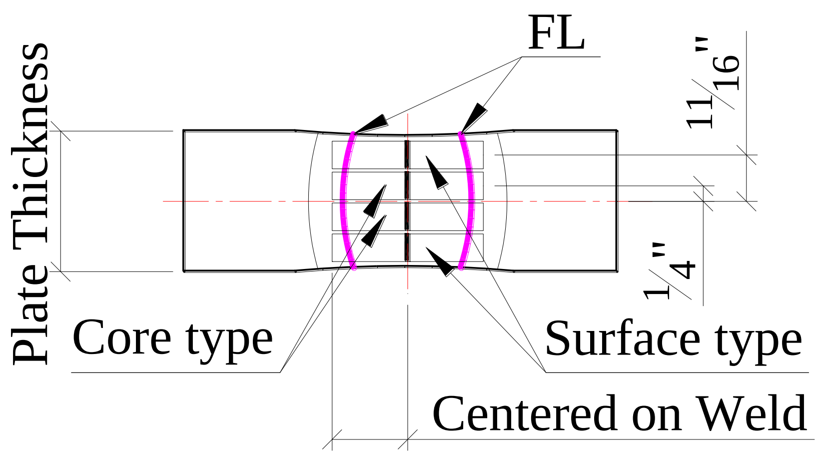

Figure 3.34. CVN at center of weld specimens

The CVN at FL specimens were positioned with the center of the notch intersecting the fusion line at the vertical center of the specimen. This approach was chosen due to highly irregular shape of the weld and geometry of the samples. Since all standards refer to orthogonal positioning, rotating the samples was not a viable option. This resulted in a combination of weld and HAZ material to be present in the break area. Figure 3.35 presents the typical CVN at FL specimens from PA and PB.

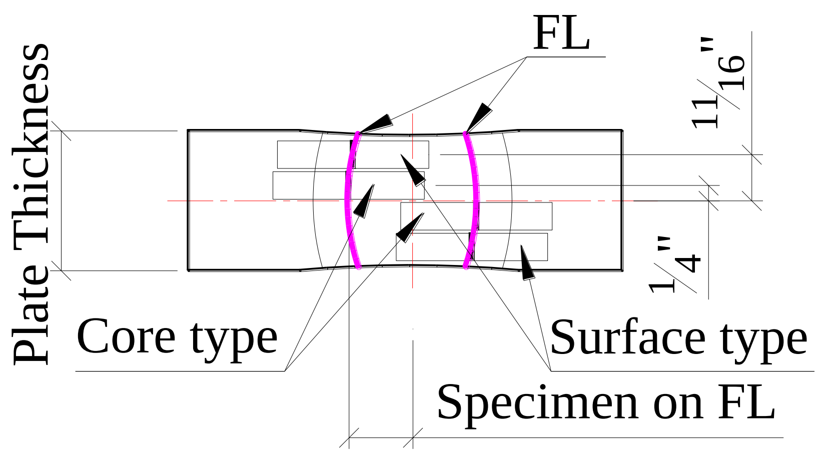

Figure 3.35. CVN at FL specimens

For the CVN at 0.04 in and 0.2 in specimens the sampling was done at the intersection of the center of the CVN with the offset from FL towards the HAZ at 0.04 in and 0.2 in respectively. Figure 3.36 presents the typical CVN at 0.04 in within HAZ specimens sampled from PA and PB.

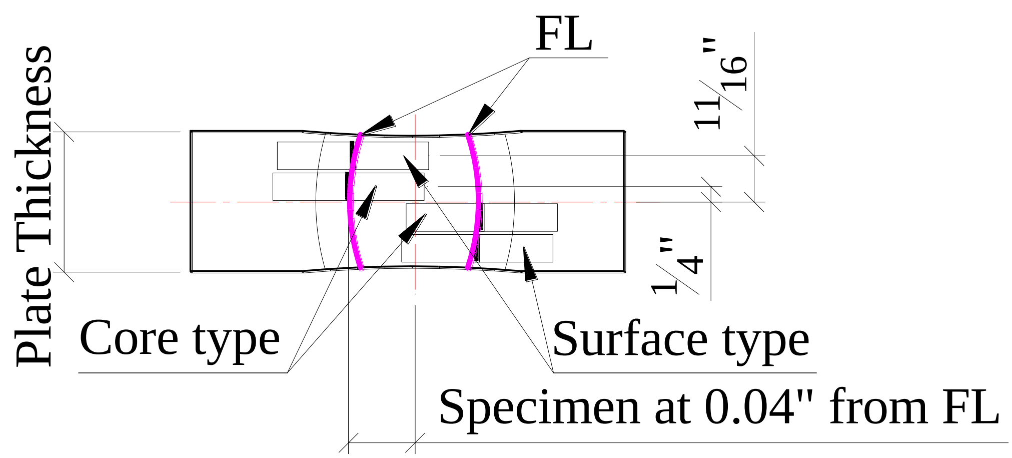

Figure 3.36. CVN at 0.04 in within HAZ specimens

There were no CVN specimens at 0.2 in within HAZ sampled due to the reduced overall size of PA. However, 22 specimens, as shown in Table 3.4, were tested from PB. Figure 3.37 presents the location of the typical CVN at 0.2 in within HAZ specimens.

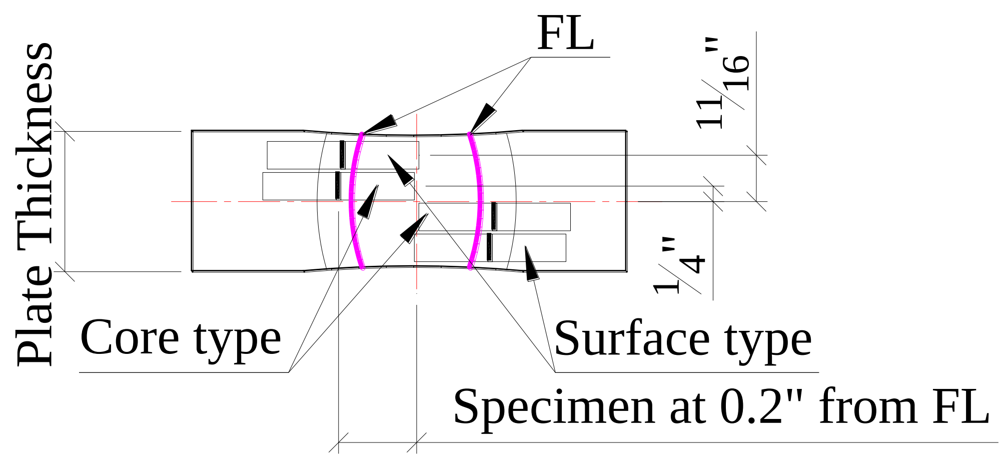

Figure 3.37. CVN at 0.2 in with-in HAZ specimens.

In Figure 3.38 a typical CVN specimen is presented. The top of the figure shows a manufactured specimen, while the bottom presents the specimen and a typical CVN slice from WPS.

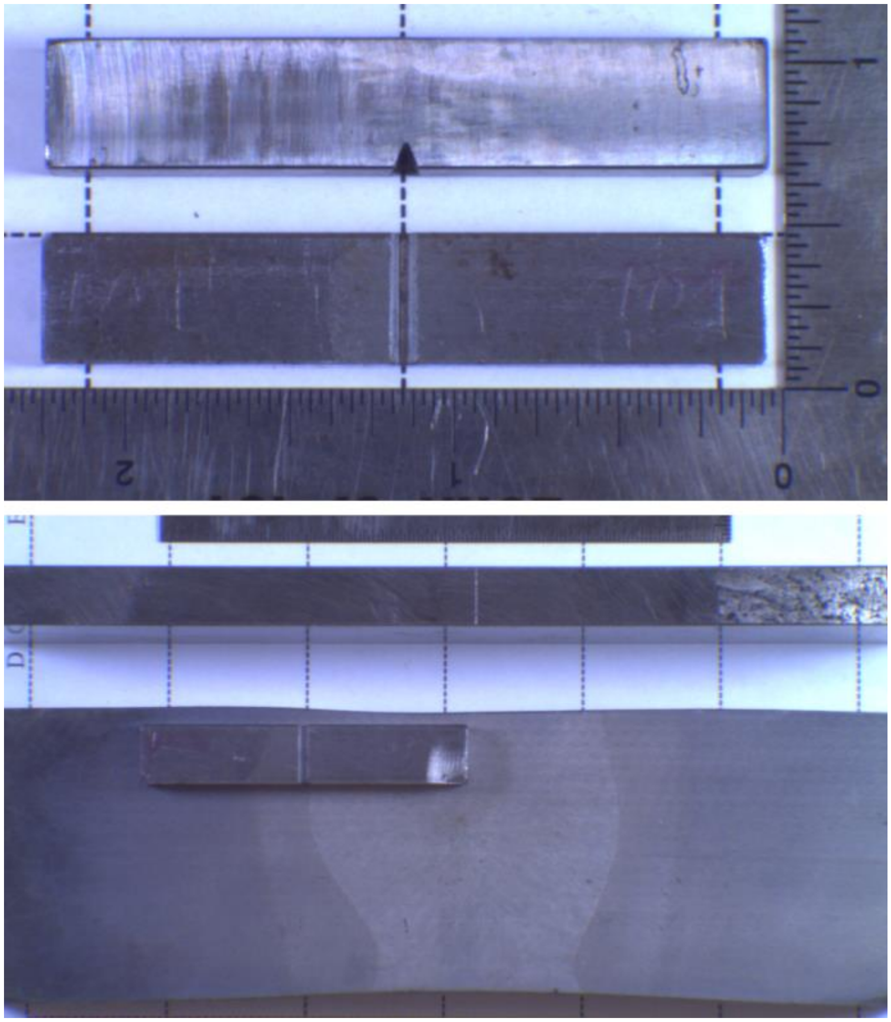

Figure 3.38. Typical CVN specimen and weld slice

For BMP, the same positioning within depth was chosen as for the WPS plates. Specimens were tested with the notch orientation aligned and normal to DOR. A schematic of the location is presented in Figure 3.39.

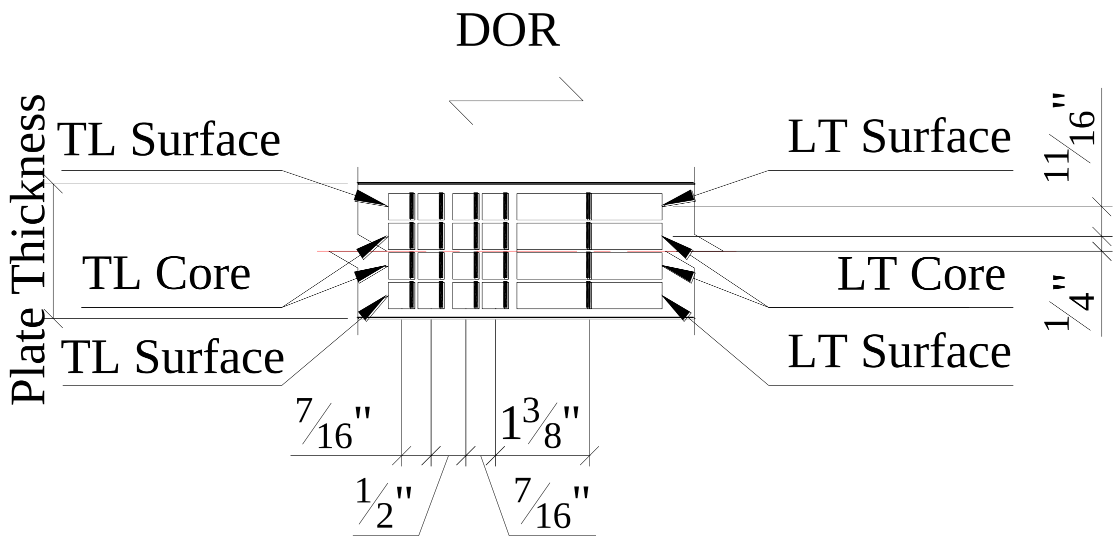

Figure 3.39. CVN specimens from BMP

3.9.2. Apparatus

The dynamic test mechanism is composed of a pendulum, a gage measuring the absorbed energy and the anvil. The pendulum is a gravity actuated mechanism composed of a standardized weight placed on a steel bar at a standardized distance from a pivoting point, which is a pin. The weight also incorporates a striker which dynamically impacts the specimen after it is placed on the anvil. After the impact test, the absorbed energy is recorded. A typical testing mechanism is presented in Figure 3.40. The testing machine must be level to within 3:1000 and bolted securely to a structural floor per the manufacturers specifications. The scale must be graduated in energy and must be able to provide readings of at least 0.25% of the energy range of the apparatus. The total friction of the machine shall not exceed in the swing direction 0.75% of the total range of the scale. The Pendulum Release Mechanism shall operate freely and permit the release of the pendulum without initial impulse, retardation or vibration. The testing environment shall be free of obstructions in the area where the specimen exists. The specimen shall be placed on the anvil in such a way that the notch will be within 0.01 in from the center of the striker. The striker shall be normal to the longitudinal axis of the specimens within 5:1000 and parallel within 1:1000. The apparatus shall be verified for accuracy and mechanical issues annually (ASTM E23-12c, 2012).

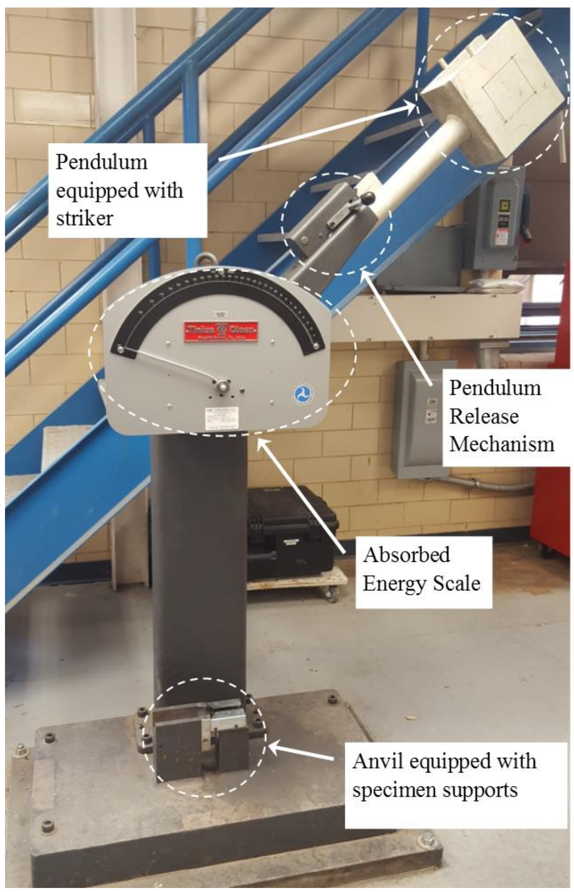

Figure 3.40. Typical Charpy test machine

Since the purpose of the toughness test is to investigate steel ductile properties, it is necessary to condition the test samples at different temperatures. Temperature conditioning of the specimen must be achieved within ±2ºF in the temperature conditioning environment. A typical means for temperature conditioning of Charpy specimens is a thermal bath as shown in Figure 3.41. The specimens are submerged in a liquid capable of withstanding the proposed testing temperatures without freezing or evaporating and removed only at the time of testing. Typical liquids used in a thermal bath when testing steel products are Methanol, Ethanol, Glycol and Water. The thermal bath presented in Figure 3.41 is capable of maintaining the temperature within ±0.1ºF. The specimens are removed from the bath and placed on the anvil with the help of self-centering steel tongues. The shape of the tongues allows for rapid placement of the specimens on the supports inside the anvil per the required specs. The steel tongues are conditioned together with the specimens in order to minimize heat transfer from the environment. At least 30 min must be allowed after the testing temperature is reached before the first specimen is tested. At least 5 min must be allowed between closing and reopening of the lid on the thermal bath before continuing testing.

Figure 3.41. Typical Charpy temperature bath

3.9.3. Method

The pendulum must be checked for accuracy prior to testing a testing cycle. The first check performed is the zero check, where after the first free swing of the pendulum the scale must return to the zero position. The second test is the friction windage loss test. The scale is moved to approximately 10% of the full range after the fifth full cycle of the pendulum. The recorded value after performing the friction windage test must not be greater than 0.4% of the maximum range of the apparatus. In the case of the test machine shown in Figure 3.40, the maximum value is 12 ft-lbs.

Before testing each specimen, the pendulum must be raised and latched, the anvil supports and striker must be cleaned and the scale must be set to the maximum value of the range. If the test is performed at any other temperature than the room temperature it must be completed within 5 seconds of the specimen removal from the temperature conditioning environment. The specimen is removed from the thermal bath, placed on the anvil supports and the pendulum is released. If a specimen jams in the machine, the test is disregarded. If a specimen does not break, it stops the pendulum and the result shall be marked as it exceeded the machine capacity.

The absorbed energy is recorded from the scale and is corrected by the windage and friction losses. If a machine is properly calibrated, verified, the losses are already accounted for, and the scale reading is the recorded value.

After testing, lateral expansion measurements (L_{ex}) are obtained by measuring the dimensions shown in Figure 3.42. The recorded values for lateral expansion are calculated based on Equation 3.5. An unbroken specimen can be reported as broken and L_{ex} calculated if it can be broken by hand after testing. All specimens shall be inspected for burrs and the burrs removed as necessary without impacting the overall shape of the specimen.

$$L_{ex} = \max(A1, A2) + \max(A3, A4) \qquad \text{Equation (3-5)}$$

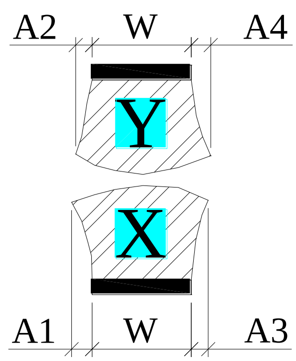

Figure 3.42. Lateral expansion measurements

The following information is required to be reported per (ASTM E23-12c):

- Reference to the standard used;
- Material and Sample identification;
- Specimen type;
- Test temperature;
- Absorbed Energy;

The following information is commonly reported per (ASTM E23-12c):

- Lateral expansion;
- Unbroken specimens;
- Fracture appearance (not reported under this investigation);
- Specimen orientation;
- Specimen location;

3.10. Hardness Testing

Hardness testing is a very useful means of evaluating the wear resistance and ductility of steel. AWS does not require hardness testing for ESW-NG, but nonetheless hardness was evaluated under this testing program. The desire is to correlate the data obtained with the tension and toughness test results. Hardness, in the same manner as the bend tests, is a relatively inexpensive testing method. As such it is beneficial to find correlation between more costly testing methods and hardness. AWS specifies micro-hardness as the preferred evaluation method for hardness, specifically The Vickers Hardness test. ASTM E384 is the spec governing Vickers micro-hardness testing. All testing performed under this investigation was performed using “ASTM E384-11e1, Standard Test Method for Knoop and Vickers Hardness of materials”.

The Vickers testing method has a minimal impact on the material. The procedure involves applying a small indentation, in the order of microns, on the test surface using a standardized weight attached to a standardized diamond indenter. The indentation is then measured and a Vickers Hardness value (HV) is found.

Hardness was performed on the macroetch specimens. For PA and PB the tested specimens are the ones presented in Table 3.8 and have the same geometry as presented in Figure 3.9 and Figure 3.10

3.10.1. Specimen Considerations

There is no standard shape or size required for the Vickers hardness test. The only requirements stated in (ASTM E384-11e1, 2012) are related to preparation, mounting, thickness and alignment.

The test sample must have a prepared surface that is flat and polished in such a manner that the test can accurately be performed. In other words, the surface preparation must allow for the indentation to be clearly defined after testing. Polishing is recommended for optimal results. The macroetch specimens were polished with progressively less abrasive paper until a mirror like finish was obtained. The specimens are to be positioned on a suitable polishing apparatus, in our case a LECO metallography belt sander, and polished at ~45º angle, changing the orientation of the specimen after each abrasive paper type used. Polishing starts at 180 grit followed by 320 and last 600 grit paper. The last step is to polish the sample with a diamond powdered cloth.

Depending on the specimen type and the testing load, mounting the sample might be required. This is usually necessary for specimens that have irregular shapes or are very thin. The samples tested under this investigation did not require mounting.

It is required that all tested specimens have a thickness at least ten times the size of the indentation. The specimens tested on PA and PB were 3/8 in thick.

The specimens must be mounted in such a way that the surface to be tested is perpendicular to the axis of the indenter. It is preferred that the specimens be machined with both bottom and tested surface parallel. If this cannot be achieved, a suitable mounting fixture must be utilized which will permit for the tested surface to properly aligned.

3.10.2. Apparatus

A Vickers testing machine is required to perform testing. The test machine shall support the test specimen and be able to control the movement of the indenter into the sample at a predefined load. The apparatus should also have a light optical microscope equipped with a measuring device. A typical Vickers Testing machine is presented in Figure 3.43.

Figure 3.43. Typical Vickers testing machine

The Vickers indenter is a highly-polished square based pyramidal pointed diamond with the face angles at 136º 0’ ± 30’. All four faces of the indenter must be equally inclined by the same angle. A schematic of a typical Vickers indenter is presented in Figure 3.44. The measuring microscope must have adjustable illumination, alignment, aperture and field diaphragms. The magnification provided by the microscope shall be such that the indented diagonal will not be smaller than 25%, nor larger than 75% of the field of view. The testing machine was verified prior to each round of testing using a standardized test specimen. The testing machine is equipped with straight shaft micrometers similar to the micrometer presented in Figure 3.30, which allows testing at precise locations on the sample.

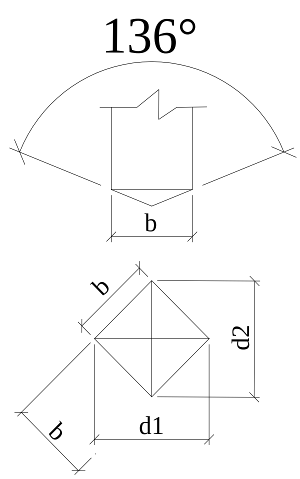

Figure 3.44. Typical Vickers indenter.

3.10.3. Method

ASTM E-384 presents all geometric and force measurements in SI units. As such, all values in this paragraph will be given in SI units. Testing must be done between 10 ºC and 35 ºC (50 ºF to 95 ºF) due to the sensitivity of metals to temperature change. A testing force is selected from the test machine settings. For the purpose of this investigation, a 500g force (P) was used. The loading time for P must be between 10 and 15s. A 15s load time was used in this research. After indentation, the location of the measurement is recorded and the indentation can be measured. After the first diagonal is measured (d1), then the eye piece is rotated 90º and diagonal 2 (d2) is measured. The measurements must not be more than 5% apart. The measurements are made in micrometers (μm) with accuracy of at least 0.5 μm. HV is then calculated and recorded using Equation 3.7. Modern testing machines are capable of computing and logging all the required information pertinent to the test: location, d1, d2, HV value. Hardness was measured as presented in Figure 3.45, Figure 3.46 and Figure 3.47.

$$HV = 1854.4 \times \frac{P}{average(d1,d2)^2} \qquad \text{Equation (3-6)}$$

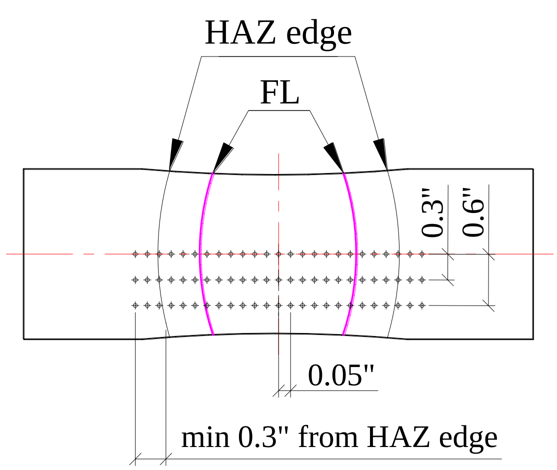

Figure 3.45. PA transverse hardness measurement layout.

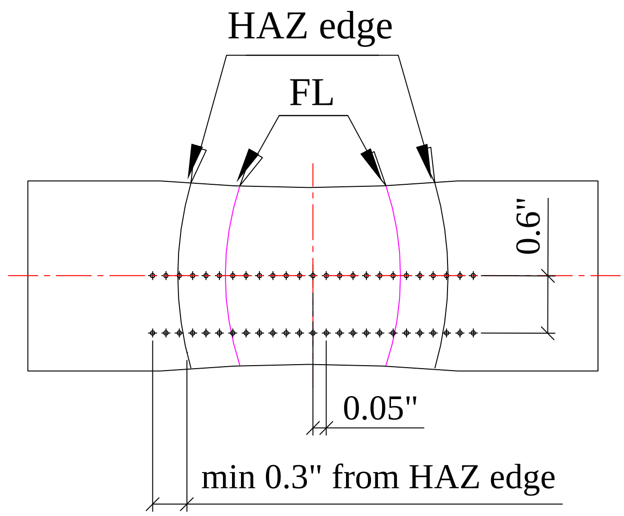

Figure 3.46. PB transverse hardness measurement layout.

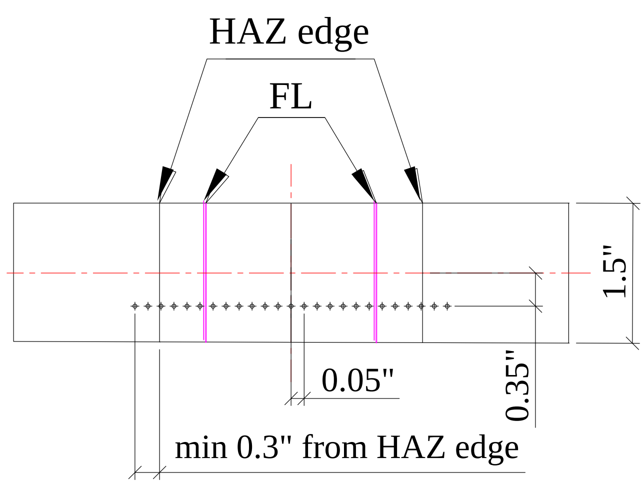

Figure 3.47. PB longitudinal hardness measurement layout.

The following information is required to be reported per (ASTM E384-11e1, 2012):

- HV result with mean and standard deviation;
- Number of tests and location;
- Test force;
- Force application time if outside of the recommended interval:
- Test temperature if outside of recommended temperatures.

3.11. Summary of Experimental Program

This Experimental Program chapter presents the testing specimens, testing methods, apparatus and required results. The chapter starts with a presentation of AWS requirements for the WPS plate followed by a detailed account of how PA, PB and BMP were cut and how the specimens were sampled. Each test specimen type and testing method used is then described in detail. This thorough account of the experimental program is meant to educate the reader on the additional testing done outside of AWS requirements, the adjustments made to the testing specimens and methods, and insure repeatability of all testing. In Chapter 4:, all of the results obtained from testing are presented and analyzed.

CHAPTER 4: RESULTS AND ANALYSIS

While the preceding chapter outlined the specific testing requirements necessary to prequalify HPS 70W steel for ESW-NG, this chapter presents the test results and analysis performed under the scope of this research. All results obtained from testing are reported as per their designated ASTM specifications. An in-depth analysis of the data was performed to provide a clear picture of the performance of an ESW-NG weld made with high performance HPS 70W steel and to provide correlation between more costly, intricate, testing methods and more accessible, economical, ones. The results were analyzed by linking them mainly to the requirements set forth in AWS. Where the scope of this research project exceeded AWS's requirements, the results were analyzed based on the bounds set by the available product specification or ASTM standards.

4.1. Macroetch Testing Results

The macroetch specimens were visually inspected and subjected to the AWS requirements for qualification. The AWS specification does not have established requirements for ESW welds, instead it only provides general requirements for all weld types. The three general requirements that apply to the weld method studied herein are no observation of cracks, good fusion between weld metal and base metal, and no undercuts exceeding 1/32 in. The general requirements were satisfied for all samples tested from both plates, PA and PB. High resolution pictures were taken of all specimens as described in chapter 3.6.

AWS also requires that the profile of the finished weld must conform to specific requirements shown through figures of fillet welds that are both acceptable and unacceptable per the code. The requirements, though, do not specifically cover ESW welds, but they are compatible with the weld method. They state that the profile must contain no impurities and no discontinuities of the weld and must maintain through the whole welding process a minimum width equivalent to the original groove width. Using the figures provided in AWS as a guideline and interpreting their significance as they relate to ESW-NG, a check of each transverse profile of the weld was performed. At this time, the maximum and minimum final groove width were recorded. Figure 4.1 to Figure 4.7 present these measurements. The designed groove width of 0.75 in is represented in the figures by the dashed rectangle.

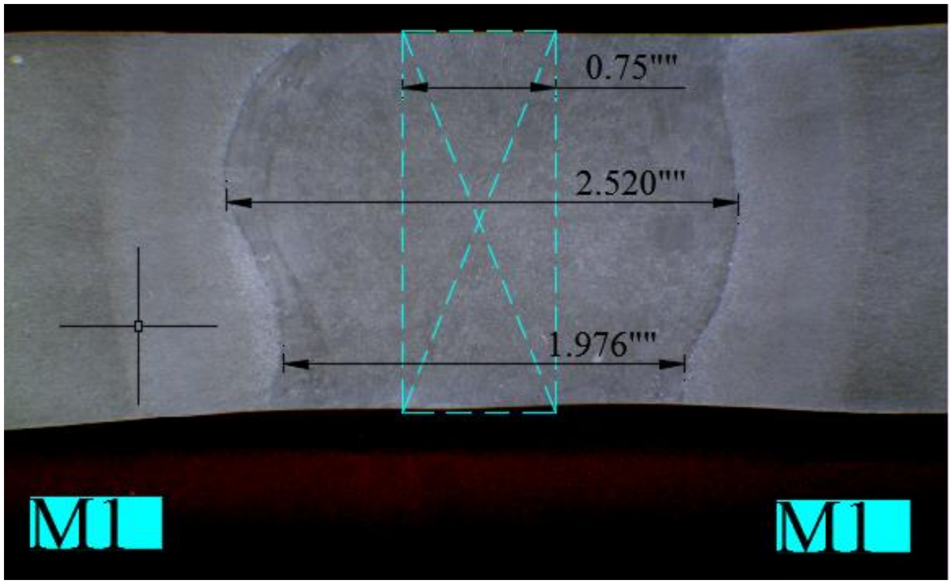

Figure 4.1. Specimen M1 groove measurements

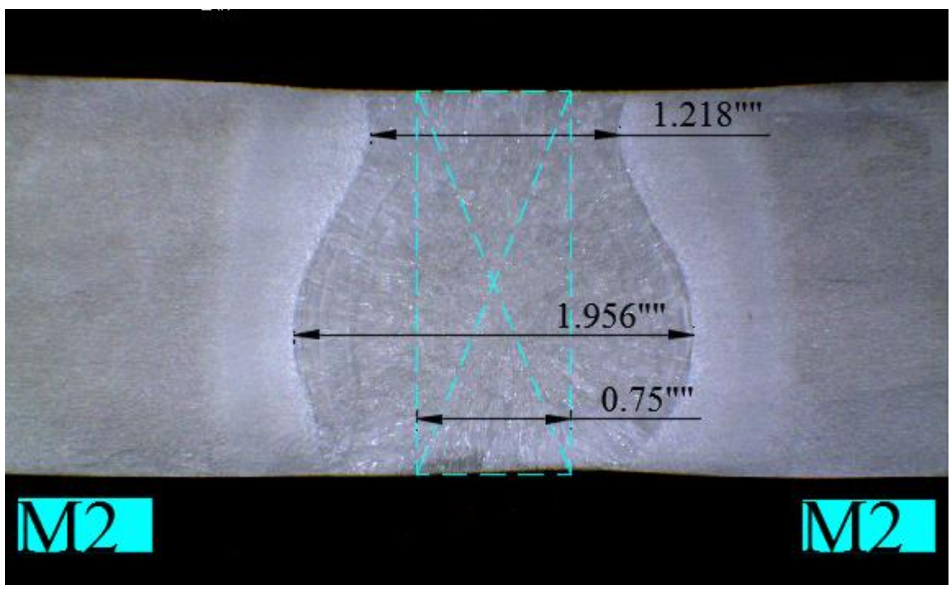

Figure 4.2. Specimen M2 groove measurements

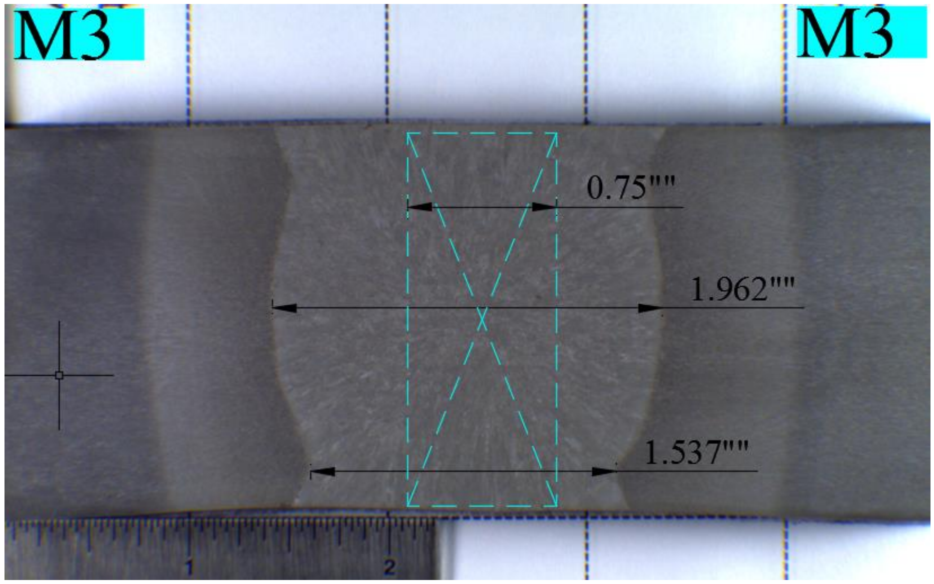

Figure 4.3. Specimen M3 groove measurements

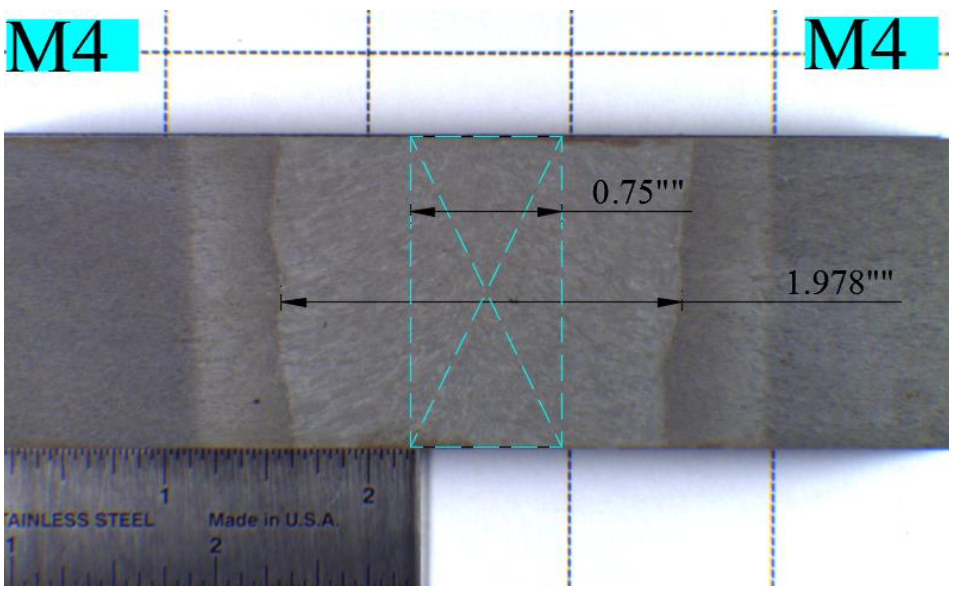

Figure 4.4. Specimen M4 groove measurements

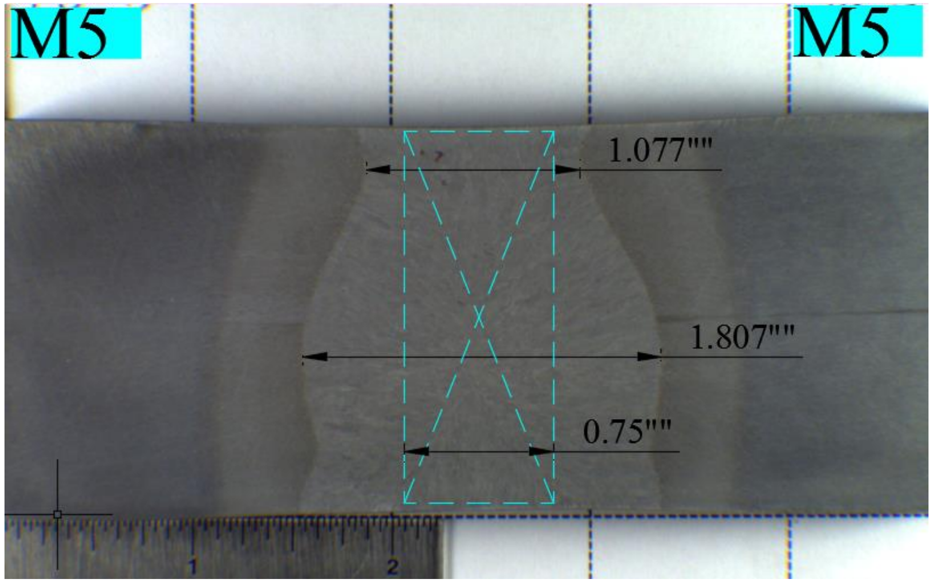

Figure 4.5. Specimen M5 groove measurements

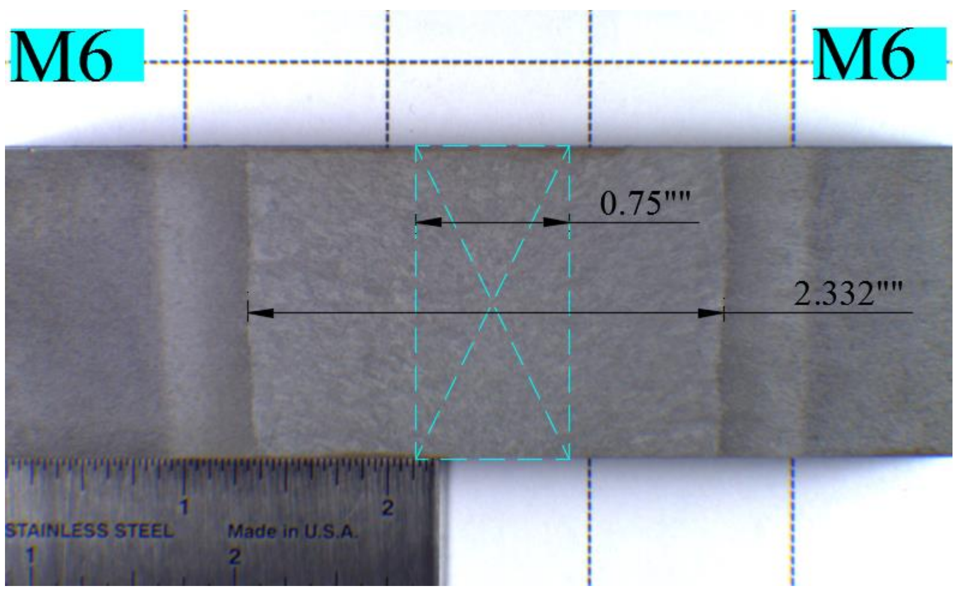

Figure 4.6. Specimen M6 groove measurements

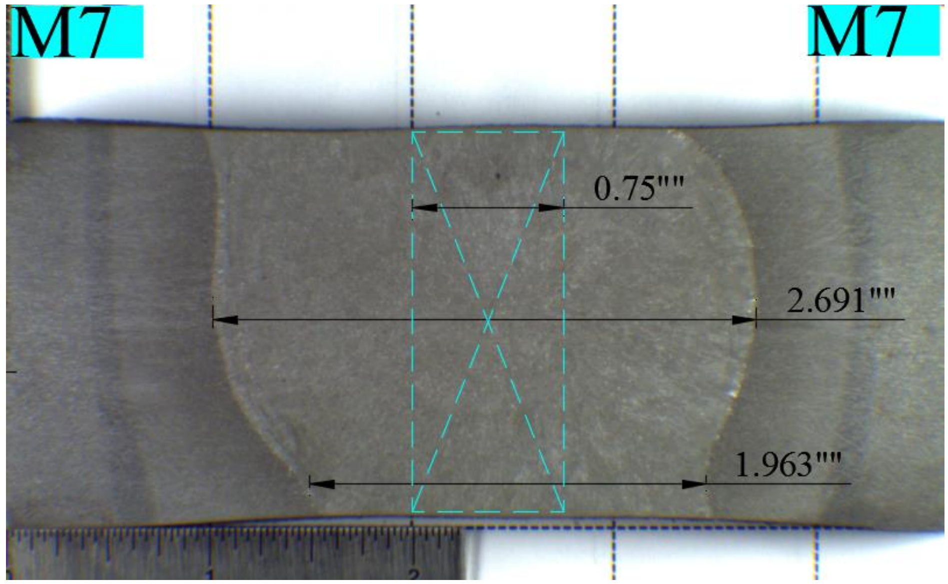

Figure 4.7. Specimen M7 groove measurements

Table 4.1 presents the tabulated measurements of the groove width for the transverse specimens. The minimum width was measured from specimen M5 at 1.077 in and the maximum width measured from specimen M7 at 2.691 in. As expected, the smallest and largest average joint widths were also recorded on specimens M5 and M7 respectively. It is worth mentioning that the average weld width recorded is between 2.5 to 3.5 times the original groove width. The sharp increase between the groove width and the size of the weld, essentially the distance between the fusion lines (FL), is a testament to how the process works by mixing exiting base material to fresh new weld metal. This provides an insight into the importance of the filler metal used. The two longitudinal specimens, M4 and M6 show relatively consistent weld widths due to their orientation and location at the core of the weld. M6 is wider than M4 by 0.354 in. Specimen pairs

M3 and M4, as well as M6 and M7, were sampled close to each other as shown in Figure 3.7 resulting in similar measurements of the final groove width. Both plates show a large variation in the size of the weld. This is due mainly to the temperature variations resulted from the location of the water inlets for the cooling shoes. See Figure 2.5 for cooling shoes location.

Table 4.1. Groove width measurements for the transverse macroetch specimens

ID	Groove width (in.)		
	min	max	average
M1	1.976	2.520	2.248
M2	1.218	1.956	1.587
M3	1.537	1.962	1.750
M5	1.077	1.807	1.442
M7	1.963	2.691	2.327

4.2. Side-bend and Face-bend Testing Results

For weld qualification, AWS states that the convex surface of a bend test must be visually inspected for discontinuities. The visual examination shall not reveal any discontinuities larger than 1/8 in, and the sum of all discontinuities larger than 1/32 in shall not be greater than 3/8 in on the surface. Corner cracks larger than ¼ in are reasons for failure, except if that crack is proven to be from slag inclusion. In that case, the 1/8 in limit from the surface condition still applies. If one of the specimens fails, two re-tests from the same WPS plate must be performed and both tests must pass the requirements.

None of the ten tested specimens exhibited any cracks, inclusions or discontinuities. Figure 4.8 shows a typical tested specimen.

Figure 4.8. Typical tested bend specimen

4.3. Tension Testing Results

The results from the tensile tests are presented in following subchapters. The results obtained from the tension tests done on the BMP are presented separately from those obtained from PA and PB. On the base metal specimens (B), and on some of the weld specimens (W) the Static Yield Stress (SYS) is also reported. SYS is reported as per the recommendation of the Structural Stability Research Council (SSRC). SSRC recommends three 90 second holds after initial yielding in order to observe the stresses under the zero strain rate condition. Static Yield is then found to be the value recorded at the intersection of the best fit line through the three static hold values and the 0.2 % offset line (Structural Stability Research Council, 2010). The following information is reported in this chapter for all tested specimens: specimen ID, orientation, Modulus, 0.2% offset yield stress, static yield stress, tensile strength, elongation at fracture and reduction in area. Additional information as required per ASTM E8 is reported in

Appendix A: Tension Testing Additional Data. The type of the specimens as it relates to tension testing is defined in Table 3.11.

4.3.1. Base Metal Testing Plate Tensile Tests

The purpose of the tensile tests done on the BMP is to evaluate the properties of the HPS 70W steel plate and provide baseline results for the WPS. The results of the tensile tests performed on the “B” specimens are tabulated in Table 4.2. Although the 0.2% yield stress values on some of the specimens were below the required 70 ksi stated in ASTM A709-13, the average value recorded per each cluster of specimens was above or equal to 70ksi. The lowest yield value was recorded on specimen B21 at 68.3 ksi, which is only 2.4 % lower than the required value. The second lowest yield value was only 1% below the requirement, a negligible difference. The lower values are a result of the use of an average to low testing speed. Typically, steel mills in order to maintain production, use the maximum testing rate allowed by ASTM E8/E8M-13a resulting in higher yield values. Where a static yield analysis was not performed, Table 4.2 shows “N/A”. All BMP test specimen were deemed to satisfy the minimum ultimate strength requirements stated in ASTM A709-13. Static Yield is a measure of the yield capabilities of the steel under static load. SSRC asserts that this is a more accurate measure of the performance of the material in the filed for dead, static, loads (Guide to Stability Design Criteria for Metal Structures, 6th Edition, 2010).

Table 4.2. Tensile tests results on base metal specimens

ID	Type	Orientation	Modulus	Yield Stress	SYS	Ultimate Tensile Strength	Elongation	Area Reduction
			(ksi)	(ksi)	(ksi)	(ksi)	%	%
B1	S	L	30,057	70.1	N/A	88.3	34	66
B2	S	L	31,159	69.9	N/A	88.2	34	67
B3	S	L	30,034	70.2	N/A	88.5	33	64
B4	R	L	29,185	69.2	66.9	87.2	27	73
B5	R	L	29,338	69.3	67.4	88.0	27	75
B6	R	L	28,769	71.0	66.9	88.5	26	74
B7	R	L	28,871	69.9	67.6	87.9	27	77
B8	R	L	29,172	70.5	67.7	88.5	27	74
B9	R	L	29,663	71.3	68.9	89.6	27	74
B10	R	T	30,199	72.1	69.6	90.1	25	73
B11	R	T	30,148	73.2	70.9	91.6	25	73
B12	R	T	30,450	72.5	70.2	91.1	25	73
B13	RR	T	30,920	74.3	N/A	91.9	27	73
B14	RR	T	31,582	74.3	N/A	91.1	26	75
B15	RR	T	31,450	69.8	N/A	89.9	26	74
B16	RR	L	30,383	70.3	67.7	88.5	27	76
B17	RR	L	30,263	72.8	70.8	90.9	28	79
B18	RR	L	30,579	70.7	68.1	89.6	28	77
B19	RR	L	29,190	70.8	68.4	89.0	28	77
B20	RR	L	28,874	71.0	68.5	89.1	28	75
B21	RR	L	32,185	68.3	66.2	89.0	27	74
B22	RR	T	31,880	71.0	69.2	91.5	27	71
B23	RR	T	31,066	70.8	69.1	91.0	28	74
B24	RR	T	30,506	69.2	N/A	88.3	25	73

4.3.1.1. BMP Tensile Specimens in the L Orientation

Plots showing engineering stress versus strain in the L orientation, aligned with the DOR, are presented in Figure 4.9 through Figure 4.11. Figure 4.9 shows the plots for the reduced section (S) type specimens and it can be easily observed that all the results are in strong correlation and closely clustered. The strain measurements for these specimens were recorded using a regular extensometer with a maximum capacity of 0.25 in/in strain at a 4 in gage length. As such, the percent elongation values reported in Table 4.2 are measurements made by joining the halves together after the completion of the test and not from the actual extensometer. This measurement method is described in section 3.8.6 of the thesis. The average yield strength of specimens B1, B2 and B3 was 70.1 ksi, while the average ultimate tensile strength was 88.3 ksi. No static yield strength analysis was performed on the S type specimens.

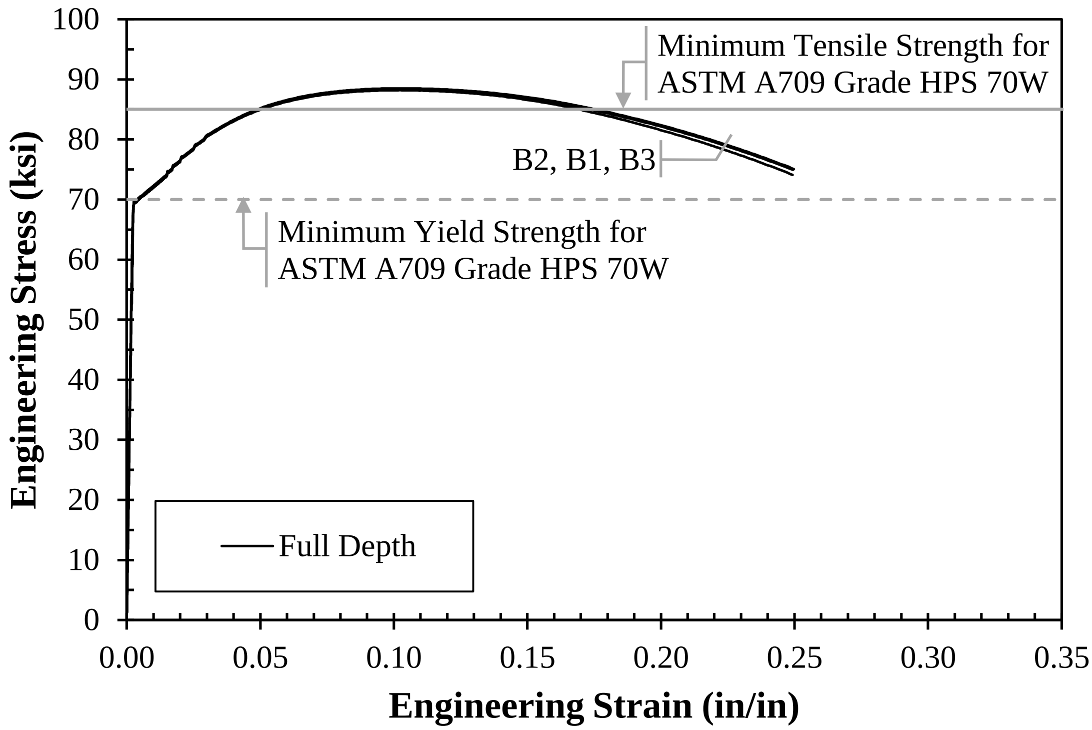

Figure 4.9. Engineering stress versus strain curve for BMP S type specimens with L orientation

Figure 4.10 shows the stress versus strain curve for the BMP round (R) type specimens in the L orientation. During testing of specimens B6 and B7, the software controlling the test stopped working and had to be restarted. The restart was done during the yield plateau portion of the test. Since the dimensions of the plate allowed for spare specimens to be manufactured, three additional specimens were tested just in case the data would not be usable. The data was processed several weeks later, which is the reason for replacing just the two tests with problems, and an extra new one for testing. After the data was processed, it was observed that the original data from the two samples (B6 and

B7) was in fact accurate and useful, hence the reason it is reported herein. The average yield strength of the BMP R type specimens in the L orientation was 70.2 ksi, the average ultimate tensile strength was 88.3 ksi and the average static yield strength was 67.6 ksi.

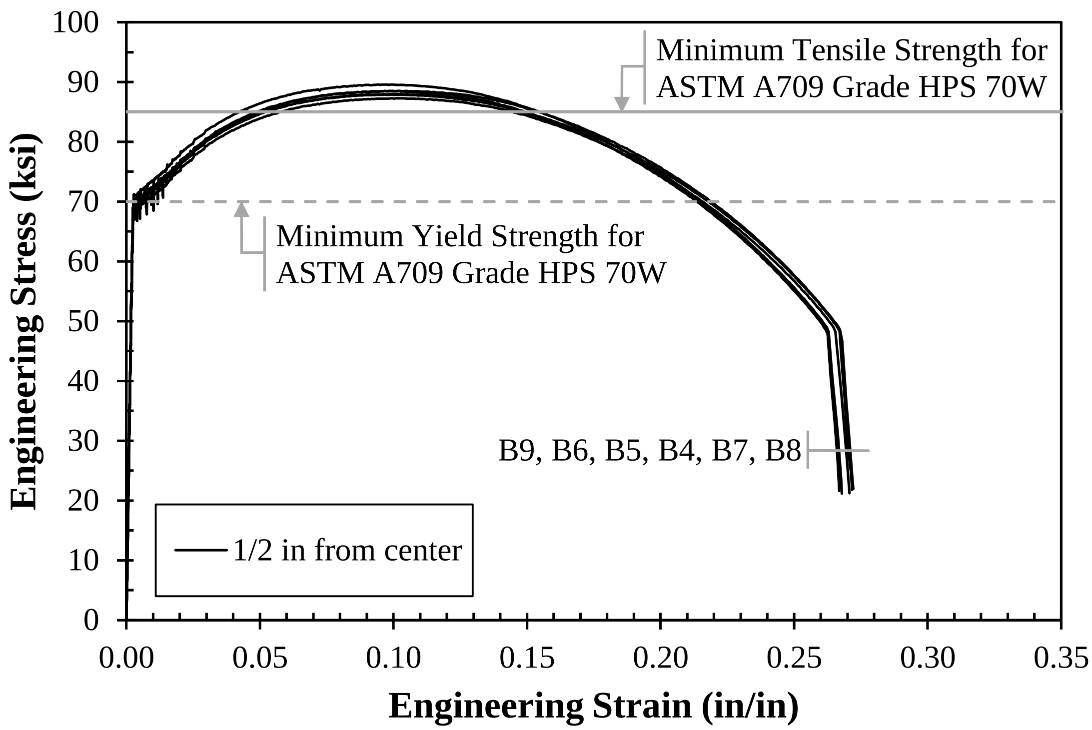

Figure 4.10. Engineering stress versus strain curve for BMP R type specimens with L orientation

The reduced round (RR) type specimens, because of their reduced dimension, allowed tensile testing on specimens sampled at 1/8 in from the center of the plate, the core, and 5/8 in from the center and the surface as presented in Figure 3.28. The resulting stress versus strain plots are presented in Figure 4.11. In this figure, the plots and labels for the samples taken at 1/8 in from center are shown in red, while the plots for the specimens sampled at 5/8 in are shown in black. Specimens B16, B17 and B18 were sampled at 5/8 in. The average yield strength for these specimens was 71.3 ksi, the average tensile strength was 89.6 ksi and the average static yield strength was 68.8 ksi. Specimen B17 exhibited a higher yield and tensile strength than all the other specimens at 72.8 ksi yield strength and 90.9 ksi ultimate tensile strength. The specimens sampled at 1/8 in were B19, B20 and B21. The average yield strength of these specimens was 70 ksi, the average tensile strength 89 ksi and the average static yield strength was 67.7 ksi. The average yield strength of the surface specimens is 4% higher than those sampled at the core due to the high strength of B17. The same is true for the ultimate strength, where the surface specimens are 2.1 % stronger. Specimens B16 and B18, which were sampled at 5/8 in, are in strong correlation to the specimens sampled at 1/8 in B19, B20 and B21 for both yield strength and ultimate strength. While the differences are not wide, they however suggest a slightly higher tensile strength towards the surface of the material.

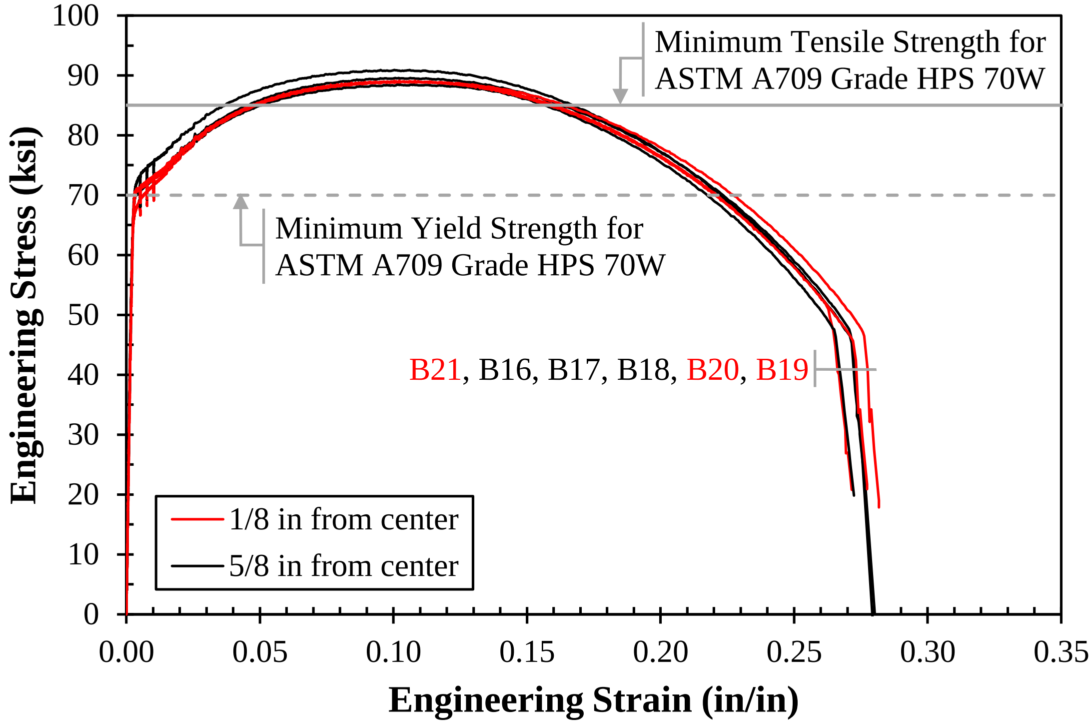

Figure 4.11. Engineering stress versus strain curve for BMP RR type specimens with L orientation

The stress versus strain curves for typical specimens of each geometry are presented in Figure 4.12. The plots are in strong relationship and prove the effectiveness of ASTM E8 in estimating tensile strength properties regardless of specimen dimensions. The average elongation at fracture for all round specimens was 27.28% with a very low standard deviation of just 0.58. The average elongation of the S specimens was 33.66% resulting in over 20% more strain at fracture than on the reduced round specimens. This can be observed in Figure 4.12 even as the curve for the S specimen is not complete. A reasonable conclusion can be drawn from these results as to the effect of the geometry and dimensions of specimens on the test results. ASTM E8 is justly calibrated to provide an accurate depiction of the ultimate strength properties of the material to the detriment of the elongation and strain at fracture which are of little importance in construction and design.

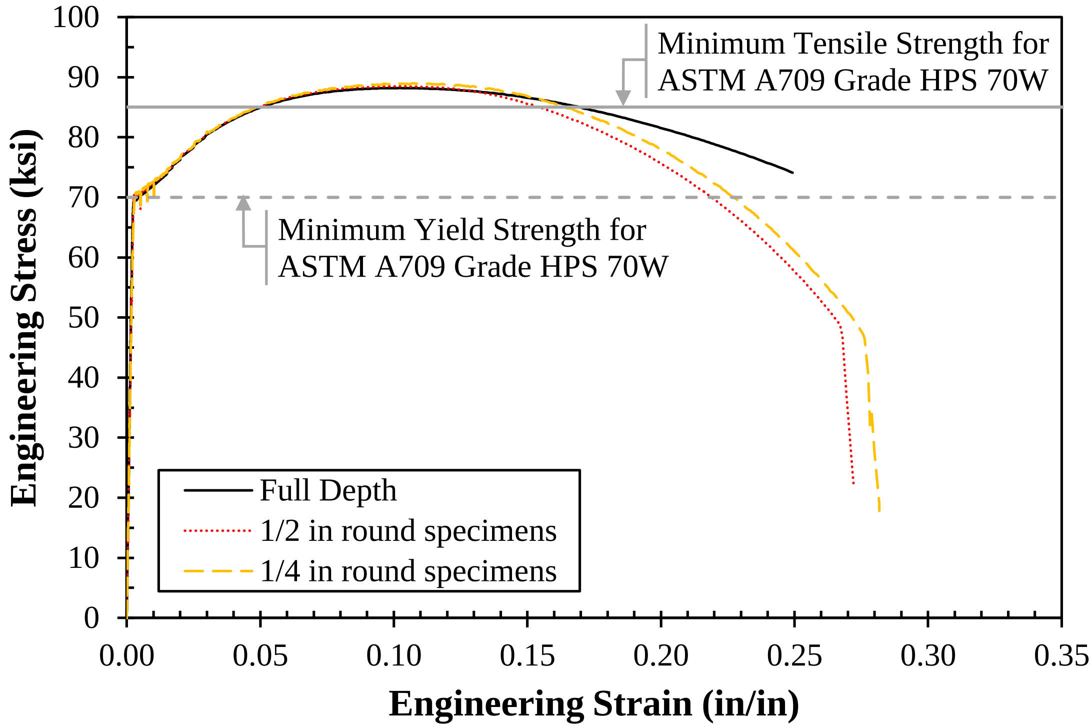

Figure 4.12. Engineering stress versus strain curve for typical average L orientation BMP tensile specimens

4.3.1.2. BMP Tensile Specimens in the T Orientation

The plots showing engineering stress versus strain for the tensile specimens sampled in the (T) orientation, transverse to DOR, are presented in Figure 4.13 and Figure 4.14. Only specimens of round (R) and reduced round (RR) geometry were manufactured on the T orientation. These specimens provided an accurate characterization of the tensile properties of BMP. No S specimens were sampled on the BMP since there is no similar WPS specimen requirement in the transverse orientation.

Figure 4.13 presents the engineering stress versus strain plots for the R specimens in the T orientation. The average yield strength of the specimens was 72.6 ksi, the average tensile strength 90.9 ksi and the average static yield strength was 70.2 ksi.

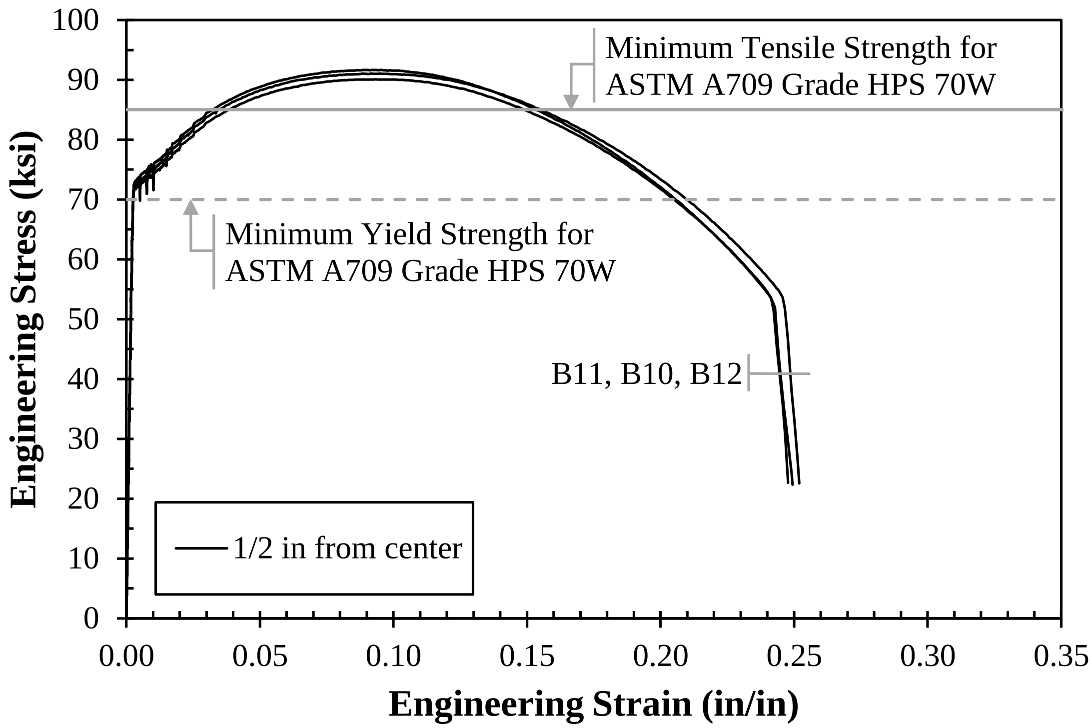

Figure 4.13. Engineering stress versus strain curve for BMP R type specimens with T orientation

The RR specimens in the T orientation were sampled as shown in Figure 3.28 at 1/8 in and 5/8 in respectably from the center. Figure 4.14 presents the engineering stress versus strain plots for the RR specimens in the T orientation. The average yield strength of the core specimens was 72.8 ksi and the average tensile strength 91.0 ksi. The static yield was not measured on these samples. For the surface specimens, the average yield strength was 70.3 ksi and the average tensile strength 90.3 ksi. Static yield was measured on specimens B23 and B24 and the average value was 69.2 ksi. Both the yield and ultimate tensile strength of the core specimens in the T orientation are marginally higher by not more than 1% of the T core and all L specimens.

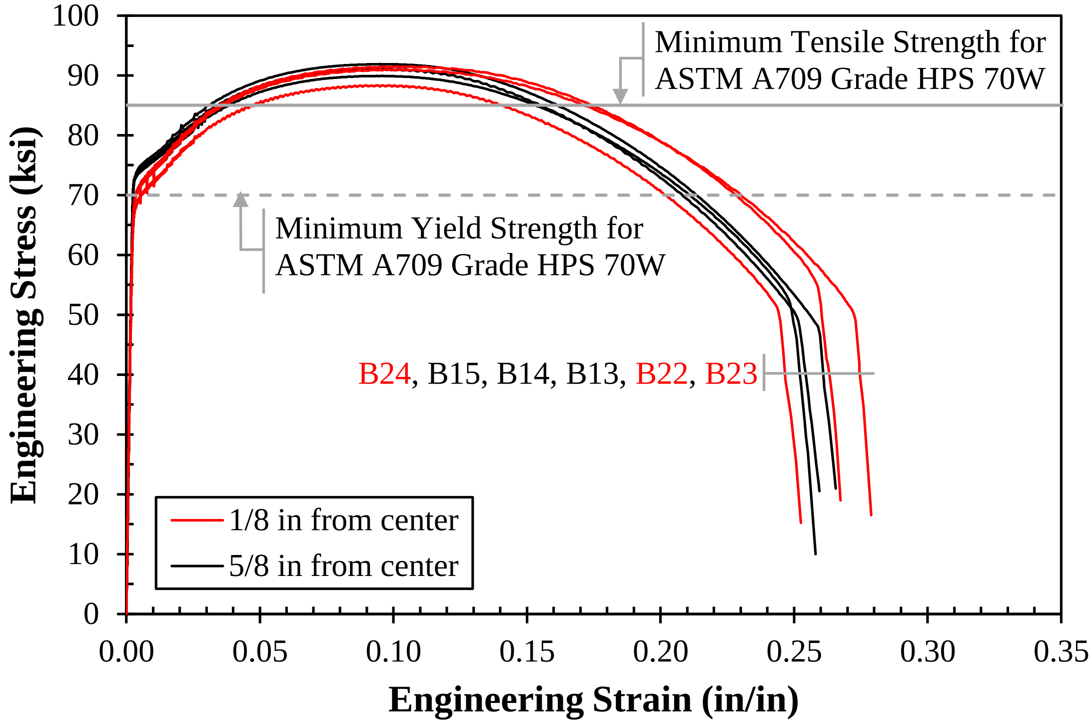

Figure 4.14. Engineering stress versus strain curve for BMP RR type specimens with T orientation

4.3.2. Plate A Tensile Tests

The results of the tensile tests performed on the PA are tabulated in Table 4.3. On specimens W1 and W2 no static yield analysis was performed in order to match the testing procedure used to test the BMP S type specimens B1, B2 and B3. All other PA tensile specimens were subjected to static holds.

Table 4.3. Tensile tests results on PA

ID	Type	Orientation	Modulus	Yield Stress	SYS	Ultimate Tensile Strength	Elongation	Area Reduction
			(ksi)	(ksi)	(ksi)	(ksi)	%	%
W1	S	L	26132	63.8	N/A	87.6	28	59
W2	S	L	25224	65.3	N/A	88.0	28	59
W3	R	L	28077	68.8	65.5	88.2	27	68
W4	R	T	29598	68.3	65.6	88.2	27	66
W5	R	T	30758	69.5	66.8	89.7	26	67
W6	R	T	30064	66.6	64.0	87.1	27	68
W7	RR	T	31526	68.0	64.5	88.2	27	70
W8	RR	T	28893	67.8	65.2	88.8	31	74
W9	RR	T	29384	65.0	62.8	86.6	30	66

AWS does not have a requirement for minimum yield and ultimate tensile strength for ESW-NG applied on HPS70W steel. However, AWS provides minimum yield and ultimate tensile strength values for all other welding methods when using HPS70W. They are 70 ksi and 90 ksi, respectably, for the filler material. As such, these values will be utilized in this research as the minimum limits for the ESW-NG weld. This is a reasonable assumption because for all other qualified steel grades the minimum strength values agree between all welding methods, including ESW-NG. None of the tested specimens from PA reached the minimum yield and tensile strength limits.

4.3.2.1. PA Tensile Specimens in the L Orientation

The stress versus strain plots for the two S type specimens sampled from PA in the L direction are shown in Figure 4.15 and Figure 4.17. No RR type specimen was tested in this direction.

The plots for the S type samples shown in Figure 4.15 show strong correlation between the two specimens. In the same manner as the BMP S type tensile tests, the strain measurements were recorded using a regular extensometer with a maximum capacity of 0.25 in/in strain at a 4 in gage length resulting in a plot that does not cover the full curve until rupture. The average yield strength of specimens W1 and W2 was 64.5 ksi and the average tensile strength was 87.8 ksi. The average yield strength of these specimens is 5.5 ksi below the minimum allowed yield strength. The average ultimate tensile strength is 2.2 ksi below what was deemed acceptable in this research, but is worth mentioning that the tensile strength of W1 and W2 is above the minimum required by ASTM A709. Typically for welded tension specimens, the expectation is that the specimen fails in the base metal or at FL and the ultimate strength of the weld be higher than that of BMP. Both of the S type specimens exhibited rupture at the center of the weld and not at FL or within base metal. This is shown in Figure 4.16, which presents specimen W1 after testing.

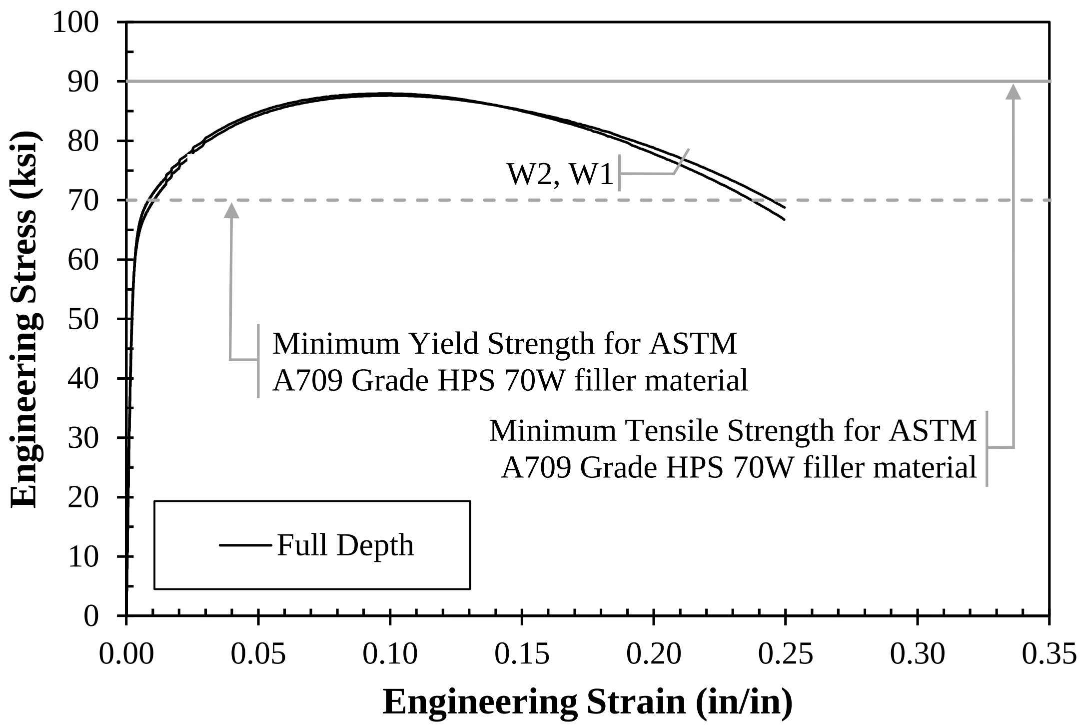

Figure 4.15. Engineering stress versus strain curve for PA S type specimens with L orientation

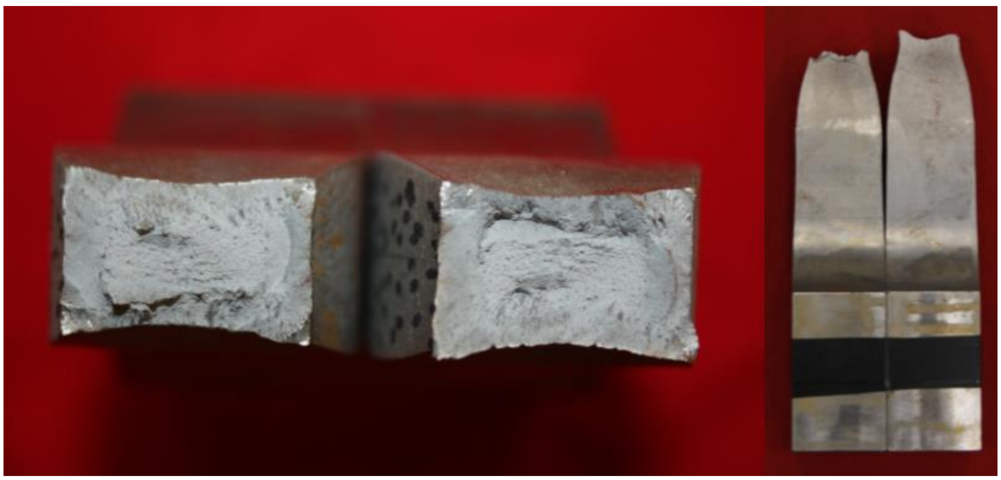

Figure 4.16. Specimen W1 after testing

Only one R type specimen (W3) originating from PA was tested in the L direction. Specimen W3 was manufactured, as mentioned in section 3.3, to explore the possibility of using smaller and more affordable testing apparatus. Only one specimen was tested because re a very small section of the testing plate was left at this point, which did not allow manufacturing additional specimens. The stress versus strain plot for specimen W3 is shown in Figure 4.17. The yield stress recorded from the sample was 68.8 ksi, 4.3 ksi higher than the average value from W1 and W2. The ultimate tensile strength of the specimen was 88.2 ksi, which is very close to the average of the S type specimens of 87.8 ksi.

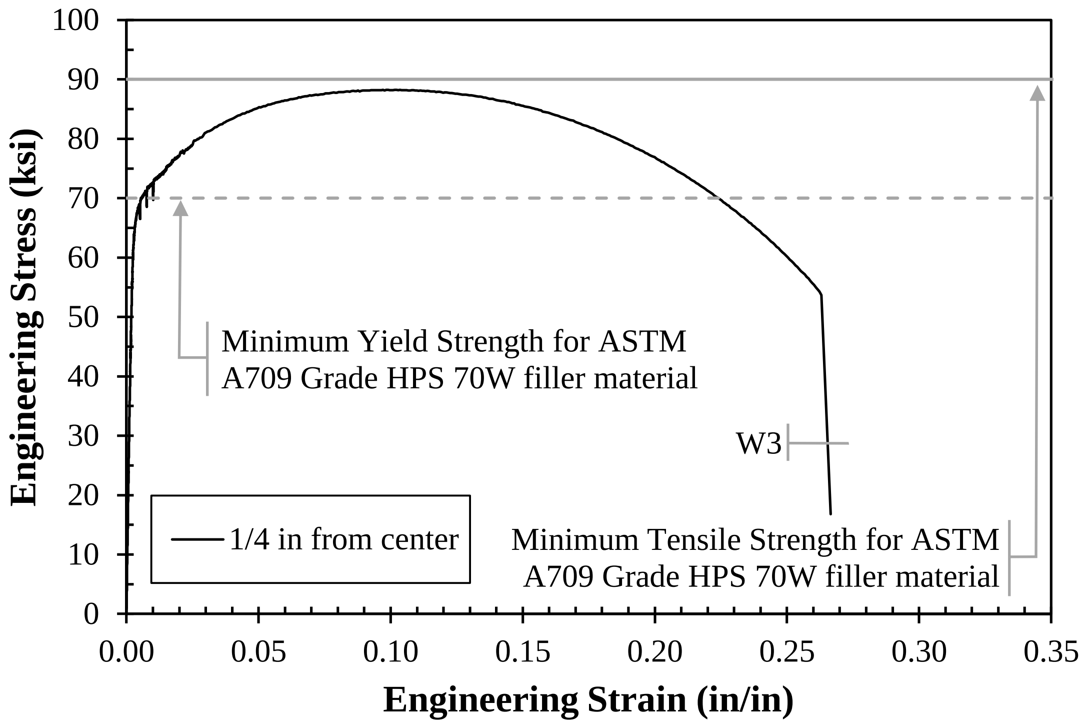

Figure 4.17. Engineering stress versus strain curve for PA R type specimens with L orientation.

A comparison between the stress versus strain curves of W1 and W3 is presented in Figure 4.18. The major difference in behavior between the two specimen types is noticeable at yield. The tensile curve after yield and the tensile strength are in close correlation. Although there are differences between the behavior of the S and R type specimens, since there was only one R type specimen tested, a reasonable conclusion cannot be drawn about the possibility of using smaller specimens for tension testing transverse to the weld. The difference in behavior at yield could be attributed either to the size of the specimen, or it could be just a difference in the composition of the weld at that location along the upward progression of the weld.

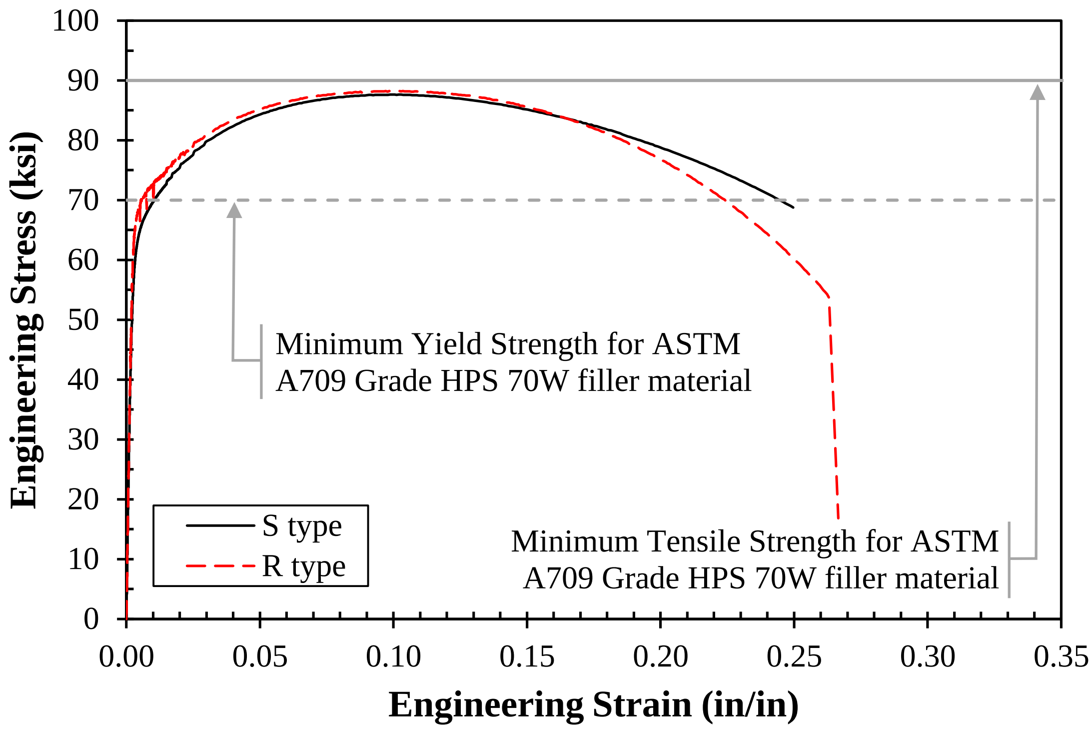

Figure 4.18. Engineering stress versus strain curve for representative L orientation PA tensile specimens

4.3.2.2. PA Tensile Specimens in the T Orientation

Two types of specimens were tested from PA in the T orientation. These were R and RR type specimens and the stress versus strain plots for these are presented in Figure 4.19 and Figure 4.20.

For WPS qualification one R specimen at center core of the weld must be tested. This specimen was specimen W6. Specimens W4 and W5 were positioned on either side of specimen W6 as shown in Figure 3.22. The average yield stress for these specimens was 68.1 ksi, the static yield was 65.5 ksi and the ultimate tensile strength 88.4 ksi. The tensile strength of these specimens is comparable to the BMP, while the yield values fall short of the desired results.

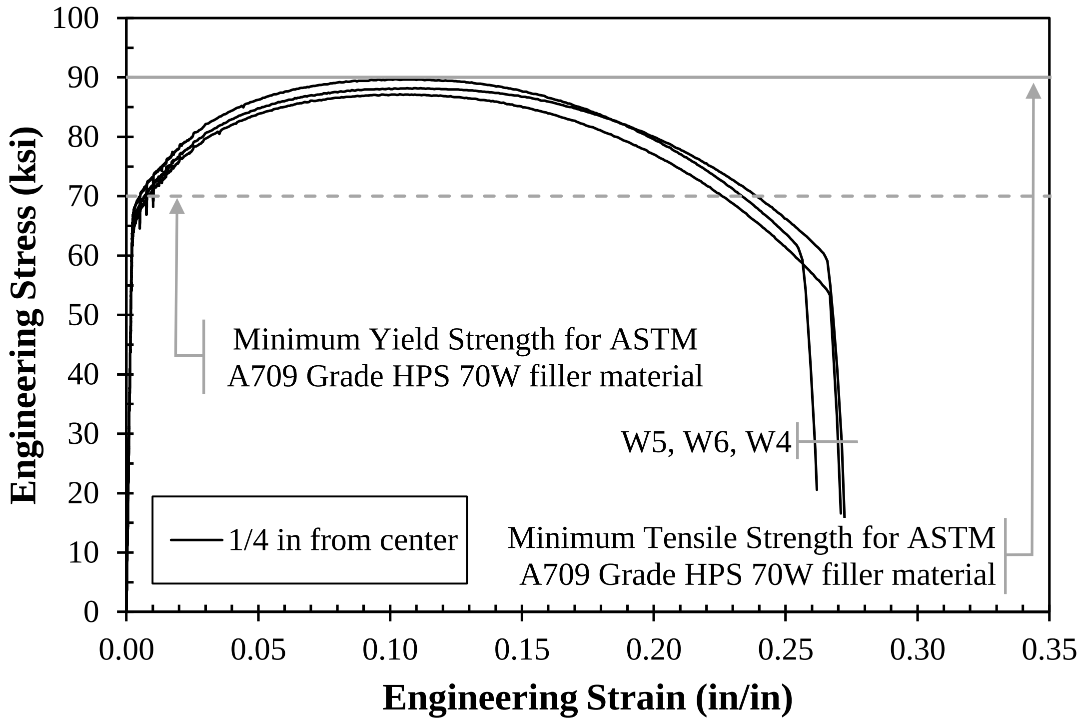

Figure 4.19. Engineering stress versus strain curve for PA R type specimens with T orientation

The reduced round (RR) specimens, W7, W8 and W9, had an average yield strength of 66.9 ksi, an average static yield of 64.2 ksi and an average ultimate tensile strength of 87.9 ksi. These values are close to the R type specimens, indicating that the statement made in section 3.3 about smaller specimens accurately depicting tensile properties is valid. The stress versus strain plots for these specimens are presented in Figure 4.20. Specimen W8 exhibited a much higher strain at rupture than the other two specimens.

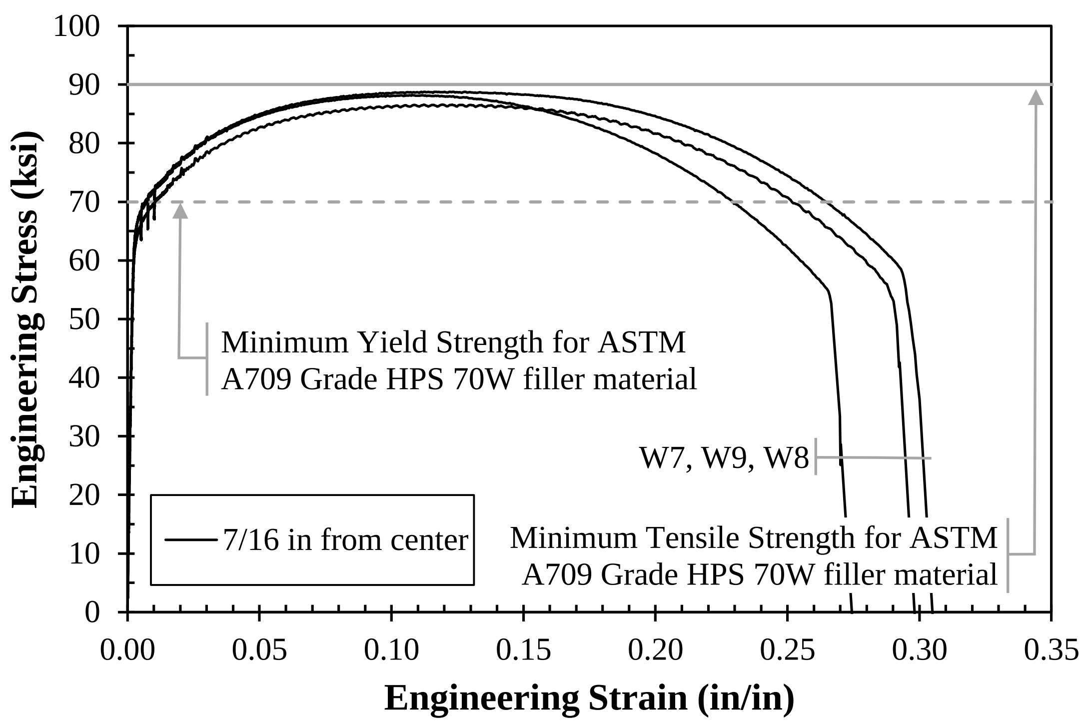

Figure 4.20. Engineering stress versus strain curve for PA RR type specimens with L orientation.

A comparison plot between W6 and W9 is presented in Figure 4.21 to showcase the similarities between the R and RR type specimens. The stress versus strain curves are similar until the ultimate stress, the RR type specimens exhibits longer elongation afterwards.

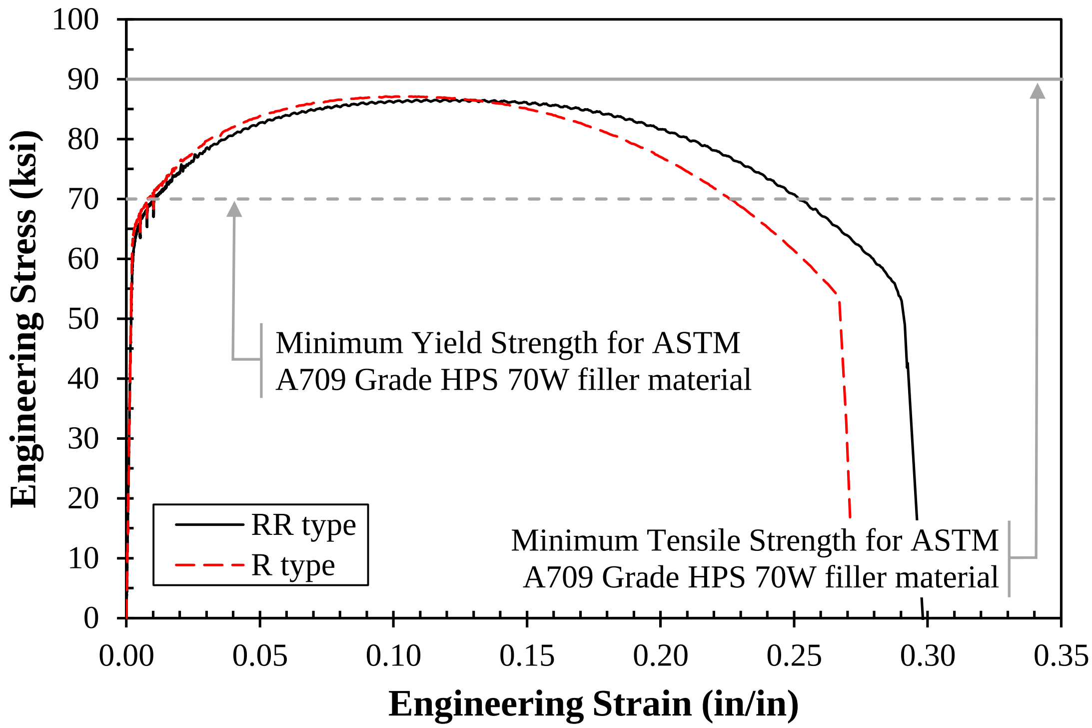

Figure 4.21. Engineering stress versus strain curve for representative T orientation PA tensile specimens.

4.3.3. Plate B Tensile Tests

The only types of tensile tests performed on plate B (PB) were those required for WPS qualification, S type in L orientation and R type in T orientation. Table 4.4 presents the results of these tensile tests. As for BMP and PA, no static holds were performed on the S type specimens, W10 and W11. All other PB tensile specimens were subjected to static holds.

Table 4.4. Tensile tests results on PB

ID	Type	Orientation	Modulus	Yield Stress	SYS	Ultimate Tensile Strength	Elongation	Area Reduction
			(ksi)	(ksi)	(ksi)	(ksi)	%	%
W10	S	L	26085	63	N/A	87.4	27	62
W11	S	L	25139	63.5	N/A	88.1	16	59
W12	R	T	30767	70.8	67.9	92	19	31
W13	R	T	29987	70.4	68.1	81	11	8
W14	R	T	29979	72	68.6	93.5	27	63
W15	R	T	-	-	-	28.4	-	-
W16	R	T	31471	71.3	68	75.9	7	18

4.3.3.1. PB Tensile Specimens in the L Orientation

Figure 4.22 presents stress versus strain diagrams for specimens W10 and W11. Specimen W10 broke at the center of the weld and exhibited a slight area reduction in the heat affected zone (HAZ). Specimen W11 broke suddenly at the fusion line (FL) after only 16% elongation. The specimen is illustrated in Figure 4.23. Neither one of the two specimens reached the required strength. The average yield strength recorded was 63.3 ksi and the average ultimate tensile strength was 87.8 ksi.

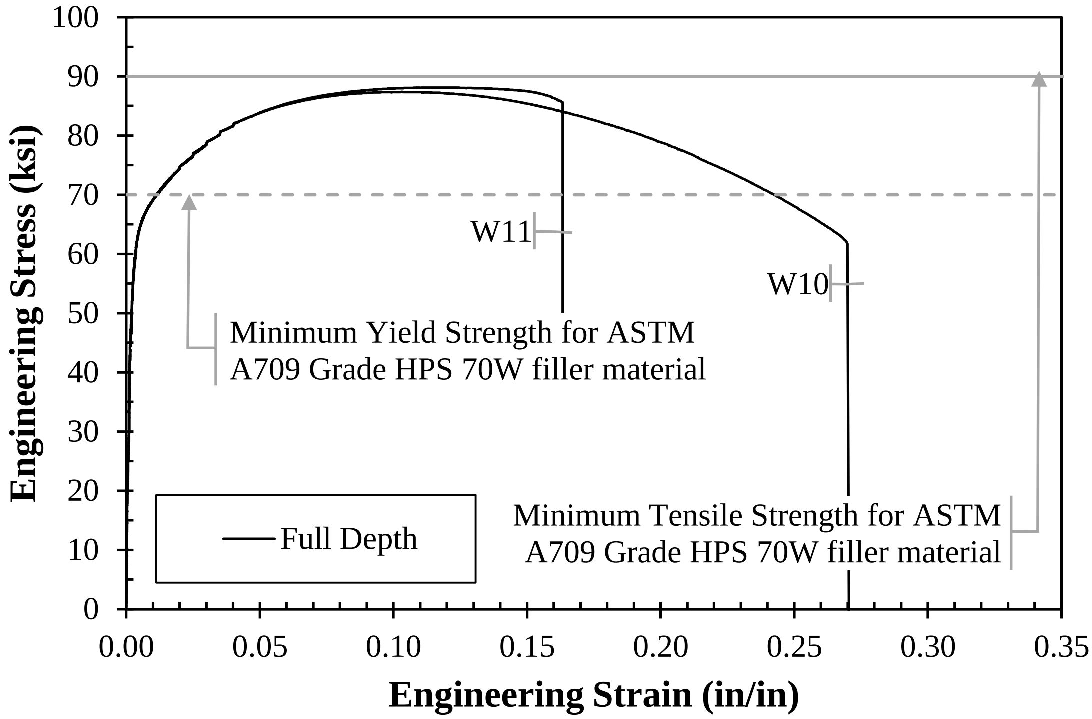

Figure 4.22. Engineering stress versus strain curve for PB S type specimens with L orientation.

Figure 4.23. Specimen W11 after testing.

4.3.3.2. PB Tensile Specimens in the T Orientation

Five R type specimens were tested in the T orientation. Specimens W12 and W14 both satisfied the minimum yield and ultimate tensile strength from AWS. Specimen W13 and W16 satisfied the minimum yield requirements from AWS, but had ductile failure shortly thereafter, well below the 90 ksi threshold. Specimen W15 failed suddenly at 28.4 ksi. Specimen W12 is shown in Figure 4.24. All the R type specimens tested from PB displayed the same typical, diagonal and repetitive failure pattern. An illustration of W14 is also shown in Figure 4.25. The reason for the abrupt failures in the samples is most probably due to poor weld quality in the area where the coupons were sampled. These specimens will be investigated at a later date at Turner Fairbanks Highway Research Center (TFHRC) in an effort to pinpoint the exact cause of failure.

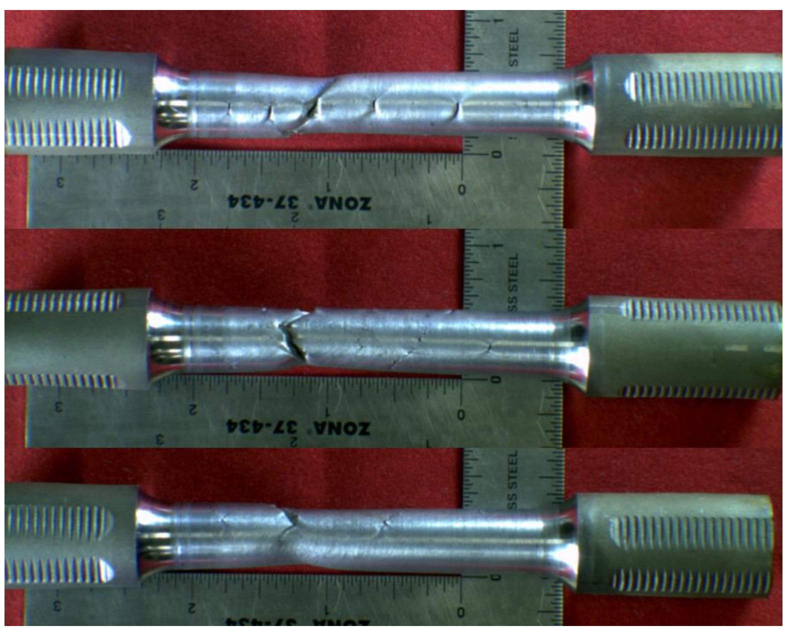

Figure 4.24. Specimen W12 after testing.

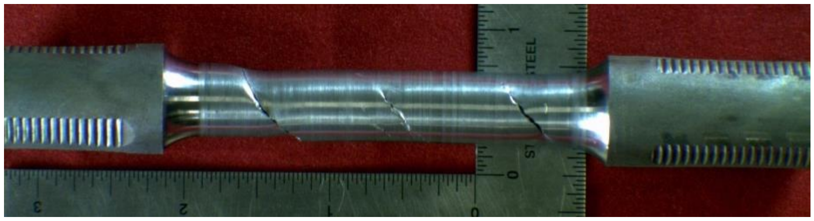

Figure 4.25. Specimen W14 after testing.

The engineering stress-strain curves for the R type specimens sampled from PB are presented in Figure 4.26.

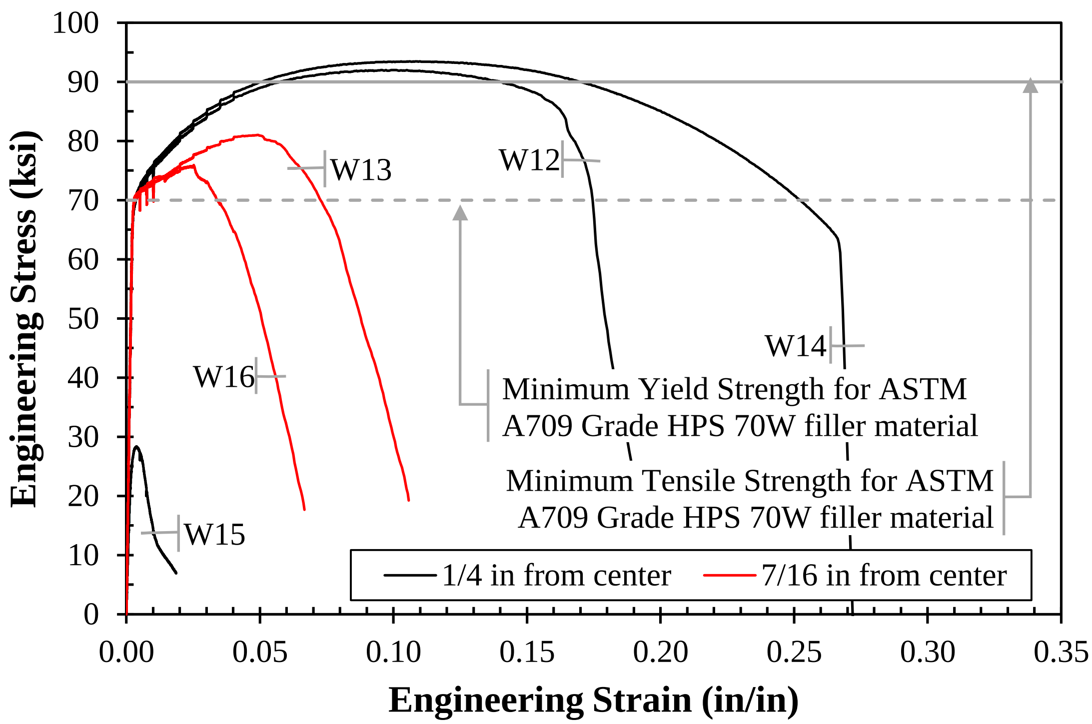

Figure 4.26. Engineering stress versus strain curve for PB R type specimens with T orientation.

4.4. Toughness Testing Results

Toughness results are presented in this section, organized per plate and sampling location. The specimens as well as the recorded tested values are presented in

Appendix B: Toughness Testing Data. All the specimens were tested according to the provisions stated in section 3.9. The measured lateral expansion values are shown in

Appendix B: Toughness Testing Data.

4.4.1. Base Metal Testing Plate Toughness Testing Results

In order to obtain a reliable transition curve portraying the toughness properties of the HPS70W plate used in this investigation, a spread of specimens was tested at temperatures ranging from -100º F to +70º F. A minimum of three specimens were tested at each temperature and the data was then input in a hyperbolic function regression as presentenced in section 2.4 to obtain the transition curves. A minimum of 27 specimens was tested for each orientation and location. In the transition zone where the data was scattered, more specimens were tested in order to produce a better model. The resulting curves and the specimen data are plotted in Figure 4.27 to Figure 4.30. The location of each specimen within depth is presented in Figure 3.39. The specimens designated LT are sampled in the L orientation, aligned to DOR, with the notch transverse to DOR. The TL specimens were transverse to DOR with the notch aligned to DOR.

The significant properties of the transition curves are shown in Table 4.5. The curve for TL-surface stands out with the lowest upper energy shelf and a very short transition range. ASTM A709 sets the lower bound for HPS70W fracture critical components as 35 ft-lbs at -10º F. All the specimens tested satisfy the requirements from ASTM A709 for minimum toughness at -10º F. In lieu of the average required by the ASTM, the value provided by the regression curve was used for comparison.

Table 4.5. Transition curve properties

Type	Location	Lower Shelf Energy	Upper Shelf Energy	Energy at -10 ºF	Temperature inflection point	Temperature range of transition
		(ft-lbs)	(ft-lbs)	(ft-lbs)	(ºF)	(ºF)
LT	Surface	0.0	221.1	158.7	-33.0	49.2
LT	Core	12.7	192.5	46.6	22.6	44.7
TL	Surface	25.6	152.2	59.4	-0.7	18.4
TL	Core	2.8	169.4	43.5	24.1	60.4

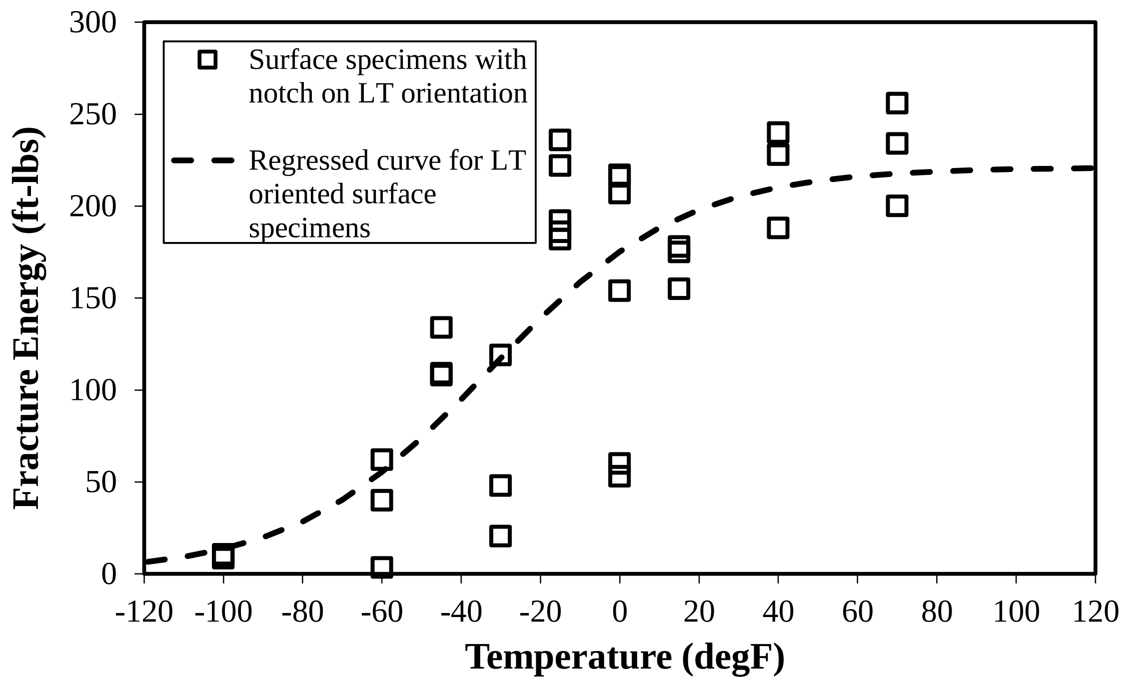

Figure 4.27. BMP LT surface toughness specimens

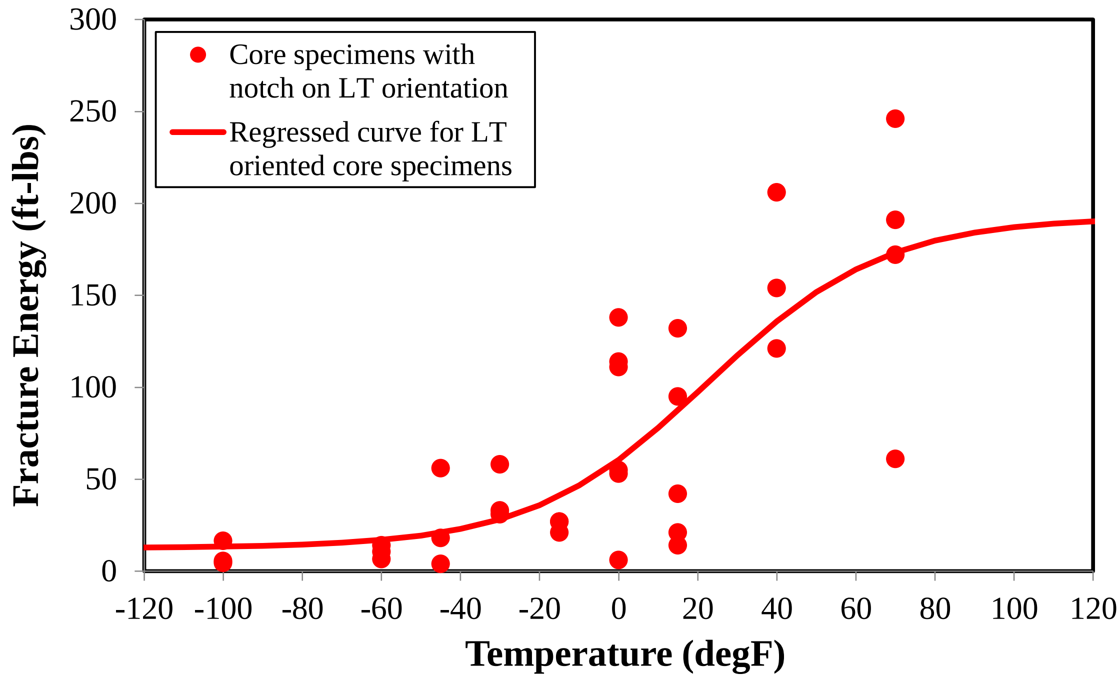

Figure 4.28. BMP LT core toughness specimens

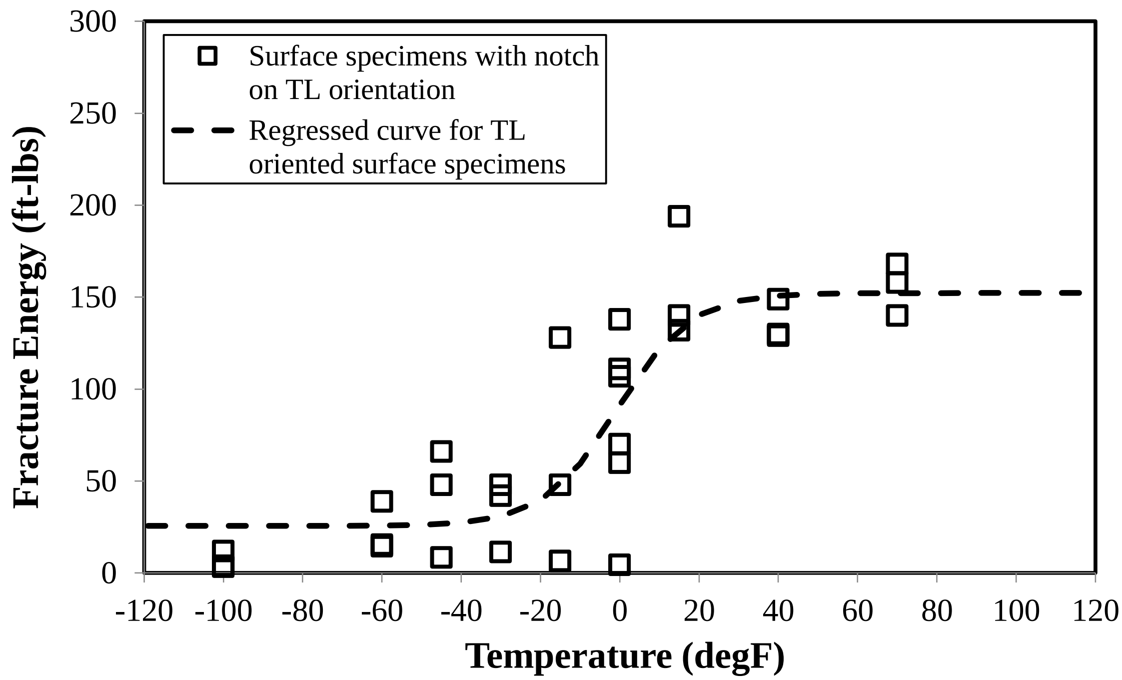

Figure 4.29. BMP TL surface toughness specimens

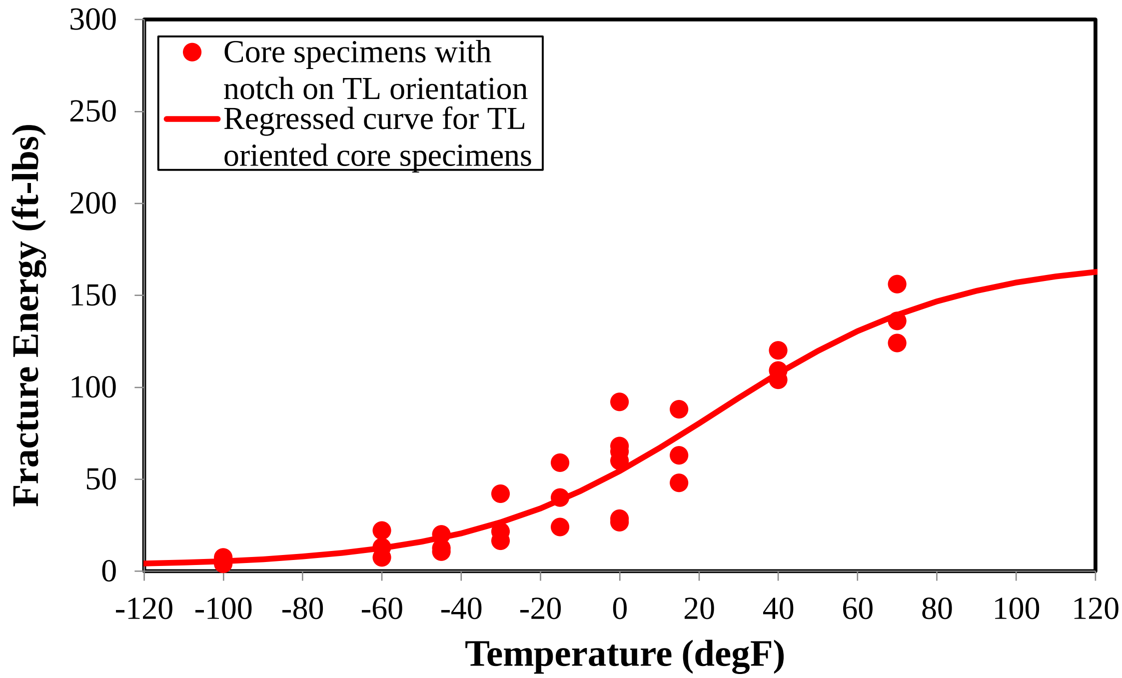

Figure 4.30. BMP TL core toughness specimens

Due to the orientation of the notch and specimens required for WPS qualification, the LT direction curves were used for comparison with the results from plates PA and PB. Steel toughness is influenced by the size of the grain and direction of roll. As such, the toughness values between the two orientations will differ. A steel plate, due to its geometry and the manufacturing process, will have a grain alignment better suited for higher toughness in the LT direction. It is expected that the toughness values from testing in the LT direction be higher than the TL direction. Our testing once again confirmed this behavior.

4.4.2. Plate A Toughness Testing Results

As a result of the reduced size of PA and the welding issues associated with the production of the welded plate, no regression analysis was performed. Instead of focusing on the toughness analysis, the samples were used to perform a comparison between side A1 and side A2 of the plate to learn about how the welding current flow influenced the toughness properties.

The specimens at the weld center were not indexed per plate side due to their location. Three samples were tested at the temperature and location required by AWS D1.5. It is noted that AWS requires eight CVN tests at center core of the WPS, and the total number of samples tested here did not satisfy that requirement. The average absorbed energy of the core specimens was 25.16 ft-lbs, above the limit of 25 ft-lbs set by AWS for CVN's tested at -10º F. Additional specimens were tested at -60º F and 70º F with the intent to locate the transition zone and lower shelf fracture energy behavior of the weld. This proved to be useful when calibrating the temperature test matrix for PB. The results are presented in Figure 4.31.

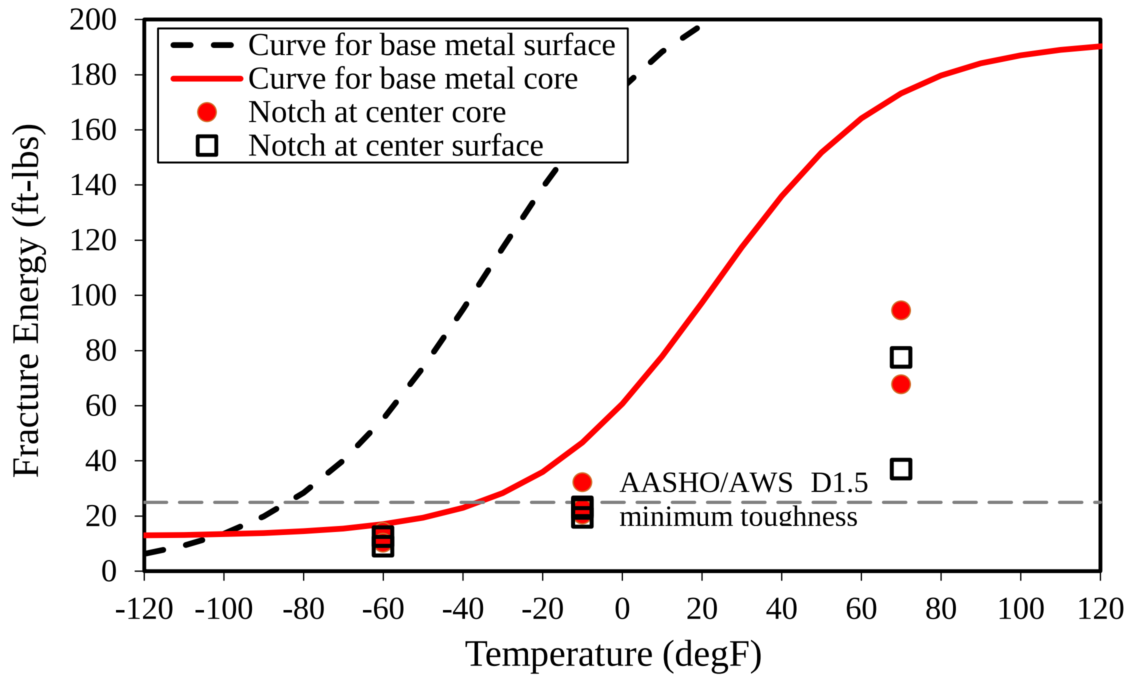

Figure 4.31. PA toughness specimens sampled at center.

The specimens sampled at FL are presented in Figure 4.32. The same principles used for choosing the test temperature for PA core were applied here. Two specimens per side were tested at each temperature at core and surface. The average energy of the specimens tested at -10º F is presented in 0. None of the results or average results was above the AWS minimum requirement 25 ft-lbs at -10º F.

Table 4.6. Average absorbed energy at FL for -10° F test temperature.

Side	Location	Average Energy (ft-lbs)
A1	Surface	16.50
A1	Core	8.25
A2	Surface	10.88
A2	Core	16.00
Both	Surface	13.69
Both	Core	12.13

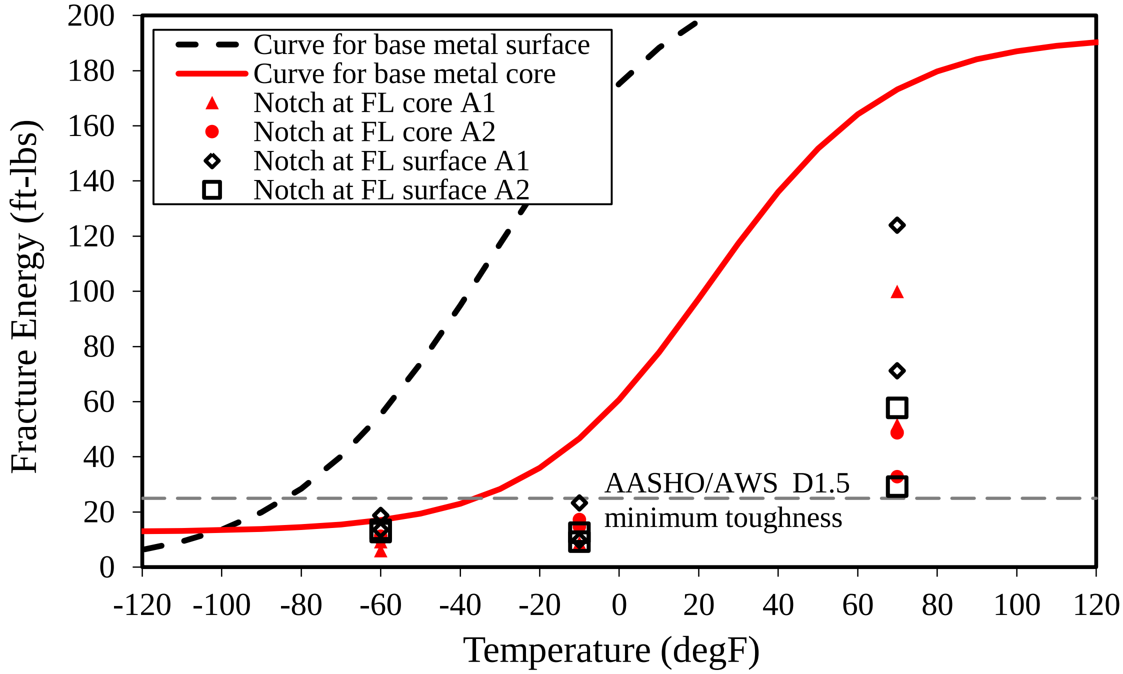

Figure 4.32. PA toughness specimens sampled at FL.

The samples tested at 0.04 offset had a much higher spread in the data than the ones at center and FL. The values suggest a transition curve with a lower upper shelf and a smaller transition area. The average energy of the specimens tested at -10° F is presented in Table 4.7. The results from the A2 side of PA were higher than those of the A1 side. The results for all specimens tested at 0.04 offset are plotted in Figure 4.33.

Table 4.7. Average absorbed energy at 0.04 offset for -10º F test temperature

Side	Location	Average Energy (ft-lbs)
A1	Surface	16.00
A1	Core	10.75
A2	Surface	20.13
A2	Core	39.88
Both	Surface	18.07
Both	Core	25.32

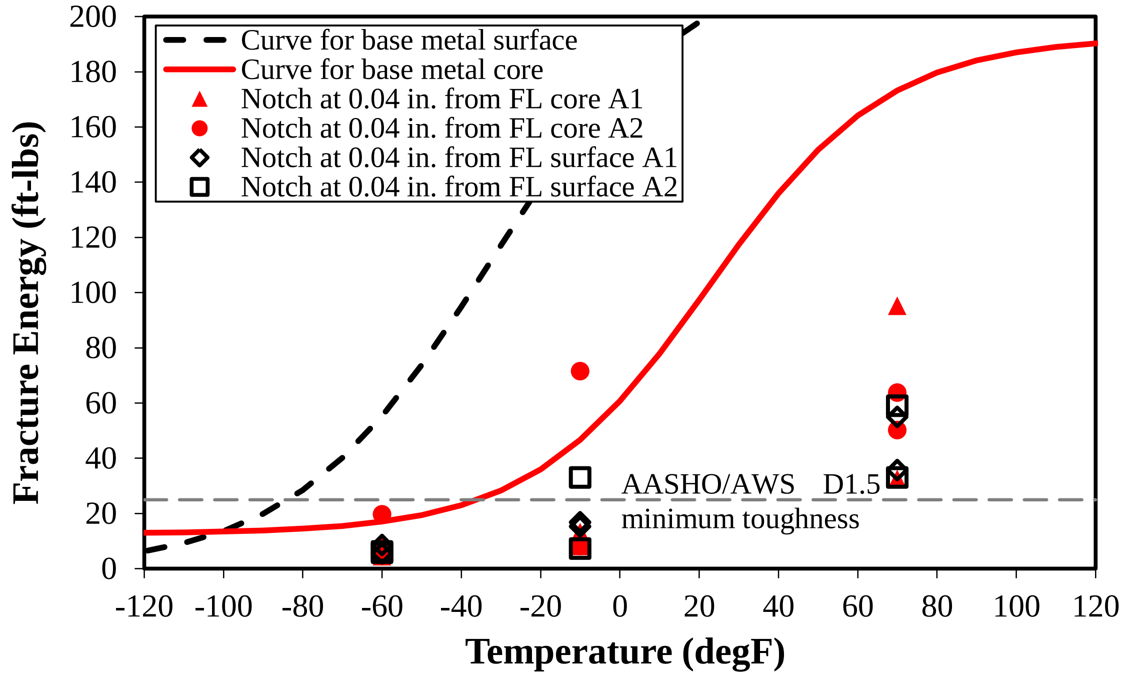

Figure 4.33. PA toughness specimens sampled at 0.04in offset from FL

4.4.3. Plate B Toughness Testing Results

For Plate B, toughness was investigated at center, FL, 0.04 in offset from FL and 0.1985 in offset from HAZ. The exact locations are shown in section 3.9.1.

For the center specimens, 10 CVN's were tested at the core and 10 more were tested at the surface, satisfying the minimum requirement criteria from AWS. The specimens were tested at -20º F, the temperature specified in AWS for AASHTO Temperature Zone III compliance. AASHTO specifies three temperature zones based on the location of the structure. Temperature Zone I is 0º F and above, Zone II is -1º F to -30º F and Zone III is -30º F to -60º F. These temperatures do not represent the testing temperature requirement for CVN in the lab, rather the climate consideration for design in each zone. The average results after removing the minimum and maximum values, as required by AWS, are presented in Table 4.8. The table also presents the lower shelf energy and the energy at -10º F obtained from the regression. There were no tests done at the upper temperature shelf. Therefor the upper shelf energy, temperature inflection point and range of transition were not determined. Due to the acceptable results obtained from PA, testing for the WPS CVN's of PB was done at -20º F. The hyperbolic regression allows for the -10º F to be extrapolated. AWS requires that the core center specimens be at least 25 ft-lbs at -20º F for AASHTO Zone III applications or at -10º F for AASHTO Zone I and II applications.

Table 4.8. Average absorbed energy at center for WPS

Location	Average Energy at -20º F	Energy obtained from regression at -10º F	Lower Shelf Energy
	(ft-lbs)	(ft-lbs)	(ft-lbs)
Surface	17.67	19.04	10.0
Core	23.96	26.11	21.4

The average toughness value for CVN core center at -20 º F is slightly lower than the requirement. The difference is marginal. Considering that there is no set lower limit for toughness of the weld in AWS, the finding is deemed acceptable. The regression values at -10 º F point to acceptance under Temperature Zone I and II conditions. Figure 4.34 and Figure 4.35 show plots of the tested specimens and regression curves. There is no requirement in AWS for testing surface specimens. These were tested in this research just to compare the difference between the toughness results at the different depths. The surface specimens exhibited much lower toughness values than the core specimens at both tested temperatures. The reason for the lower values is most probably the rapid reduction in heat at the time of welding from the direct contact with the cooling shoes. The rapid heat reduction was one of the problems with the early ESW welds and was investigated by FHWA as presented in Section 2.3.

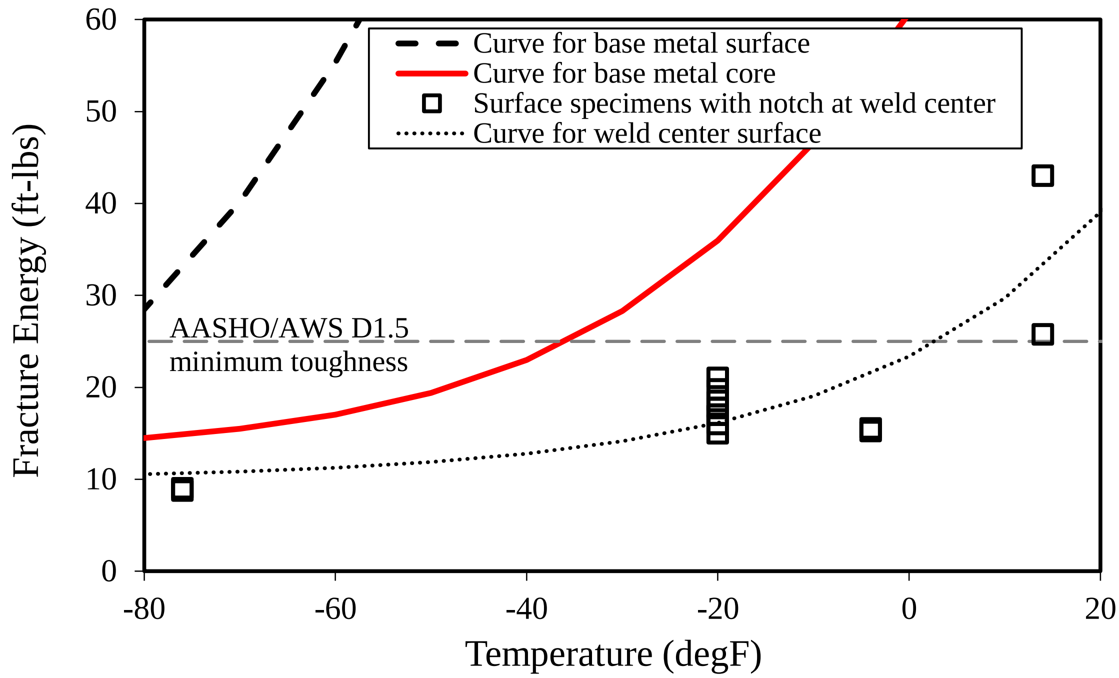

Figure 4.34. PB toughness specimens sampled at surface center

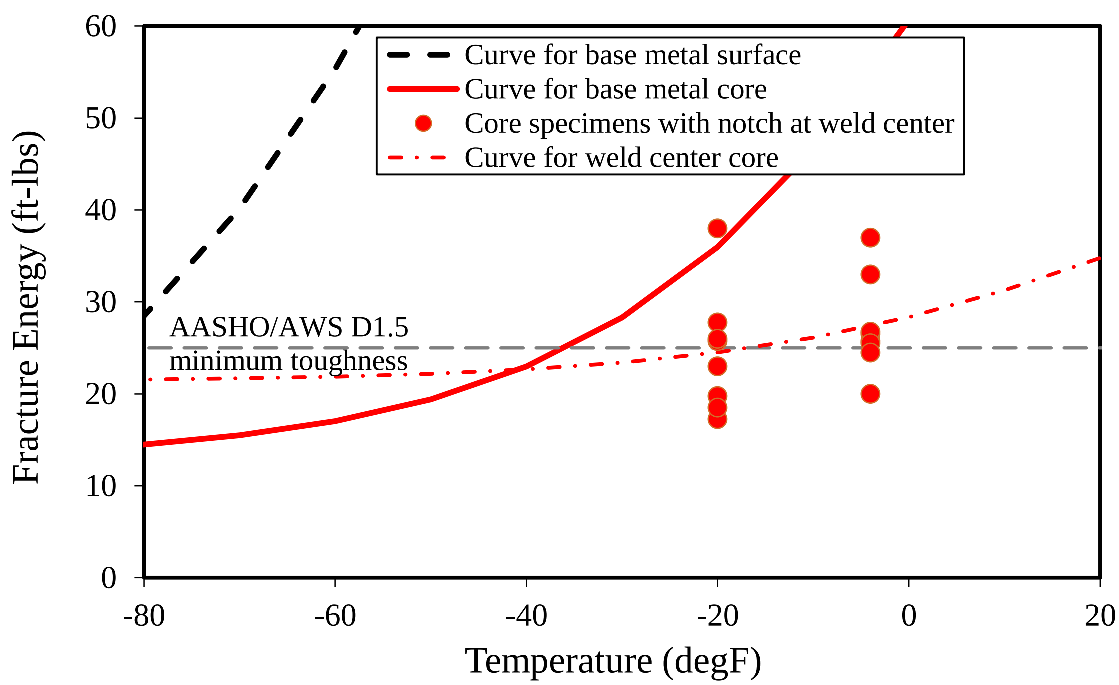

Figure 4.35. PB toughness specimens sampled at core center

The significant properties of the transition curves for FL, 0.04 offset from FL and 0.1985 offset from FL are presented in Table 4.9. The data obtained from these samples is very scattered. This is mainly due to the complex geometry of the finished weld and the very straight nature of the notch. Since the notch was positioned parallel to the center of the weld, the samples encompassed weld and HAZ material resulting in inconsistent and scattered data. To establish the upper shelf energy for the specimens located at FL core and surface, and those located at 0.04 offset from FL surface, more tests would have been required. For these, only the lower shelf energy at -10 °F was determined. However, the values in Table 4.9 provide a reliable picture for the toughness properties at the lower shelf. The PB toughness results are summarized in Figure 4.36 through Figure 4.41.

Table 4.9. Transition curve properties

Type	Location	Lower Shelf Energy	Upper Shelf Energy	Energy at -10 ºF	Temperature inflection point	Temperature range of transition
		(ft-lbs)	(ft-lbs)	(ft-lbs)	(ºF)	(ºF)
FL	Surface	2.1	-	16.7	-	-
FL	Core	21.6	-	30.5	-	-
0.04 offset	Surface	4	-	11.8	-	-
0.04 offset	Core	6.1	129.9	11.0	67.5	48.6
0.1985 offset	Surface	0	184.3	62.5	25.2	105.2
0.1985 offset	Core	24.2	205.5	63.6	27	67.7

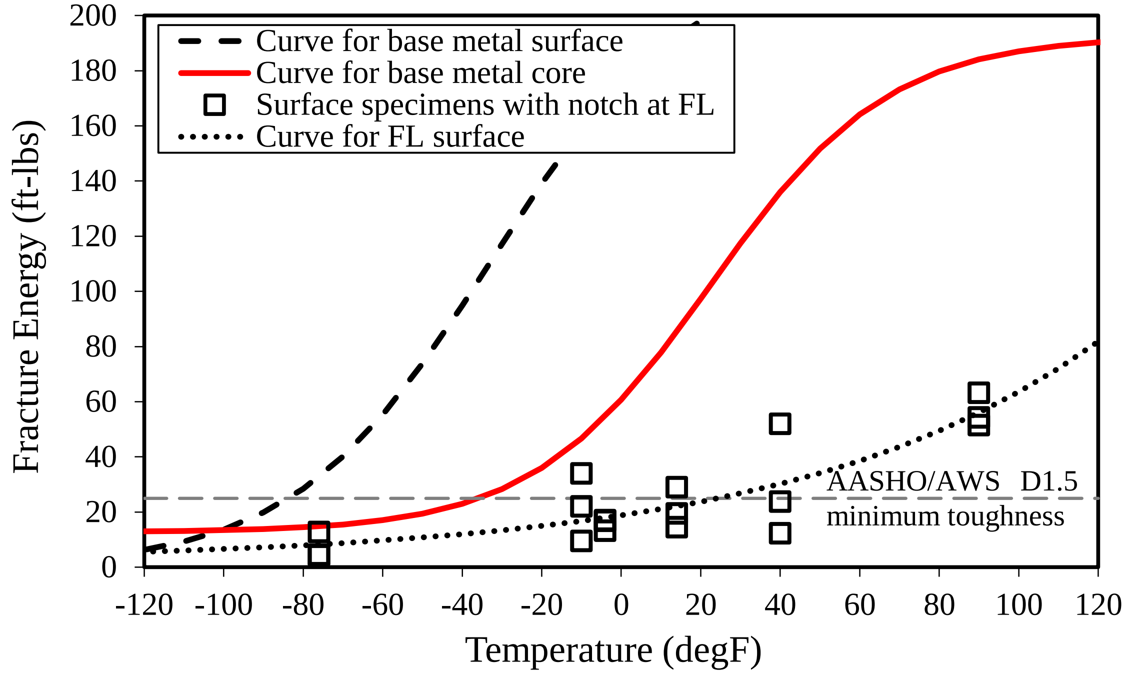

Figure 4.36. PB toughness specimens sampled at FL surface

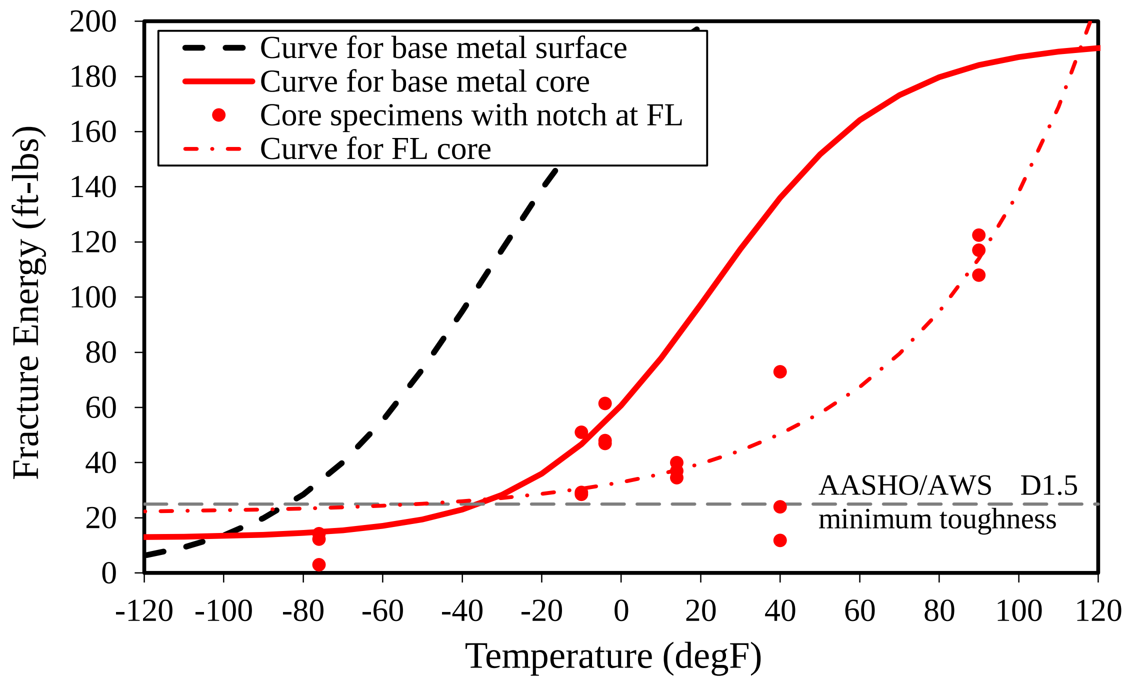

Figure 4.37. PB toughness specimens sampled at FL core

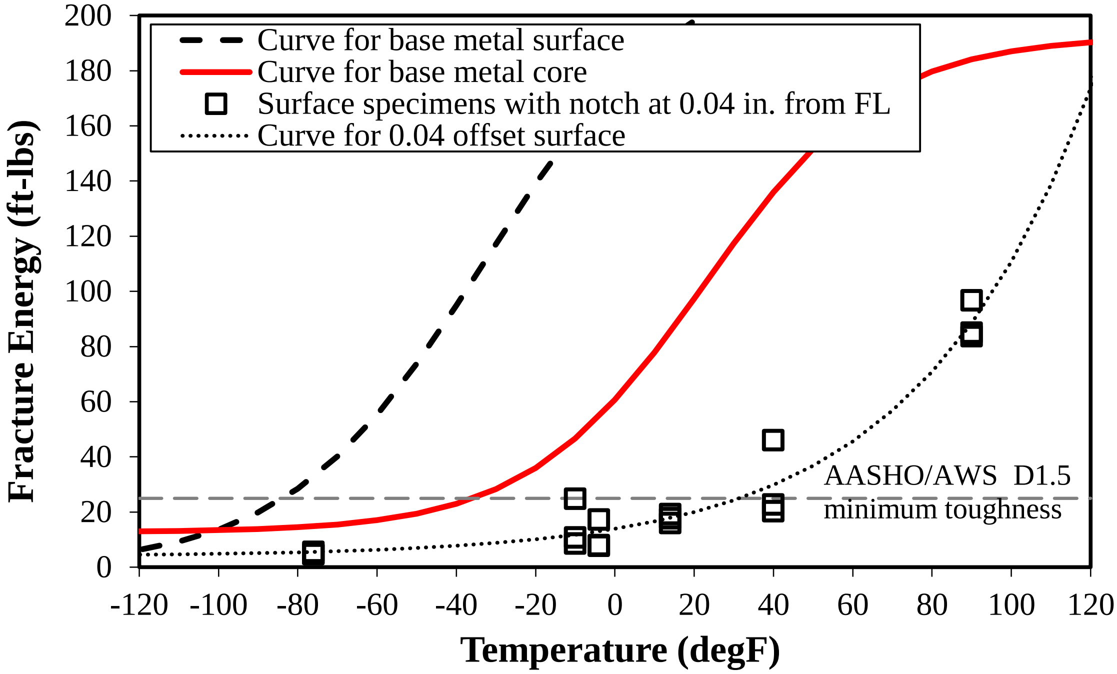

Figure 4.38. PB toughness specimens sampled at 0.04 in offset from FL surface

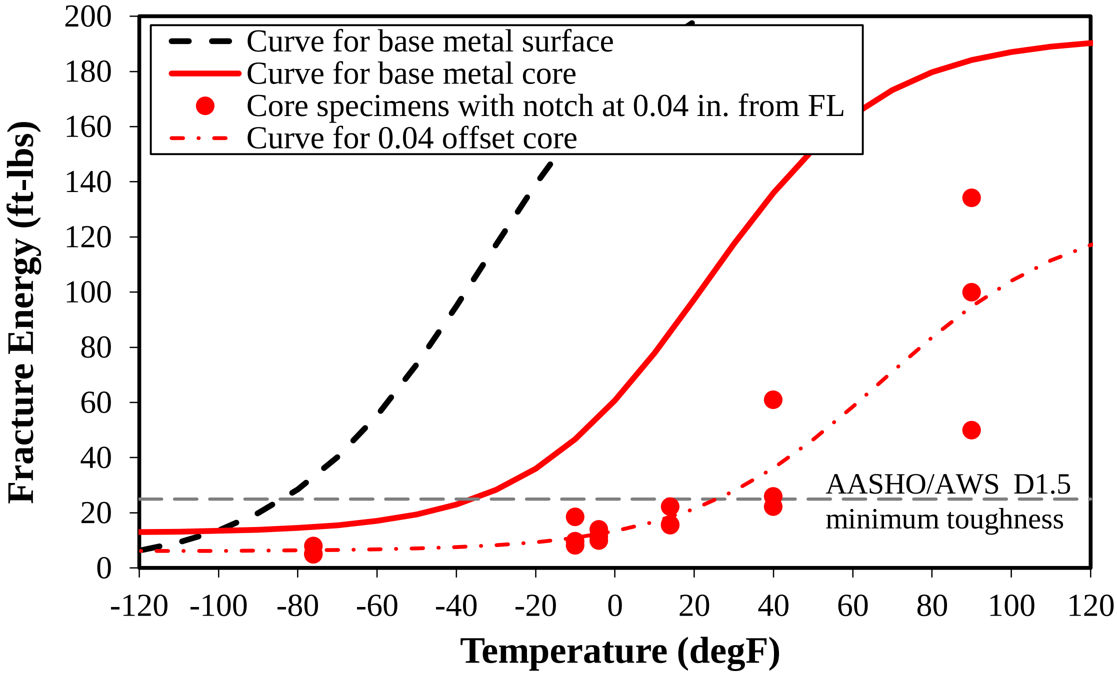

Figure 4.39. PB toughness specimens sampled at 0.04 in offset from FL core

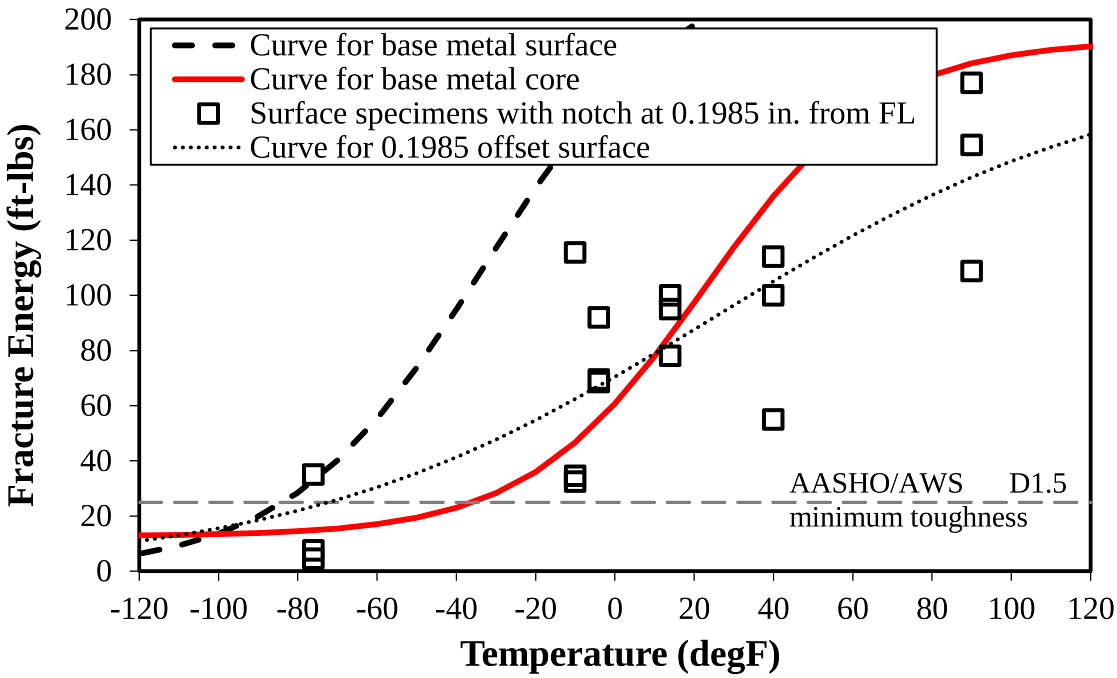

Figure 4.40. PB toughness specimens sampled at 0.1985 in offset from FL surface

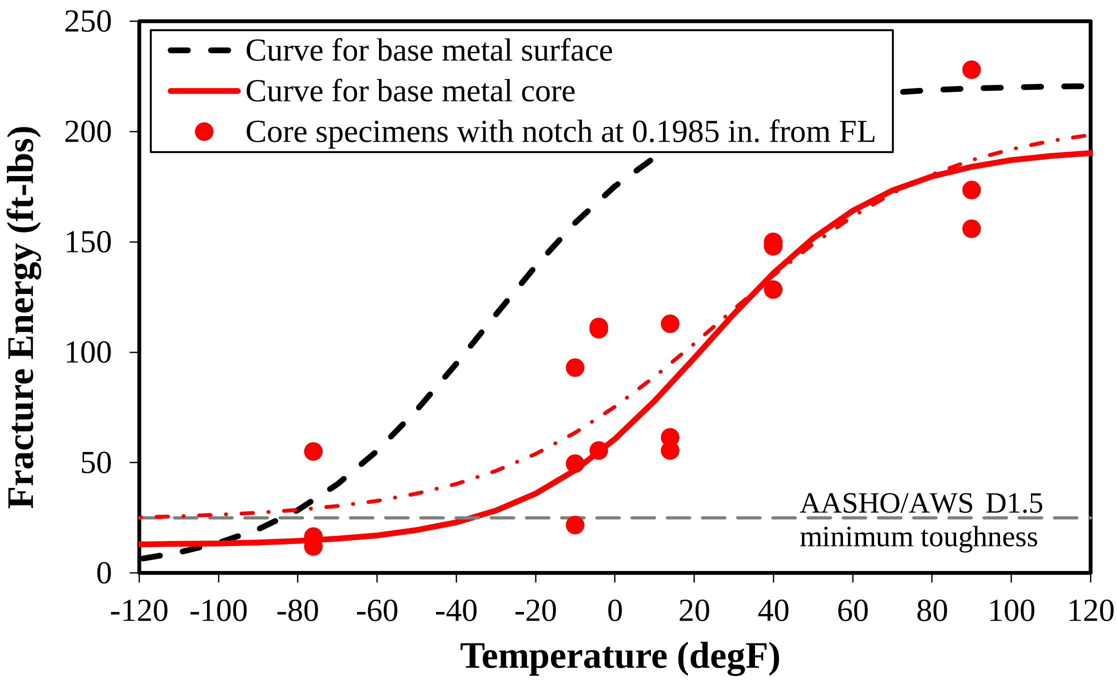

Figure 4.41. PB toughness specimens sampled at 0.1985 in offset from FL core

4.5. Hardness Testing Results

Hardness was measured on each macroetch specimen per the pattern shown in section 0. The maximum, minimum, average and standard deviation of the Vickers Hardness values (HV) for each specimen are tabulated in 0. Specimens M1 and M2 were sampled from PA, while all other specimens were sampled from PB. The location of each specimen is reported in section 3.4 and the geometric properties of the samples is reported in section 3.6. All measurements are tabulated in the

Appendix C: Hardness Testing data. The hardness readings are presented in the form of bubble plots in Figure 4.42 through Figure 4.48. The magnitude of the HV is represented through the size and color of the bubbles. Samples M1 and M2 were tested on three parallel strips in order to study the variation of HV within the depth. Since no significant differences were observed, a more reduced testing matrix of just two strips was applied to the remaining transverse specimens, M3, M5 and M7. On the longitudinal specimens, M4 and M6, there was no added benefit in performing multiple testing strips because the section represents a single plane within depth.

Table 4.10. Hardness testing results per specimen

ID	Plate of origin	Type	HV min	HV max	Average HV	St dev. (σ)	Number of tests
M1	PA	Transverse	199.1	353.7	236.5	15.77	260
M2	PA	Transverse	180.8	250.8	222.1	12.70	236
M3	PB	Transverse	169	264.9	218.5	18.97	160
M4	PB	Longitudinal	172.5	241.7	209.1	13.99	80
M5	PB	Transverse	179.8	262.7	217.5	13.01	160
M6	PB	Longitudinal	170.6	251.6	209.9	14.02	80
M7	PB	Transverse	170.4	248.4	216.2	12.88	160

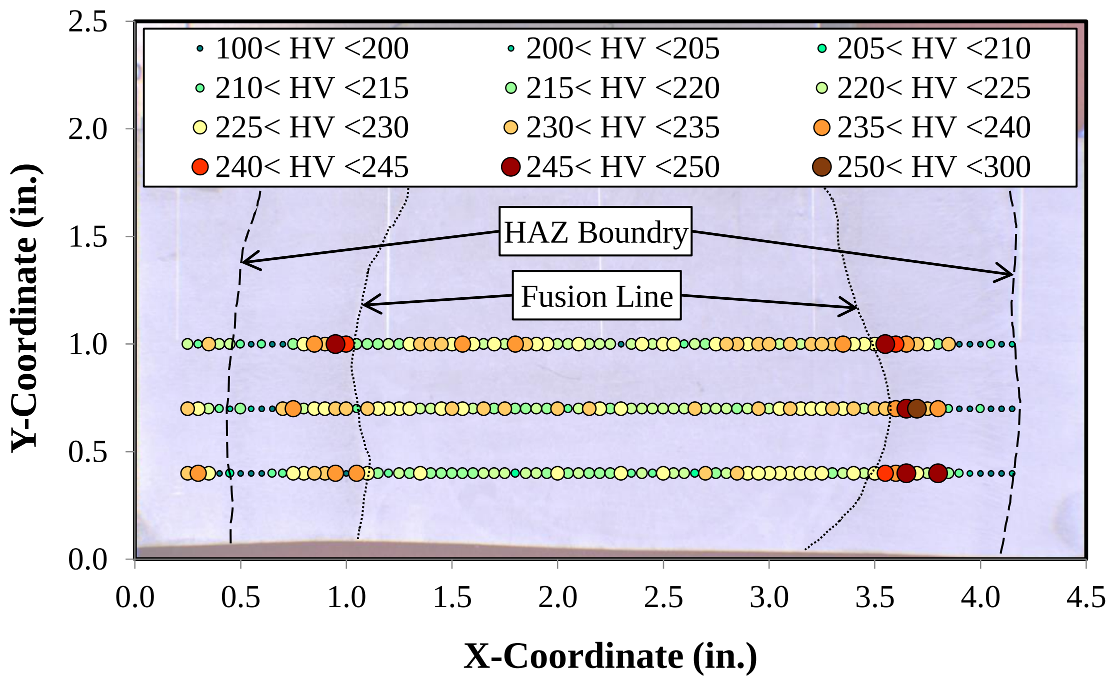

Figure 4.42. Bubble plot for specimen M1

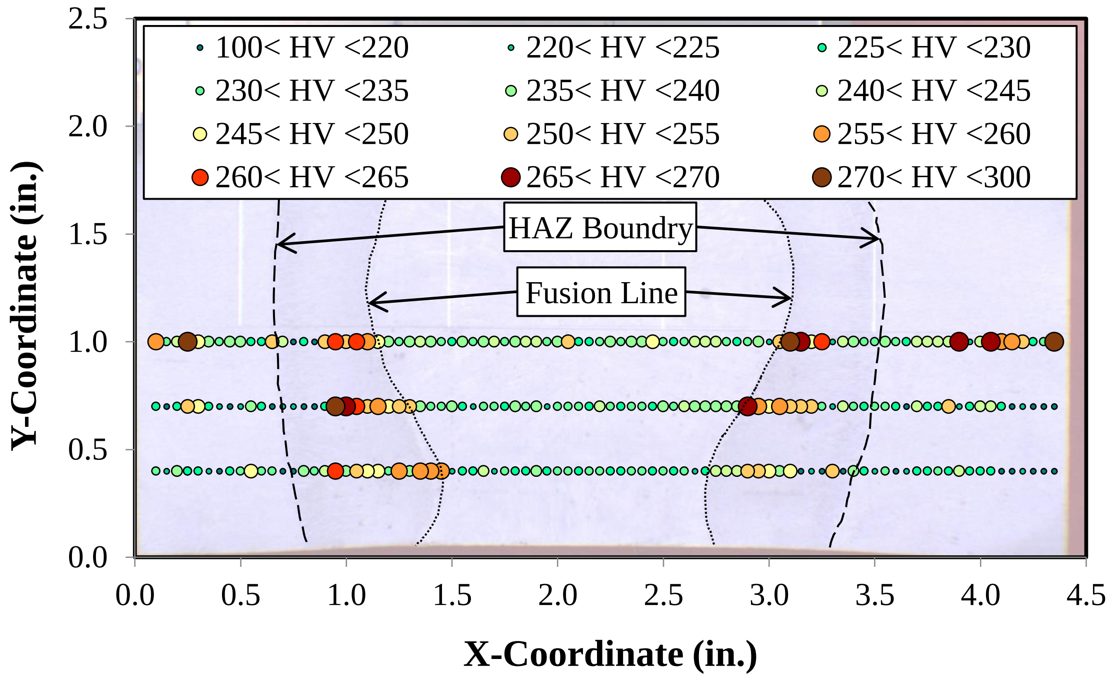

Figure 4.43. Bubble plot for specimen M2

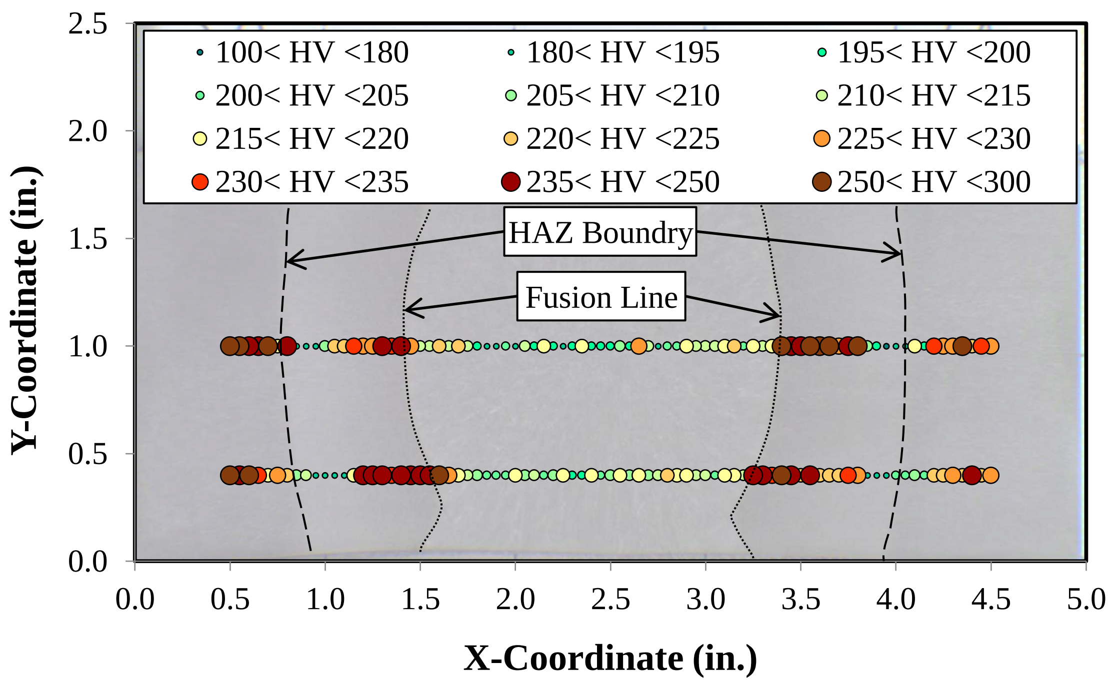

Figure 4.44. Bubble plot for specimen M3

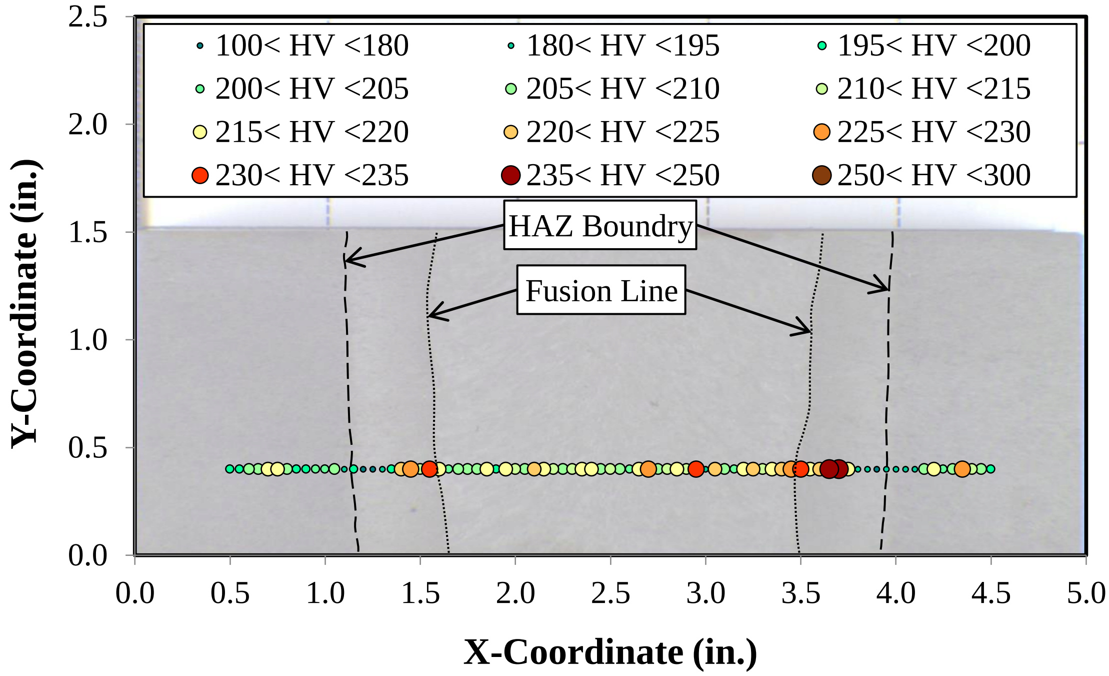

Figure 4.45. Bubble plot for specimen M4

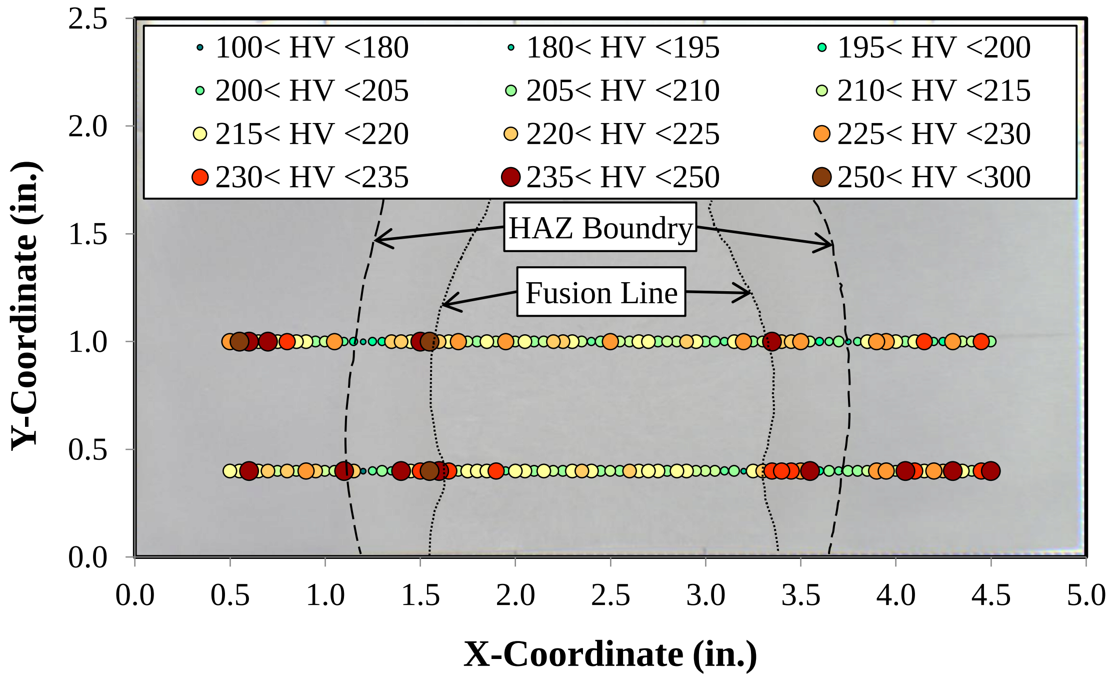

Figure 4.46. Bubble plot for specimen M5

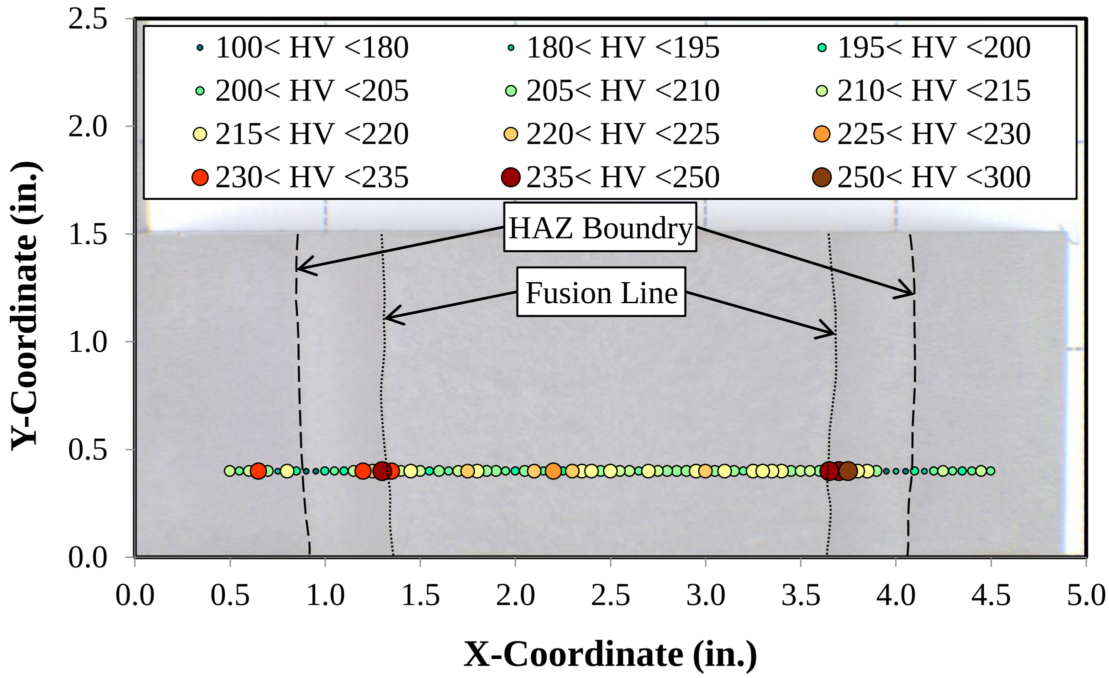

Figure 4.47. Bubble plot for specimen M6

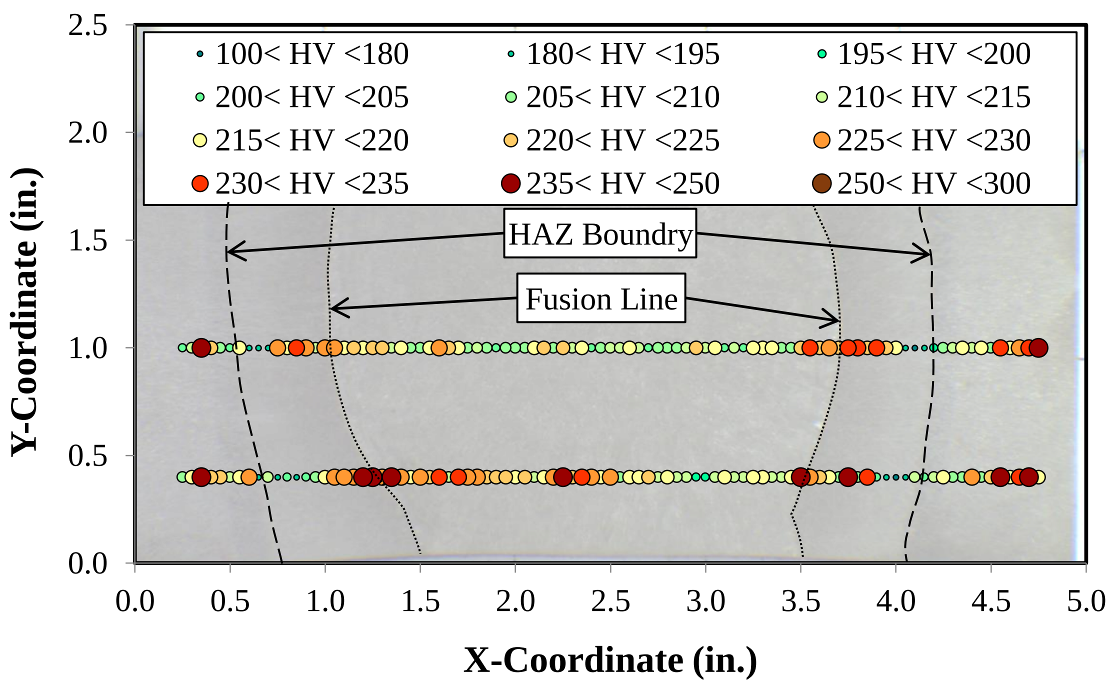

Figure 4.48. Bubble plot for specimen M7

In Figure 4.49 through Figure 4.55 the same data is presented in three point average strip plots. A spike in hardness can be observed on all specimens at the approximate location of FL and significant dip at the approximate edge of the HAZ.

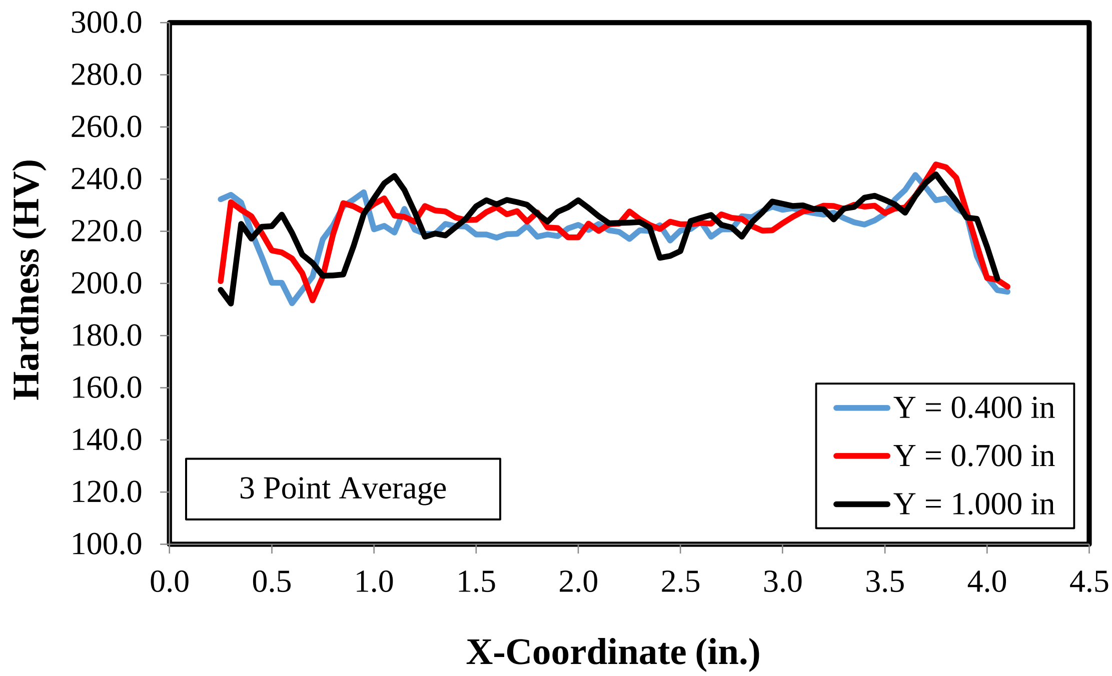

Figure 4.49. Hardness strip plot for specimen M1.

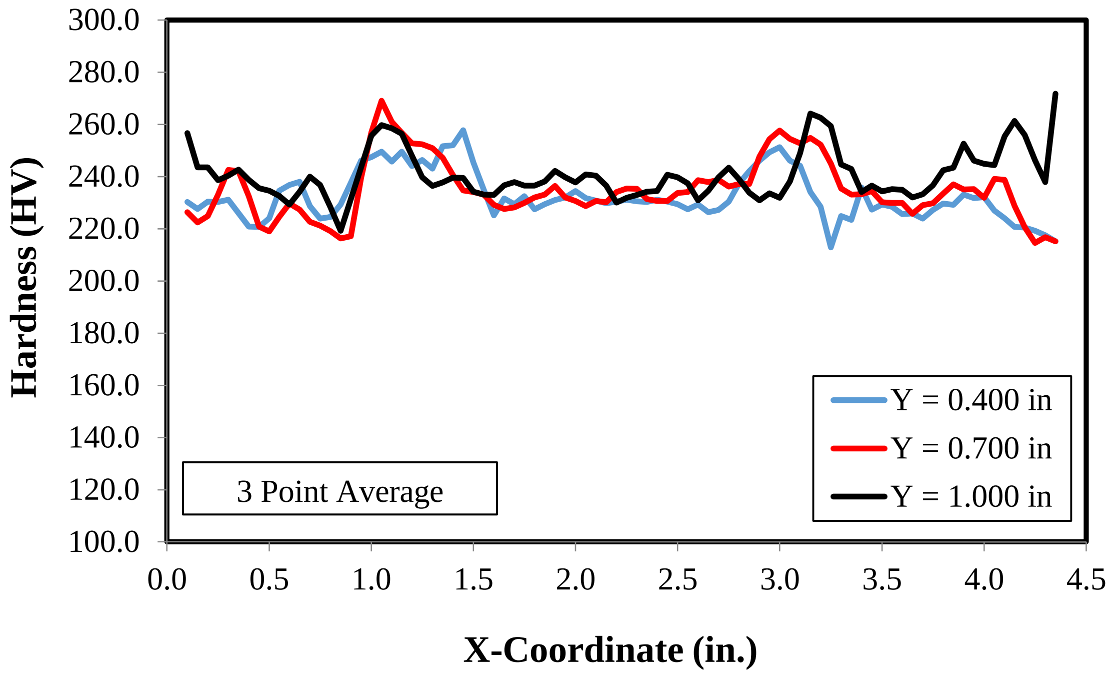

Figure 4.50. Hardness strip plot for specimen M2.

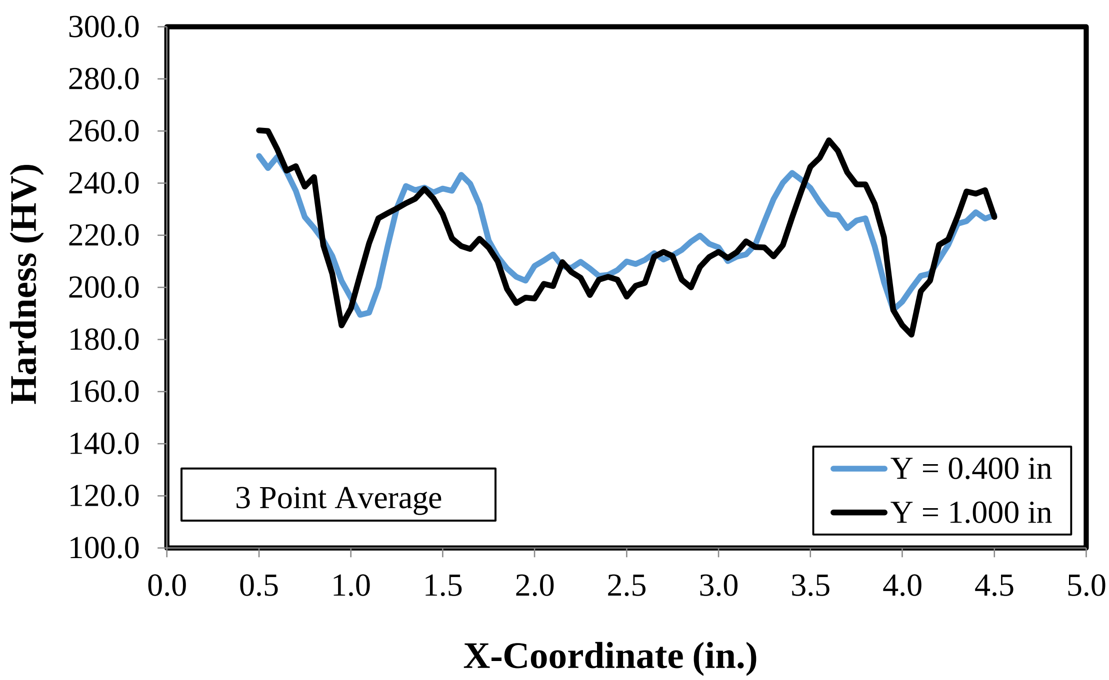

Figure 4.51. Hardness strip plot for specimen M3.

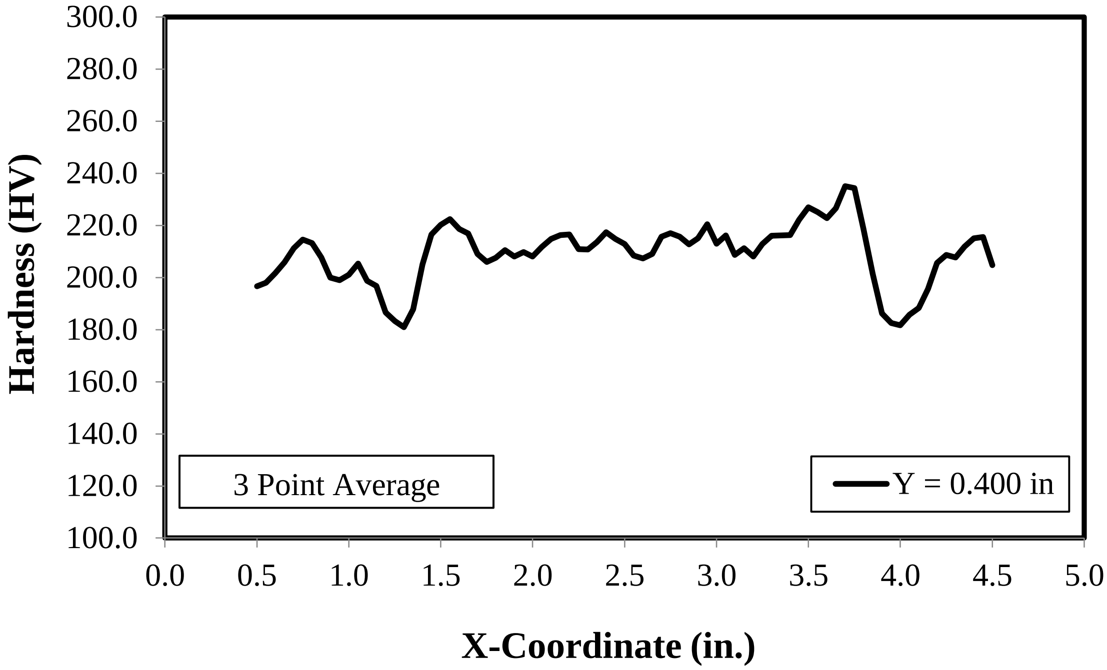

Figure 4.52. Hardness strip plot for specimen M4.

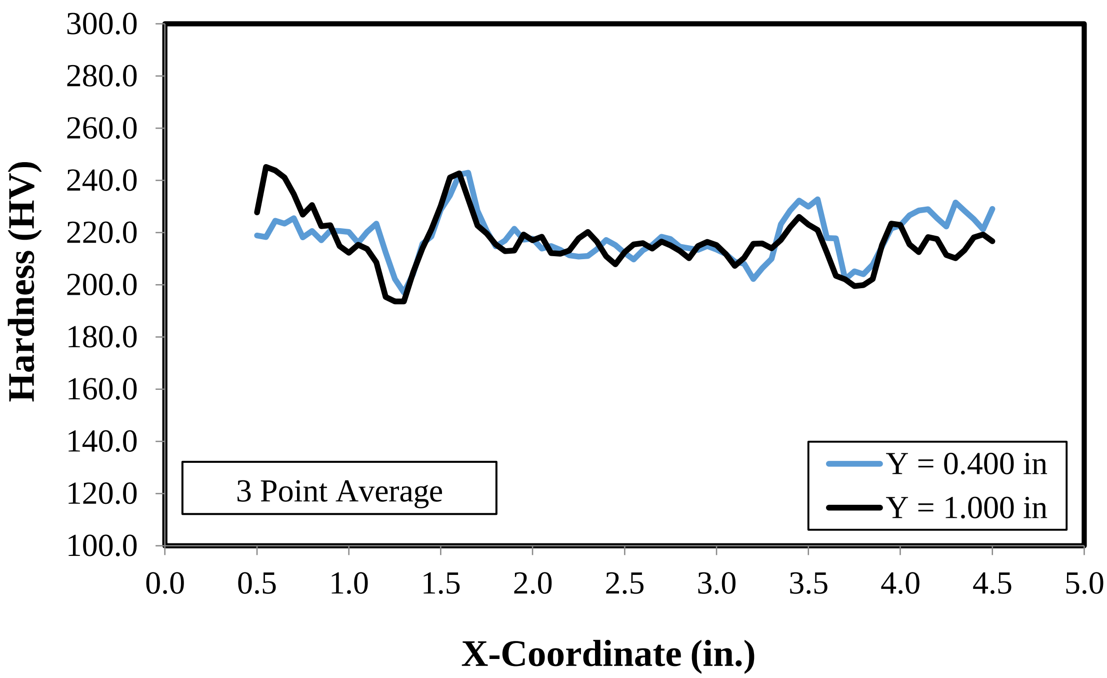

Figure 4.53. Hardness strip plot for specimen M5.

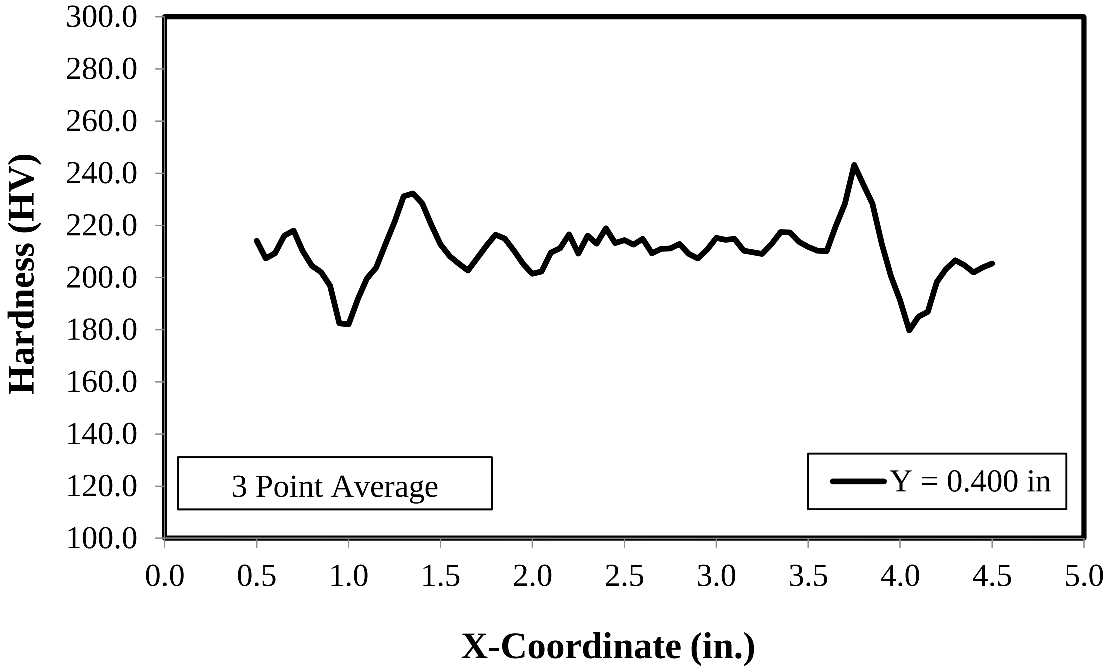

Figure 4.54. Hardness strip plot for specimen M6.

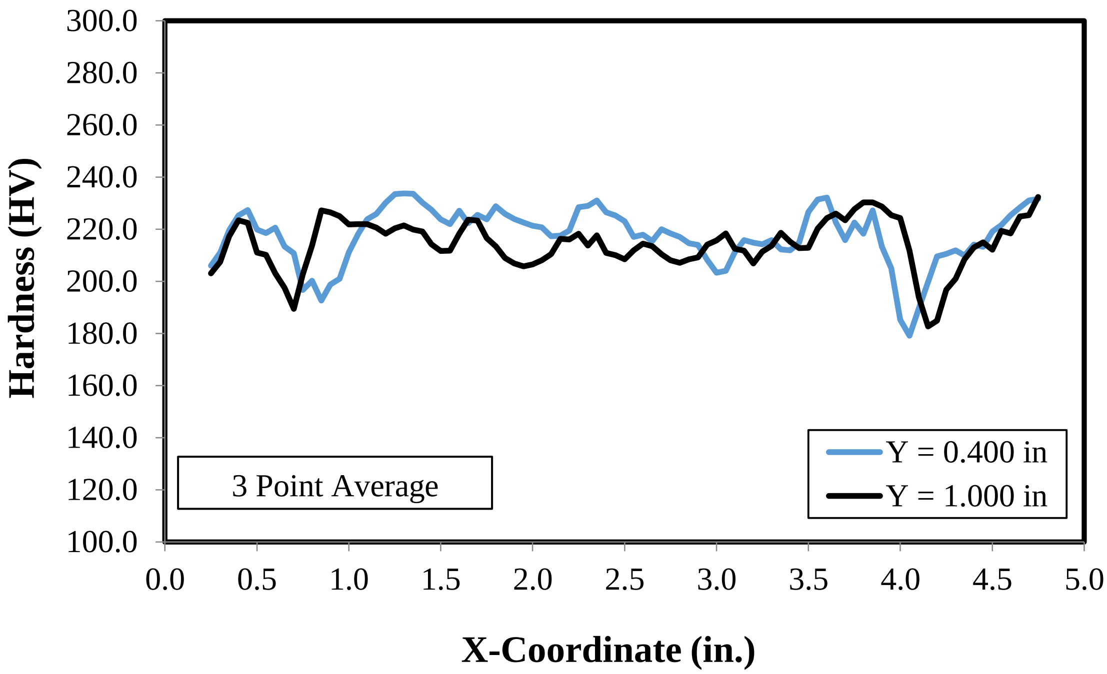

Figure 4.55. Hardness strip plot for specimen M7.

High HV values were recorded in the HAZ and around FL, while in general the center of the weld and the base metal outside the HAZ showed smaller HV values. This is consistent with toughness testing done at FL and near FL in the sense that lower toughness values translated into higher hardness values, showing the material is least ductile at FL. Hardness and toughness variations appear to behave in reflective fashion, and pending further investigation, suggest that higher HV values result in lower toughness values and vice versa. If this assumption can be proven through further research, HV would be a viable alternative to determine toughness deficiencies at FL and variations within HAZ. The hardness profiles showed consistent and acceptable hardness values throughout the weld nugget.

4.6. Summary of Analysis and Results

In this chapter, the results from all the tests performed per Chapter 3: are presented accompanied by a comprehensive analysis of the results. The results and analysis was organized per the test type and specimen location and orientation. Where applicable, a comparison between different types of specimens was also provided. The major conclusions obtained from the experimental program are outlined in chapter 5.

CHAPTER 5: CONCLUSIONS

An exhaustive experimental testing program was performed on two welded HPS 70W plates and accompanying BMP. The testing program was designed to investigate the possibility of pre-qualification of ESW-NG on HPS 70W per the AWS code, explore the mechanical properties of the weld thoroughly, and study the use of non-AWS testing specimens for weld qualification. A total of 389 individual specimens were tested. The tests were performed per their designated ASTM, and the results were recorded and analyzed. In this chapter, the main findings from the experimental program are summarized, and the known limitations and possible future research topics are identified.

5.1. Conclusions

A summary of the conclusions from the analysis performed in Chapter 4: is presented as follows:

- The manufacturer, who supplied the welded plate, performed NDT tests to screen for rejectable discontinuities, and none were identified. However, the early failure of three all-weld tension specimens from Plate B suggests there might have been a defect present.

- The macroetch specimens exhibited a highly irregular nugget shape. The weld opening width varied across specimens from 1.077 in to 2.691 in, suggesting that there was a large variation of temperature within the weld encasement.
- The longitudinal macroetch specimens do not show sudden shape change, which suggests that shape variations occur gradually and pose no stress concentration issues.
- All bend tests yielded positive results with no cracks, inclusions or discontinuities. This shows that the weld had good fusion to base metal and was cohesive with no defects at the location of the tests.
- All tension coupons for the base metal testing plate, regardless of geometry and size, exhibited similar tensile properties.
- The Base Metal Plate tension coupons had low yield strength. Typically, a HPS 70W steel would exhibit between 73 ksi and 78 ksi yield strength even though the requirement under ASTM A709 is 70 ksi. This lower than expected yield strength might have lowered the yield capabilities of the weld metal.
- On the Base Metal Testing Plate, no sensible strength difference was recorded between the tension specimens manufactured aligned to the direction of roll (L) and the ones manufactured transverse to the direction of roll (T).
- Five of the tension specimens from Plate B and none from Plate A met AWS D1.5 minimum filler metal strength requirements. However, they met minimum ASTM A709 ultimate tensile strength requirements.
- Two of the all weld tension specimens from Plate B met the minimum requirements for qualification under the AWS code.

- Both reduced section tension specimens (S) from Plate A and one specimen from Plate B failed at the center of the weld metal instead of the expected failure location at the Fusion Line (FL) or within the Heat Affected Zone (HAZ). Only one S type specimen from Plate B failed at FL following conventional wisdom. A metallurgical study that captures the amount of heat input, maximum temperature reached and rate of cooling is needed to explain the plausible causes of failure locations by identifying microstructure changes.
- On Plate A, two different types of tension specimens were tested in the L orientation in order to explore the possibility of using smaller samples for ESW-NG WPS qualification. These were reduced section and round type tension specimens. The two specimens behaved similarly at the upper portion of the stress strain curve, but had different behaviors at the yield plateau. The difference in behavior at yield could be attributed either to the size of the specimen, or it could be just a difference in the composition of the weld at that location along the upward progression of the weld. While this is promising, further testing is required in order to find out if tension on testing smaller size coupons is viable for the L orientation.
- The results from the comparison between round and reduced round tension specimens sampled in the T orientation from Plate A were very similar. This observation suggests that the use of smaller coupons is a practical option for WPS tension testing in the T orientation.
- Defects in the weld prevented three of the Round tension specimens in the T orientation sampled from Plate B to develop full yield and ultimate tensile strength.

The remaining two specimens achieved both the required yield and ultimate tensile strength requirements set forth in AWS.

- The base metal testing plate toughness specimens passed all the requirements for toughness from ASTM A709.
- There were no sensible differences in the toughness values between the two sides of Plate A. The electric current flow issue, which occurred on this plate, had no effect on toughness.
- Toughness requirements for the weld at center for both Plate A and Plate B were satisfied for Zone I and II applications under AWS.
- The geometry of the nugget yields very scattered toughness testing results at the Fusion Line (FL) as there is no means to align the straight notch of the Charpy specimens with the curved profile of the FL without encompassing some weld metal. It is recommended that testing of toughness at FL actually be done at 0.04 in offset within HAZ, which would allow for only HAZ material to be tested.
- Toughness values drop at the Fusion Line compared with center and progressively increase towards the edge of the Heat Affected Zone.
- Hardness testing values were high at and around the Fusion Line (FL), which resulted in low toughness values. The hardness plots showed high Vickers Hardness values (HV) at the Fusion Line and a progressive decrease towards the edge of the Heat Affected Zone (HAZ). Due to this highly localized testing method, the investigation proved to be useful in identifying variations in hardness within HAZ.

- Hardness and Toughness variations appear to behave in reflective fashion, and pending further investigation, suggest that higher HV values result in lower toughness values and vice versa. If this assumption can be proven through further research, HV would be a viable alternative to determine toughness deficiencies at FL and variations within HAZ.
- The hardness profiles showed consistent and acceptable hardness values throughout the weld nugget.
- Plate B, which was designated as the welding process qualification plate per AWS, did not pass qualification. Plate B failed the all-weld tension testing due to the defect within the weld at that location where the specimens were sampled. The plate passed two of the all-weld tension tests and all other required tests.

Overall, the objective of determining and characterizing the mechanical properties of HPS 70W high-performance steel when welded with the ESW-NG welding method was achieved. However, the research revealed that ESW-NG cannot currently be pre-qualified for HPS 70W per the AWS code due to the failure of the all-weld tension specimens.

5.2. Limitations

The main limitation involving this experimental research comes from the fact that the commissioned plates were provided by only one manufacturer and they involved only one heat of steel. More plates are needed to provide a statistical meaning to results. Due to the issues at the time of welding, the two resulting tested plates were reduced in size and additional testing specimens had to be manufactured for each plate in order to qualify at least one of the plates. This severely reduced the scope of the original testing plan as many of the testing specimens had to be manufactured on each plate, essentially duplicating them and reducing the number of planed additional specimens. Originally, more than 500 toughness specimens on the weld qualification plates alone were planned to be manufactured for providing a curve for the variation of toughness within the Heat Affected Zone. There were also additional reduced size tension tests planed meant to analyze comprehensively the possibility of their use for qualification instead of the full size specimens currently required by the AWS code.

5.3. Future Testing and Recommendations

The following future tests are proposed:

- A metallurgical study will be conducted at TFHRC to identify the exact reason why the Plate B all-weld tension specimens failed and confirm the weld inclusion theory.
- TFHRC is investigating more WPS testing plates made out of HPS 70 W steel joined with ESW-NG from a different manufacturer. The investigation proposes to further explore the possibility of using smaller tension specimens and provide a curve for the toughness properties at the Fusion Line and within the Heat Affected Zone.
- Tension testing will be performed at TFHRC on the two large dog bones from Plate B at low temperature to investigate the correlation between low toughness values and tension properties at low temperatures.

The following future analysis is recommended:

- Linear elastic fracture mechanics theory has been widely used to predict fracture for steels that exhibit brittle behavior. The critical stress intensity factor, K_{IC}, is the toughness measure that is conventionally used to predict when fracture will occur from a fatigue crack. Limited information is available that relates K_{IC} with CVN data. This can be explored in future studies.
- A metallurgical study and analysis of the Heat Affected Zone that captures the amount of heat input, maximum temperature reached and rate of cooling can be used to explain the plausible causes of low toughness and high hardness locations by identifying microstructure changes.
- Further analysis can be conducted to identify numerical relationships between hardness, toughness, and tension results corresponding to ESW-NG weld and the Heat Affected Zone.

APPENDIX A: TENSION TESTING ADDITIONAL DATA

Table A.1. Tension Specimens additional data

ID	Type	Initial Gage Length	Final Thickness	Final Width	Final Area	Final Gage Length	Measure ment to Break	Pass[a]
		(inch)	(inch)	(inch)	($inch^2$)	(inch)	(inch)	
W1	S	3.9940	1.2566	0.5841	0.7340	5.1270	2.590	Yes
W2	S	4.0105	1.2830	0.5853	0.7509	5.1265	2.550	yes
W3	R	2.0000	0.2770	0.2850	0.0620	2.5331	1.448	yes
W4	R	2.0000	0.2870	0.2960	0.0667	2.5452	1.360	yes
W5	R	2.0000	0.2840	0.2860	0.0638	2.5238	1.286	yes
W6	R	2.0000	0.2870	0.2770	0.0624	2.5419	1.424	yes
W7	RR	1.0000	0.1350	0.1420	0.0151	1.2744	0.932	yes
W8	RR	1.0000	0.1130	0.1430	0.0127	1.3051	0.742	yes
W9	RR	1.0000	0.1450	0.1470	0.0167	1.2987	0.809	yes
W10	S	4.000	0.9692	0.5775	0.5597	-0.002	2.457	no
W11	S	4.000	1.1161	0.5847	0.6526	0.000	0.000	no
W12	R	2.000	0.41100	0.4200	0.1356	2.381	0.812	yes
W13	R	2.000	0.47600	0.4800	0.1794	2.212	0.310	no
W14	R	2.000	0.29800	0.3110	0.0728	2.544	1.020	yes
W15	R	2.000	0.49900	0.4990	0.1956	2.037	0.000	no
W16	R	2.000	0.44700	0.4580	0.1608	2.133	0.312	no
B1	S	4.0005	1.0589	0.6033	0.6389	5.3580	2.365	yes
B2	S	4.0155	1.0482	0.5909	0.6194	5.3670	2.220	yes
B3	S	4.0350	1.0647	0.6415	0.6830	5.3830	2.161	yes
B4	R	2.0000	0.2230	0.3040	0.0532	2.5415	1.172	yes

B5	R	2.0000	0.2110	0.2890	0.0479	2.5357	1.296	yes
B6	R	2.0000	0.2130	0.3090	0.0517	2.5267	1.391	yes
B7	R	2.0000	0.2000	0.2870	0.0451	2.5389	1.485	yes
B8	R	2.0000	0.2070	0.3110	0.0506	2.5443	1.336	yes
B9	R	2.0000	0.2140	0.3010	0.0506	2.5338	1.038	yes
B10	R	2.0000	0.2310	0.2850	0.0517	2.4988	1.287	yes
B11	R	2.0000	0.2280	0.2940	0.0526	2.4956	1.311	yes
B12	R	2.0000	0.2330	0.2860	0.0523	2.5038	1.398	yes
B13	RR	1.0000	0.1150	0.1470	0.0133	1.2656	0.616	yes
B14	RR	1.0000	0.1200	0.1320	0.0124	1.2595	0.634	yes
B15	RR	1.0000	0.1200	0.1330	0.0125	1.2580	0.760	yes
B16	RR	1.0000	0.0990	0.1440	0.0112	1.2724	0.602	yes
B17	RR	1.0000	0.0940	0.1360	0.0100	1.2802	0.661	yes
B18	RR	1.0000	0.0990	0.1440	0.0112	1.2795	0.453	yes
B19	RR	1.0000	0.1000	0.1420	0.0112	1.2818	0.690	yes
B20	RR	1.0000	0.1030	0.1530	0.0124	1.2773	0.512	yes
B21	RR	1.0000	0.1120	0.1430	0.0126	1.2716	0.487	yes
B22	RR	1.0000	0.1170	0.1530	0.0141	1.2674	0.726	yes
B23	RR	1.0000	0.1130	0.1430	0.0127	1.2789	0.641	yes
B24	RR	1.0000	0.1150	0.1470	0.0133	1.2525	0.758	yes

[a]ASTM E8 requires that the break occurs at more than 25% of gage length from gage mark

APPENDIX B: TOUGHNESS TESTING DATA

Table B.1. Toughness results for PA and PB

ID	Type	Depth	T (degF)	CVN (ft-lbs)
PA				
DW2	W	Core	-60	14.25
DW3	W	Core	-60	10.25
AW2	W	Core	-10	32.25
AW3	W	Core	-10	20.5
MW3	W	Core	-10	22.75
PW2	W	Core	70	67.75
WW3	W	Core	70	94.5
DW1	W	Surface	-60	9
DW4	W	Surface	-60	12.5
AW1	W	Surface	-10	23.25
MW1	W	Surface	-10	19.5
AW4	W	Surface	-10	22.75
PW1	W	Surface	70	37
PW4	W	Surface	70	77.5
BF1	FL	Surface	-10	9.75
EF1	FL	Surface	70	71.25
GF1	FL	Surface	-10	23.25
IF1	FL	Surface	-60	18.75
KF1	FL	Surface	70	124
NF1	FL	Surface	-60	13.5
BF2	FL	Core	-10	8.75
EF2	FL	Core	70	51.75

GF2	FL	Core	-10	7.75
IF2	FL	Core	-60	6
KF2	FL	Core	70	100
NF2	FL	Core	-60	9.25
BF3	FL	Core	-10	17.25
EF3	FL	Core	70	32.75
GF3	FL	Core	-10	14.75
IF3	FL	Core	-60	11.25
KF3	FL	Core	70	48.75
NF3	FL	Core	-60	10.25
BF4	FL	Surface	-10	12.5
EF4	FL	Surface	70	29.25
GF4	FL	Surface	-10	9.25
IF4	FL	Surface	-60	12.75
KF4	FL	Surface	70	57.75
NF4	FL	Surface	-60	13.5
C11	0.04 in offset	Surface	-10	15.25
F11	0.04 in offset	Surface	-60	8.5
H11	0.04 in offset	Surface	-60	5.5
J11	0.04 in offset	Surface	70	55
L11	0.04 in offset	Surface	70	35.75
O11	0.04 in offset	Surface	-10	16.75
C12	0.04 in offset	Core	-10	13.25
F12	0.04 in offset	Core	-60	6.75
H12	0.04 in offset	Core	-60	4.5
J12	0.04 in offset	Core	70	95.25
L12	0.04 in offset	Core	70	32.5
O12	0.04 in offset	Core	-10	8.25
C13	0.04 in offset	Core	-10	8.25
F13	0.04 in offset	Core	-60	19.75
H13	0.04 in offset	Core	-60	7.75
J13	0.04 in offset	Core	70	50.25
L13	0.04 in offset	Core	70	63.75
O13	0.04 in offset	Core	-10	71.5
C14	0.04 in offset	Surface	-10	7.25
F14	0.04 in offset	Surface	-60	6.25
H14	0.04 in offset	Surface	-60	5.75

J14	0.04 in offset	Surface	70	33
L14	0.04 in offset	Surface	70	59
O14	0.04 in offset	Surface	-10	33
PB				
191	W	Surface	14	25.75
381	W	Surface	-76	8.75
341	W	Surface	-4	15.5
401	W	Surface	-20	19.75
391	W	Surface	-20	17
411	W	Surface	-20	16
51	W	Surface	-20	15
54	W	Surface	14	43
344	W	Surface	-76	9
194	W	Surface	-4	15.25
404	W	Surface	-20	17.75
384	W	Surface	-20	18.5
14	W	Surface	-20	21
414	W	Surface	-20	17
12	W	Core	32	25.75
52	W	Core	32	26.5
342	W	Core	32	26.75
382	W	Core	32	37
402	W	Core	-20	19.75
392	W	Core	-20	17.25
192	W	Core	-20	25.75
412	W	Core	-20	23
13	W	Core	32	25.5
53	W	Core	32	33
343	W	Core	32	20
383	W	Core	32	24.5
403	W	Core	-20	27.75
393	W	Core	-20	26
413	W	Core	-20	38
193	W	Core	-20	18.5
131	FL	Surface	32	19.5
141	FL	Surface	32	14.5
231	FL	Surface	32	4.25

241	FL	Surface	32	4.5
221	FL	Surface	32	17
41	FL	Surface	-10	22
31	FL	Surface	40	12.25
121	FL	Surface	40	52
311	FL	Surface	90	51.5
144	FL	Surface	32	29
244	FL	Surface	32	12.75
224	FL	Surface	32	13.25
234	FL	Surface	32	16.75
124	FL	Surface	-10	9.5
34	FL	Surface	-10	34
134	FL	Surface	40	23.75
24	FL	Surface	90	63.25
314	FL	Surface	90	54.25
232	FL	Core	32	3
242	FL	Core	32	12.25
243	FL	Core	32	14.25
22	FL	Core	-10	51
123	FL	Core	-10	29.25
133	FL	Core	-10	28.5
222	FL	Core	32	48
223	FL	Core	32	61.5
233	FL	Core	32	47
132	FL	Core	32	34.5
142	FL	Core	32	40
143	FL	Core	32	37
32	FL	Core	40	11.75
122	FL	Core	40	24
33	FL	Core	40	73
312	FL	Core	90	108
23	FL	Core	90	117
313	FL	Core	90	122.5
171	0.04 in offset	Surface	32	17.75
271	0.04 in offset	Surface	32	4.75
251	0.04 in offset	Surface	32	8
261	0.04 in offset	Surface	32	17.25

71	0.04 in offset	Surface	-10	24.75
61	0.04 in offset	Surface	-10	10.75
161	0.04 in offset	Surface	40	22.75
331	0.04 in offset	Surface	90	83.75
351	0.04 in offset	Surface	90	96.75
164	0.04 in offset	Surface	32	16
174	0.04 in offset	Surface	32	19.25
264	0.04 in offset	Surface	32	4.75
274	0.04 in offset	Surface	32	5.5
254	0.04 in offset	Surface	32	7.75
354	0.04 in offset	Surface	-10	8.5
74	0.04 in offset	Surface	40	46
334	0.04 in offset	Surface	40	20.25
64	0.04 in offset	Surface	90	85
162	0.04 in offset	Core	32	15.5
172	0.04 in offset	Core	32	22.25
262	0.04 in offset	Core	32	8
272	0.04 in offset	Core	32	5.25
252	0.04 in offset	Core	32	10
352	0.04 in offset	Core	-10	8.25
72	0.04 in offset	Core	40	26
332	0.04 in offset	Core	40	61
62	0.04 in offset	Core	90	50
173	0.04 in offset	Core	32	15.75
273	0.04 in offset	Core	32	5
253	0.04 in offset	Core	32	14
263	0.04 in offset	Core	32	11.5
83	0.04 in offset	Core	-10	18.5
153	0.04 in offset	Core	-10	9.75
73	0.04 in offset	Core	40	22.25
63	0.04 in offset	Core	90	100
353	0.04 in offset	Core	90	134.25
301	0.1985 in offset	Surface	32	7.5
361	0.1985 in offset	Surface	32	4.5
304	0.1985 in offset	Surface	32	35
201	0.1985 in offset	Surface	-10	32.5
181	0.1985 in offset	Surface	-10	115.5

364	0.1985 in offset	Surface	-10	34.5
291	0.1985 in offset	Surface	32	68.5
284	0.1985 in offset	Surface	32	69.5
294	0.1985 in offset	Surface	32	92
211	0.1985 in offset	Surface	32	78
281	0.1985 in offset	Surface	32	100
214	0.1985 in offset	Surface	32	95
111	0.1985 in offset	Surface	40	114
114	0.1985 in offset	Surface	40	55
374	0.1985 in offset	Surface	40	100
91	0.1985 in offset	Surface	90	154.5
371	0.1985 in offset	Surface	90	177
94	0.1985 in offset	Surface	90	108.75
292	0.1985 in offset	Core	32	12
302	0.1985 in offset	Core	32	16.5
303	0.1985 in offset	Core	32	55
182	0.1985 in offset	Core	-10	21.75
362	0.1985 in offset	Core	-10	49.5
203	0.1985 in offset	Core	-10	93
282	0.1985 in offset	Core	32	111.5
283	0.1985 in offset	Core	32	55.5
293	0.1985 in offset	Core	32	110.5
202	0.1985 in offset	Core	32	61.5
212	0.1985 in offset	Core	32	55.5
213	0.1985 in offset	Core	32	113
112	0.1985 in offset	Core	40	148
113	0.1985 in offset	Core	40	128.5
373	0.1985 in offset	Core	40	150
92	0.1985 in offset	Core	90	228
372	0.1985 in offset	Core	90	173.5
93	0.1985 in offset	Core	90	156

Table B.2. Toughness results for BMP.

ID	Type	Depth	T (degF)	CVN (ft-lbs)
1	LT	Surface	-100	8.5
2	LT	Surface	-100	10.5
3	LT	Surface	-100	10
4	LT	Core	-100	5.5
5	LT	Core	-100	16.5
6	LT	Core	-100	4.5
7	TL	Surface	-100	3.5
8	TL	Surface	-100	12
9	TL	Surface	-100	4
10	TL	Core	-100	5.5
11	TL	Core	-100	4
12	TL	Core	-100	7.5
13	LT	Surface	-60	62
14	LT	Surface	-60	40
15	LT	Surface	-60	3.5
16	LT	Core	-60	14
17	LT	Core	-60	6.5
18	LT	Core	-60	10.5
19	TL	Surface	-60	39
20	TL	Surface	-60	15.5
21	TL	Surface	-60	14.5
22	TL	Core	-60	13
23	TL	Core	-60	7.5
24	TL	Core	-60	22
25	LT	Surface	-45	134
26	LT	Surface	-45	109
27	LT	Surface	-45	108
28	LT	Core	-45	56
29	LT	Core	-45	18
30	LT	Core	-45	4
31	TL	Surface	-45	66
32	TL	Surface	-45	48
33	TL	Surface	-45	8.5

34	TL	Core	-45	10.5
35	TL	Core	-45	20
36	TL	Core	-45	12.5
37	LT	Surface	-30	119
38	LT	Surface	-30	20.5
39	LT	Surface	-30	48
40	LT	Core	-30	58
41	LT	Core	-30	33
42	LT	Core	-30	31
43	TL	Surface	-30	42
44	TL	Surface	-30	11.5
45	TL	Surface	-30	48
46	TL	Core	-30	16.5
47	TL	Core	-30	21.5
48	TL	Core	-30	42
49	LT	Surface	-15	236
50	LT	Surface	-15	186
51	LT	Surface	-15	222
52	LT	Surface	-15	192
53	LT	Surface	-15	182
54	LT	Core	-15	27
55	LT	Core	-15	21
56	LT	Core	-15	27
57	TL	Surface	-15	128
58	TL	Surface	-15	48
59	TL	Surface	-15	6.5
60	TL	Core	-15	59
61	TL	Core	-15	24
62	TL	Core	-15	40
63	LT	Surface	0	60
64	LT	Surface	0	216
65	LT	Surface	0	207
66	LT	Surface	0	217
67	LT	Surface	0	154
68	LT	Surface	0	53
69	LT	Core	0	6
70	LT	Core	0	138

71	LT	Core	0	55
72	LT	Core	0	111
73	LT	Core	0	53
74	LT	Core	0	114
75	TL	Surface	0	4.5
76	TL	Surface	0	107
77	TL	Surface	0	138
78	TL	Surface	0	70
79	TL	Surface	0	111
80	TL	Surface	0	60
81	TL	Core	0	28.5
82	TL	Core	0	65
83	TL	Core	0	26.5
84	TL	Core	0	92
85	TL	Core	0	60
86	TL	Core	0	68
87	LT	Surface	15	175
88	LT	Surface	15	155
89	LT	Surface	15	178
90	LT	Core	15	14
91	LT	Core	15	21
92	LT	Core	15	42
93	LT	Core	15	132
94	LT	Core	15	95
95	TL	Surface	15	140
96	TL	Surface	15	132
97	TL	Surface	15	194
98	TL	Core	15	48
99	TL	Core	15	88
100	TL	Core	15	63
101	LT	Surface	40	228
102	LT	Surface	40	188
103	LT	Surface	40	240
104	LT	Core	40	206
105	LT	Core	40	154
106	LT	Core	40	121
107	TL	Surface	40	149

108	TL	Surface	40	129
109	TL	Surface	40	130
110	TL	Core	40	109
111	TL	Core	40	120
112	TL	Core	40	104
113	LT	Surface	70	256
114	LT	Surface	70	234
115	LT	Surface	70	200
116	LT	Core	70	191
117	LT	Core	70	172
118	LT	Core	70	61
119	LT	Core	70	246
120	TL	Surface	70	140
121	TL	Surface	70	168
122	TL	Surface	70	158
123	TL	Core	70	124
124	TL	Core	70	136
125	TL	Core	70	156

Table B.3. Lateral expansion measuremnts for PA.

ID	A1	A3	A2	A4	max (A1,A2)	max (A3,A4)	L_{ex}
C12	4.25	2.75	4.75	6	4.75	6	10.75
C14	2.25	2.25	1.5	1.75	2.25	2.25	4.5
EF1	27.75	26.25	24.25	21.75	27.75	26.25	54
EF2	18	16.75	20.5	17.75	20.5	17.75	38.25
EF3	16.25	15.25	8	9	16.25	15.25	31.5
EF4	15.75	14	8	7.5	15.75	14	29.75
F12	1.75	2.5	1.75	2	1.75	2.5	4.25
GF2	2.75	1.75	1.5	2	2.75	2	4.75
GF4	2.75	2.5	4	2.25	4	2.5	6.5
J14	17.75	18.25	24	17.75	24	18.25	42.25
J12	38.5	29.5	33.5	30	38.5	30	68.5
J13	14.75	14.75	22	23	22	23	45
J11	10	19	16.75	16	16.75	19	35.75
KF1	41	28	26.25	43	41	43	84

KF2	35.25	20.25	35.25	26.25	35.25	26.25	61.5
KF3	15.25	16.25	15	15.25	15.25	16.25	31.5
KF4	20.75	20.25	18.25	19	20.75	20.25	41
L14	20.5	26.25	14.75	16	20.5	26.25	46.75
L11	11.5	10.25	17.75	20	17.75	20	37.75
L12	10.25	11	13	11.25	13	11.25	24.25
L13	23.75	21	20.75	19.5	23.75	21	44.75
PW1	15.5	14.75	16	15.75	16	15.75	31.75
PW2	20.25	21.25	24	28	24	28	52
PW3	26	31.5	31	36.25	31	36.25	67.25
PW4	27.25	23	29	24	29	24	53
MW1	8.5	8.75	6	7	8.5	8.75	17.25
MW3	7	7	10.25	8	10.25	8	18.25
C13	5.25	5.5	1	1.25	5.25	5.5	10.75
O11	8	7.5	5	3	8	7.5	15.5
BF1	3	3	2.25	3.5	3	3.5	6.5
BF2	2.75	3	2	2.75	2.75	3	5.75
BF3	5.75	6.75	5	6	5.75	6.75	12.5
BF4	3.5	3.75	4.25	0	4.25	3.75	8
C11	5.25	6	5.75	5.25	5.75	6	11.75
GF3	8.75	7	2.5	2.75	8.75	7	15.75
O14	19.25	17.75	5	7.75	19.25	17.75	37
O13	24	22	18	27.75	24	27.75	51.75
O12	2	2	2	2	2	2	4
GF1	1	2	19	18.75	19	18.75	37.75
AW1	10.75	9.25	6.25	8.5	10.75	9.25	20
AW2	10.5	11.75	13	12.75	13	12.75	25.75
AW3	10	8	6	7	10	8	18
AW4	9.25	6.5	6	9.25	9.25	9.25	18.5
DW2	3.5	3	6	5.25	6	5.25	11.25
DW3	2.75	3.75	3.25	3	3.25	3.75	7
DW4	5.25	5.25	3.75	3.5	5.25	5.25	10.5
H11	1.75	1.5	1.25	2	1.75	2	3.75
H12	1	1	2	0.75	2	1	3
H13	2.25	2	2	1.75	2.25	2	4.25
H14	1.5	2	1.5	3	1.5	3	4.5
IF1	4	4	13	9.25	13	9.25	22.25

IF2	1.25	1.75	1.25	1.5	1.25	1.75	3
IF3	0.75	0.75	16.25	13	16.25	13	29.25
IF4	12.75	11	11	12.25	12.75	12.25	25
NF1	12	10.5	1	2	12	10.5	22.5
NF2	2.75	5.5	3	2.75	3	5.5	8.5
NF3	0.75	0.5	13	11.75	13	11.75	24.75
NF4	1.25	1.25	15.5	14	15.5	14	29.5
F14	3	3	1	1	3	3	6
F11	1.5	1.5	4	5	4	5	9

Table B.4. Lateral expansion measuremnts for PB.

ID	A1	A3	A2	A4	max (A1,A2)	max (A3,A4)	L_{ex}
54	18	19	15	15.75	18	19	37
131	5	4.75	9.75	9.75	9.75	9.75	19.5
132	14.25	12	13.75	11.5	14.25	12	26.25
141	6.25	8.25	2	2.25	6.25	8.25	14.5
142	8.75	7.75	24	20.25	24	20.25	44.25
143	10	8.75	22	19.5	22	19.5	41.5
144	18.75	18	5	6	18.75	18	36.75
162	5	5.25	5	6	5	6	11
164	5	5	5.5	5	5.5	5	10.5
171	5.25	5.25	6.75	6.25	6.75	6.25	13
172	9.25	8.5	7.25	8.25	9.25	8.5	17.75
173	6	7.25	4.75	5	6	7.25	13.25
174	2.75	3.75	9	8.75	9	8.75	17.75
191	7.25	7.5	6.5	7.25	7.25	7.5	14.75
202	22.5	21.75	26.25	22.5	26.25	22.5	48.75
211	28.75	26.25	29	27	29	27	56
212	20	18.5	23	19.75	23	19.75	42.75
213	38	40.75	39	31	39	40.75	79.75
214	35.25	31	33.5	35	35.25	35	70.25
281	28.75	38.25	33.25	33.5	33.25	38.25	71.5
12	7.75	7.5	12	10.5	12	10.5	22.5
13	9.25	8.25	11.25	8.25	11.25	8.25	19.5
52	12	10.25	10	11.25	12	11.25	23.25

53	14.75	12	20	19	20	19	39
194	4.75	5.5	7.5	6.75	7.5	6.75	14.25
221	21.25	21	1.5	3	21.25	21	42.25
222	19.5	18.5	21.5	12.5	21.5	18.5	40
223	20.75	15.25	18	28	20.75	28	48.75
224	9.5	3.5	6.25	5.8	9.5	5.8	15.3
233	11.75	14.5	17.25	23	17.25	23	40.25
234	1	1.5	14	11.25	14	11.25	25.25
251	1.75	2	2.75	2.75	2.75	2.75	5.5
252	2.75	3	2.75	2.5	2.75	3	5.75
253	3.75	4.25	4.75	3.5	4.75	4.25	9
254	1.5	2.75	2.25	2	2.25	2.75	5
261	5.75	5.25	5	4	5.75	5.25	11
263	3.75	3.25	3	3	3.75	3.25	7
282	34.25	37	41.75	29	41.75	37	78.75
283	22	19.75	19.75	18	22	19.75	41.75
284	27.25	26.5	25.25	24	27.25	26.5	53.75
291	24.25	21.25	22.25	24	24.25	24	48.25
293	31	41.25	39.25	32	39.25	41.25	80.5
294	28.5	31	32	33	32	33	65
341	5.25	5	7	5.5	7	5.5	12.5
342	10.75	15	9.5	9.75	10.75	15	25.75
343	6.5	9.25	6.75	6.75	6.75	9.25	16
382	14	11	14.75	15.5	14.75	15.5	30.25
383	13.25	1.5	7.25	7.5	13.25	7.5	20.75
231	0.5	0.75	2	2	2	2	4
232	2	0.5	0.5	0	2	0.5	2.5
241	2.75	1	0.75	1.25	2.75	1.25	4
242	6	7	2	2.5	6	7	13
243	12.25	9	0.5	1	12.25	9	21.25
244	1	1.75	2.75	1.25	2.75	1.75	4.5
262	2.5	2.25	3	2.75	3	2.75	5.75
264	0.25	0.75	1.25	0.25	1.25	0.75	2
271	1	2	1	1	1	2	3
272	4	1	2	0.75	4	1	5
273	1.75	1	1.25	3.25	1.75	3.25	5
274	2	0	0	1.25	2	1.25	3.25

292	3.75	3.75	3.25	3.25	3.75	3.75	7.5
301	2	2.75	1.5	1.25	2	2.75	4.75
302	6	4.25	6	4.75	6	4.75	10.75
303	22	19.5	22	20	22	20	42
304	13	14.25	12	13	13	14.25	27.25
344	2	3.5	2	1.25	2	3.5	5.5
361	15.75	13.5	19.75	18.75	19.75	18.75	38.5
381	5.75	5	1.75	2	5.75	5	10.75
31	4	4	4	4	4	4	8
32	4	3.75	4	4	4	4	8
33	21	22.25	28.25	27.25	28.25	27.25	55.5
121	20.25	23.5	15.5	20.75	20.25	23.5	43.75
122	10	12	8	9	10	12	22
134	6	5.75	11	14	11	14	25
72	8	8.25	13	9.5	13	9.5	22.5
73	4.5	5	9	11.25	9	11.25	20.25
74	15.25	15.5	14.75	15.5	15.25	15.5	30.75
161	7.5	8	8	7	8	8	16
332	19.75	22	21	20	21	22	43
334	7.75	8.5	7.75	6.5	7.75	8.5	16.25
111	35.75	33.25	35.25	36	35.75	36	71.75
113	40	32	31.75	41.25	40	41.25	81.25
114	16.75	17	19.75	26	19.75	26	45.75
373	35	47.5	24	47.25	35	47.5	82.5
374	34.25	36.25	34	32	34.25	36.25	70.5
112	44	26.5	41.75	36.26	44	36.26	80.26
23	17.5	40.75	40.25	32	40.25	40.75	81
24	20.5	18.75	23	22	23	22	45
311	16.25	16.25	26	23	26	23	49
312	33	36.75	27	36.5	33	36.75	69.75
313	31.25	43.25	25.25	41.5	31.25	43.25	74.5
314	16.25	21.75	20.75	19	20.75	21.75	42.5
62	18.25	19.5	19	17.75	19	19.5	38.5
63	31	33	34	30.5	34	33	67
64	25.75	26	30.25	29	30.25	29	59.25
331	29.25	26.5	30	29	30	29	59
351	32.75	33	30.25	33	32.75	33	65.75

353	37	39.25	41.25	36.25	41.25	39.25	80.5
91	33	38	29	40.75	33	40.75	73.75
92	43.75	31	40	27.75	43.75	31	74.75
94	33	31	33	34.25	33	34.25	67.25
371	49.25	30	26.25	49.75	49.25	49.75	99
372	31.25	48.75	49	29	49	48.75	97.75
93	24.45	45	27.25	45.25	27.25	45.25	72.5

Table B.5. Lateral expansion measuremnts for BMP.

ID	Type	Depth	A1	A3	A2	A4	max (A1,A2)	max (A3,A4)	L_{ex}
1	LT	Surface	26	26.25	26	26.25	26	26.25	52.25
2	LT	Surface	27.5	27	26	26.75	27.5	27	54.5
3	LT	Surface	25.25	26	26.5	27.5	26.5	27.5	54
4	LT	Core	23.5	23.5	23	24	23.5	24	47.5
5	LT	Core	29	29	28	30	29	30	59
6	LT	Core	24.25	24	24.5	24.25	24.5	24.25	48.75
7	TL	Surface	26	24	23.25	23.5	26	24	50
8	TL	Surface	28	27.5	26.25	27	28	27.5	55.5
9	TL	Surface	24.75	22	24	22.25	24.75	22.25	47
10	TL	Core	24	24.75	24	24	24	24.75	48.75
11	TL	Core	22	23.5	25.5	24.5	25.5	24.5	50
12	TL	Core	28	24.75	26	24.75	28	24.75	52.75
13	LT	Surface	49.25	52	48.5	48.25	49.25	52	101.25
14	LT	Surface	41	42	40	40	41	42	83
15	LT	Surface	24	24	25	26.25	25	26.25	51.25
16	LT	Core	28	27.5	28.25	29	28.25	29	57.25
17	LT	Core	24.5	24.5	25	25	25	25	50
18	LT	Core	25.75	25.25	28.75	28	28.75	28	56.75
19	TL	Surface	39.25	41	37	37.5	39.25	41	80.25
20	TL	Surface	24.5	24	31.25	24	31.25	24	55.25
21	TL	Surface	28	28	26.75	27.5	28	28	56
22	TL	Core	33.75	32	30	30	33.75	32	65.75
23	TL	Core	26.25	25.5	24	23.25	26.25	25.5	51.75
24	TL	Core	28.5	27	26.5	28.25	28.5	28.25	56.75
25	LT	Surface	68	58	67	71	68	71	139

26	LT	Surface	51.5	59.25	52	58	52	59.25	111.25
27	LT	Surface	61.5	62	54.75	62.25	61.5	62.25	123.75
28	LT	Core	46	46	48.5	48	48.5	48	96.5
29	LT	Core	30	29.25	30	30	30	30	60
30	LT	Core	23.25	23.75	25.25	24.75	25.25	24.75	50
31	TL	Surface	48	47	49.5	50.75	49.5	50.75	100.25
32	TL	Surface	41	43	40.5	41	41	43	84
33	TL	Surface	26	26	24.25	25.25	26	26	52
34	TL	Core	26	26.25	27	28	27	28	55
35	TL	Core	31.5	32	30	29	31.5	32	63.5
36	TL	Core	26.5	26	28	28	28	28	56
37	LT	Surface	31	30	31.25	32	31.25	32	63.25
38	LT	Surface	43	41	43.25	43.25	43.25	43.25	86.5
39	LT	Surface	61.75	65.5	68.5	69.5	68.5	69.5	138
40	LT	Core	35.5	36	36.5	36	36.5	36	72.5
41	LT	Core	37	37	36.5	38	37	38	75
42	LT	Core	50	49	47.5	48	50	49	99
43	TL	Surface	38	38	39	40	39	40	79
44	TL	Surface	44	43	39	40	44	43	87
45	TL	Surface	26.5	26	27.5	28	27.5	28	55.5
46	TL	Core	40	40	39.25	36.25	40	40	80
47	TL	Core	32	31.5	30	30	32	31.5	63.5
48	TL	Core	28	28	31	31	31	31	62
49	LT	Surface	69	44.25	45	66.25	69	66.25	135.25
50	LT	Surface	66	72	65	67	66	72	138
51	LT	Surface	69	49	45	70	69	70	139
52[a]	LT	Surface					0	0	0
53[a]	LT	Surface					0	0	0
54	LT	Core	33	34	34	34	34	34	68
55	LT	Core	32	32	32	33	32	33	65
56	LT	Core	35	34.25	34	33.5	35	34.25	69.25
57	TL	Surface	66.25	58	63.5	59.5	66.25	59.5	125.75
58	TL	Surface	39	40.5	42	41.75	42	41.75	83.75
59	TL	Surface	23	23	25.5	25	25.5	25	50.5
60	TL	Core	47.5	47.25	46	47	47.5	47.25	94.75
61	TL	Core	33.5	35	32	31.25	33.5	35	68.5
62	TL	Core	38	37	40	38.5	40	38.5	78.5

63	LT	Surface	54.25	73	50	73	54.25	73	127.25
64	LT	Surface	31	30	58.5	45	58.5	45	103.5
65	LT	Surface	70.5	49	48	71	70.5	71	141.5
66	LT	Surface	51.5	71.25	50.5	71	51.5	71.25	122.75
67	LT	Surface	NB	NB	NB	NB	0	0	0
68	LT	Surface	45	42	44.5	44	45	44	89
69	LT	Core	25	25	25.5	25	25.5	25	50.5
70	LT	Core	62.75	64.25	69	53	69	64.25	133.25
71	LT	Core	47	46.5	45.5	44.25	47	46.5	93.5
72	LT	Core	66	57.75	65.5	60	66	60	126
73	LT	Core	44.75	44.5	44.25	46	44.75	46	90.75
74	LT	Core	62.5	68	68.75	67.75	68.75	68	136.75
75	TL	Surface	63	61	62	66	63	66	129
76	TL	Surface	24	23.75	24	24	24	24	48
77	TL	Surface	62.25	69	58.75	71.75	62.25	71.75	134
78	TL	Surface	48	50	48	49	48	50	98
79	TL	Surface	59.5	67	64	68.25	64	68.25	132.25
80	TL	Surface	45.75	45	49.5	46.5	49.5	46.5	96
81	TL	Core	33	32	34	36.75	34	36.75	70.75
82	TL	Core	51	51	49	47	51	51	102
83	TL	Core	33	32.5	33.75	34	33.75	34	67.75
84	TL	Core	58.5	55.25	59.25	58.25	59.25	58.25	117.5
85	TL	Core	46	45	48	49.75	48	49.75	97.75
86	TL	Core	50	50.75	48.5	49	50	50.75	100.75
87	LT	Surface	NB	NB	NB	NB	0	0	0
88	LT	Surface	69.75	67	71	69	71	69	140
89	LT	Surface	NB	NB	NB	NB	0	0	0
90	LT	Core	64	70	63	70.75	64	70.75	134.75
91	LT	Core	33	31.5	31.25	32	33	32	65
92	LT	Core	39	39.5	40.25	40.5	40.25	40.5	80.75
93[a]	LT	Core					0	0	0
94[a]	LT	Core					0	0	0
95	TL	Surface	68.25	56.5	54.25	69	68.25	69	137.25
96	TL	Surface	72	62.5	62.5	67	72	67	139
97	TL	Surface	61.75	66	61.75	65	61.75	66	127.75
98	TL	Core	42.25	41.25	41	42	42.25	42	84.25
99	TL	Core	55	55.5	58.5	56	58.5	56	114.5

100	TL	Core	45.25	46.5	48.75	47.25	48.75	47.25	96
101	LT	Surface	52.5	71	72	54	72	71	143
102	LT	Surface	53.75	68.75	51.75	70	53.75	70	123.75
103	LT	Surface	45.5	68	69	40.25	69	68	137
104	LT	Core	64	63.75	48.75	69.75	64	69.75	133.75
105	LT	Core	73	55.75	73	55.5	73	55.75	128.75
106	LT	Core	59.75	64.75	63.5	66	63.5	66	129.5
107	TL	Surface	54	70	56.75	67	56.75	70	126.75
108	TL	Surface	61	64.75	58.5	63.5	61	64.75	125.75
109	TL	Surface	70	56.75	69.75	58	70	58	128
110	TL	Core	59	64.5	59	58.25	59	64.5	123.5
111	TL	Core	61	60	59.75	62	61	62	123
112	TL	Core	64	64	59.5	56.25	64	64	128
113	LT	Surface	NB	NB	NB	NB	0	0	0
114	LT	Surface	57.25	64.5	49.25	71.5	57.25	71.5	128.75
115[a]	LT	Surface					0	0	0
116	LT	Core	70.5	48	46	72	70.5	72	142.5
117	LT	Core	70	52.25	69.5	48.5	70	52.25	122.25
118	LT	Core	42.5	46	44	44.5	44	46	90
119[a]	LT	Core					0	0	0
120	TL	Surface	70.25	51	67.5	51.25	70.25	51.25	121.5
121	TL	Surface	68.5	54	71.75	51.75	71.75	54	125.75
122	TL	Surface	65	51	69.5	52	69.5	52	121.5
123	TL	Core	57.25	69.5	64	52	64	69.5	133.5
124	TL	Core	62.25	56	58	67	62.25	67	129.25
125	TL	Core	54.5	67.75	57	69.25	57	69.25	126.25

[a] No lateral expansion measurement performed

APPENDIX C: HARDNESS TESTING DATA

Table C.1. Hardness measurements for PA.

M1						
Point	X	Y	D1	D2	HV	3 Point Average
3	0.25	0.4000	63.18	63.19	232.2	232.2
4	0.3	0.4000	62.26	63.18	235.7	233.95
9	0.35	0.4000	64.23	64.1	225.2	231.03333
10	0.4	0.4000	67.78	68.97	198.3	219.73333
15	0.45	0.4000	66.5	67.29	207.2	210.23333
16	0.5	0.4000	68.92	68.92	195.2	200.23333
21	0.55	0.4000	67.23	69.58	198.2	200.2
22	0.6	0.4000	71.13	70.9	183.8	192.4
27	0.65	0.4000	68.21	64.5	210.6	197.53333
28	0.7	0.4000	66.22	65.72	213.1	202.5
33	0.75	0.4000	64.01	63.83	227	216.9
34	0.8	0.4000	64	63.93	226.6	222.23333
39	0.85	0.4000	62.74	62.9	235	229.53333
40	0.9	0.4000	63.73	61.96	234.8	232.13333
45	0.95	0.4000	62.69	62.91	235.1	234.96667
46	1	0.4000	69.98	68.88	192.3	220.73333
51	1.05	0.4000	62.92	61.72	238.7	222.03333
52	1.1	0.4000	63.67	64.04	227.4	219.46667
57	1.15	0.4000	66.21	63.79	219.5	228.53333
A	1.2	0.4000	65.18	66.23	214.8	220.56667
60	1.25	0.4000	64.91	64.17	222.6	218.96667
61	1.3	0.4000	65.28	64.67	219.6	219
66	1.35	0.4000	65.02	63.07	226.1	222.76667

67	1.4	0.4000	64.7	65.13	220	221.9
72	1.45	0.4000	64.76	65.28	219.3	221.8
73	1.5	0.4000	65.16	65.59	216.9	218.73333
78	1.55	0.4000	64.72	65.13	220	218.73333
79	1.6	0.4000	66.49	64.62	215.8	217.56667
84	1.65	0.4000	63.94	65.63	220.9	218.9
85	1.7	0.4000	65.56	64.18	220.3	219
90	1.75	0.4000	64.13	64.3	224.9	222.03333
91	1.8	0.4000	66.44	66.99	208.3	217.83333
96	1.85	0.4000	63.79	65.13	223.1	218.76667
97	1.9	0.4000	64.03	64.96	222.9	218.1
102	1.95	0.4000	65.63	65.05	217.2	221.06667
103	2	0.4000	63.36	64.42	227.2	222.43333
108	2.05	0.4000	65.14	65.55	217.1	220.5
109	2.1	0.4000	63.93	64.71	224.1	222.8
114	2.15	0.4000	65.14	64.79	219.7	220.3
B	2.2	0.4000	65.12	66.11	215.4	219.73333
117	2.25	0.4000	64.87	66.19	215.9	217
118	2.3	0.4000	63.61	63.44	229.8	220.36667
123	2.35	0.4000	65.93	65.52	214.6	220.1
124	2.4	0.4000	63.02	66.03	222.7	222.36667
129	2.45	0.4000	66.23	66.09	211.8	216.36667
130	2.5	0.4000	63.64	64.46	226	220.16667
135	2.55	0.4000	64.48	63.96	224.8	220.86667
136	2.6	0.4000	64.33	65.48	220.1	223.63333
141	2.65	0.4000	66.74	66.58	208.7	217.86667
142	2.7	0.4000	62	64.06	233.4	220.73333
147	2.75	0.4000	64.98	64.91	219.9	220.66667
148	2.8	0.4000	65.24	63.46	223.9	225.73333
153	2.85	0.4000	63.84	62.54	232.2	225.33333
154	2.9	0.4000	63.93	63.91	226.9	227.66667
159	2.95	0.4000	62.89	64.34	229.1	229.4
160	3	0.4000	62.86	64.48	228.7	228.23333
165	3.05	0.4000	63.71	63.68	228.5	228.76667
166	3.1	0.4000	64.39	63.69	226.1	227.76667
171	3.15	0.4000	63.49	64.56	226.2	226.93333
C	3.2	0.4000	64.11	63.79	226.7	226.33333
174	3.25	0.4000	63.83	63.56	228.5	227.13333
175	3.3	0.4000	64.56	65.35	219.7	224.96667

180	3.35	0.4000	64.71	64.57	221.9	223.36667
181	3.4	0.4000	63.95	64.19	225.9	222.5
186	3.45	0.4000	64.14	64.34	224.7	224.16667
187	3.5	0.4000	65.13	62.11	229.1	226.56667
192	3.55	0.4000	63.95	59.72	242.5	232.1
193	3.6	0.4000	62.23	63.12	236	235.86667
198	3.65	0.4000	60.51	62.21	246.3	241.6
199	3.7	0.4000	64.27	63.19	228.3	236.86667
204	3.75	0.4000	65.53	64.05	220.9	231.83333
205	3.8	0.4000	59.89	62.19	248.8	232.66667
210	3.85	0.4000	64.36	66.57	216.3	228.66667
211	3.9	0.4000	64.73	66.96	213.9	226.33333
216	3.95	0.4000	67.54	68.29	201	210.4
217	4	0.4000	69.03	69.92	192.1	202.33333
222	4.05	0.4000	68.16	68.38	198.9	197.33333
223	4.1	0.4000	67.58	68.89	199.2	196.73333
228	4.15	0.4000	67.28	67.38	204.5	200.86667
2	0.25	0.7000	62.29	64.41	231.1	231.1
5	0.3	0.7000	63.53	64.77	225.3	228.2
8	0.35	0.7000	63.12	66.44	221	225.8
11	0.4	0.7000	65.87	66.5	211.7	219.33333
14	0.45	0.7000	67.56	66.94	205	212.56667
17	0.5	0.7000	64.73	65.42	218.9	211.86667
20	0.55	0.7000	66.65	67.88	204.9	209.6
23	0.6	0.7000	70.76	69.76	187.8	203.86667
26	0.65	0.7000	69.9	70.66	187.7	193.46667
29	0.7	0.7000	65.78	60.65	232	202.5
32	0.75	0.7000	64.05	61.21	236.4	218.7
35	0.8	0.7000	63.54	65.09	224.1	230.83333
38	0.85	0.7000	64.45	63.02	228.3	229.6
41	0.9	0.7000	63.18	63.82	230	227.46667
44	0.95	0.7000	62.94	63.18	233.1	230.46667
47	1	0.7000	63.53	62.14	234.8	232.63333
50	1.05	0.7000	67.19	65.63	210.2	226.03333
53	1.1	0.7000	62.64	63.91	231.6	225.53333
56	1.15	0.7000	63.5	63.76	229	223.6
D	1.2	0.7000	63.65	63.81	228.3	229.63333
59	1.25	0.7000	63.86	64.06	226.6	227.96667
62	1.3	0.7000	63.71	63.85	227.9	227.6

65	1.35	0.7000	64.28	65.21	221.2	225.23333
68	1.4	0.7000	63.87	64.92	223.6	224.23333
71	1.45	0.7000	63.31	64.13	228.4	224.4
74	1.5	0.7000	63.15	63.82	230.1	227.36667
77	1.55	0.7000	63.91	63.3	229.2	229.23333
80	1.6	0.7000	64.33	65.48	220.1	226.46667
83	1.65	0.7000	63.17	62.76	233.9	227.73333
86	1.7	0.7000	66.44	64.33	216.9	223.63333
89	1.75	0.7000	63.34	63.36	231	227.26667
92	1.8	0.7000	65.24	65.62	216.6	221.5
95	1.85	0.7000	65.09	65.88	216.2	221.26667
98	1.9	0.7000	66.63	63.14	220.3	217.7
101	1.95	0.7000	65.84	65.09	216.3	217.6
104	2	0.7000	63.61	62.82	232	222.86667
107	2.05	0.7000	65.35	66.94	211.9	220.06667
110	2.1	0.7000	64.05	64.62	224	222.63333
113	2.15	0.7000	63.8	62.39	232.9	222.93333
E	2.2	0.7000	64.12	63.97	226	227.63333
116	2.25	0.7000	66.39	64.92	215.1	224.66667
119	2.3	0.7000	64.92	63.14	226.1	222.4
122	2.35	0.7000	64.33	65.14	221.2	220.8
125	2.4	0.7000	66.01	62.79	223.5	223.6
128	2.45	0.7000	64.97	63.93	223.2	222.63333
131	2.5	0.7000	65.29	64.14	221.4	222.7
134	2.55	0.7000	64.76	63.65	224.9	223.16667
137	2.6	0.7000	64.48	64.61	222.6	222.96667
140	2.65	0.7000	62.93	63.54	231.9	226.46667
143	2.7	0.7000	63.01	66.52	221	225.16667
146	2.75	0.7000	63.88	65.57	221.3	224.73333
149	2.8	0.7000	64.51	64.35	223.4	221.9
152	2.85	0.7000	65.55	65.5	215.9	220.2
155	2.9	0.7000	63.88	65.42	221.8	220.36667
158	2.95	0.7000	63.13	63.44	231.5	223.06667
161	3	0.7000	64.68	64.22	223.2	225.5
164	3.05	0.7000	62.88	64.64	228.1	227.6
167	3.1	0.7000	63.65	62.39	233.5	228.26667
170	3.15	0.7000	64.96	62.64	227.8	229.8
F	3.2	0.7000	63.75	63.81	227.9	229.73333
173	3.25	0.7000	63.4	63.63	229.9	228.53333

176	3.3	0.7000	62.61	63.64	232.7	230.16667
179	3.35	0.7000	63.19	64.99	225.7	229.43333
182	3.4	0.7000	63.61	63.13	230.9	229.76667
185	3.45	0.7000	64.33	64.27	224.3	226.96667
188	3.5	0.7000	63.34	63.41	230.8	228.66667
191	3.55	0.7000	62.99	63.45	232	229.03333
194	3.6	0.7000	62.43	62.39	238	233.6
197	3.65	0.7000	61.24	61.01	248.2	239.4
200	3.7	0.7000	60.54	61.07	250.8	245.66667
203	3.75	0.7000	62.84	62.85	234.7	244.56667
206	3.8	0.7000	62.08	63.31	235.9	240.46667
209	3.85	0.7000	65.13	67.06	212.2	227.6
212	3.9	0.7000	69.74	67.78	196.1	214.73333
215	3.95	0.7000	69.23	67.71	197.8	202.03333
218	4	0.7000	65.24	67.62	210.1	201.33333
221	4.05	0.7000	68.54	71.83	188.2	198.7
224	4.1	0.7000	69.72	68.44	194.3	197.53333
227	4.15	0.7000	69.58	68.54	194.4	192.3
1	0.25	1.0000	63.74	65.28	222.8	222.8
6	0.3	1.0000	65.85	66.56	211.5	217.15
7	0.35	1.0000	63.03	63.71	230.9	221.73333
12	0.4	1.0000	63.94	64.88	223.5	221.96667
13	0.45	1.0000	64.97	63.54	224.6	226.33333
18	0.5	1.0000	64.99	67.86	210.1	219.4
19	0.55	1.0000	67.93	68.78	198.4	211.03333
24	0.6	1.0000	66.03	65.37	214.8	207.76667
25	0.65	1.0000	69.88	67.84	195.5	202.9
30	0.7	1.0000	67.78	68.8	198.8	203.03333
31	0.75	1.0000	65.61	65.44	215.9	203.4
36	0.8	1.0000	64.29	63.27	227.9	214.2
37	0.85	1.0000	63.56	61.81	236	226.6
42	0.9	1.0000	62.18	63.72	234	232.63333
43	0.95	1.0000	61.33	61.68	245.1	238.36667
48	1	1.0000	62.2	60.94	244.6	241.23333
49	1.05	1.0000	65.71	64.85	217.6	235.76667
54	1.1	1.0000	64.73	65.13	219.9	227.36667
55	1.15	1.0000	65.42	65.61	216	217.83333
G	1.2	1.0000	64.51	64.89	221.5	219.13333
58	1.25	1.0000	64.71	65.79	217.8	218.43333

63	1.3	1.0000	64.44	63.77	225.6	221.63333
64	1.35	1.0000	63.48	63.23	231	224.8
69	1.4	1.0000	62.4	64.02	232.1	229.56667
70	1.45	1.0000	62.64	63.68	232.4	231.83333
75	1.5	1.0000	63.63	64.33	226.5	230.33333
76	1.55	1.0000	61.7	63.34	237.2	232.03333
81	1.6	1.0000	63.38	63.66	229.8	231.16667
82	1.65	1.0000	64.53	64.28	223.5	230.16667
87	1.7	1.0000	64.36	63.45	227	226.76667
88	1.75	1.0000	63.66	66.08	220.3	223.6
93	1.8	1.0000	62.67	62.89	235.2	227.5
94	1.85	1.0000	62.14	64.3	232	229.16667
99	1.9	1.0000	63.16	64.3	228.3	231.83333
100	1.95	1.0000	64.32	63.66	226.5	228.93333
105	2	1.0000	64.65	64.48	222.4	225.73333
106	2.05	1.0000	64.84	64.96	220.2	223.03333
111	2.1	1.0000	64.3	63.59	226.8	223.13333
112	2.15	1.0000	64.24	64.74	223	223.33333
H	2.2	1.0000	65.01	64.58	220.8	223.53333
115	2.25	1.0000	65.8	63.82	220.7	221.5
120	2.3	1.0000	70.49	69.96	188	209.83333
121	2.35	1.0000	63.78	65.22	222.9	210.53333
126	2.4	1.0000	63.76	64.29	226.2	212.36667
127	2.45	1.0000	64.75	64.32	222.6	223.9
132	2.5	1.0000	64.89	63.04	226.6	225.13333
133	2.55	1.0000	63.71	63.42	229.5	226.23333
138	2.6	1.0000	65.78	66.78	211.1	222.4
139	2.65	1.0000	63.64	65.1	223.8	221.46667
144	2.7	1.0000	64.96	65.26	218.7	217.86667
145	2.75	1.0000	64.21	63.29	228.1	223.53333
150	2.8	1.0000	62	63.72	234.7	227.16667
151	2.85	1.0000	63.3	63.28	231.5	231.43333
156	2.9	1.0000	65.24	63.05	225.4	230.53333
157	2.95	1.0000	63.11	63.28	232.2	229.7
162	3	1.0000	63.94	62.42	232.3	229.96667
163	3.05	1.0000	65.54	63.93	221.3	228.6
168	3.1	1.0000	62.86	63.69	231.6	228.4
169	3.15	1.0000	63.54	66.1	220.7	224.53333
I	3.2	1.0000	62.85	63.15	233.6	228.63333

172	3.25	1.0000	62.66	63.35	233.6	229.3
177	3.3	1.0000	63.27	63.31	231.5	232.9
178	3.35	1.0000	62.52	62.94	235.6	233.56667
183	3.4	1.0000	64.09	63.17	229	232.03333
184	3.45	1.0000	63.14	64.84	226.4	230.33333
189	3.5	1.0000	63.77	64.34	226	227.13333
190	3.55	1.0000	60.64	61.63	248.1	233.5
195	3.6	1.0000	61.03	62.86	241.6	238.56667
196	3.65	1.0000	62.21	63.2	235.8	241.83333
201	3.7	1.0000	63.41	63.01	232.1	236.5
202	3.75	1.0000	63.48	64.42	226.7	231.53333
207	3.8	1.0000	64.71	65.99	217.1	225.3
208	3.85	1.0000	63.74	63.1	230.5	224.76667
213	3.9	1.0000	68.98	69.23	194.2	213.93333
214	3.95	1.0000	70.54	72.69	180.8	201.83333
219	4	1.0000	70.14	69.75	189.5	188.16667
220	4.05	1.0000	63.87	68.48	211.7	194
225	4.1	1.0000	68.89	68.96	195.2	198.8
226	4.15	1.0000	67.86	67.91	201.2	202.7
M2						
3	0.1	0.4	64.08	62.81	230.3	230.3
4	0.15	0.4	62.49	65.97	224.8	227.55
9	0.2	0.4	62.27	63.03	236.2	230.43333
A	0.25	0.4	63.15	63.86	229.9	230.3
15	0.3	0.4	64.23	63.5	227.3	231.13333
16	0.35	0.4	63.95	65.68	220.7	225.96667
21	0.4	0.4	63.94	67.52	214.6	220.86667
22	0.45	0.4	64.58	63.28	226.9	220.73333
27	0.5	0.4	63.26	63.58	230.5	224
30	0.55	0.4	60.88	61.78	246.5	234.63333
31	0.6	0.4	61.84	64.19	233.5	236.83333
36	0.65	0.4	63.02	62.85	234.1	238.03333
37	0.7	0.4	63.79	66.5	218.5	228.7
42	0.75	0.4	64.44	65.66	219.1	223.9
43	0.8	0.4	62.62	62.74	236	224.53333
48	0.85	0.4	61.48	64.78	232.7	229.26667
49	0.9	0.4	60.23	63.04	244.1	237.6
54	0.95	0.4	59.28	59.76	261.7	246.16667
55	1	0.4	62.4	62.81	236.6	247.46667

60	1.05	0.4	60.27	61.42	250.5	249.6
61	1.1	0.4	61.41	60.39	250	245.7
66	1.15	0.4	62.19	60.07	248.1	249.53333
67	1.2	0.4	63.11	62.75	234.1	244.06667
72	1.25	0.4	60.4	59.73	257	246.4
73	1.3	0.4	62.74	62.08	238	243.03333
78	1.35	0.4	59.91	59.53	260	251.66667
79	1.4	0.4	60.06	59.85	257.9	251.96667
84	1.45	0.4	59.01	61.47	255.5	257.8
87	1.5	0.4	65.22	63.86	222.6	245.33333
90	1.55	0.4	64.15	63.58	227.3	235.13333
91	1.6	0.4	64.91	63.32	225.6	225.16667
96	1.65	0.4	61.74	62.04	242.1	231.66667
97	1.7	0.4	64.16	65.51	220.6	229.43333
102	1.75	0.4	62.43	63.24	234.9	232.53333
103	1.8	0.4	64.64	63.19	227	227.5
108	1.85	0.4	63.6	64.42	226.3	229.4
109	1.9	0.4	62.49	61.89	239.8	231.03333
114	1.95	0.4	62.81	64.22	229.9	232
115	2	0.4	61.58	64.4	233.7	234.46667
120	2.05	0.4	62.43	64.06	231.8	231.8
121	2.1	0.4	63.98	63.94	226.7	230.73333
126	2.15	0.4	63.39	63.32	231	229.83333
127	2.2	0.4	62.34	63.65	233.7	230.46667
132	2.25	0.4	63.52	63.78	228.9	231.2
133	2.3	0.4	64.12	63.18	228.9	230.5
138	2.35	0.4	64.13	62	233.1	230.3
139	2.4	0.4	62.74	63.89	231.3	231.1
144	2.45	0.4	63.41	64.46	226.9	230.43333
147	2.5	0.4	63.01	63.96	230.1	229.43333
150	2.55	0.4	63.57	64.67	225.5	227.5
151	2.6	0.4	63.01	63.33	232.4	229.33333
156	2.65	0.4	65.11	64.35	221.3	226.4
157	2.7	0.4	63.67	63.94	227.8	227.16667
162	2.75	0.4	60.83	62.91	242.2	230.43333
163	2.8	0.4	61.13	62.56	242.4	237.46667
168	2.85	0.4	63.21	60.68	241.7	242.1
169	2.9	0.4	59.84	60.9	254.4	246.16667
174	2.95	0.4	59.86	61.49	251.9	249.33333

175	3	0.4	61.75	60.63	247.6	251.3
180	3.05	0.4	61.3	63.28	239	246.16667
181	3.1	0.4	60.46	62.37	245.8	244.13333
186	3.15	0.4	65.8	64.81	217.4	234.06667
187	3.2	0.4	64.04	65.21	222	228.4
192	3.25	0.4	68.58	67.91	199.1	212.83333
193	3.3	0.4	63.16	57.79	253.5	224.86667
198	3.35	0.4	64.23	66.29	217.7	223.43333
199	3.4	0.4	63.29	61.96	236.4	235.86667
204	3.45	0.4	63.97	63.61	227.9	227.33333
207	3.5	0.4	65.23	63.49	223.8	229.36667
208	3.55	0.4	62.08	63.9	233.7	228.46667
213	3.6	0.4	63.59	66.39	219.5	225.66667
214	3.65	0.4	63.49	65.04	224.5	225.9
219	3.7	0.4	62.37	65.19	227.9	223.96667
220	3.75	0.4	62.13	65.08	229.2	227.2
225	3.8	0.4	62.39	64.03	232.1	229.73333
226	3.85	0.4	64.29	63.78	226.1	229.13333
231	3.9	0.4	61.93	62.05	241.3	233.16667
232	3.95	0.4	63.14	64.4	228	231.8
237	4	0.4	61.52	66.29	227.1	232.13333
238	4.05	0.4	63.98	64.19	225.8	226.96667
243	4.1	0.4	64.61	65.42	219.3	224.06667
244	4.15	0.4	64.21	66.49	217.1	220.73333
249	4.2	0.4	63.96	64.46	224.9	220.43333
250	4.25	0.4	66.69	64.44	215.7	219.23333
255	4.3	0.4	63.19	69.11	211.9	217.5
256	4.35	0.4	64.51	65.99	217.8	215.13333
2	0.1	0.7	64.36	63.63	226.4	226.4
5	0.15	0.7	63.64	66.66	218.4	222.4
8	0.2	0.7	64.32	62.73	229.8	224.86667
B	0.25	0.7	61.41	60.15	251	233.06667
14	0.3	0.7	60.04	62.51	246.9	242.56667
17	0.35	0.7	62.83	64.59	228.4	242.1
20	0.4	0.7	64.56	64.61	222.3	232.53333
23	0.45	0.7	64.28	68.07	211.7	220.8
26	0.5	0.7	62.83	66.13	223	219
29	0.55	0.7	61.56	63.09	238.7	224.46667
32	0.6	0.7	61.58	66.17	227.3	229.66667

35	0.65	0.7	65.67	65.39	215.9	227.3
38	0.7	0.7	63.98	64.42	224.9	222.7
41	0.75	0.7	64.13	64.89	222.8	221.2
44	0.8	0.7	65.1	67.86	209.8	219.16667
47	0.85	0.7	66.33	64.6	216.4	216.33333
50	0.9	0.7	64.14	64.21	225.1	217.1
53	0.95	0.7	57.18	58.51	277.1	239.53333
56	1	0.7	59.21	58.28	268.7	256.96667
59	1.05	0.7	58.86	60.2	261.6	269.13333
62	1.1	0.7	60.44	60.69	252.8	261.03333
65	1.15	0.7	60.89	59.44	256.1	256.83333
68	1.2	0.7	61.15	60.76	249.5	252.8
71	1.25	0.7	60.14	61.25	251.7	252.43333
74	1.3	0.7	59.4	62.07	251.4	250.86667
77	1.35	0.7	61.68	63.04	238.4	247.16667
80	1.4	0.7	61.46	64.94	232.1	240.63333
83	1.45	0.7	62.52	63.51	233.5	234.66667
86	1.5	0.7	61.72	63.48	236.6	234.06667
89	1.55	0.7	63.7	63.45	229.4	233.16667
92	1.6	0.7	65.16	64.23	221.6	229.2
95	1.65	0.7	62.55	63.96	231.7	227.56667
98	1.7	0.7	63.36	63.24	231.4	228.23333
101	1.75	0.7	63.2	64.76	226.5	229.86667
104	1.8	0.7	61.96	62.87	238	231.96667
107	1.85	0.7	62.16	63.47	235	233.16667
110	1.9	0.7	62.04	63.23	236.3	236.43333
113	1.95	0.7	62.93	65.51	224.8	232.03333
116	2	0.7	63	63.72	231	230.7
119	2.05	0.7	63.28	63.59	230.4	228.73333
122	2.1	0.7	63.34	63.54	230.4	230.6
125	2.15	0.7	63.65	63.4	229.8	230.2
128	2.2	0.7	61.53	62.24	242.1	234.1
131	2.25	0.7	63.16	62.58	234.6	235.5
134	2.3	0.7	63.61	63.57	229.3	235.33333
137	2.35	0.7	62.96	64	230.1	231.33333
140	2.4	0.7	64.9	61.41	232.5	230.63333
143	2.45	0.7	63.51	63.64	229.4	230.66667
146	2.5	0.7	62.48	62.06	239.1	233.66667
149	2.55	0.7	63.99	62.01	233.6	234.03333

152	2.6	0.7	62.26	61.23	243.2	238.63333
155	2.65	0.7	62.97	62.18	236.8	237.86667
158	2.7	0.7	62.78	62.56	236.1	238.7
161	2.75	0.7	62.48	62.99	235.6	236.16667
164	2.8	0.7	62.95	61.4	239.8	237.16667
167	2.85	0.7	61.31	64.05	236	237.13333
170	2.9	0.7	59.52	58.22	267.5	247.76667
173	2.95	0.7	59.36	60.19	259.5	254.33333
176	3	0.7	62.32	60.51	245.8	257.6
179	3.05	0.7	58.11	61.76	258.1	254.46667
182	3.1	0.7	60.24	60.5	254.4	252.76667
185	3.15	0.7	60.25	61.06	252	254.83333
188	3.2	0.7	62.46	59.28	250.2	252.2
191	3.25	0.7	62.6	63.59	232.9	245.03333
194	3.3	0.7	63.51	65.39	223.2	235.43333
197	3.35	0.7	61.78	61.67	243.4	233.16667
200	3.4	0.7	62.99	63.19	233	233.2
203	3.45	0.7	62.65	65.21	226.9	234.43333
206	3.5	0.7	63.18	63.67	230.5	230.13333
209	3.55	0.7	62.91	63.43	232.4	229.93333
212	3.6	0.7	64.21	63.64	226.9	229.93333
215	3.65	0.7	64.66	65.79	217.9	225.73333
218	3.7	0.7	62.38	61.34	242.3	229.03333
221	3.75	0.7	63.49	63.74	229.1	229.76667
224	3.8	0.7	62.05	65.18	229.1	233.5
227	3.85	0.7	58.5	62.57	253	237.06667
230	3.9	0.7	65.25	63.71	223	235.03333
233	3.95	0.7	63.08	64.04	229.5	235.16667
236	4	0.7	63.01	60.53	243	231.83333
239	4.05	0.7	59.05	63.99	245	239.16667
242	4.1	0.7	61.42	66.04	228.3	238.76667
245	4.15	0.7	65.34	66.56	213.2	228.83333
248	4.2	0.7	63.4	66.41	220.1	220.53333
251	4.25	0.7	65.09	67.64	210.5	214.6
254	4.3	0.7	64.53	65.37	219.8	216.8
257	4.35	0.7	65.31	65.96	215.2	215.16667
1	0.1	1	58.35	61.84	256.7	256.7
6	0.15	1	63.84	63.06	230.3	243.5
7	0.2	1	61.09	62.34	243.5	243.5

C	0.25	1	61.02	62.75	242.1	238.63333
13	0.3	1	59.16	63.73	245.6	240.375
18	0.35	1	62.41	62	239.6	242.7
19	0.4	1	62.73	63.96	231.1	238.76667
24	0.45	1	60.3	65.05	236	235.56667
25	0.5	1	62.48	62.71	236.7	234.6
28	0.55	1	63.88	64.48	225.1	232.6
33	0.6	1	63.88	64.23	226	229.26667
34	0.65	1	60.82	60.59	251.6	234.23333
39	0.7	1	60.85	62.91	242.2	239.93333
40	0.75	1	64.75	66.17	216.4	236.73333
45	0.8	1	63.55	64.41	226.5	228.36667
46	0.85	1	64.94	66.42	214.9	219.26667
51	0.9	1	60.44	60.71	252.7	231.36667
52	0.95	1	59.66	59.07	263.1	243.56667
57	1	1	60.74	60.76	251.2	255.66667
58	1.05	1	58.83	59.53	264.8	259.7
63	1.1	1	58.67	60.89	259.4	258.46667
64	1.15	1	62.51	60.49	245.1	256.43333
69	1.2	1	61.89	62.55	239.5	248
70	1.25	1	62.88	62.89	234.5	239.7
75	1.3	1	63.73	61.82	235.3	236.43333
76	1.35	1	61.31	62.08	243.6	237.8
81	1.4	1	61.13	63.22	239.8	239.56667
82	1.45	1	62.94	62.71	234.9	239.43333
85	1.5	1	63.33	64.25	227.9	234.2
88	1.55	1	62.54	62.66	236.6	233.13333
93	1.6	1	61.59	64.14	234.6	233.03333
94	1.65	1	61.06	63.53	238.9	236.7
99	1.7	1	62.41	61.87	240.1	237.86667
100	1.75	1	63.89	62.88	230.8	236.6
105	1.8	1	61.69	62.98	238.6	236.5
106	1.85	1	60.65	62.39	245	238.13333
111	1.9	1	61.19	62.41	242.8	242.13333
112	1.95	1	63.47	63.11	231.5	239.76667
117	2	1	60.78	63.79	239	237.76667
118	2.05	1	60.18	61.1	252.2	240.9
123	2.1	1	62.54	64.48	229.9	240.36667
124	2.15	1	62.19	65.44	227.7	236.6

129	2.2	1	62.12	64.18	232.5	230.03333
130	2.25	1	61.32	64.19	235.4	231.86667
135	2.3	1	62.78	63.93	231	232.96667
136	2.35	1	61.58	63.76	236.1	234.16667
141	2.4	1	62.06	63.18	236.4	234.5
142	2.45	1	59.51	62.4	249.6	240.7
145	2.5	1	62.63	63.52	233.1	239.7
148	2.55	1	62.93	64.2	229.5	237.4
153	2.6	1	62.93	64.03	230.1	230.9
154	2.65	1	61.03	62.24	244	234.53333
159	2.7	1	60.34	62.69	245	239.7
160	2.75	1	62.68	61.32	241.2	243.4
165	2.8	1	63.4	63.38	230.7	238.96667
166	2.85	1	62.61	64.48	229.6	233.83333
171	2.9	1	62.44	63.91	232.3	230.86667
172	2.95	1	63.11	61.46	239	233.63333
177	3	1	64.13	64.45	224.3	231.86667
178	3.05	1	62.11	59.43	251.1	238.13333
183	3.1	1	56.94	59.85	271.9	249.1
184	3.15	1	58.88	58.43	269.5	264.16667
189	3.2	1	61.02	61.69	246.3	262.56667
190	3.25	1	58.44	60.43	262.5	259.43333
195	3.3	1	63.94	64.44	225	244.6
196	3.35	1	60.62	63.33	241.4	242.96667
201	3.4	1	62.8	62.63	235.8	234.06667
202	3.45	1	63.23	63.08	232.5	236.56667
205	3.5	1	62.5	63.19	234.8	234.36667
210	3.55	1	61.31	63.46	238.3	235.2
211	3.6	1	61.66	64.89	231.6	234.9
216	3.65	1	62.56	65.5	226.2	232.03333
217	3.7	1	59.74	64.09	241.8	233.2
222	3.75	1	62.18	61.65	241.9	236.63333
223	3.8	1	60.21	63.14	243.7	242.46667
228	3.85	1	58.83	64.34	244.5	243.36667
229	3.9	1	59.96	57.33	269.6	252.6
234	3.95	1	63.31	65.26	224.4	246.16667
235	4	1	61.55	62.58	240.7	244.9
240	4.05	1	57.21	60.43	268	244.36667
241	4.1	1	60.61	59.4	257.5	255.4

246	4.15	1	60.89	58.86	258.6	261.36667
247	4.2	1	60.39	60.98	251.8	255.96667
252	4.25	1	63.81	63.64	228.3	246.23333
253	4.3	1	62.64	63.38	233.5	237.86667
258	4.35	1	49.77	52.63	353.7	271.83333

Table C.2. Hardness measurements for PB.

M3						
Point	X	Y	D1	D2	HV	3 Point Average
1	0.5	1	60.38	59	260.2	260.2
2	0.55	1	59.88	59.58	259.9	260.05
3	0.6	1	62.61	61.99	238.9	253
4	0.65	1	63.44	62.02	235.6	244.8
5	0.7	1	58.43	59.9	264.9	246.46667
6	0.75	1	65.59	65.59	215.5	238.66667
7	0.8	1	61.26	61.43	246.4	242.26667
8	0.85	1	70.35	70.69	186.4	216.1
9	0.9	1	71.42	71.05	182.7	205.16667
10	0.95	1	70.8	70	187.1	185.4
11	1	1	66.72	67.49	205.9	191.9
12	1.05	1	64.36	65.14	221.2	204.73333
13	1.1	1	64.51	64.33	223.5	216.86667
14	1.15	1	63.38	62.28	234.9	226.53333
15	1.2	1	65.34	62.48	227	228.46667
16	1.25	1	63.06	64.16	229.1	230.33333
17	1.3	1	62.43	61.74	240.6	232.23333
18	1.35	1	63.11	63.24	232.3	234
19	1.4	1	61.24	62.97	240.4	237.76667
20	1.45	1	64.26	62.83	229.6	234.1
21	1.5	1	66.1	65.51	214.1	228.03333
22	1.55	1	66.55	65.5	212.7	218.8
23	1.6	1	64.89	64.73	220.8	215.86667
24	1.65	1	67.08	65.63	210.6	214.7
25	1.7	1	64.76	63.76	224.5	218.63333
26	1.75	1	66.52	66.26	210.4	215.16667
27	1.8	1	69.54	68.38	195	209.96667
28	1.85	1	71.03	67.73	192.6	199.33333
29	1.9	1	68.74	69.41	194.3	193.96667
30	1.95	1	66.86	68.92	201.2	196.03333
31	2	1	69.23	69.91	191.6	195.7
32	2.05	1	67.6	64.98	211	201.26667

33	2.1	1	66.96	69.58	198.9	200.5
34	2.15	1	65	65.06	219.2	209.7
35	2.2	1	68.01	68.38	199.4	205.83333
36	2.25	1	67.93	70.93	192.3	203.63333
37	2.3	1	67.23	69.19	199.3	197
38	2.35	1	65.14	65.54	217.2	202.93333
39	2.4	1	69.25	68.42	195.7	204.06667
40	2.45	1	69.38	68.18	196	202.96667
41	2.5	1	68.92	68.13	197.5	196.4
42	2.55	1	66.6	66.85	208.3	200.6
43	2.6	1	69.44	66.98	199.3	201.7
44	2.65	1	64.02	63.59	227.8	211.8
45	2.7	1	65.51	66.26	213.6	213.56667
46	2.75	1	68.28	69.77	194.6	212
47	2.8	1	67.48	68.53	200.5	202.9
48	2.85	1	66.87	67.7	204.8	199.96667
49	2.9	1	65.95	64.43	218.2	207.83333
50	2.95	1	66.61	65.68	211.9	211.63333
51	3	1	66.01	66.66	210.7	213.6
52	3.05	1	66.56	66	211.1	211.23333
53	3.1	1	65.46	64.75	218.7	213.5
54	3.15	1	64.92	63.96	223.3	217.7
55	3.2	1	68.28	66.45	204.3	215.43333
56	3.25	1	64.41	65.88	218.5	215.36667
57	3.3	1	66.26	65.75	212.8	211.86667
58	3.35	1	65.48	65.17	217.3	216.2
59	3.4	1	60.24	61.43	250.6	226.9
60	3.45	1	62.68	61.09	242.1	236.66667
61	3.5	1	61.43	61.31	246.2	246.3
62	3.55	1	59.41	59.81	260.9	249.73333
63	3.6	1	60.74	60.58	252	256.45
64	3.65	1	60.81	60.33	252.7	252.35
65	3.7	1	64.33	63.32	227.6	244.1
66	3.75	1	61.73	63.11	238	239.43333
67	3.8	1	60.11	60.96	253	239.53333
68	3.85	1	67.07	67.42	205.1	232.03333
69	3.9	1	67.59	68.64	199.8	219.3
70	3.95	1	74.88	73.24	169	191.3
71	4	1	70.65	69.99	187.5	185.43333
72	4.05	1	70.11	70.05	188.8	181.76667
73	4.1	1	65.12	64.98	219.1	198.46667
74	4.15	1	67.19	69.04	199.8	202.56667
75	4.2	1	63.72	63.23	230.1	216.33333
76	4.25	1	63.41	64.96	225.1	218.33333
77	4.3	1	63.56	64.47	226.3	227.16667
78	4.35	1	60.03	59.69	258.8	236.73333

79	4.4	1	63.24	65.79	222.8	235.96667
80	4.45	1	63.69	63.22	230.3	237.3
81	4.5	1	63.18	64.42	227.8	226.96667
82	0.5	0.4	61.19	60.52	250.4	250.4
83	0.55	0.4	61.41	62.65	241	245.7
84	0.6	0.4	60.46	59.29	258.6	250
85	0.65	0.4	62.4	63.71	233.2	244.26667
86	0.7	0.4	63.98	66	219.5	237.1
87	0.75	0.4	64.41	63.11	228.1	226.93333
88	0.8	0.4	65.31	64.29	220.8	222.8
89	0.85	0.4	68.36	66.14	205	217.96667
90	0.9	0.4	66.63	66.19	210.2	212
91	0.95	0.4	68.99	70	192	202.4
92	1	0.4	71.22	69.95	186.1	196.1
93	1.05	0.4	70.29	69.43	190	189.36667
94	1.1	0.4	68.84	69.2	194.6	190.23333
95	1.15	0.4	64.46	66.67	215.7	200.1
96	1.2	0.4	61.52	63.55	237.1	215.8
97	1.25	0.4	62.81	61.79	238.9	230.56667
98	1.3	0.4	62.86	61.26	240.7	238.9
99	1.35	0.4	61.48	64.89	232.2	237.26667
100	1.4	0.4	61.89	61.93	241.9	238.26667
101	1.45	0.4	63.17	62.38	235.3	236.46667
102	1.5	0.4	62.75	62.51	236.4	237.86667
103	1.55	0.4	62.08	62.42	239.3	237
104	1.6	0.4	60.21	60.66	253.9	243.2
105	1.65	0.4	64.04	64.08	225.9	239.7
106	1.7	0.4	66.14	65.17	215.1	231.63333
107	1.75	0.4	65.73	66.33	212.7	217.9
108	1.8	0.4	66.43	67.33	207.3	211.7
109	1.85	0.4	67.15	68.53	201.5	207.16667
110	1.9	0.4	66.76	68.38	203.1	203.96667
111	1.95	0.4	69.26	65.89	203	202.53333
112	2	0.4	66.19	64.09	218.5	208.2
113	2.05	0.4	67.35	65.81	209.2	210.23333
114	2.1	0.4	66.94	65.87	210.3	212.66667
115	2.15	0.4	67.8	66.79	204.7	208.06667
116	2.2	0.4	66.35	67.44	207.2	207.4
117	2.25	0.4	65.74	64.87	217.4	209.76667
118	2.3	0.4	68.63	68.62	196.9	207.16667
119	2.35	0.4	69.08	67.51	198.8	204.36667
120	2.4	0.4	65.98	64.28	218.6	204.76667
121	2.45	0.4	67.21	68.14	202.4	206.6
122	2.5	0.4	66.32	66.92	208.9	209.96667
123	2.55	0.4	65.6	65.58	215.5	208.93333
124	2.6	0.4	67.33	66.42	207.3	210.56667

125	2.65	0.4	65.99	64.88	216.5	213.1
126	2.7	0.4	65.86	67.62	208.2	210.66667
127	2.75	0.4	66.79	65.46	212	212.23333
128	2.8	0.4	64.92	64.08	222.9	214.36667
129	2.85	0.4	65.58	64.96	217.7	217.53333
130	2.9	0.4	64.17	66.03	218.8	219.8
131	2.95	0.4	65.79	66.01	213.5	216.66667
132	3	0.4	65.76	66.03	213.5	215.26667
133	3.05	0.4	67.32	67.77	203.2	210.06667
134	3.1	0.4	65.83	64.47	218.4	211.7
135	3.15	0.4	65.36	65.57	216.4	212.66667
136	3.2	0.4	66.58	64.92	214.5	216.43333
137	3.25	0.4	61.75	61.41	244.5	225.13333
138	3.3	0.4	62.29	61.33	242.7	233.9
139	3.35	0.4	64.25	61.86	233.2	240.13333
140	3.4	0.4	60.21	60.22	255.7	243.86667
141	3.45	0.4	62.34	63.29	235	241.3
142	3.5	0.4	64.88	63.9	223.6	238.1
143	3.55	0.4	61.93	62.56	239.3	232.63333
144	3.6	0.4	64.73	64.74	221.2	228.03333
145	3.65	0.4	63.96	65.09	222.7	227.73333
146	3.7	0.4	64.17	64.51	224	222.63333
147	3.75	0.4	63.65	63.33	230	225.56667
148	3.8	0.4	63.92	64.34	225.4	226.46667
149	3.85	0.4	69.96	69.09	191.8	215.73333
150	3.9	0.4	70.35	69.88	188.6	201.93333
151	3.95	0.4	68.33	69.99	193.8	191.4
152	4	0.4	68.33	67.51	201	194.46667
153	4.05	0.4	66.76	68.04	204.1	199.63333
154	4.1	0.4	66.41	67.14	207.9	204.33333
155	4.15	0.4	68.92	65.94	203.9	205.3
156	4.2	0.4	65.14	64.67	220.1	210.63333
157	4.25	0.4	64.94	63.51	224.8	216.26667
158	4.3	0.4	63.65	63.83	228.2	224.36667
159	4.35	0.4	64.15	64.78	223.1	225.36667
160	4.4	0.4	63.32	62.29	235.1	228.8
161	4.45	0.4	65.06	64.48	221	226.4
162	4.5	0.4	63.79	64.06	226.9	227.66667
M4						
1	0.5	0.4	69.34	67.98	196.7	196.7
2	0.55	0.4	69.22	67.22	199.2	197.95
3	0.6	0.4	66.76	66.36	209.3	201.73333
4	0.65	0.4	67.76	65.41	209.1	205.86667
5	0.7	0.4	67.25	63.98	215.4	211.26667
6	0.75	0.4	66.09	63.99	219.2	214.56667

7	0.8	0.4	66.97	67.48	205.2	213.26667
8	0.85	0.4	68.51	68.09	198.7	207.7
9	0.9	0.4	68.77	68.77	196.1	200
10	0.95	0.4	68.77	66.66	202.2	199
11	1	0.4	66.83	67.69	204.9	201.06667
12	1.05	0.4	66.91	66.3	209	205.36667
13	1.1	0.4	72.82	69.77	182.4	198.76667
14	1.15	0.4	67.91	68.61	199	196.8
15	1.2	0.4	72.76	71.51	178.2	186.53333
16	1.25	0.4	74.24	72.38	172.5	183.23333
17	1.3	0.4	69.72	69.24	192.1	180.93333
18	1.35	0.4	68.83	67.78	198.7	187.76667
19	1.4	0.4	65.02	63.59	224.2	205
20	1.45	0.4	64.73	63.2	226.6	216.5
21	1.5	0.4	66.83	66.06	210	220.26667
22	1.55	0.4	63.49	63.28	230.8	222.46667
23	1.6	0.4	66.38	64.94	215.1	218.63333
24	1.65	0.4	67.13	67.42	204.9	216.93333
25	1.7	0.4	67.15	66.59	207.3	209.1
26	1.75	0.4	67.54	66.73	205.7	205.96667
27	1.8	0.4	66.75	66.17	209.9	207.63333
28	1.85	0.4	66.33	64.78	215.8	210.46667
29	1.9	0.4	69.14	67.52	198.6	208.1
30	1.95	0.4	64.96	66.34	215.1	209.83333
31	2	0.4	67.16	65.56	210.6	208.1
32	2.05	0.4	66.13	66.96	209.4	211.7
33	2.1	0.4	64.24	64.29	224.5	214.83333
34	2.15	0.4	66.17	65.12	215.1	216.33333
35	2.2	0.4	65.99	66.88	210.1	216.56667
36	2.25	0.4	67.13	66.52	207.6	210.93333
37	2.3	0.4	65.96	65.48	214.7	210.8
38	2.35	0.4	65.85	64.48	218.4	213.56667
39	2.4	0.4	64.57	65.56	219	217.36667
40	2.45	0.4	67.37	66.48	207	214.8
41	2.5	0.4	65.5	66.54	212.7	212.9
42	2.55	0.4	68.17	66.09	205.7	208.46667
43	2.6	0.4	68.18	66.81	203.5	207.3
44	2.65	0.4	65.41	65.1	217.8	209
45	2.7	0.4	64.79	63.41	225.7	215.66667
46	2.75	0.4	67.41	66.23	207.7	217.06667
47	2.8	0.4	67	64.73	213.7	215.7
48	2.85	0.4	66.02	64.79	216.7	212.7
49	2.9	0.4	66.56	64.85	214.8	215.06667
50	2.95	0.4	62.68	64.3	230	220.5
51	3	0.4	69.28	68.98	194	212.93333
52	3.05	0.4	64.99	63.47	224.7	216.23333

53	3.1	0.4	66.88	66.82	207.5	208.73333
54	3.15	0.4	68.12	67.49	201.7	211.3
55	3.2	0.4	66.03	65.24	215.2	208.13333
56	3.25	0.4	64.21	65.2	221.5	212.8
57	3.3	0.4	67.06	65.38	211.4	216.03333
58	3.35	0.4	65.67	65.44	215.7	216.2
59	3.4	0.4	65.33	63.95	221.9	216.33333
60	3.45	0.4	64.12	63.16	228.9	222.16667
61	3.5	0.4	64.63	62.29	230.2	227
62	3.55	0.4	66.19	64.75	216.3	225.13333
63	3.6	0.4	65.84	63.48	221.8	222.76667
64	3.65	0.4	61.96	61.92	241.7	226.6
65	3.7	0.4	61.79	62.09	241.6	235.03333
66	3.75	0.4	65.56	64.33	219.9	234.4
67	3.8	0.4	69.01	69.01	194.7	218.73333
68	3.85	0.4	71.41	68.39	189.8	201.46667
69	3.9	0.4	73.36	72.54	174.2	186.23333
70	3.95	0.4	71.67	70.48	183.5	182.5
71	4	0.4	69.16	71.51	187.4	181.7
72	4.05	0.4	71.58	69.46	186.4	185.76667
73	4.1	0.4	70.46	68.78	191.3	188.36667
74	4.15	0.4	67.73	65.41	209.2	195.63333
75	4.2	0.4	65.67	65.26	216.4	205.63333
76	4.25	0.4	68.33	67.66	200.6	208.73333
77	4.3	0.4	68.04	66.11	206.1	207.7
78	4.35	0.4	63.79	63.5	228.9	211.86667
79	4.4	0.4	66.92	65.94	210.1	215.03333
80	4.45	0.4	67.58	66.06	207.7	215.56667
81	4.5	0.4	70.5	66.97	196.3	204.7
M5						
1	0.5	1	64.14	63.48	227.7	227.7
3	0.55	1	58.53	60.29	262.7	245.2
5	0.6	1	62.27	61.76	241.1	243.83333
7	0.65	1	64.6	65.46	219.3	241.03333
9	0.7	1	61.38	61.99	243.7	234.7
11	0.75	1	63.95	66.65	217.4	226.8
13	0.8	1	62.58	64.24	230.6	230.56667
15	0.85	1	64.22	65.79	219.4	222.46667
17	0.9	1	65.56	64.71	218.5	222.83333
19	0.95	1	68.14	65.83	206.7	214.86667
21	1	1	65.85	66.54	211.6	212.26667
23	1.05	1	64.26	63.34	227.8	215.36667
25	1.1	1	67.39	68.15	201.9	213.76667
27	1.15	1	68.44	69.1	196	208.56667
29	1.2	1	70.28	70.09	188.2	195.36667

31	1.25	1	68.47	68.92	196.5	193.56667
33	1.3	1	69.24	68.23	196.2	193.63333
35	1.35	1	64.84	64.48	221.7	204.8
37	1.4	1	63.29	65.35	224.1	214
39	1.45	1	64.96	65.47	218	221.26667
41	1.5	1	61.66	60.51	248.5	230.2
43	1.55	1	59.97	60.2	256.8	241.1
45	1.6	1	64.69	64.39	222.6	242.63333
47	1.65	1	65.36	64.68	219.3	232.9
49	1.7	1	63.54	64.58	226	222.63333
51	1.75	1	66.32	65.42	213.7	219.66667
53	1.8	1	67.71	66.3	206.5	215.4
55	1.85	1	65.24	65.13	218.2	212.8
57	1.9	1	65.31	66.11	214.7	213.13333
59	1.95	1	63.99	64.41	225	219.3
61	2	1	66.06	66.43	211.3	217
63	2.05	1	65.21	65	218.8	218.36667
65	2.1	1	67.42	66.66	206.3	212.13333
67	2.15	1	66.44	66.26	210.6	211.9
69	2.2	1	63.97	65.15	222.5	213.13333
71	2.25	1	64.86	64.89	220.3	217.8
73	2.3	1	65.07	65.36	218	220.26667
75	2.35	1	67.09	65.33	211.5	216.6
77	2.4	1	68.01	67.09	203.2	210.9
79	2.45	1	65.96	67.38	208.6	207.76667
81	2.5	1	64.09	64.09	225.7	212.5
83	2.55	1	66.59	65.71	211.9	215.4
85	2.6	1	66.33	66.49	210.2	215.93333
87	2.65	1	64.98	64.96	219.6	213.9
89	2.7	1	64.6	65.32	219.7	216.5
91	2.75	1	66.81	67.37	206	215.1
93	2.8	1	66.02	65.83	213.3	213
95	2.85	1	67.41	65.19	211	210.1
97	2.9	1	65.04	64.73	220.2	214.83333
99	2.95	1	65.31	65.06	218.2	216.46667
101	3	1	67.65	66.16	207.1	215.16667
103	3.05	1	67.05	65.89	209.8	211.7
105	3.1	1	67.52	67.06	204.8	207.23333
107	3.15	1	65.53	65.38	216.4	210.33333
109	3.2	1	64.21	63.99	225.7	215.63333
111	3.25	1	66.44	67.93	205.4	215.83333
113	3.3	1	66.11	66.55	210.8	213.96667
115	3.35	1	62.06	63.49	235.3	217.16667
117	3.4	1	64.74	65.04	220.2	222.1
119	3.45	1	65.09	64.06	222.3	225.93333
121	3.5	1	63.24	64.73	226.5	223

123	3.55	1	66.13	65.55	213.9	220.9
125	3.6	1	69.13	68.31	196.3	212.23333
127	3.65	1	67.01	69.09	200.2	203.46667
129	3.7	1	65.32	67.73	209.5	202
131	3.75	1	69.58	70.54	188.9	199.53333
133	3.8	1	67.9	67.94	201	199.8
135	3.85	1	65.99	64.89	216.5	202.13333
137	3.9	1	62.93	64.6	228.1	215.2
139	3.95	1	63.16	64.99	225.8	223.46667
141	4	1	64.34	67	215	222.96667
143	4.05	1	67.05	67.33	205.4	215.4
145	4.1	1	65.76	65.02	216.9	212.43333
147	4.15	1	63.66	62.69	232.3	218.2
149	4.2	1	67.58	67.44	203.4	217.53333
151	4.25	1	67.78	68.99	198.3	211.33333
153	4.3	1	63.13	64.21	228.7	210.13333
155	4.35	1	64.58	67.46	212.7	213.23333
157	4.4	1	66.61	65.34	213	218.13333
159	4.45	1	63.13	63.29	232	219.23333
161	4.5	1	66.24	68.26	205	216.66667
2	0.5	0.4	65.48	64.69	218.9	218.9
4	0.55	0.4	64.09	66.45	217.6	218.25
6	0.6	0.4	62.74	62.38	236.9	224.46667
8	0.65	0.4	65.41	65.75	215.6	223.36667
10	0.7	0.4	63.59	65.07	224.1	225.53333
12	0.75	0.4	64.3	67.17	214.6	218.1
14	0.8	0.4	64.38	64.6	222.9	220.53333
16	0.85	0.4	64.92	66.84	213.6	217.03333
18	0.9	0.4	64.36	63.87	225.5	220.66667
20	0.95	0.4	63.45	65.63	222.6	220.56667
22	1	0.4	66.66	65.44	212.5	220.2
24	1.05	0.4	65.89	66.03	213.1	216.06667
26	1.1	0.4	61.78	63.86	235	220.2
28	1.15	0.4	64.71	64.46	222.3	223.46667
30	1.2	0.4	71.42	72.19	179.8	212.36667
32	1.25	0.4	67.11	67.62	204.3	202.13333
34	1.3	0.4	65.81	68.07	206.9	197
36	1.35	0.4	67.66	68.03	201.4	204.2
38	1.4	0.4	62.26	62.34	238.9	215.73333
40	1.45	0.4	66.5	64.76	215.3	218.53333
42	1.5	0.4	62.96	63.55	231.7	228.63333
44	1.55	0.4	60.61	59.85	255.6	234.2
46	1.6	0.4	62.09	62.43	239.2	242.16667
48	1.65	0.4	62.74	63.17	234	242.93333
50	1.7	0.4	66.64	65.76	211.6	228.26667
52	1.75	0.4	65.76	65.22	216.2	220.6

54	1.8	0.4	66.04	64.9	216.3	214.7
56	1.85	0.4	65.74	64.66	218.1	216.86667
58	1.9	0.4	63.96	62.99	230.1	221.5
60	1.95	0.4	66.99	67.96	203.6	217.26667
62	2	0.4	65.43	64.6	219.3	217.66667
64	2.05	0.4	64.63	65.59	218.7	213.86667
66	2.1	0.4	67.29	66.73	206.5	214.83333
68	2.15	0.4	66.01	65.34	215	213.4
70	2.2	0.4	66.55	65.59	212.4	211.3
72	2.25	0.4	67.17	67.31	205.1	210.83333
74	2.3	0.4	65.65	65.53	215.5	211
76	2.35	0.4	64.61	65.15	220.3	213.63333
78	2.4	0.4	65.24	65.9	215.6	217.13333
80	2.45	0.4	65.83	67.23	209.5	215.13333
82	2.5	0.4	66.42	66.04	211.4	212.16667
84	2.55	0.4	67.41	66.06	208.2	209.7
86	2.6	0.4	65.57	64.28	220	213.2
88	2.65	0.4	65.3	65.32	217.4	215.2
90	2.7	0.4	64.84	65.66	217.8	218.4
92	2.75	0.4	65.16	65.48	217.3	217.5
94	2.8	0.4	66.84	66.48	208.7	214.6
96	2.85	0.4	65.91	65.17	215.8	213.93333
98	2.9	0.4	64.66	66.51	215.5	213.33333
100	2.95	0.4	65.53	66.35	213.3	214.86667
102	3	0.4	65.53	66.84	211.7	213.5
104	3.05	0.4	66.54	66.29	210.2	211.73333
106	3.1	0.4	67.19	67.51	204.4	208.76667
108	3.15	0.4	66.58	66.49	209.5	208.03333
110	3.2	0.4	69.89	68.85	192.7	202.2
112	3.25	0.4	65.39	65.38	216.9	206.36667
114	3.3	0.4	63.51	66.24	220.3	209.96667
116	3.35	0.4	63.88	62.44	232.4	223.2
118	3.4	0.4	63.5	62.76	232.7	228.46667
120	3.45	0.4	62.6	63.96	231.5	232.2
122	3.5	0.4	64.62	63.61	225.5	229.9
124	3.55	0.4	62.59	61.42	241.2	232.73333
126	3.6	0.4	69.04	68.28	196.7	217.83333
128	3.65	0.4	66.37	66.69	209.5	217.775
130	3.7	0.4	67.31	68.84	200.1	202.1
132	3.75	0.4	66.52	67.75	205.7	205.1
134	3.8	0.4	66.84	67.29	206.1	203.96667
136	3.85	0.4	66.61	65.86	211.3	207.7
138	3.9	0.4	63.55	64.41	226.5	214.63333
140	3.95	0.4	64.24	63.55	227.1	221.63333
142	4	0.4	64.95	66.5	214.6	222.73333
144	4.05	0.4	61.57	63.24	238.1	226.6

146	4.1	0.4	64.06	62.16	232.8	228.5
148	4.15	0.4	65.58	65.49	215.9	228.93333
150	4.2	0.4	64.37	63.21	227.9	225.53333
152	4.25	0.4	64.38	64.49	223.3	222.36667
154	4.3	0.4	60.41	63.02	243.5	231.56667
156	4.35	0.4	64.84	65.51	218.3	228.36667
158	4.4	0.4	65.53	66.29	213.5	225.1
160	4.45	0.4	62.01	64.49	231.8	221.2
162	4.5	0.4	60.42	63.4	241.9	229.06667
M6						
1	0.5	0.4	67.38	64.23	214.1	214.1
2	0.55	0.4	68.09	67.88	200.6	207.35
3	0.6	0.4	66.53	65.41	213.1	209.26667
4	0.65	0.4	62.56	63.18	234.6	216.1
5	0.7	0.4	67.36	66.67	206.5	218.06667
6	0.75	0.4	69.86	69.94	189.8	210.3
7	0.8	0.4	64.56	66.04	217.4	204.56667
8	0.85	0.4	68.17	68.39	198.9	202.03333
9	0.9	0.4	74.26	71.53	174.5	196.93333
10	0.95	0.4	72.71	73.31	173.9	182.43333
11	1	0.4	68.19	68.73	197.9	182.1
12	1.05	0.4	66.97	67.98	203.6	191.8
13	1.1	0.4	69.07	67.99	197.4	199.63333
14	1.15	0.4	67.2	65.57	210.4	203.8
15	1.2	0.4	63.23	63.61	230.5	212.76667
16	1.25	0.4	64.33	64.55	223.3	221.4
17	1.3	0.4	63.41	60.99	239.7	231.16667
18	1.35	0.4	61.71	64.23	233.8	232.26667
19	1.4	0.4	66.35	65.94	211.9	228.46667
20	1.45	0.4	65.11	66.17	215.2	220.3
21	1.5	0.4	66.05	66.54	211	212.7
22	1.55	0.4	67.71	69	198.4	208.2
23	1.6	0.4	66.92	67.17	206.3	205.23333
24	1.65	0.4	66.8	68.25	203.3	202.66667
25	1.7	0.4	65.59	66.5	212.6	207.4
26	1.75	0.4	63.33	66.26	220.9	212.26667
27	1.8	0.4	64.74	66.31	215.9	216.46667
28	1.85	0.4	65.53	67.97	208.1	214.96667
29	1.9	0.4	67.18	66.67	207	210.33333
30	1.95	0.4	66.34	69.78	200.2	205.1
31	2	0.4	69.86	67.27	197.2	201.46667
32	2.05	0.4	66.79	66.26	209.5	202.3
33	2.1	0.4	64.53	64.78	221.8	209.5
34	2.15	0.4	66.99	68.39	202.4	211.23333
35	2.2	0.4	64.58	63.68	225.4	216.53333

36	2.25	0.4	68.71	67.49	199.9	209.23333
37	2.3	0.4	64.11	64.91	222.8	216.03333
38	2.35	0.4	65.71	65.29	216.1	212.93333
39	2.4	0.4	65.53	64.92	217.9	218.93333
40	2.45	0.4	66.94	67.33	205.7	213.23333
41	2.5	0.4	65.64	64.34	219.5	214.36667
42	2.55	0.4	65.46	66.56	212.8	212.66667
43	2.6	0.4	66.83	65.42	212	214.76667
44	2.65	0.4	67.08	68.09	203	209.26667
45	2.7	0.4	65.33	65.04	218.2	211.06667
46	2.75	0.4	66.05	66.09	212.4	211.2
47	2.8	0.4	67.31	66.26	207.9	212.83333
48	2.85	0.4	66.91	66.98	206.9	209.06667
49	2.9	0.4	67.63	66.2	207.1	207.3
50	2.95	0.4	65.22	65.26	217.8	210.6
51	3	0.4	64.06	65.61	220.6	215.16667
52	3.05	0.4	68.25	66.21	205.1	214.5
53	3.1	0.4	65.12	65.04	218.9	214.86667
54	3.15	0.4	66.92	66.93	207	210.33333
55	3.2	0.4	67.78	67.32	203.2	209.7
56	3.25	0.4	65.58	65.16	217	209.06667
57	3.3	0.4	65.71	64.74	217.9	212.7
58	3.35	0.4	66.35	64.31	217.3	217.4
59	3.4	0.4	65.92	64.96	216.5	217.23333
60	3.45	0.4	66.96	66.76	207.4	213.73333
61	3.5	0.4	65.59	66.88	211.3	211.73333
62	3.55	0.4	66.31	65.96	212	210.23333
63	3.6	0.4	67.44	66.37	207.1	210.13333
64	3.65	0.4	62.72	61.64	239.8	219.63333
65	3.7	0.4	62.66	62.13	238.2	228.36667
66	3.75	0.4	61.37	60.04	251.6	243.2
67	3.8	0.4	64.59	65.97	217.6	235.8
68	3.85	0.4	65.83	65.25	215.9	228.36667
69	3.9	0.4	67.88	66.45	205.5	213
70	3.95	0.4	72.04	71.55	179.9	200.43333
71	4	0.4	70.23	69.94	188.8	191.4
72	4.05	0.4	74.33	73.11	170.6	179.76667
73	4.1	0.4	69.78	67.92	195.6	185
74	4.15	0.4	70.14	67.96	194.5	186.9
75	4.2	0.4	67.38	67.27	204.6	198.23333
76	4.25	0.4	66.56	66.13	210.7	203.26667
77	4.3	0.4	67.54	67.11	204.6	206.63333
78	4.35	0.4	68.23	68.31	199	204.76667
79	4.4	0.4	67.69	67.74	202.2	201.93333
80	4.45	0.4	66.78	65.93	210.6	203.93333
81	4.5	0.4	69	66.08	203.3	205.36667

M7						
1	0.25	1	68.23	66.92	203	203
2	0.3	1	67.07	65.23	211.9	207.45
3	0.35	1	62.41	62.67	237.1	217.33333
4	0.4	1	64.61	64.88	221.2	223.4
5	0.45	1	67.14	66.07	209	222.43333
6	0.5	1	66.36	68.85	202.9	211.03333
7	0.55	1	64.65	65.64	218.5	210.13333
8	0.6	1	70.21	70.35	187.7	203.03333
9	0.65	1	70.35	70.71	186.4	197.53333
10	0.7	1	69.93	68.24	194.3	189.46667
11	0.75	1	64.06	63.64	227.4	202.7
12	0.8	1	64.79	65.18	219.5	213.73333
13	0.85	1	63.16	62.56	234.6	227.16667
14	0.9	1	63.67	64.63	225.3	226.46667
15	0.95	1	65.99	65.34	215	224.96667
16	1	1	65.03	63.34	225.1	221.8
17	1.05	1	64.35	63.88	225.6	221.9
18	1.1	1	65.13	66.14	215.3	222
19	1.15	1	65.29	64.28	220.9	220.6
20	1.2	1	65.64	64.59	218.7	218.3
21	1.25	1	64.56	64.9	221.3	220.3
22	1.3	1	64.31	64.31	224.2	221.4
23	1.35	1	65.58	66.03	214.1	219.86667
24	1.4	1	64.33	65.79	219.1	219.13333
25	1.45	1	66.8	66.21	209.6	214.26667
26	1.5	1	68.04	66.03	206.3	211.66667
27	1.55	1	65.12	64.88	219.5	211.8
28	1.6	1	63.86	63.43	228.9	218.23333
29	1.65	1	64.73	64.42	222.4	223.6
30	1.7	1	65.28	64.95	218.7	223.33333
31	1.75	1	65.98	67.33	208.7	216.6
32	1.8	1	66.45	65.5	213	213.46667
33	1.85	1	68.01	66.48	205.1	208.93333
34	1.9	1	67.72	67.61	202.5	206.86667
35	1.95	1	65.99	67	209.7	205.76667
36	2	1	66.72	67.05	207.3	206.5
37	2.05	1	67.39	66.38	207.2	208.06667
38	2.1	1	65.59	65.23	216.7	210.4
39	2.15	1	64.21	64.21	224.9	216.26667
40	2.2	1	67.83	66.24	206.4	216
41	2.25	1	65.53	63.31	223.5	218.26667
42	2.3	1	66.71	65.78	211.3	213.73333
43	2.35	1	66.2	64.23	218	217.6
44	2.4	1	67.58	67.44	203.4	210.9

45	2.45	1	66.43	66.88	208.7	210.03333
46	2.5	1	65.82	66.01	213.4	208.5
47	2.55	1	65.81	66.04	213.4	211.83333
48	2.6	1	65.51	65.36	216.5	214.43333
49	2.65	1	66.77	65.98	210.5	213.46667
50	2.7	1	67.46	67.31	204.2	210.4
51	2.75	1	67.09	65.93	209.6	208.1
52	2.8	1	65.88	67.81	207.5	207.1
53	2.85	1	66.58	66.92	208.1	208.4
54	2.9	1	67.13	65.15	211.9	209.16667
55	2.95	1	64.83	64.32	222.4	214.13333
56	3	1	66.92	65.07	212.9	215.73333
57	3.05	1	65.55	64.37	219.7	218.33333
58	3.1	1	67.98	66.58	204.9	212.5
59	3.15	1	67.14	65.59	210.5	211.7
60	3.2	1	68.46	66.04	205	206.8
61	3.25	1	65.26	64.95	218.7	211.4
62	3.3	1	65.24	65.44	217.2	213.63333
63	3.35	1	64.74	65.14	219.9	218.6
64	3.4	1	66.4	67.02	208.3	215.13333
65	3.45	1	66.4	66.51	209.9	212.7
66	3.5	1	65.13	64.58	220.5	212.9
67	3.55	1	63.89	63.08	230.1	220.16667
68	3.6	1	65.14	64.09	222.1	224.23333
69	3.65	1	64.03	64.16	225.7	225.96667
70	3.7	1	65.25	63.86	222.5	223.43333
71	3.75	1	62.24	63.39	235	227.73333
72	3.8	1	63.17	62.92	233.3	230.26667
73	3.85	1	65.37	63.73	222.5	230.26667
74	3.9	1	63.24	63.71	230.1	228.63333
75	3.95	1	64.92	63.83	223.7	225.43333
76	4	1	65.07	64.99	219.2	224.33333
77	4.05	1	68.78	70.15	192.2	211.7
78	4.1	1	73.38	74.15	170.4	193.93333
79	4.15	1	70.14	71.29	185.4	182.66667
80	4.2	1	67.13	69.45	198.8	184.86667
81	4.25	1	67.48	66.67	206.1	196.76667
82	4.3	1	67.06	64.76	213.4	200.925
83	4.35	1	65.99	65.2	215.5	208.45
84	4.4	1	66.73	66.11	210.2	213.03333
85	4.45	1	65.26	64.82	219.2	214.96667
86	4.5	1	67.19	66.69	206.9	212.1
87	4.55	1	61.64	64.78	232.1	219.4
88	4.6	1	65.21	65.73	216.3	218.43333
89	4.65	1	64.54	63.52	226.1	224.83333
90	4.7	1	62.69	63.22	233.9	225.43333

91	4.75	1	61.32	63.75	237.1	232.36667
92	0.25	0.4	68.83	65.36	206	206
93	0.3	0.4	65.77	65.24	216.1	211.05
94	0.35	0.4	63.06	62.14	236.6	219.56667
95	0.4	0.4	65.21	63.73	223.1	225.26667
96	0.45	0.4	64.43	64.72	222.4	227.36667
97	0.5	0.4	66.16	65.51	213.9	219.8
98	0.55	0.4	63.88	66.17	219.3	218.53333
99	0.6	0.4	62.85	64.51	228.7	220.63333
100	0.65	0.4	69.04	69.98	191.9	213.3
101	0.7	0.4	64.44	67.92	211.7	210.76667
102	0.75	0.4	71.6	69.51	186.3	196.63333
103	0.8	0.4	66.74	68.59	202.5	200.16667
104	0.85	0.4	70.85	69.24	189	192.6
105	0.9	0.4	68.28	66.33	204.7	198.73333
106	0.95	0.4	67.48	65.67	209.2	200.96667
107	1	0.4	65.36	64.61	219.6	211.16667
108	1.05	0.4	63.61	64.62	225.5	218.1
109	1.1	0.4	63.28	64.74	226.3	223.8
110	1.15	0.4	64.24	63.96	225.7	225.83333
111	1.2	0.4	62.51	62.21	238.4	230.13333
112	1.25	0.4	62.23	63.06	236.3	233.46667
113	1.3	0.4	64.24	63.75	226.4	233.7
114	1.35	0.4	62.33	62.46	238.2	233.63333
115	1.4	0.4	64.28	63.84	225.9	230.16667
116	1.45	0.4	66.42	63.89	218.4	227.5
117	1.5	0.4	63.74	64.11	226.9	223.73333
118	1.55	0.4	63.98	65.66	220.7	222
119	1.6	0.4	62.35	63.64	233.7	227.1
120	1.65	0.4	66.66	65.47	212.4	222.26667
121	1.7	0.4	63.56	63.32	230.4	225.5
122	1.75	0.4	63.44	63.89	228.7	223.83333
123	1.8	0.4	63.76	63.98	227.3	228.8
124	1.85	0.4	64.96	64.42	221.6	225.86667
125	1.9	0.4	64.79	64.23	222.8	223.9
126	1.95	0.4	64.15	64.79	223.1	222.5
127	2	0.4	65.98	64.43	218.1	221.33333
128	2.05	0.4	64.41	65.2	220.8	220.66667
129	2.1	0.4	65.53	66.46	212.9	217.26667
130	2.15	0.4	65.69	64.54	218.7	217.46667
131	2.2	0.4	63.18	64.66	226.9	219.5
132	2.25	0.4	62.53	61.81	239.9	228.5
133	2.3	0.4	64.38	65.44	220.1	228.96667
134	2.35	0.4	63.82	62.29	233.2	231.06667
135	2.4	0.4	63.1	64.95	226.2	226.5
136	2.45	0.4	66.06	64.88	216.3	225.23333

137	2.5	0.4	63.85	64.04	226.8	223.1
138	2.55	0.4	67.08	66.5	207.9	217
139	2.6	0.4	65.24	64.92	218.9	217.86667
140	2.65	0.4	64.57	65.42	219.5	215.43333
141	2.7	0.4	64.81	64.56	221.6	220
142	2.75	0.4	65.89	65.79	213.9	218.33333
143	2.8	0.4	65.97	65.16	215.7	217.06667
144	2.85	0.4	65.96	65.68	214	214.53333
145	2.9	0.4	66.12	66.11	212.1	213.93333
146	2.95	0.4	68.49	68.24	198.4	208.16667
147	3	0.4	68.74	67.71	199.2	203.23333
148	3.05	0.4	66.49	64.97	214.6	204.06667
149	3.1	0.4	64.62	65.28	219.8	211.2
150	3.15	0.4	65.06	66.94	212.9	215.76667
151	3.2	0.4	65.74	66.57	211.8	214.83333
152	3.25	0.4	65.17	65.29	217.9	214.2
153	3.3	0.4	64.92	65.61	217.7	215.8
154	3.35	0.4	66.18	65.84	212.8	212.24167
155	3.4	0.4	65.51	66.76	212	211.93333
156	3.45	0.4	63.77	66.21	219.5	214.76667
157	3.5	0.4	61.88	60.32	248.4	226.63333
158	3.55	0.4	62.79	65.25	226.2	231.36667
159	3.6	0.4	65.18	64.09	221.9	232.16667
160	3.65	0.4	65.81	64.18	219.5	222.53333
161	3.7	0.4	66.23	68	205.9	215.76667
162	3.75	0.4	61.63	62.14	242.1	222.5
163	3.8	0.4	66.71	67.18	206.9	218.3
164	3.85	0.4	62.71	63.56	232.6	227.2
165	3.9	0.4	67.5	68.59	200.3	213.26667
166	3.95	0.4	71.69	71.05	182	204.96667
167	4	0.4	72.36	73.82	173.6	185.3
168	4.05	0.4	71.28	71.61	181.6	179.06667
169	4.1	0.4	65.94	65.92	213.3	189.5
170	4.15	0.4	67.49	67.28	204.2	199.7
171	4.2	0.4	65.95	66.52	211.3	209.6
172	4.25	0.4	65.45	65.59	216	210.5
173	4.3	0.4	66.01	67.45	208.2	211.83333
174	4.35	0.4	67.07	67.19	205.7	209.96667
175	4.4	0.4	64.24	63.15	228.5	214.13333
176	4.45	0.4	67.73	66.65	205.4	213.2
177	4.5	0.4	63.91	64.95	223.4	219.1
178	4.55	0.4	62.76	62.58	236.1	221.63333
179	4.6	0.4	65.58	65.22	216.8	225.43333
180	4.65	0.4	62.89	63.54	232	228.3
181	4.7	0.4	61.35	61.91	244.1	230.96667
182	4.75	0.4	65.34	64.87	218.8	231.63333

REFERENCES

American Association of State Highway and Transportation Officials. (2010). *AASHTO LRFD Bridge Design Specifications, Fifth Edition.* AASHTO.

American Welding Society. (2009). Welding Handbook - 9 Edition, Volume 2. American Welding Society.

American Welding Society. (2010). Bridge Welding Code AASHTO/AWS D1.5M/D1.5. AWS.

American Welding Society. (n.d.). AWS B4.0:2007. In *Standard Method for Mechanical Testing of Welds.*

ASTM International. (2012). ASTM E23-12c. In *Standard Test Method for Notched Impact Testing of Metallic Materials.* ASTM International.

ASTM International. (2012). ASTM E384-11e1. In *Standard Test Method for Knoop and Vickers Hardness of Materials.* ASTM International.

ASTM International. (2013). ASTM A709 - 13. In *Standard Specification for Structural Steel for Bridges.*

ASTM International. (2013). ASTM E8/E8M - 13a. In *Standard Test methods for Tension Testing of Metallic Materials.* ASTM International.

ASTM International. (n.d.). ASTM A370 - 12a. In *Standard Test Methods and Definitions for Mechaniocal Testing of Steel Products.*

Bennett, C. R., Swanson, J. A., & Linzell, D. G. (2009). *Fatigue Resistance of HPS-485 W(70W) Welded Butt-Splice Connections Using Narroe Gap Improved Electroslag Welding.* ASCE.

Blodgett, O. W., Funderburk, S. R., Miller, D. K., & Quintana, M. (1999). *Fabricators' and Erectors' Guide to Welded Steel Construction.* Miami: The James F. Lincoln Arc Welding Foundation.

Chambers, J. J. (2015). *Electroslag Welding Facts for Structural Engineers.* Steel Tips, Structural Steel Education Council.

Chambers, J. J., & Medlock, R. D. (2015). *Electroslag Welding Facts for Structural Engineers* . Steel Tips, Structural Steel Education Council.

Choi, S. W. (2016). *Non-linear Curve Fitting of High Perfoemance Steel Charpy Impact Test Data, MS Project.* George Mason University.

Culmo, M. P. (2011). *Accelerated Bridge Construction - Experience in Design, Fabrication and Erection of Prefabricated Bridge Elements and Systems.* Washington D.C.: Federal Highway Administration.

Federal Highway Administration. (1996). *Technical Information Guide For Narrow-Gap Improved Electroslag Welding.* U.S. Department of Transportation.

Federal Highway Administration. (2002). *High Performance Steel Designers' Guide.* Washington D.C.: FHWA.

Structural Stability Research Council. (2010). *Guide to Stability Design Criteria for Metal Structures, 6th Edition.*

Swanson, J. A., Linzell, D. G., & Bennett, C. R. (2006). *Verification of Performance and Design Criteria for High Performance Steel Bridges.* University of Cincinnaty, FHWA.

Ted L. Anderson, D. A. (2000). API 579: a comprehensive fitness-for-service guide.

Verma, K. K. (2001). Narrow-Gap Improved Electroslag Welding For Bridges. 11.

Yeager, K. (n.d.). *Nonlinear curve fitting and the Charpy impact test: statistical, mathematical, and physical considerations.*

BIOGRAPHY

Andrei Denes received his Bachelor of Science in Roads, Bridges and Railway Engineering from the Technical University of Cluj-Napoca, Romania, in 2005. He started working in 2002, as a student intern, for a transportation infrastructure design-build firm called 4I Invest which was based in Cluj-Napoca. There, he participated in the design of multiple highway and railway projects, most notably two bridges and one tunnel. After graduating in 2005, he continued his employment with the same company as a Project and Design Engineer. During this time, he was the main designer on a vast amount of highway design projects and two railroad projects as well as project engineer on two major local projects. In 2005, while employed with 4I Invest, he was the main project engineer for the biggest traffic improvement project that the city had implemented at the time. He emigrated to the United States of America in 2006. Here, using the experience gained in Romania, Andrei together with a partner, started his own residential contracting company called A&C Custom Flooring LLC. As an owner and manager of the company he performed project budgeting, planning, bidding, invoicing and cost evaluations while managing client and stakeholder's relations. In 2012 from the desire to further his engineering knowledge and experience, Andrei moved to Northern Virginia to join Professional Service Industries at Turner Fairbanks Highway Research Center (TFHRC) as a contractor for Federal Highway Administration (FHWA) in the Structures Research Lab. Here, he performed the role of staff scientist which allowed him to participate in industry leading research on High Performance Steel, Ultra High Performance Concrete and Structural Building Methods. As a staff scientist, he was charged with updating, maintaining and upgrading instrumentation and Lab equipment, as well as to train new technicians and develop safety plans. At TFHRC Andrei built on his previous experience with engineering practices and software's by adding specialty testing equipment and software knowledge to his curriculum. Andrei is well versed in AutoCAD, Excel, MatLAB, MTS Testing Systems and software, FARO Laser equipment and software, Instron and LECO metallography tools. In 2014, Andrei joined the Civil Engineering department at George Mason University as a graduate student with a concentration in Structural Engineering. In 2015, while at TFHRC Andrei was tasked to perform the experimental program presented in this thesis. Currently, Andrei Denes works as a Bridge Design Engineer with the Bridge Design Office of FHWA-Eastern Federal Lands.